IMPROVING COAL MINE SAFETY BY IDENTIFYING FACTORS THAT INFLUENCE THE SUDDEN RELEASE OF GASES IN OUTBURST PRONE ZONES.

A thesis submitted in fulfilment of the
requirements for the award of the degree

DOCTOR OF PHILOSOPHY

from

UNIVERSITY OF WOLLONGONG

by

FARHANG SERESHKI

B.Sc. (Hon.), M.Sc. Mining Engineering

School of Civil, Mining and Environmental Engineering

May 2005

IN THE NAME OF GOD

This thesis is dedicated to my dear parents:

My mother and father: Iran and Firooz

My brother and sister: Farrokh, Frouzan and their families

My dear uncle and his family

and

My dear daughter:

Sarina

For their love, encouragement, support and patience.

AFFIRMATION

I, Farhang Sereshki, declare that this thesis, submitted in fulfilment of the requirements for the award of Doctor of Philosophy, in the School of Civil, Mining and Environmental Engineering, Faculty of Engineering, University of Wollongong, is wholly my own work unless otherwise referenced or acknowledged. The thesis was completed under the supervision of A/Prof. N. I. Aziz and A/Prof. I. Porter and has not been submitted for qualification at any other academic institution.

Farhang Sereshki

May 2005

The following publications are the result of this thesis project:

Sereshki, F., Aziz, N. I., and Porter, I. (2003). Impact of Coal Permeability on Gas Sorption and Coal Volume Change. *Proceedings of the 7th Annual Environmental Engineering Research Event Conference*, The Cumberland, Marysville, Victoria, Australia, pp. 333-342.

Sereshki, F., Aziz, N. I., and Porter, I. (2003). Improving Mine Safety by Identifying Factors that Influence the Sudden Release of Gases in Outburst Prone Zones. *Proceedings of the 5th Congress on Safety, Occupational and Environmental health in Mines and related Industries*, Kerman, Iran, pp. 33-44. (*This conference paper was approved by the editorial committee as the best technical paper and won the best paper prize.*)

Sereshki, F., Aziz, N. I., and Porter, I. (2004). Influence of Gas Type and Pressure on Permeability and Volumetric Characteristics of Coal. *Proceedings of the International Coalbed Methane Symposium*, Univ of Alabama, Tuscaloosa, Alabama, USA, Paper No. 415.

Aziz, N. I., Porter, I., and **Sereshki, F.** (2004). The Influence of Gas Environment on Coal Properties- Experimental Studies on Outburst Control. *Proceedings of the 5th Underground Coal Operators' Conference*, Convened by the Illawarra Branch of The Australian Institute of Mining and Metallurgy, Univ. of Wollongong, NSW, Australia, pp.195-201.

Sereshki, F., Aziz, N. I., and Porter, I. (2004). Cracking the Coal Matrix (Report on coal permeability tests using various gas pressures and axial loads). World Coal, Vol 13, No. 9, pp. 85-90.

Sereshki, F., Bruggemann, D., Aziz, N. I., and Porter, I. (2005). Change in effective stress associated with coal shrinkage and gas sorption. Journal of the Mine Ventilation Society of South Africa, January/March, pp. 28-31.

Sereshki, F., Aziz, N. I., Porter, I., and Godbole, A. (2005). Impact of Different Confining Gas Pressures on Coal Permeability and Modelling the Movement of Coalbed Gas. *International Coalbed Methane Symposium*, Uni. of Alabama, Tuscaloosa, Alabama, USA, pp. No. 502.

Hutton, A., Bruggemann, D., Aziz, N. I. and **Sereshki, F.,** (2005). Effect of Coal Properties on Gas Drainage. *International Coalbed Methane Symposium*, Uni. of Alabama, Tuscaloosa, Alabama, USA. Paper No. 501.

Hutton, A., Bruggemann, D., **Sereshki, F.,** and Aziz, N. I. (2005). Gas and Coal Properties Associated with Experimental studies in Outburst Control. The International Journal of Coal Geology (Refereed).

Sereshki, F., Aziz, N. I. and Porter, I. (2005). Influences of coal type and rank on volumetric changes of coal and their impact on coal and gas outbursts. *20th World Mining Conference*, Tehran, Iran (Abstract approved and manuscript submitted).

Aziz, N. I., **Sereshki, F.,** and Bruggemann, D. (2005). Status of Outburst Research at The University of Wollongong. *6th Underground Coal Operators' Conference (Coal 2005)*. Convened by the Queensland Branch of The Australian Institute of Mining and Metallurgy, Brisbane, Queensland, Australia, pp. 283-289.

Aziz, N. I., **Sereshki, F.**, Bruggemann, D. and Porter, I. (2005). Parameters affecting mine gas drainage and outburst control research. *19th International Mining Congress and Fair*. Izmir, Turkey (In press).

ACKNOWLEDGMENTS

The author would like to express his sincere gratitude to A/ Prof. N. I. Aziz for his supervision, encouragement, guidance and inspiration provided during the course of this research and providing the necessary facilities for this research. I would also like to express my sincere thanks to A/ Prof. I. Porter my thesis co-supervisor for his advice, encouragement and critical review of several aspects of this study.

The author also wishes to express his sincere thanks for helpful contributions made by the following professionals during the period of this study:

I wish to express my appreciation to A/ Prof. A. Hutton, Dr. T. Silver, Dr. A. Godbole, Mr. Saeid Hesami and Mrs Lorelle Pollard for their helpful comments and assistance.

I also would like to thank the technical staff in the School of Civil, Mining and Environmental Engineering, especially Ian Laird and Alan Grant for their laboratory assistance and also Bob Rowlan, Ian Bridge, Nick MacKie and Greg Tillman.

The author wishes to thank Mrs. Leonie McIntyre, Mr. Des Jemison and Mr. Peter Turner of the ITS staff for their contributions. The assistance provided by the Faculty of Engineering, University of Wollongong is also appreciated.

I would also like to acknowledge with sincere appreciation, the financial support of the Ministry of Science, Research and Technology of the Islamic Republic of Iran and the University of Shahrood.

Most importantly, I would like to express my deepest thanks to my parents and members of my family in Iran who have provided continued support throughout this study and indeed for my entire life.

This study would not have been finished without support and encouragement from all my fellow Iranians at the University of Wollongong and their families. In particular, the author is indebted to Mr. Vahid Mottaghitalab, Mr. Mehrdad Bahrami Samani, Mr. Mohammad Mahdi Emamjomeh, Mr. Fardin Akhlaghiyan, Mr. Behzad Fatahi and Dr. Faramarz Doulati together with their respective families.

ABSTRACT

In recent decades, the subject of coal and gas outburst in underground coal mines has been a focus of interest in Australia and worldwide. Much of this interest has been the result of the alarming increase in outburst related incidents and associated fatalities world wide, particularly in China, Russia, Ukraine and other major coal producing countries. Australia, on the other hand, has seen a relative decline in outburst related incidents, for the last three years no outburst related incident has been reported. Effective gas drainage programmes, better management of outburst prone zones, tougher regulations and a continuing programme of dedicated vigilance and research have collectively contributed to improvements in outburst prevention. Still, however, difficult problems remain to be addressed. Geological disturbances such as dykes, shear planes and increased mineralisation can influence coal permeability and porosity. These disturbances must be fully understood in order to develop an effective on gas drainage programme and reduce outburst risks. Accordingly, a programme of laboratory studies was undertaken to investigate the relationship between coal composition, coal volumetric change and coal permeability. Coal samples for this study were obtained from four different coalmines in Australia (Tahmoor, Metropolitan, Dartbrook and North Goonyella) and Tabas coalmine in Iran.

Coal samples were tested in different types of gases and under different gas pressures and stress conditions. Coal permeability tests were conducted in the gas pressure chamber of the multi-function outburst research rig (MFORR), and the volumetric

change tests were carried out in a modified pressure bomb. Microscopic studies provided a better correlation between coal composition permeability and shrinkage characteristics. A numerical model was developed to simulate single gas flow through a coal sample. The simulation further supported the experimental studies.

The petrographical tests showed that most of the Australian coals tested were inertinite rich coals. The mineral matter in the Australian coal samples were mostly carbonate (calcite) and clay, but the Iranian Tabas coal had pyrite as the dominant mineral matter. Tabas coal has the highest vitrinite concentration (70%) and lowest proportion of inertinite elements (8.18%), the lowest vitrinite content was obtained from North Goonyella coal.

There was a definite correlation between coal composition, coal volumetric change and coal permeability. Volumetric strain changes during the adsorption stage in all gas environments were greater than the volumetric strains in the desorption stage. The level of coal shrinkage was affected by the type of gas desorbed. Carbon dioxide appears to have the greatest influence on the matrix and nitrogen the least.

The permeability of coal was also influenced by the gas type and pressure. Greater gas permeability was obtained in N_2 gas, and the lowest permeability was obtained in a CO_2 environment. The sorption characteristics of CO_2 are a major factor. The degree of coal permeability is reduced exponentially by increasing the applied stress and also by increasing the confining gas pressure, irrespective of the gas type. The permeability tests showed that with an increased inertinite content the permeability of

coal increased, except in the case of Tahmoor Colliery 900 Panel which showed a decrease. Comparison of the Tahmoor coals from 800 and 900 Panels showed that the permeability of coal was influenced by the mineral content and the carbonates, as well as the cavities. In particular; there was a reduction in coal permeability with increasing mineral content and carbonate content of the coal. With an increase in the percentage of inertinite, the permeability of coal increased.

The numerical modelling provided an opportunity to quantify the flow mechanism in coal. It was possible to simulate the flow duration across the coal samples as a function of time with different gases and coal types. It was recommended that the study be extended to include more coal deposits and coals with different geological variations, so that an effective data bank can be established for Australian coals.

TABLE OF CONTENTS

LIST OF FIGURES

PAGE

LIST OF TABLES

Page

LIST OF SYMBOLS AND ABBREVIATIONS

SYMBOLS

A	Cross sectional area
a	Langmuir's constant
b	Langmuir's constant
b	fracture width
C	The exponent of $-(E_1-E_e)/RT$
c_P	Pore volume compressibility
c_m	Matrix shrinkage compressibility
C	Reservoir gas concentration
C_i	Initial reservoir gas concentration
C_o	Langmuir dimensionless volumetric strain constant
C_m	Shrinkage coefficient
ΔC_i	Maximum concentration change based on the initial desorb
dV_m	Change in volume
dP	Change in applied pressure
$\frac{dP}{dx}$	Gradient of pressure
f	Grain thermal expansivity fraction
f	Protodyakonov strength coefficient of the coal sample
h	The height of sample
$\frac{\Delta h}{h}$	Average strains in axial direction
K	Bulk modulus
K	Gas emission index / outburst tendency index
Δk	The change in permeability

k	Permeability
k_f	Permeability of fracture
k_m	Permeability of coal to mixture
ℓ	Height of the sample
M	Constrained axial modulus
M	Mass
M_m	Molecular mass
N	Volumetric percentage of gas in mixture
n	The quantity of gas
$P_\circ$	Saturation vapour pressure of the gas
P	Reservoir pore pressure
P_i	Initial reservoir pore pressure
P_o	Absolute pressure in the chamber
P_u	Absolute pressure in the outlet
P	Pressure
P'	Dimensionless pressure
P_{max}	Inlet pressure
$P\ (r_i, t_j)$	Gas pressure in j time step
Δ_{P10-60}	Emission rate of gas released from the coal sample
ΔP_i	Maximum pressure change based on the initial desorb
$\frac{\Delta P}{L}$	Pressure differential over channel length
Q	Quantity of methane gas adsorbed at a given pressure p
Q	Swelling parameter (swollen volume/ un swollen volume)
Q	Volumetric flow
Q	Flow rate
q_w	Mass of coal at equilibrium/initial mass.
R	Universal gas constant
r	The radius of coal sample

r_o	External radius of sample
r_i	Internal radius of sample
r'	Dimensionless radius
$r_\circ$	Radius of hole, cm
$\frac{\Delta r}{r}$	Average strains in radial direction
S	Weight of the adsorbate at pressure P
$S_\circ$	Monolayer capacity
S	Fracture spacing
T	Temperature
t	Time
Δt	Time steps
$\mathbf{u}$	Darcy velocity of gas phase
V	The volume of sample
V_2	Volume fraction of coal in the swollen coal sample
V_m	Matrix volume
V_{des}	Volume of gas desorbed
V_m	Matrix volume
ΔV_m	Matrix volume change
$\frac{\Delta V}{V}$	Volumetric strain
W	Fracture width

a	Constant depends on the coal type and its characteristics
b	Constant, which depends on the coal type
g	Grain compressibility
m	Viscosity of the fluid
m_m	Viscosity of mixture gas

r	Gas density
r_1	Density of the sorbate in the liquid state
r_2	Density of coal in the liquid sorbate
s	Effective triaxial confining stress
f	Formation porosity
Φ	Fracture system porosity
Φ_i	Initial fracture system porosity

ABBREVIATIONS

CAR	Carbonate
CAV	Cavity
DAR	Dartbrook coal sample
FRA	Fracture
INT	Inertinite
LIP	Liptinite
MMP	Metropolitan coal sample
NGO	North Goonyella coal sample
OMM	Other mineral matter
PYR	Pyrite
TAB	Tabas coal sample
TAH	Tahmoor coal sample
VIT	Vitrinite

CHAPTER ONE

GENERAL INTRODUCTION

1.1 INTRODUCTION

Australia is one of the world's leading coal exporters, with an annual export capacity exceeding 200 mt. The total annual production of coal in Australia amounts to 10% of the total world production of around three billion tonnes. The majority of the coal mined in Australia comes from the eastern states of Queensland and NSW. The total annual saleable coal production from all Australian coalmines in 2003 amounted to around 275 mt. 56% of this total production came from Queensland, 41 % came from NSW and the remaining 3% came from the other states of Western Australia, South Australia and Tasmania. Almost one third of the coal production comes from 63 underground coalmines. There were 29 operating longwall faces in 2003, producing around 73m tonnes out of a total underground production of 80mt. This represented around 90% of the total underground coal production. Coal seam depth and the prevailing geological conditions influence the productivity of an underground operation.

Generally, the productivity of an underground operation, be it by longwall mining or the bord and pillar system, is highly influenced by the presence of mine gases and the ease with which the coal seam can be drained. Gas outburst is influenced by the

ground stress and sorbed gases present in high quantities and at high pressures in coal seams and surrounding stratifications.

Most coalmine gas if undrained could contribute to the phenomenon of gas outburst with varied consequences, depending on the severity of the outburst. The present practice of mine gas drainage is playing a vital part in allowing the mines to operate safely and with increased production. Costing around $ 0.50 per tonne mined (Cram, 2002), the draining of coal seams has significant obvious economic benefits in addition to the safety benefit of reducing the onset of coal and gas outbursts. Coal outbursts constitute one of the important factors that can influence any mine production and productivity. From Figure 1.1 It can be seen that five mines with

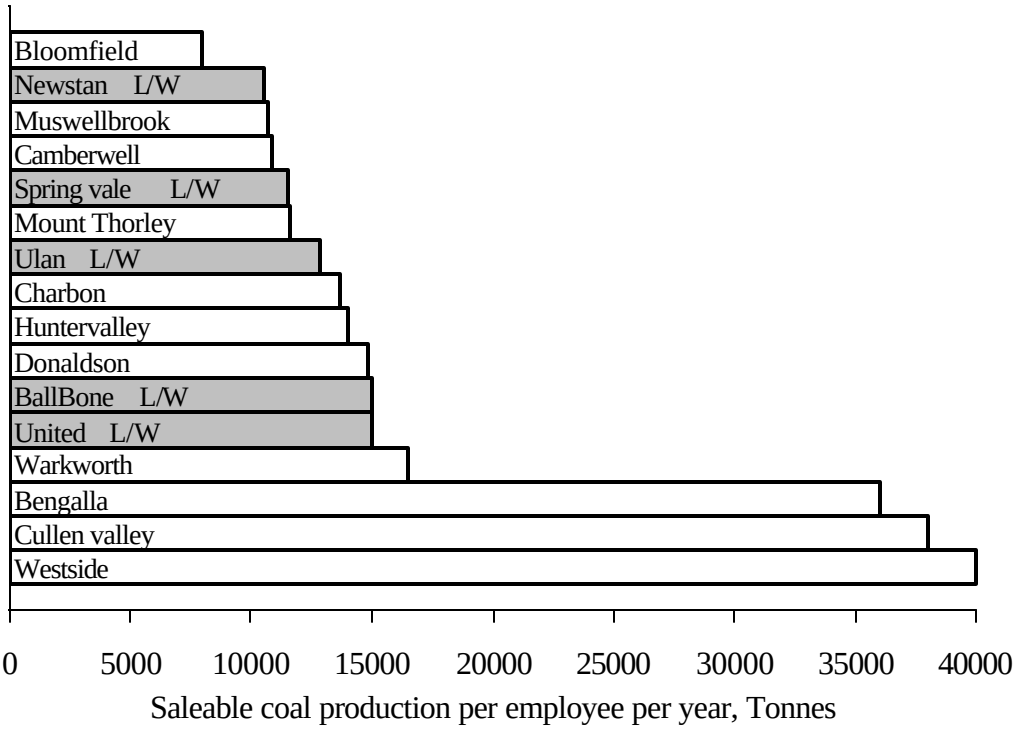

Figure 1.1 Productivity comparisons NSW of top longwall mine output with opencast mines for 2002-2003 (Cram, 2003)

longwall faces are achieving outputs in parity with the high output opencast mines (Cram, 2003). It has been shown that in coalmines with reduced risk of outburst, the productivity can match that of the opencast operations.

Clearly, for the mines to remain economically viable, it is essential that an effective gas drainage programme form an integral part of the mining operation. The success of such drainage operations is dependent on the drainage properties of the coal and the geological conditions. The permeability and porosity of the coal are important factors influencing the efficiency of a gas drainage programme, and accordingly, any mine contemplating introducing a drainage system must undertake close scrutiny of the coal deposit conditions.

Volume change of coal as measured in laboratory tests has been shown to have a direct correlation with the efficiency of gas drainage insitu. Accordingly, it is the main objective of this study to examine the extent of the coal shrinkage and its influence on coal permeability with respect to the type of the gas drained and the deposit pressure.

1.2 COAL AND GAS OUTBURST

Outburst can be defined as a sudden release of coal (coal and rock) accompanied by large quantities of gas into the working face or other mine workings (Harvey, 2001). Outburst represents a major coalmining hazard, which may lead to a dust or gas explosion, with subsequent destruction of mine structure, leading to the loss of equipment and possible injury or death to miners.

Gas outburst is influenced by the ground stress and by sorbed gases in high quantities and at high pressures. The following circumstances may contribute to the occurrence of outbursts (Hargraves, 1983):

- Presence of a sufficient quantity of gas in the coal seam (high gas content)
- Local fracturing and partial crushing of coal at faults, dyke intrusions in the seam, etc. (coal seam geology)
- Coal of low permeability to the passage of gas
- Coal strength (coal characteristics)
- Stress regime

Some factors are easily controllable while control of others, has been proven to be more difficult. Gas drainage has been proven to be successful in reducing the outburst hazard by reducing the in-situ gas pressure. Influencing the effectiveness of gas drainage is coal permeability.

Permeability is a property of any porous medium and can be simply explained as the measure of the ability of a medium (rock) to conduct fluids. The permeability of coal is influenced by the viscosity of the fluid contained in the coal (gas type in this case) and changes to the coal matrix. Coal matrix changes occur as a result of change in the stress regime, which in turn may be influenced by the release (drainage) of in-situ gas, i.e., all factors are inter-related (Gunther, 1968; Patching, 1965; Puri and Seidle, 1992).

1.3 STATEMENT OF THE PROBLEM

To conduct an effective gas drainage programme for any underground mining operation, the programme requires a better understanding of the permeability and porosity of coal as well as the geological conditions of the seam section drained. A clear understanding of the consequences of a gas drainage programme with respect to its influence on coal moisture content and volumetric changes in the coal, in what is known as coal shrinkage, is vitally important. Also important are the level and intensity of the geological anomalies and igneous intrusions in the coal seam. Such intrusions have been found to reduce and at times completely nullify the gas drainage effectiveness. With igneous intrusions such as thick dykes and shear planes the properties of the coal understandably will be influenced. Accordingly, a better approach would be to assess the drainage properties of the coal on either side of the intrusion through assessment of the influence of the gas type and gas pressures on the volumetric changes of the coal and to use the change to assess the drainage potential of the coal seam. This issue represents a clear challenge and constitutes the real statement of the problem.

Despite the increased number of mines with mature programmes of gas drainage, there remains the lack of a common database system of all Australian coal deposits which would list properties such as permeability, porosity and the like. Accordingly there is an urgent need to establish such a database for the future benefit of the industry. This thesis provides the basis for development of this database.

1.4 OBJECTIVES OF RESEARCH

a) To evaluate the influence of gas type and gas pressure on the permeability characteristics of various coal seams.

b) To establish parameters affecting the coal volumetric changes.

c) To establish a credible procedure to predict the drainability of coal in advance of mine development by examining the shrinkage characteristics of coal under different gas types and gas pressures. Also to assess the merits of the methodology as a standard for future assessment of other coal seams.

d) To determine the influence of geological intrusions on permeability and porosity based on the real analysis of coal samples in advance of mine development headings.

Thus the main significance of the research work will be the establishment of a reliable and easily repeatable technique for assessing the outburst proneness of coal ahead of the heading development, thus enabling a suitable approach to be put in place to allow for safe mining of the coal deposit.

1.5 RESEARCH PROGRAMME

The research programme undertaken consisted of eight distinct phases. Table 1.1 indicates the research timetable and the main research activities pursued.

Table 1.1 Research activities and timetable

TASK	2002		2003		2004		2005
	S_1	S_2	S_1	S_2	S_1	S_2	S_1
Literature survey of the coalbed gas and associated hazards.							
A survey of the latest tests on adsorption – desorption, permeability and volumetric changes of coal, their equipment and procedures.							
Familiarisation with the existing equipment and its modification for the proposed research.							
Collecting coal samples from different coalmines, their preparation, and then petrological studies on them.							
Testing volumetric changes and permeability of coal, data collecting and processing of the collected data.							
Modelling single-phase flow through coal samples.							
Thesis preparation and submission of final thesis.							

S_1= 1st Academic Session, S_2= 2nd Academic Session

1.6 THESIS OUTLINE

The thesis is presented in 8 chapters. A flowchart of the arrangement of this thesis is shown in Figure 1.2.

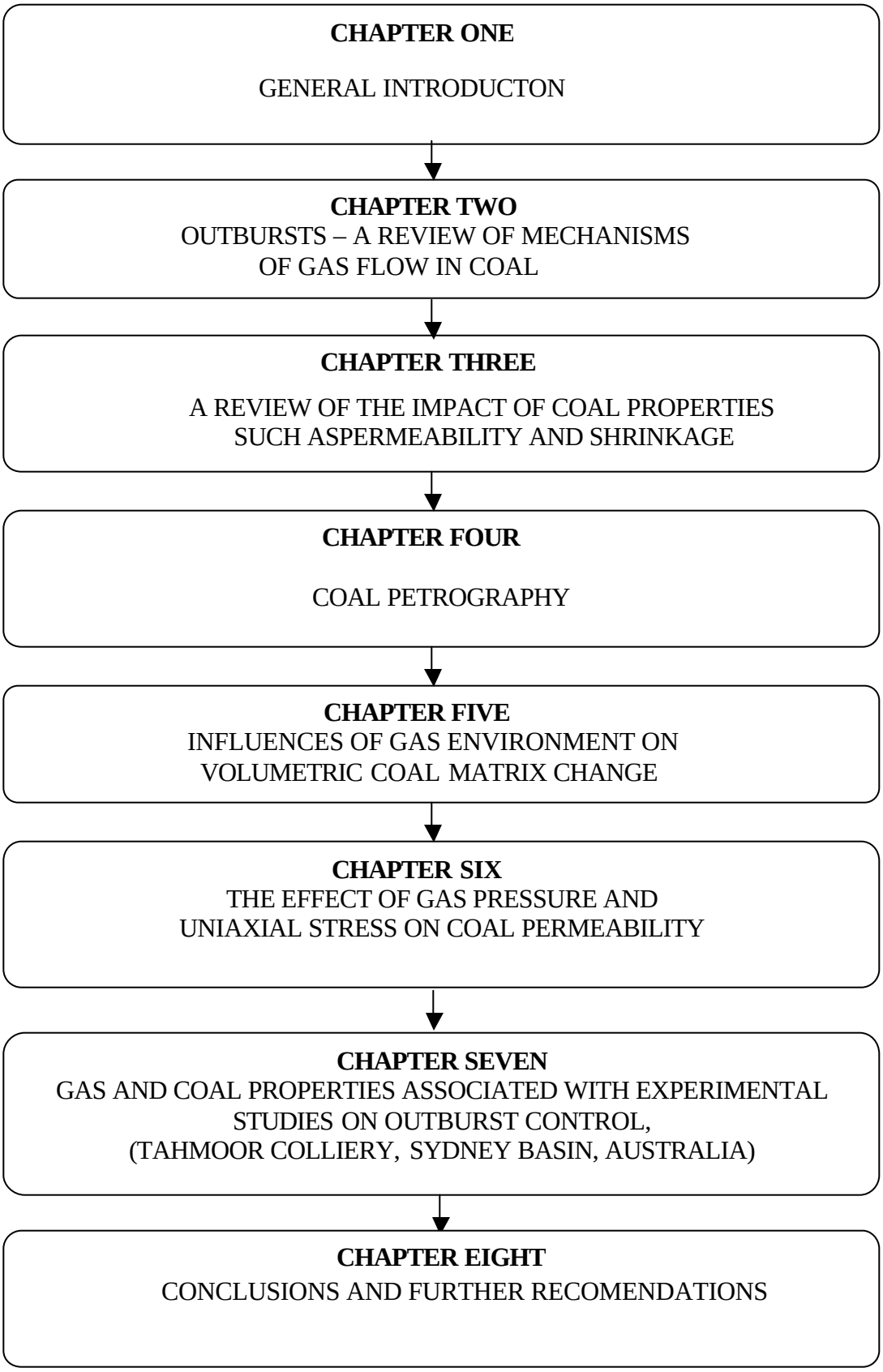

Figure 1.2 Structure of chapters in thesis.

- Chapter 1 presents the general purpose of the research aims and objectives of the thesis work.

- Chapter 2 includes the studies carried out on the instantaneous outburst mechanism and the factors that contribute to this mechanism, such as coal seam thickness, depth of burial, coal geology, coal structure, strength of coal, igneous intrusions, and the ground stress regime. These factors, together with gas migration in coal seams, form the subject of review and discussion in this chapter.

- Chapter 3 details a review of fundamental studies on shrinkage and permeability of coal.

- Chapter 4 contains theoretical aspects of coal petrography, including the tests performed and a discussion of the results.

- Chapter 5 describes extensive tests conducted to investigate swelling and shrinkage of the coal matrix by various gases at different pressures for measuring the shrinkage coefficients and comparing the determined coefficients with those of other researchers.

- In chapter 6 a brief description of the coal permeability tests is given together with their results. These tests were carried out to determine the permeability

behaviour of the coal matrix as a function of applied axial stress at different gas pressures for various gases (CH_4, CO_2, N_2 and a mixture of CH_4/CO_2). It also contains results of the modelling of single–phase (gas) flow phenomena through different coal cores.

- Chapter 7 describes tests carried out on coal samples from Tahmoor coal mine (Australia) as a case study and analysed them to show the interrelating data which could be obtained.

- Chapter 8 summarises the results and principal conclusions of the research work presented in the thesis and gives suggestions for further research.

CHAPTER TWO

OUTBURSTS – A REVIEW OF MECHANISMS OF GAS FLOW IN COAL

2.1 INTRODUCTION

The influence of coal gas on the occurrence of outbursts in underground coalmines requires a good understanding of the mechanism of gas flow and the gas sorption characteristics of coal. This is important in addressing the challenges presented to the mine operators and planners in extracting coal safely and efficiently.

The production of gas from the coal seams is a by-product of the coalification process, in which vegetable matter like wood and peat is converted to coal. The amount of gases remaining in a coal deposit during mining is dependent on seam thickness, depth of burial, coal geology, coal structure, strength of coal, igneous intrusions and the ground stress regime. These factors, together with gas migration in coal seams, form the subject of review and discussion in this chapter.

2.2 COALIFICATION PROCESS

Gases associated with coal and coal measure rocks are a by-product of the coalification process (Stach et al., 1975), which is defined as the process of increasing

the carbon content of the buried organic material such as peat and wood, and can be distinguished as a biochemical stage (diagenesis).

During the first stages of the coalification process, methane is produced from the degradation of plant and animal material by aerobic and anaerobic bacteria. Reduced acidic conditions and temperatures are required. Unless the peat is deeply buried at this stage, the methane and other gases generated are emitted to the atmosphere or trapped in the overlying sediments. As the depth of burial of the peat increases, rising temperature and pressure allow the geochemical stage of coalification to occur, and low-grade coal slowly metamorphoses into bituminous coal. At this stage, coal gases such as methane, carbon dioxide, nitrogen and water are released due to natural physical and chemical reactions.

2.2.1 Stages of the coalification process

Figure 2. 1 shows the stages of the coalification process. The process is divided into three stages known as humification, diagenesis and metamorphism (Van Krevelen, 1981). A number of theories have been proposed, and one theory suggests that "time" is the major factor in the coalification process. This theory has become unpopular because it has been recognized that there is no orderly increase in the metamorphic rank of coal with increasing age. Van Krevelen (1981) based on observations from the Moscow Coal Basin asserted that time has no major influence on the coalification process. In the second theory pressure is regarded as the major factor in coal metamorphosis.

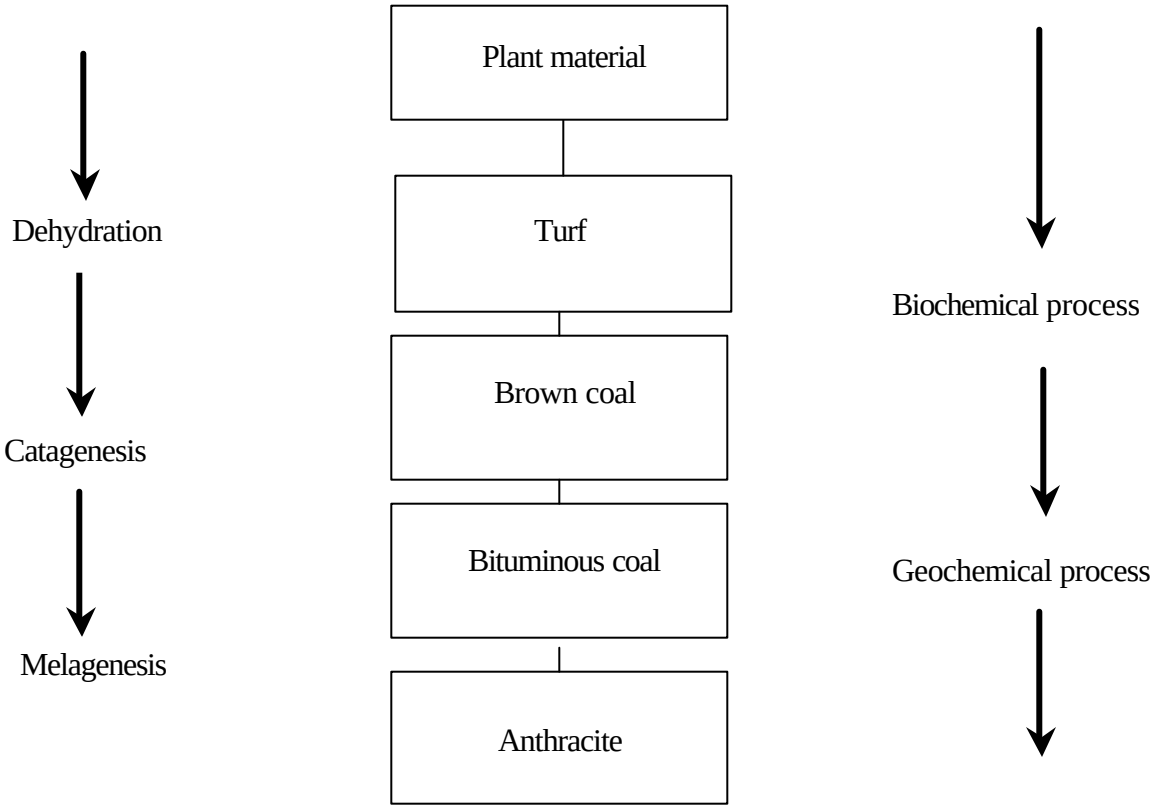

Figure 2.1 Coalification process (after Lama and Bodziony, 1996)

The theory is refuted by numerous geological examples, such as the fact that suppressing excessive methane formation (one of the coalification reactions) results in slower reaction (coalification) at higher pressures or where the metamorphic rank does not increase in highly deformed and folded strata (Speight, 1983). An increase in pressure can actually retard the chemical alteration of peat to coal but produces some physical changes in its texture (porosity, compactness). A third theory suggests that the maximum temperature to which the coal has been subjected over geological time is the important factor in coal metamorphosis. Geological examples (igneous intrusions into coal seams) demonstrate that elevated temperature could cause

coalification, which can easily be confirmed by laboratory experiments (Mackay, 1983).

2.2.2 Gases in Coal

Lohe (1990) states that water, carbon dioxide and methane are generated during the progressive metamorphism of coal, that water and carbon dioxide are produced chemically during metamorphism of lower ranks of coal, but that methane is the predominant fluid generated in bituminous and anthracitic coal formation. Carbon dioxide, methane and water are produced during increasing coal ranking as illustrated by Hargraves (1966) in Figure 2. 2.

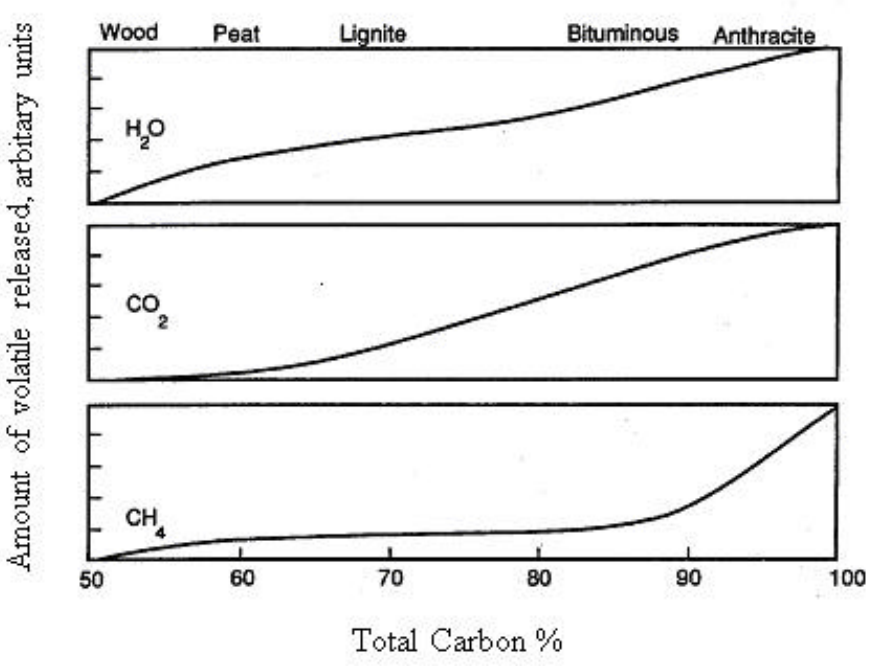

Figure 2.2 General release profiles for methane, carbon dioxide and water as coalification proceeds (after Hargraves,1966).

The quantity of gas formed during the coalification process has been the subject of study for decades. Figure 2.3 shows the quantities of gas generated from different ranks of coal during the coalification process.

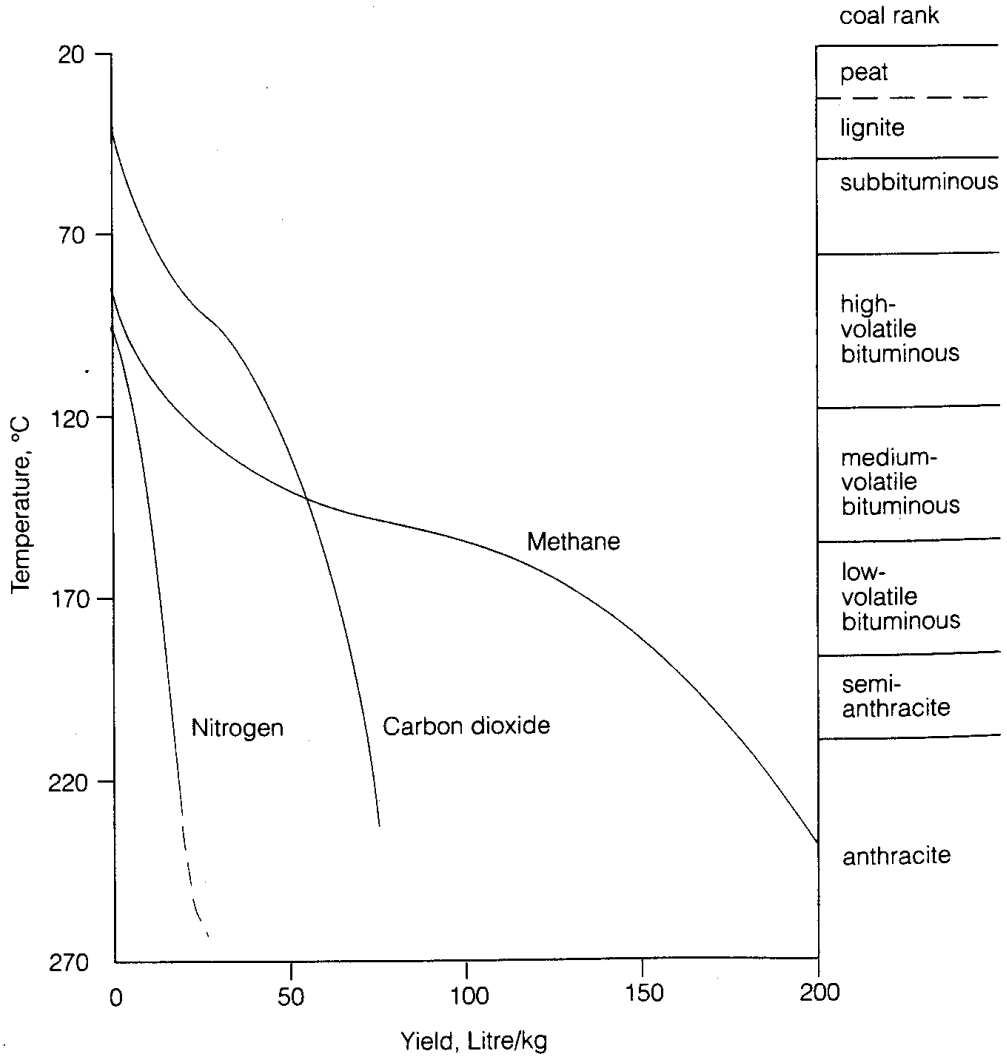

Figure 2.3 Different gas quantities generated during coalification (after Levine and Deul (1989)

According to Patching (1970) nearly 1300 m^3 /t of gas can be generated from the formation of coal. Thakur and Dahl (1982) claimed that for each ton of coal formed, about 765m^3 methane and 565m^3 carbon dioxide are generated. Eddy, Rightmire and

Byrer (1982), Temmel (1990) reported that the amount of methane liberated during coalification ranges from 200 m^3/t to as high as 765 m^3/t.

The composition of coal seam gases varies worldwide, with methane being the dominant gas content, however, the proportion can vary from one locality to another in the same seam or between different seams. Creedy (1991) reported that the seam gas content includes 80-90% methane as the dominant gas and between 0.2 and 6% CO_2. Mostade (1999) estimated for the southern coal basin of Belgium that the average gas composition is 97.5% CH_4, and 0.9% CO_2. Rice (1993) reported that US coal was predominantly CH_4 with CO_2 in the Piceance Basin ranging between 0% and 25.5%.

Lama (1991) estimated that Australian coals contain less than 1.5% of the total gas generated during the formation of the coal, and Hargraves (1990) estimated the gas content of the Bulli coal at a depth of around 500m as 15 m^3/t. The major gas in Australian coal beds is normally methane (Gould, Hargraves and Smith 1987; Bustin and Clarkson, 1998) but in some mines such as Tahmoor and Metropolitan Colliers, carbon dioxide forms the dominant gas in some sections of the mine (Williams, 1991). Bishop and Battino (1989) described the composition of Australian coal seam gas as consisting of more than 90% methane, but with smaller quantities of carbon dioxide, nitrogen, and other gases.

However, Lama and Bodziony (1996) reported on coal and gas outburst histories in Australia and worldwide. Their comprehensive reporting on outbursts in the Australian scene, mainly from the two major coal producing basins, namely the southern coalfields of Sydney Basin in NSW and the Bowen Basin of Queensland,

has demonstrated the variations in the nature of the outburst occurrence and the types of gases associated with various blasts. For example the outburst at Collinsville Colliery was CO_2 (> 90%) based whereas the outburst at Leichhardt Colliery was mainly a methane-based explosion. Others studies on the Australian outbursts scene include Hargraves (1963 b, 1983), More and Hanes (1980), Smith and Gould (1980), Hanes, Lama and Shepherd (1983), Clark, Battino and Lunarzewski (1983), Williams (1991), Lama (1995b) and Faiz and Hutton (1995).

Faiz and Hutton (1995) reported that geological structures were the cause of the CO_2/CH_4 variations in the Illawarra coal measures. The highest concentration of carbon dioxide is localized laterally along major faults as a local pocket, and near anticlines and domes (structural highs) areas of pure CO_2 gas can occur. Garner (1999) reported that some places in the southern and eastern margins of the Illawarra coal measure have been subjected to magmatic (igneous intrusions) activity such as dykes and sills resulting in a high percentage of carbon dioxide.

2.2.3 Effect of igneous intrusions

Experience has shown that CO_2 gas occurs in an increased amount in the vicinity of dykes and other magmatic intrusions. This is due to the fact that these intrusions sometimes act as a barrier and prevent carbon dioxide gas from migrating until they are fractured, releasing trapped gases.

The increased percentages of CO_2 associated with igneous intrusions is attributed to the physico-chemical aspect of the process, in which coal in the vicinity of igneous

intrusions is burned and its carbon and hydrogen content are oxidized as (Speight, 1983):

$$C(s) + O_2(g) \rightarrow CO_2(g) \quad (2\text{-}1)$$

$$2H_2(g) + O_2(g) \rightarrow 2H_2O(g) \quad (2\text{-}2)$$

Sometimes the procedure may occur in two stages, for which its equations are:

$$2C(s) + O_2(g) \rightarrow 2CO(g) \quad (2\text{-}3)$$

and then:

$$2CO(g) + O_2(g) \rightarrow 2CO_2(g) \quad (2\text{-}4)$$

The letter (g) indicates the gaseous state and the letter (s) the solid state. Another possibility for increasing the amount of carbon dioxide may result from the following equation:

$$CH_4 + 2O_2 \rightarrow CO_2 + 2H_2O \quad (2\text{-}5)$$

It can be seen that CO_2 is formed as a result of a reaction between CH_4 and a sufficient amount of oxygen. This is a clear explanation for the increased CO_2/CH_4 ratio, and shows that, by burning, the seam gas methane in the vicinity of magmatic intrusions is converted to carbon dioxide. It should be mentioned that the entrapment of coal gas by solid and non-permeable surrounding strata must occur so that the existing gas cannot escape.

2.3 PHYSICAL STRUCTURE OF COAL

The gas in coal is stored in a fundamentally different way than in conventional sandstone or carbonate (sedimentary rock) natural gas reservoirs. In conventional reservoirs, the primary storage is in the form of compressed gas in void spaces within the rock matrix (Creel and Rollins, 1993). At lower pressures, coal can store more gas per unit volume than conventional reservoirs. The reason for this enhanced storage capacity is attributed to the large pore surface area of coal. Coal is considered to be a dual porosity rock (Gamson, Beamish and Johnson 1996; Harpalani and Chen, 1997; Harpalani and Ouyang, 1999; Cui, Bustin and Dipple, 2004a-b).

The matrix structure of coal is characterized by both micropores <2nm and macropores >50 nm in size, and based on the Maidebor (1973) classification for porous and non- porous fractured reservoirs, coal reservoirs are classified as a porous fractured reservoir. Between the two systems of micro and macropores, there appeared to be no clear transitory pore system (Van Krevelin, 1981). Later Littke and Leythaeuser (1993) showed that there were three distinct pore systems of micropores (<50 Å), mesopores (50 to 500 Å) and macropores (500 Å to about 50 mm). The macropore system consisted of a naturally occurring network of fractures called the cleat system. Doscher, Kuuskraa and Hammershaib (1980) stated that "coal is not a porous medium", and this was soon challenged by other researchers (Gray, 1995), who showed that coal can be a porous medium because its structure is occupied partly by a solid (matrix) and partly by a void space, with the latter being occupied by one or more gases. Figure 2.4 a-b shows electron micrographs of a coal matrix.

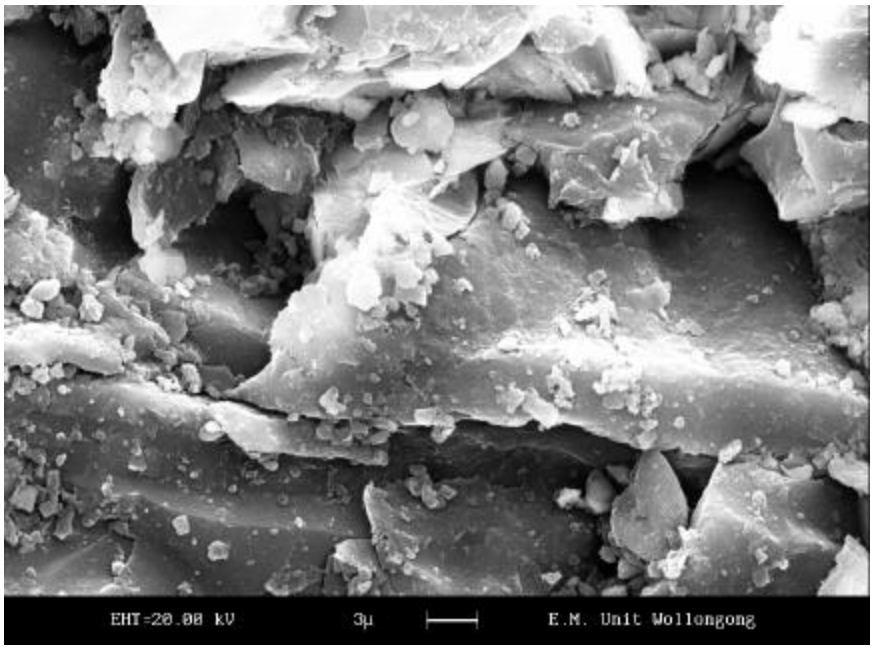

(a)

(b)

Figure 2.4 Electron micrographs of a coal matrix.

During the burial of decayed plant material, a large amount of gases is lost, and the amount of gas retained per ton is known as the seam gas content. The storage of the remaining gases in the coal structure occurs in two different forms, in one by sorption into pores and microfractures which account for most of the surface area of coals (Mahajan and Walker, 1978; Kim and Kissell, 1986; Ettinger and Serpinsky, 1991 and Yee, Seidle and Hanson, 1993), while the rest occurs as free gas. Saghafi (2001) and Gray (1987) showed that sorbed gas constitutes about 85-90% of the total gas content of the coal, and its amount increases with the free gas pressure. Rightmire (1984) introduced a third option in which gas can be stored in a dissolved form in groundwater within the coal seam (Figure 2.5).

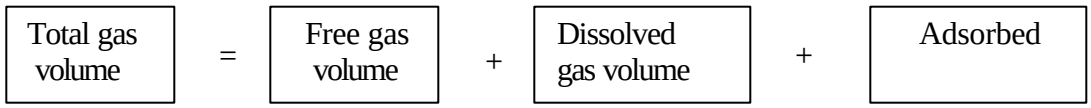

Figure 2.5 Gas storage mechanism.

However, Murry (1991) went further and suggested that gases could be retained in a coal bed in four different ways:

- Adsorbed molecules within micropores (<2 nm in diameter)
- Trapped gas within matrix porosity
- Free gas
- As dissolved gas in ground water within a coal fracture

Figure 2.6 shows how the gas is stored in coal as free gas or adsorbed gas in the form of a monomolecular layer on the internal surface of the coal .

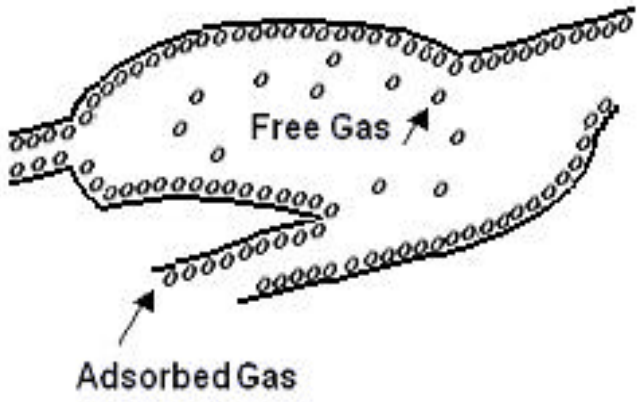

Figure 2.6 Gas storage in coal (after Harpalani and Schraufngel, 1990).

2.4 GAS SORPTION IN COAL

Gas adsorption and desorption or simply gas sorption is a physical process of gas movement in and out of coal under given environmental pressures. Adsorption describes a more or less uniform penetration of gases into the molecular structure of coal. Molecules and atoms can attach themselves onto surfaces in two ways, physisorption and chemisorption.

In physisorption (physical adsorption), there is a weak Van der Waals attraction of the adsorbate (the gas attached on the pore surface) to the surface, and the attraction to the surface is weak. During the process of physisorption, the chemical identity of

the adsorbate remains intact. Adsorption has a surface effect whereby gases are physically held on the surface of coal. Desorption refers to the movement of gas out of coal. Chemisorption is an irreversible process where gases are held on the surface of the coal by chemical forces.

Moffat and Weale (1955) and Zwietring and Van Krevelen (1954) worked on these different kinds of sorption and described the process of gas sorption on coal as easily reversible. This easy progress towards equilibrium between sorption and desorption thus implies that the gas on the surface of coal is adsorbed physically and that this phenomenon is not chemisorption.

The bigger its internal surface area, the more molecules that can be trapped on the coal surface. Generally this means that a good adsorbent (the solid that takes gas up) will be very porous and full of many tiny holes on its surface that effectively increase its surface area by many times. Sorption depends on various factors such as the moisture, temperature and mineral content of the coal, as well as the porosity of the coal, especially with respect to the micropore structure, because these pore spaces can account for up to 85% of the total porosity (Mahajan, 1982). The coal gas is held in place by the hydrostatic pressure of the pore fluids in the surrounding strata. As pressure increases with depth, deeper coal seams generally contain more gas. Faiz and Cook (1991), by studying various coal samples from New South Wales, found that depth of cover is the most important factor controlling the gas retention capacity of coal, while mineral content is the secondary factor. As can be seen from Figure 2.7 there is a relationship between the depth and the volume of adsorbed gas, and by increasing the depth the capacity for gas sorption will increase.

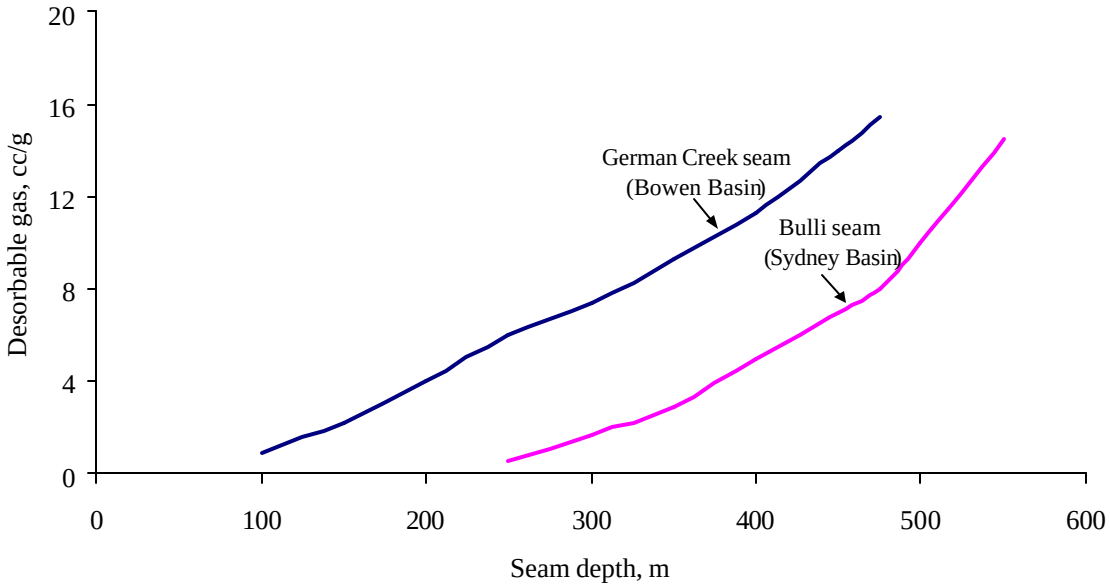

Figure 2.7 Effect of increase in depth on desorbable gas content of coal seams (after Lama, 1991)

On the other hand, by increasing the mineral content the sorption capacity will decrease. As stated previously, almost 95 % of stored gas in coal is in an adsorbed state as a monomolecular layer on the surfaces of fissures, cracks and cleavages, and only a small percentage (<5%) is in the free State. Jolley, Morris and Hinsley (1968) estimated that the surface area of one kilogram of coal could be between 20,000 m^2 and 200,000 m^2, and later Saghafi (2001) estimated that the pore surface area varies between 50,000 m^2 and 300,000 m^2, which corresponds to 25 m^3/t of gas held in coal (Creedy, 1991). The amount of free gas present is related to the porosity of the rock and depends upon the gas absolute pressure and temperature. The free gas content in coal can be calculated using the following relationship (Boxho et al., 1980; Vutukuri and Lama, 1986; Rabia, 1988):

$$C_v = \Phi \frac{P}{P_o} \times \frac{273}{T} \qquad (2\text{-}6)$$

where;

C_v = Free gas, m^3/t

Φ = Rock porosity, m^3/t

P = Absolute gas pressure, kPa

P_o = Barometric pressure, kPa

T = Absolute strata temperature in degrees, K

Patching (1970) assumed the porosity of coal is in the order of 3% to 10%, and McPherson (1993) estimated between 1% and 20%, and therefore, even at comparatively high pressures, the amount of free gas present in coal is small. In contrast, Bustin and Clarkson (1999) suggested that free gas in matrix porosity must be considered in all coal-bed methane explorations, especially in low rank coals, because there are free gases trapped in the matrix porosity, such as free gases in coal fractures, and the amount of them cannot be measured by conventional tests. From Figure 2.8 it can be seen by mercury porosimetry for different coals that the cumulative porosity and mean pore size varies for different ranks and that lower rank coals have a higher pore diameter for the same porosity.

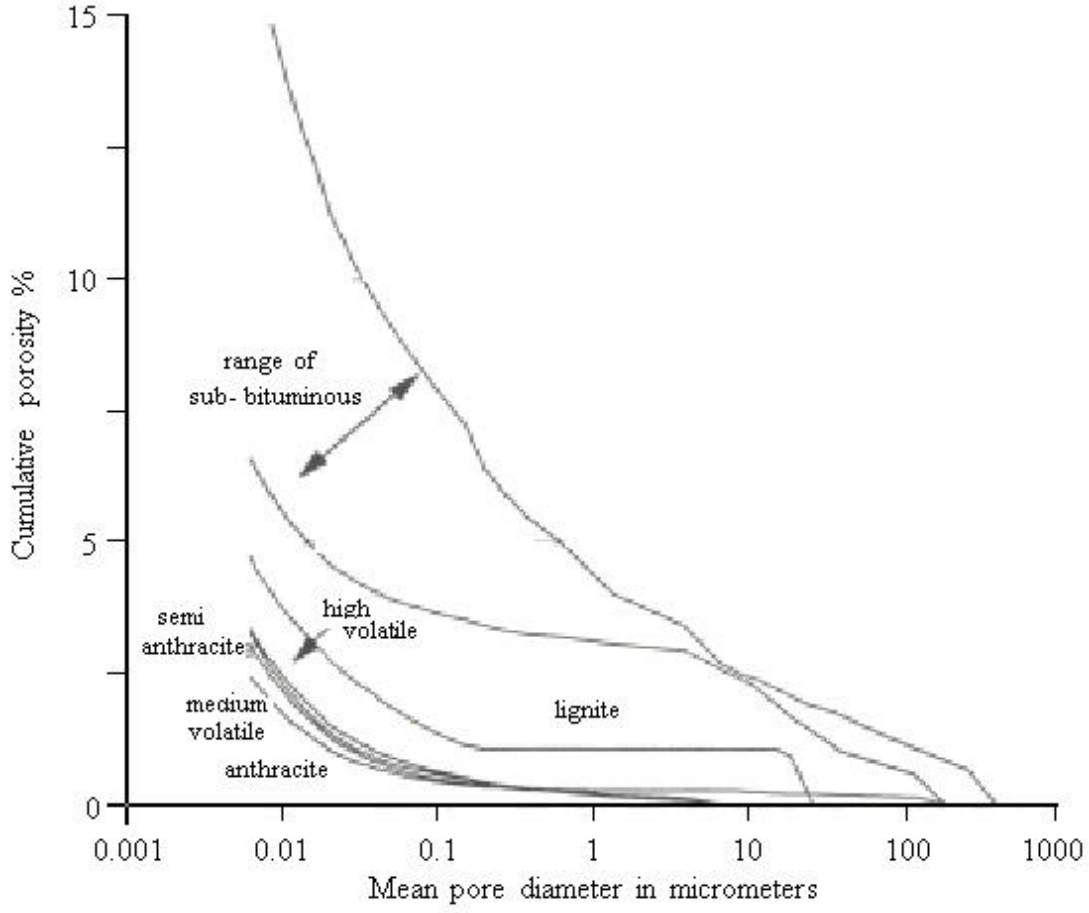

Figure 2.8 Cumulative porosity for different coals. (after Bustin and Clarkson, 1999)

Changes in pressure, temperature and mining conditions can cause part of the free gas to adsorb. Conversely, some of the adsorbed gas may be released to become free gas (Peng and Chiang, 1984).

Adsorbed methane gas in coal at pressures normally encountered in coalmines is adequately described by Langmuir's isotherm (Ruppel, Grein and Bienstock, 1974; Gregg and Sing, 1982; Yee, Seidle and Hanson, 1993; Beamish and Gamson, 1993). The relation between the quantities of gas that can be contained in coal at given temperatures and at different pressures can be plotted as sorption isotherms. Ogle

(1984) and Bartosiewicz and Hargraves (1984) derived the isotherms for CH_4 and CO_2 gases at the same temperature (Figure 2.9) and found that coal has a substantially greater capacity for CO_2 than for methane, implying that coal generally adsorbs carbon dioxide much more readily and strongly than methane.

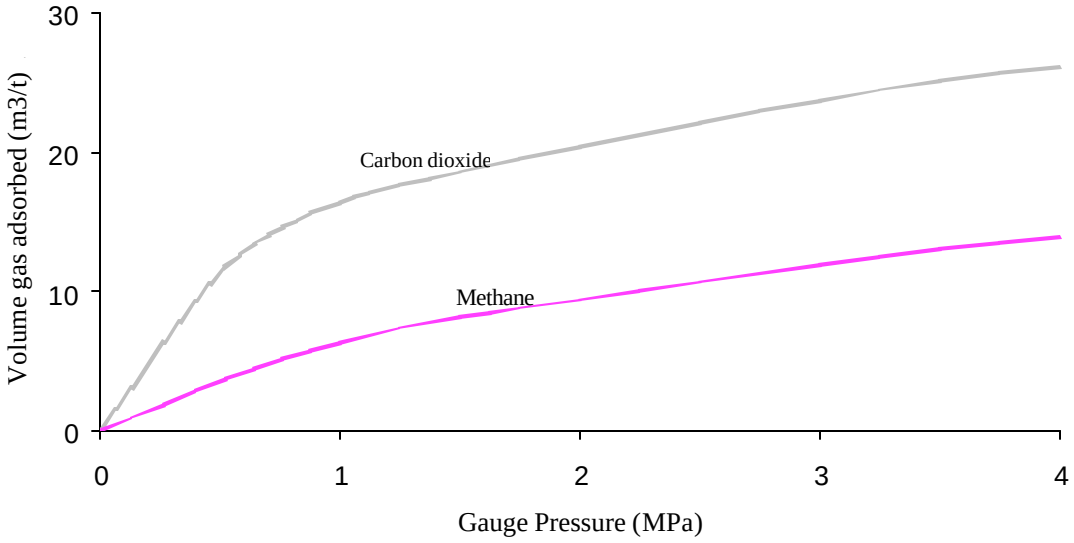

Figure 2.9 Volume of different gases adsorbed by coal under various pressures.

Langmuir (1918) derived an equation for the idealized monolayer adsorption of methane on coal matrix, which is now known as the Langmuir equation:

$$Q = \frac{abp}{1 + bp} \qquad (2\text{-}7)$$

where

Q = Quantity of methane gas adsorbed at a given pressure p, m^3/t

P = Pressure of adsorbate gas, kPa

a = Langmuir's constant representing methane gas absorbed as pressure $\rightarrow \infty$, m^3/t

b = Langmuir's constant with dimensions of $(\frac{1}{p})$

Constants a and b are more dependent upon a number of factors such as:

- Nature of gas
- Temperature
- Moisture
- Effects of Oxidization
- Rank of coal
- Coal constituents

Langmuir's model of adsorption gives a simple picture of adsorption, the one most favored for use at pressures encountered in coal seams. This model assumes only monolayer adsorption, and the possibility of the initial overlayer of adsorbate acting like an absorbent surface is not considered. The occurrence of additional adsorption beyond monolayer coverage has been treated by Brunauer, Emmett and Teller (1938), and their treatment results in what are known as BET isotherms. BET isotherms are useful in cases where multilayer adsorption is considered. The BET model was based on the Langmuir (single layer of molecules) model. The theory assumed that the gas molecules could be adsorbed in multimolecular layers. Once a state of equilibrium was reached, the number of molecules arriving at a particular layer from the gas phase, in unit time, will be equal to the number leaving that layer by evaporation. The general relationship for the multimolecular layer isotherms is given as follows (Ellis, 1953):

$$\frac{P}{S(P_\circ - P)} = \frac{1}{S_\circ C} + \frac{(C-1)P}{S_\circ C P_\circ} \qquad (2\text{-}8)$$

where:

$P_\circ$ = Saturation vapour pressure of the gas, Pa

$S_\circ$ = Monolayer capacity, kg

S = Weight of the adsorbate at pressure P, kg

C = Constant (The exponent of $-(E_1-E_e)/RT$ where E_1 is the latent heat of adsorption (J mol^{-1}) of the first layer and E_e is the latent heat of condensation of the gas (J mol^{-1}))

R = Universal gas constant = 8.3144 J mol^{-1} K^{-1}

T = Temperature, K

This equation it suitable for high vapour pressures, in which multilayer adsorption may occurs after the micropores are filled (Gregg and Sing, 1967).

2.5 TRANSPORT OF GAS IN COAL

Methane will flow out of pores of coal if there is a pressure gradient acting as a driving force. When the pressure in the coal seam is reduced through mining, methane begins to desorb and migrate through the coal matrix and through natural fractures known as cleats. As shown in Figure 2.10 the migration of methane through the coal matrix can occur through diffusion, whereas its movement through cleats is by laminar flow (Cervik, 1969 and Giron, Pavone and Schwere, 1984) governed by Darcy's law, and termed Darcy flow.

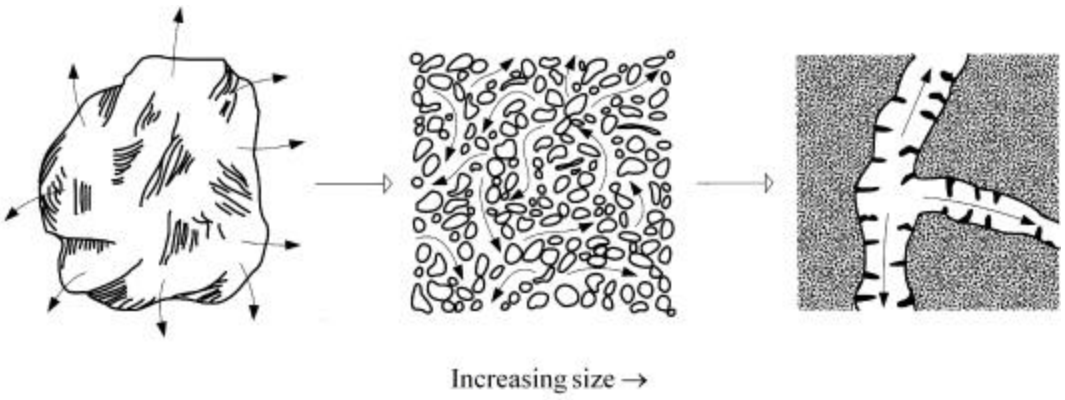

Figure 2.10 Transport of gas in coal. (after Harpalani and Schraufnagel,1990)

Generally, there are at least two sets of nearly perpendicular fractures that intersect to form an interconnected network throughout a coal-bed (McCulloch, Duel and Jeran, 1974). These two fracture systems are known as face and butt cleats. Scott (1994) showed the general structure of coal in relation to face and butt cleat spacing (Figure 2.11). The shorter butt cleat terminates at a face cleat, which is the prominent type of cleat (Figure 2.12).

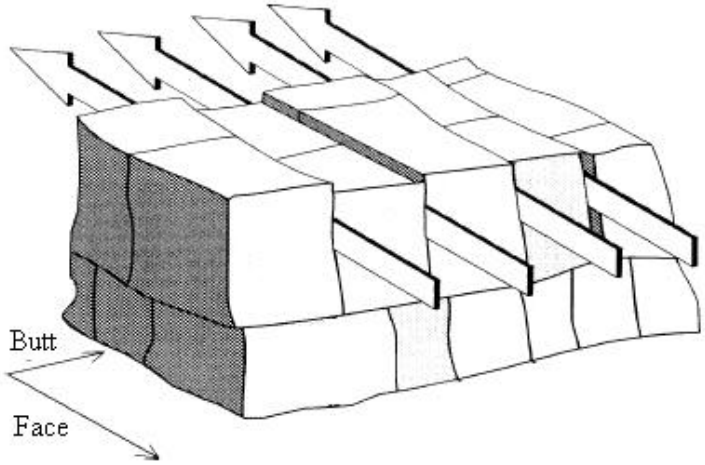

Figure 2.11 Face and butt cleats in the coal structure (after Scott,1994)

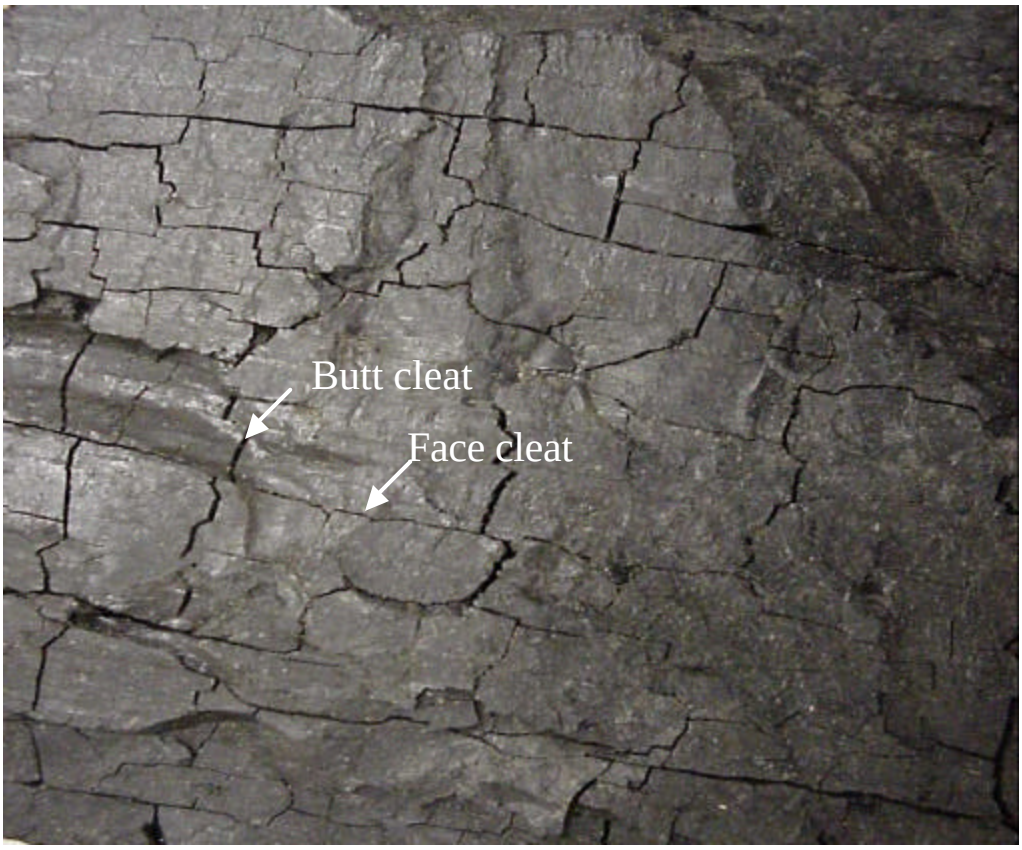

Figure 2.12 Face and butt cleats

The angle between the between the face and butt cleats is around 90° (McCulloch, Duel and Jeran, 1974; Cui, Bustin and Dipple, 2004a). McElhiney, Paul and Young (1993) noted that the spacing between cleats varies according to factors such as the coal maturity, the mineral matter and the carbon content, but normally is of the order of 25 mm and more in dimension.

Research carried out by Massarotto, Rudolph and Golding (2000) on some Australian coal samples determined the approximate width of the aperture and the length of the face and butt cleat spacing (Table 2.1).

Table 2.1 Length of cleat spacing and aperture in coal. (after Massarotto, Rudolph and Golding, 2000)

Cleat	Spacing
Face cleat spacing	10-25 mm
Butt cleat spacing	10-22 mm
Aperture	0.1-2 mm

According to Close (1993) and Ryan (1995) coals with bright lithotype layers, with a high percentage of vitrinite macerals, have a greater amount of cleats than dull coals.

The mechanism of coal cleating has been long discussed by many researchers, and a common understanding is that cleats are formed due to the effects of the intrinsic tensile force, fluid pressure, and tectonic stress (Laubach et al., 1998; Su et al., 2001). The intrinsic tensile force arises from matrix shrinkage of coal, and the fluid pressure arises from hydrocarbons within the coal. These two factors are considered to be intrinsic reasons for cleat formation.

On the other hand, the tectonic stress is regarded as extrinsic to cleat formation and is the major factor that controls the geometric pattern of cleats. Face cleats extend in the direction of maximum in situ stress, and butt cleats extend in the direction of minimum in situ stress. This is why regular cleats are formed in face and butt pairs.

Microscopic observations by Gamson and Beamish (1992) indicated three sets of cleats present in coal: face, butt and the curviplanar cleat direction, which intersects both face and butt cleats as shown in Figure2.13.

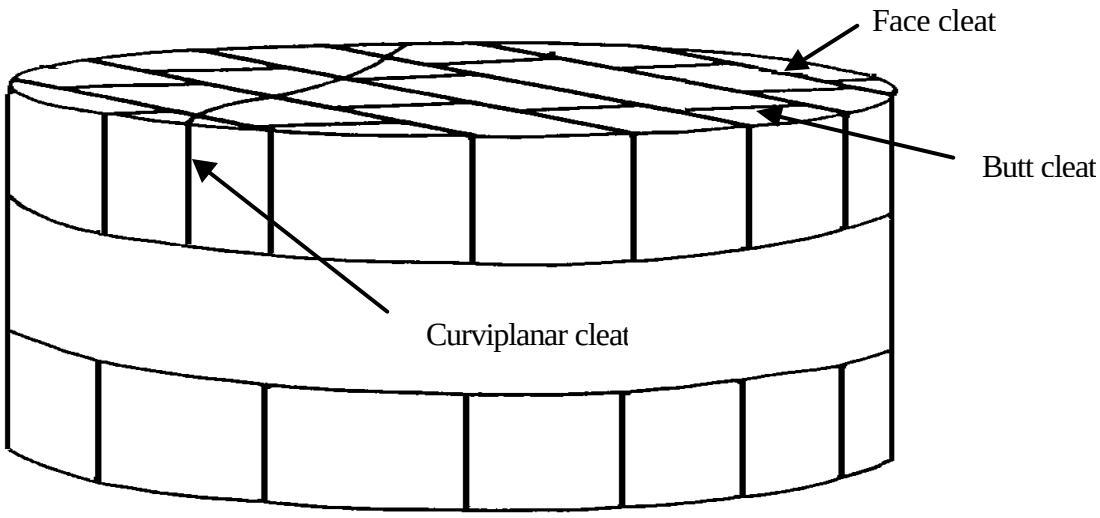

Figure 2.13 Idealized representation of microstructures in coal.
(modified from Gamson and Beamish, 1992)

Reiss (1980) presented three different network geometric models for simulating the fractured reservoirs network. As shown in Figure 2.14 a-d, these fracture network models consist of a "sheets model", a "matchsticks" model and a "cubes" model. In the sheets model (Figure 2.14a) only one set of fractures is considered. The matchsticks model (Figure 2.14b) shows two sets of fracture planes, which are perpendicular to each other. Three different orthogonal fracture planes lead to the formation of the cubic model, which consists of several cubes put together. According to the width of fractures, the cubic model is further subdivided into two different models. In one of these, the width of the horizontal set is very thin, while in the other all fractures have the same width (Figure 2.14 c-d).

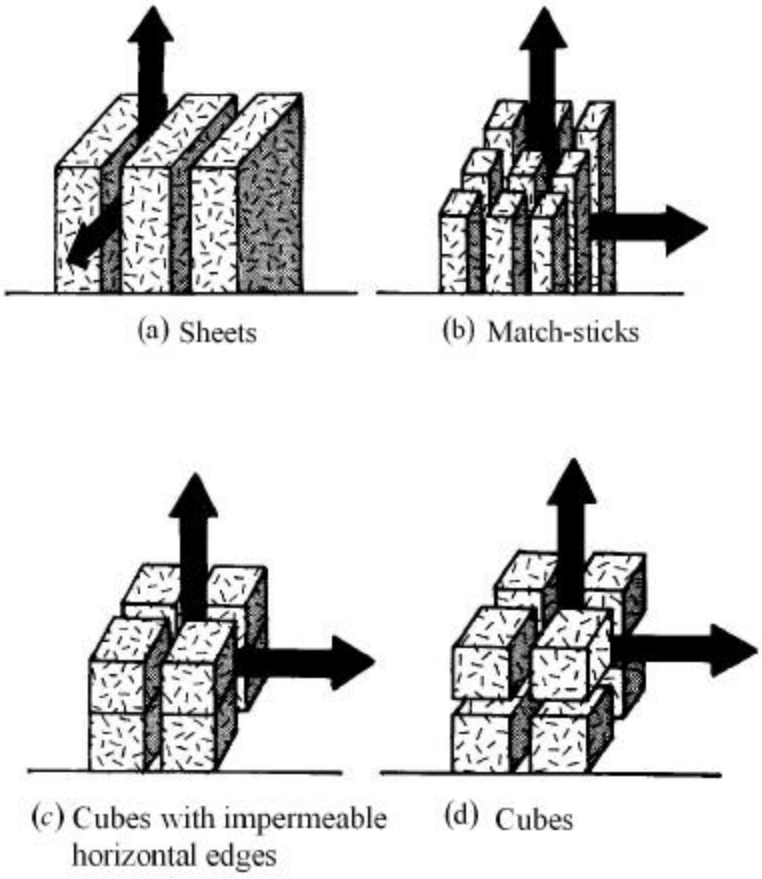

Figure 2.14 Typical fracture networks including the possible directions of flow. (after Reiss, 1980)

Harpalani and Chen (1997) used the matchsticks model to represent the coal-bed reservoir. However, this model ignored the existence of the three sets of fracture systems as they considered the third fracture system as bedding planes being closed because of the overburden weight and thus lacking any role in conducting coal gases.

The most recent model reported by Li, Ogawa and Shimada (2003) considered gas flow behaviour in sheared coals. As can be seen from Figure 2.15, three different gas flow categories through the coal matrix were classified. These categories were based on the form of the coal, i.e. normal, brittle and ductile deformed coal.

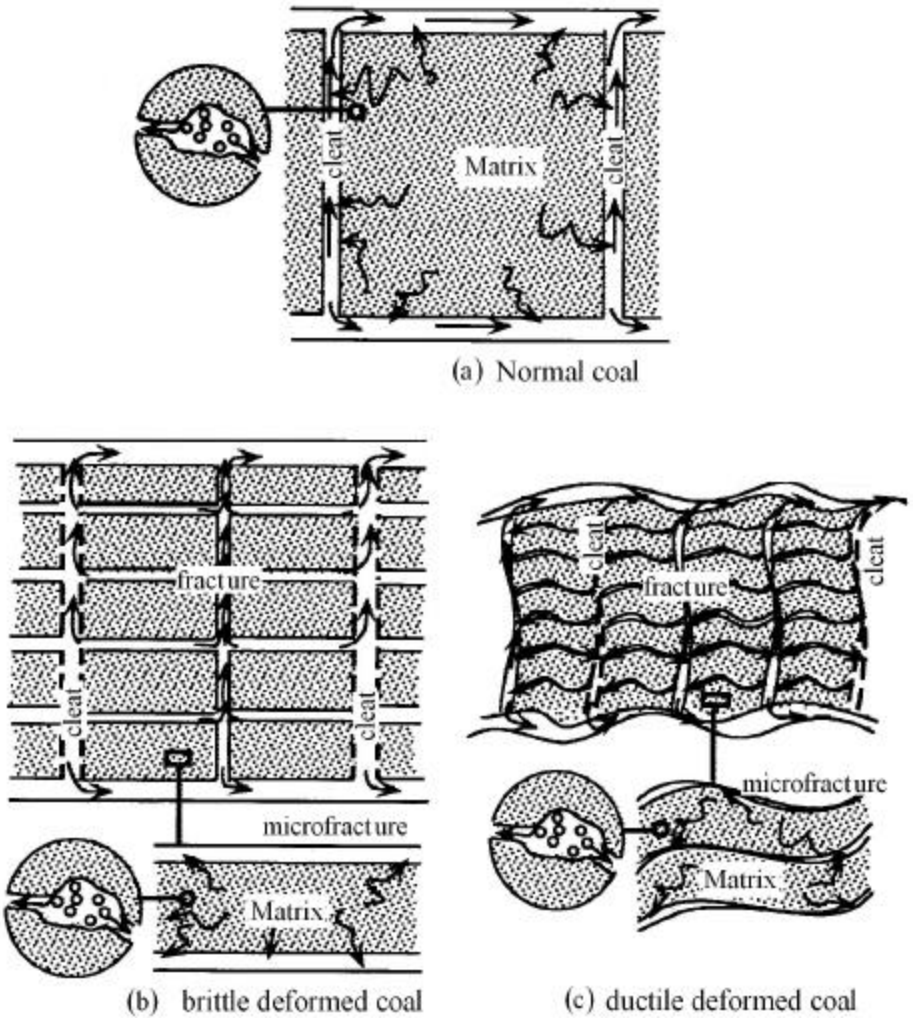

Figure 2.15 The most recent model of gas flow through coal.
(after Li, Ogawa and Shimada, 2003)

In normal coal, as previously described, gas desorbs from the internal coal surfaces to diffuse through the coal matrix and micropores to cleats and then enters the laminar flow regime. Cataclastic coals, which result from the formation of sheared coals through a brittle deformation mechanism, have interconnected pores and continuous cleats. They are divided into blocks of sizes intermediate between the cleat and microfractures size. It is clear that in as much as the dimensions of these blocks are

smaller, the mean diffusion distances are shorter, implying that the gas quickly reaches fractures and cleats for laminar flow. From Figure 2.14 it can be concluded that there are three different stages in the transport of gases through sheared coals. The first stage involves diffusion from and through the micropores to microfractures. Secondly, the flow of gas proceeds through microfractures to cleats or fractures, and the last stage is gas movement through cleats and fractures to the open surface. Ductile deformed coals are called mylonitic coal and are located in special structural positions such as thrust ramps and small-scale vergent folds. In this kind of coal all fractures are tightly compressed, which means less ability to conduct the gas as well as a vast specific surface area, which is the specification of a good gas reservoir. This type of coal always exhibits low connectivity and results in the appearance of high-pressure gas pockets, which represent one of the most well defined outburst prone places in coalmines.

In this research, because the coal samples are chosen from normally formed coal and come from deep coalmines, it is therefore assumed that the matchsticks model for the flow of gas through the coal matrix is appropriate.

2.6 STRENGTH OF COAL

Change in coal strength due to gas sorption has been a subject of interest for several decades. The interest in the effect of sorbed gas type and pressure on the strength of coal is in relation to better understanding of the outburst proneness of the coal. Studies by Czaplinski and Holda (1982, 1985), Gustkiewcz (1985), Tankard (1958), Jackson (1984), Hiramatsu, Saito and Oda (1983), and Holda (1986), showed that

there was a clear relationship ship between gas pressure and coal strength. Increased gas pressures caused a reduction in coal strength. However, Ates and Barron (1987) challenged this finding, and based on their experimental study and on the work of Tankard (1958), they did not find a significant reduction in the coal strength they tested. More recently, Aziz and Ming-Li (1999) studied the influence of gas type and pressure on the strength of coal. Based on their analysis of the rate of drilling and particle size analysis of drill flushings from pressurized coal samples and in different gaseous environments, they concluded that there was a clear influence of gas type and gas pressures on coal strength. Wang and Yang (1987) proposed the following relationship, based on their observations on Chinese coals, and dealt with an important index that combined gas emission rate and coal strength for outburst assessment:

$$K = \Delta_{P10-60} / f \qquad (2\text{-}9)$$

where,

K = Gas emission index / outburst tendency index; kPa/s

Δ_{P10-60} = Emission rate of gas released from the coal sample; kPa/s

f = Protodyakonov strength coefficient of the coal sample.

When gas pressure reaches or exceeds 0.6 MPa, outburst tendency increases with increasing K value: K < 15, a coal seam is not liable to outburst; $15 \leq K$ < 40, a coal seam is liable to outburst; $K \geq 40$, a coal seam is likely to have a serious outburst. As can be seen in Equation (2-9), the K value is directly proportional to the gas emission rate Δ_{P10-60} and inversely proportional to the coal strength (f). When Δ_{P10-60} is

constant, the outburst tendency is determined only by coal strength. The Protodyakonov strength coefficient (f) is measured by a simple test designed to determine the degree of pulverization of rock on impact (Protodyakonov, 1963; Lama and Bodziony, 1996).

2.7 SUMMARY

In this chapter, a review of coal coalification processes and the various changes in coal have provided a clear understanding of the ways that gases are formed and accumulated in coal seams. Factors influencing their pressurization, their sorption and their influence on the strength of coal have provided a better understanding of the role and effectiveness of the coal structures for enabling effective future planning of mine gas drainage systems for efficient gas drainage. Effective drainage can only be achieved through determination of the permeability and porosity of the coal and the changes in the coal matrix due to gas pressures, which are the subject of the next chapter.

CHAPTER THREE

A REVIEW OF THE IMPACT OF COAL PROPERTIES ON GAS SORPTION

3.1 INTRODUCTION

The current practice of controlling outburst is by a concentrated program of gas drainage by borehole drilling. The position and orientation of the holes varies from one location to another and also depends on the mining methods. The success of the drainage relies upon efficient sorption of the gases from the coal deposit. Coal rank, coal temperature and ambient temperature, as well as the gas composition, depth of the working and intrusions are a number of parameters that are known to influence coal sorption characteristics. The direct effect of these parameters will be on volumetric matrix changes, related to the coal permeability as well as the strength properties, which are the subject of review in this chapter.

3.2 COAL MATRIX CHANGE

The coal matrix swells and shrinks as the gas is first adsorbed and then desorbed in the coal, and the extent of the changes is influenced by the type of gas and the pressure. Carbon dioxide causes a greater degree of coal matrix change compared to methane, and these changes are not confined to the matrix structures alone, but rather

they also embrace cleats and other fractures in coal and thus have a profound influence on coal permeability and porosity.

Clearly, the issue of volumetric changes and its implications for the Australian coal scene is in its infancy, and very few coal seams in Australia have been studied in detail to evaluate the extent of the use of coal shrinkage to better understand the potential of the seam for effective drainage capability with respect to coal rank and coal purity.

This section aims to shed light on the importance of coal volume change and its influence on the gas drainage capability of seams through changes in the coal matrix structure, as well as the fractures and cleavage systems that are influenced by the coal matrix changes.

3.2.1 Early research on coal matrix shrinkage related to sorption

Interest in coal shrinkage and swelling dates back almost 100 years, Table 3.1 lists various studies undertaken from the turn of the last century to the present day.

Table 3.1 Coal matrix shrinkage indices

Reference	Gas	Swelling/shrinkage coefficient, MPa^{-1})
Moffat & Weale (1955)	CH_4	1.17×10^{-8}
Gunther (1968)	CH_4	1.90×10^{-8} - 4.76×10^{-8}
Wubben, Seewald and Jurgen (1986)	CH_4	9.65×10^{-9} - 4.76×10^{-8}
Reucroft & Patel (1986)	CO_2	4.52×10^{-7}

Gray (1987)	CH_4	1.25×10^{-4}
Gray (1987)	CO_2	1.82×10^{-3}
Juntgen (1987)	CH_4	1.77×10^{-6}
Harpalani & Schraufnagel (1990)	CH_4	4.27×10^{-8}
Harpalani & Chen (1997)	CH_4	2.30×10^{-8}
St. George & Barakat (2001)	CH_4	1.20×10^{-3}
St. George & Barakat (2001)	CO_2	5.20×10^{-3}
Seidle & Huitt (1995)	CH_4	1.96×10^{-4}
Seidle & Huitt (1995)	CO_2	1.78×10^{-4}
Levine (1996)	CH_4	1.30×10^{-3}
Levine (1996)	CO_2	5.50×10^{-3}
Dunn & Alehossein (2002)	CH_4	1.77×10^{-3} - 1.95×10^{-3}

The research undertaken on the subject includes both experimental and theoretical reports, as well as numerical simulations. A chronological description of some experimental work is given here, while the numerical models are dealt with in the next section.

a) Studies prior to 1950

In the early 1930's Briggs and Sinha (1933) tested the swelling and shrinkage of different varieties of UK (Scottish) coals with both firedamp and carbon dioxide, over

various pressures ranging from atmospheric to 2.07 MPa (300lbs). Using the specially constructed apparatus shown in Figure 3.1(some details omitted for clarity

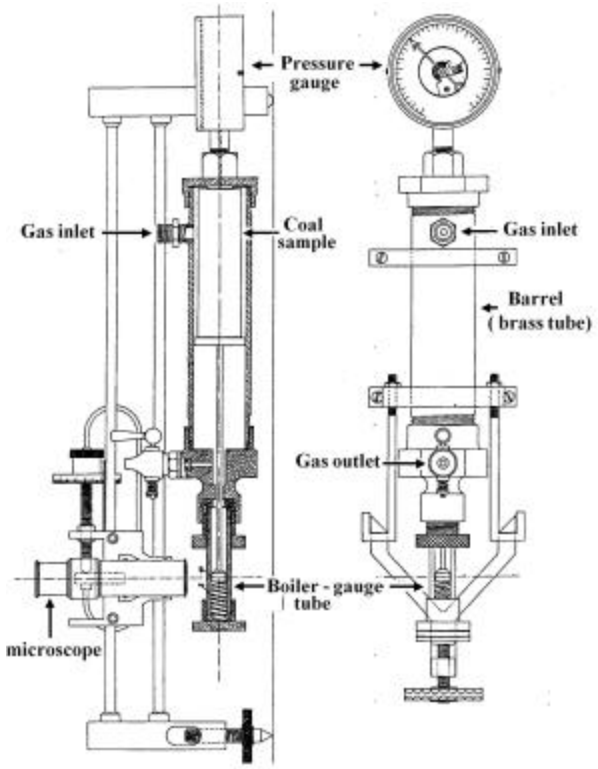

End elevation Front view

Figure 3.1 Apparatus used for the measurement of the expansion and contraction of coal (after Briggs and Sinha, 1933).

from end elevation), the change in sample size was monitored only along its axis, which was cut parallel with the samples' bedding. The axial elongation of the coal samples ranged from 0.06% to 0.3% in firedamp and 5% in carbon dioxide gas. Once the gas pressure was removed most samples returned to near original size, however there was a elongation of 0.14% for antracite.

The elongation or shrinkage of the coal was measured by a micrometer, with resolution down to ± 0.0021 mm. Figure 3.2 shows Briggs and Sinha's test results.

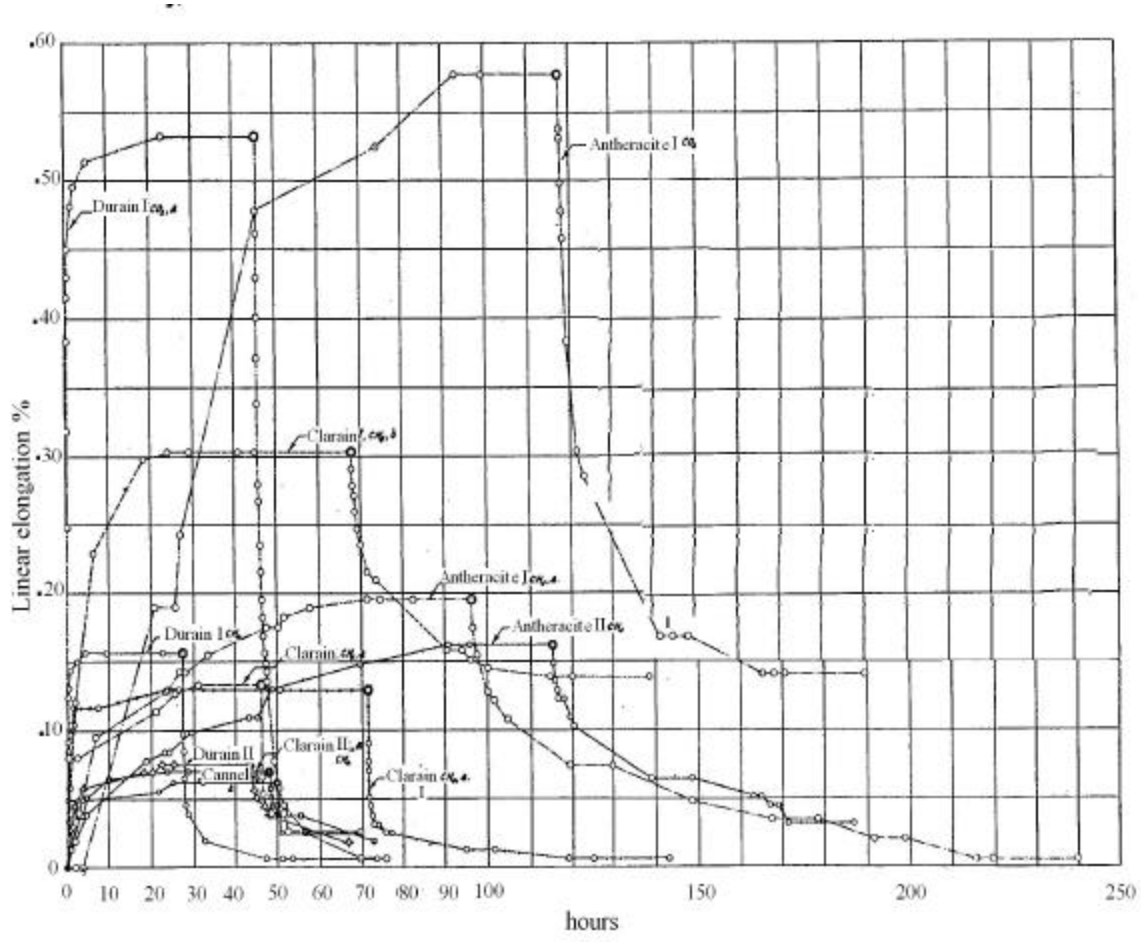

Figure 3.2 Time – dimension change chart at 2.07 MPa (300 psi) gas pressure for different coal samples(after Briggs and Sinha, 1933).

The researchers did not address the radial shrinking or swelling of coal samples in CH_4, but recognised that coal can expand in all directions when absorbing gas, reacting less strongly with methane than with carbon dioxide. Coal also absorbs moisture with greater eagerness than methane, and if coal charged with gas is placed in water, much of the gas will be expelled and replaced with water. Others with

interest in the field in the pre 1950s period include Meehan (1927), Kvalnes and Gaddy (1931), Audibert (1935) and Coppens (1937).

b) Research studies between 1950 and 1960

During the 1950s Moffat and Weale (1955) attempted to define a correlation between the sorption mechanism and the isotherm diagram. They interpreted the sorption mechanism by measuring the coal matrix expansion caused by methane sorption under pressure. Tests were conducted on coal samples parallel and perpendicular to the bedding planes, and were combined to determine the bulk expansion of coal. A constant volume sorption apparatus (Figure 3.3) was used for the test.

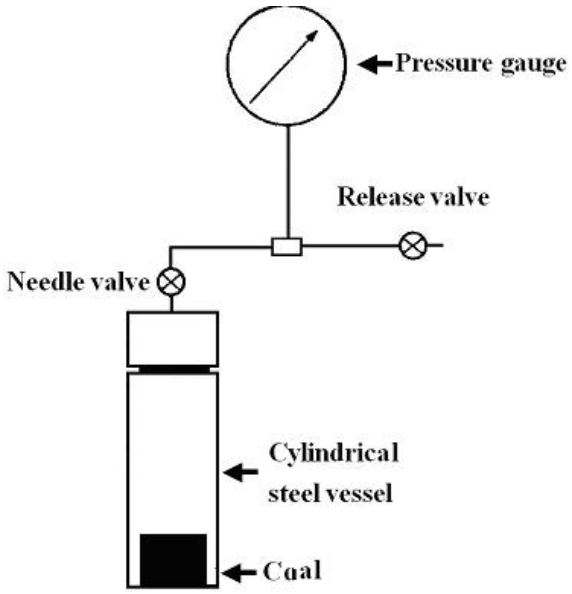

Figure 3.3 A constant volume sorption apparatus. (Moffat and Weale, 1955)

Electrical strain gauges, attached to the surface of suitably cut blocks of coal, with connections from the pressure vessels to a Wheatstone bridge were used to monitor

coal volume change. The tests were made in methane gas at different pressures ranging between 0 and 70 MPa. Tests were made on different coal types ranging from low rank coal to anthracite. Tests conducted perpendicular to the bedding plane attained a linear expansion ranging from 0.2% to 1.6%, at 15.0 to 20 MPa (150 to 200 atm). Higher rank coal expansion was generally less than for low rank coals. Typical graphs of coal expansion are shown in Figure 3.4.

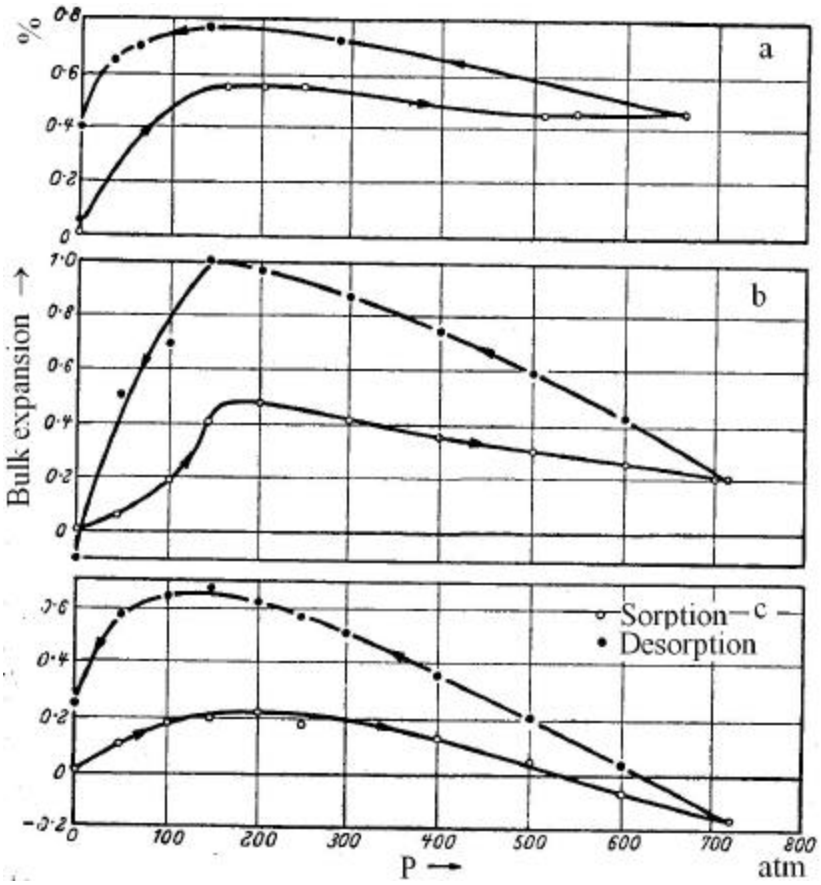

Figure 3.4 Bulk expansion as a function of gas pressure.
(after Moffat and Weale, 1955)

Less expansion was reported on coals tested parallel to the bedding plane. Similar observations were also reported by Audibert (1942) and confirmed by De braaf, Itz and Mass (1952).

c) Research between the 1960s and 1970s

Hargraves (1963a) conducted a series of tests on the Bulli seam coal at Metropolitan Colliery, NSW. Using a simplified shrinkage apparatus as shown in Figures 3.5 and 3.6, he was able to determine the sorption coefficient of expansion of the Bulli coal to

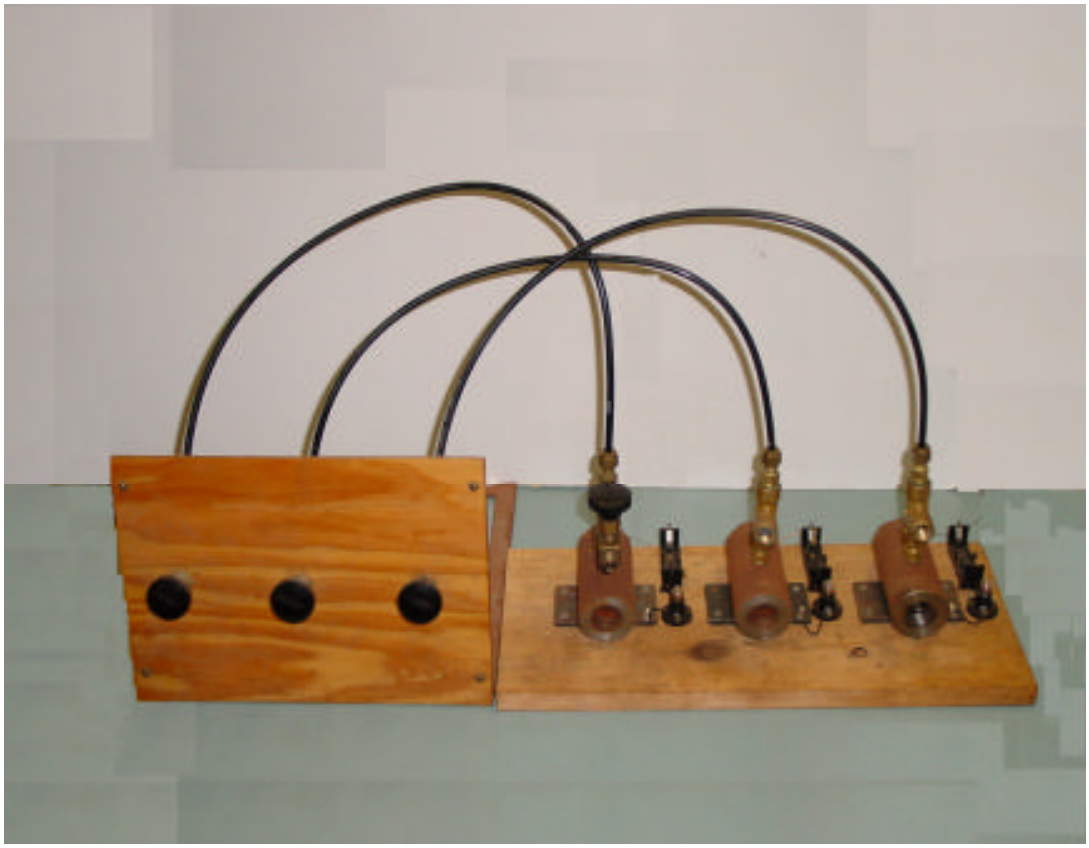

Figure 3.5 Apparatus for determination of sorption coefficient of expansion. (after Hargraves, 1963a)

be approximately 1.75 x 10^{-3} cm/cm at 1 MPa. The test was conducted using 25.4 mm (1 in) cubes, which was subjected to CO_2 gas pressures.

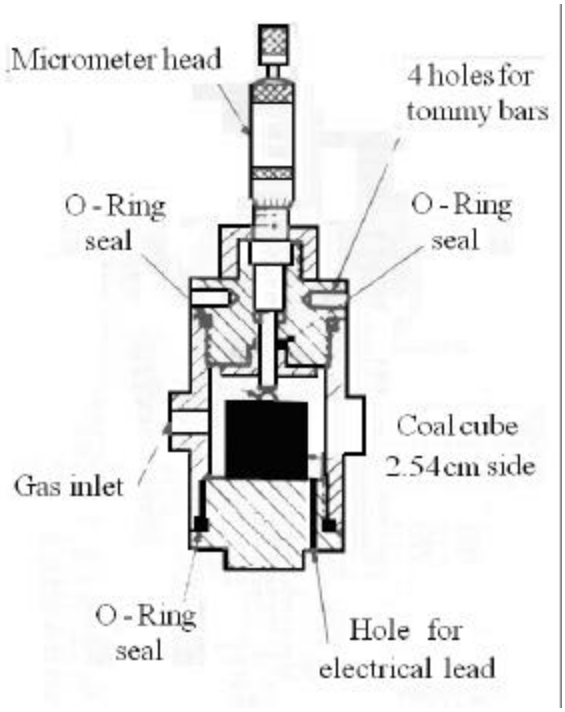

Figure 3.6 Schematic of apparatus for determination of sorption coefficient of expansion.

Gunther (1968) investigated swelling of different ranks of coal using both methane and carbon dioxide, and calculated the swelling coefficients for different types of coal, ranging from low rank, high volatile coals to anthracite. He observed greater swelling of coal in CO_2 than in CH_4. The reported swelling coefficients ranged from 1.90 x10^{-8} to 4.76 x 10^{-8} MPa^{-1} (2.76 to 6.90 E-6 psi^{-1}).

Czaplinski (1971) examined the relationship between the kinetics of sorption and the swelling of coal. Tests were conducted parallel and perpendicular to beddings as shown in Figure3.7 and Figure3.8. He showed that at low pressures, the sorption of

carbon dioxide was faster than the development of swelling strain, but at higher pressures (> 4 MPa) the two occur simultaneously.

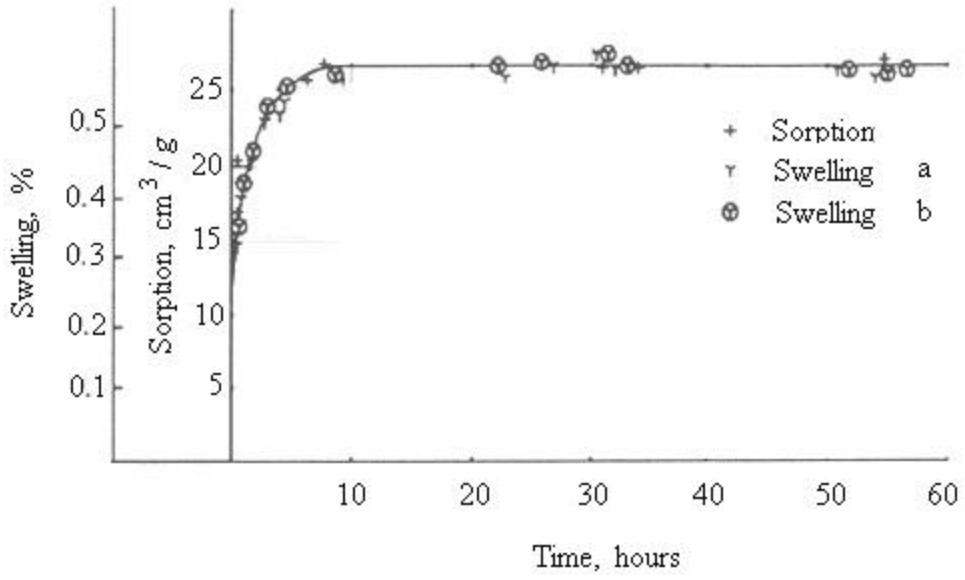

Figure 3.7 Kinetics of sorption and swelling at 4.42 MPa pressure of CO_2.
("a" swelling parallel to bedding, "b" swelling perpendicular to bedding)
(after Czaplinski,1971)

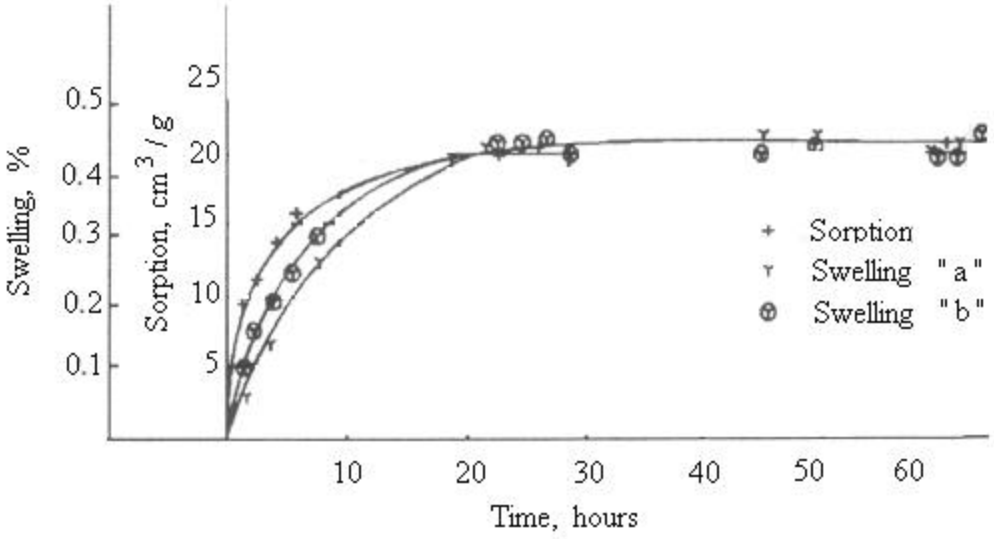

Figure 3.8 Kinetics of sorption and swelling at 2.85 MPa pressure of CO_2.
("a" swelling parallel to bedding, "b" swelling perpendicular to bedding).
(after Czaplinski,1971)

Lama and Bodziony (1996) based on Czaplinski's (1971) studies, stated that "the delay in coal dilation can be explained as follows: At the initial low pressure levels, the gas can only enter the coal macro-pores, causing a minimum of volume change. Increased swelling of coal takes place when the gas, at higher pressures, is forced into the micro-pores."

Ettinger (1977) reported extensive studies on the swelling of different ranks of coal from different coal deposits in Russia, Ukraine and other former Soviet republics. Tables 3.2 and 3.3 show some data on coals from the Donetsk basin and other regions of the Ukraine. The stresses due to swelling cause the release of free energy in coal which, according to Ettinger; contributes to the onset of outburst. Lama, and Bodziony (1996) listed a number of factors to support this claim.

Table 3.2 Linear swelling of Donetsk coals in methane at 5 MPa gas pressure. (after Ettinger, 1979)

Coal deposit	Yield of volatile substances vg, %	Swelling of coal, %	Swelling stress P_0, MPa	Relative free energy of stress state F_s , J/kg
Komsomlets pit, Mazurka seam, (fat coal)	30.6	0.14	21.5	0.5×10^2
Karl Marx pit, Mazurka seam, (coking coal)	18.2	0.17	25.5	0.88×10^2
Kondratevka pit, Derezovka seam, (lean coal)	11.4	0.24	42.3	1.5×10^2

Table 3.3 Bulk swelling in CO_2 at 0.5 MPa gas pressure.
(after Ruff and Gessele, 1930&1940)

Index of coals	Specimens of coal		
	Swelling, %	P_0, MPa	F_s , J/kg
High volatile Bituminous	0.90	50.0	0.24×10^3
Medium volatile Bituminous	0.44	21.8	0.58×10^3
Low volatile Bituminous	0.53	26.4	0.90×10^3

d) Research in the 1980's

Reucroft and Patel (1983) measured the surface area and porosity of coal with respect to sorption with of different gases and vapours, in a similar way to the tests conducted by Mahajan (1982), which measured the porosity as a function of volumetric change. The following equation was used for measuring the volumetric changes of coal:

$$Q = \frac{1}{V_2} = 1 + \frac{r_2}{r_1}(q_w - 1) \qquad (3\text{-}1)$$

where:

r_1 = Density of the sorbate in the liquid state, g/cm^3

r_2 = Density of coal in the liquid sorbate, g/cm^3

V_2 = Volume fraction of coal in the swollen coal sample at equilibrium

q_w = Mass of coal at equilibrium/initial mass.

Q = Swelling parameter (swollen volume/ unswollen volume)

Reucroft and Patel (1983) found that the apparent surface area was higher when, measured using carbon dioxide as the sorbate rather than other gases like nitrogen. Using the weighting method, they estimated the volumetric changes of coal, but without mentioning in which direction it happened and by how much.

Later, Reucroft and Patel (1986) continued with their experiments by investigating the swelling of coal, which was induced by gas, in order to obtain a better understanding of the internal structure and surface area of coal. They observed the swelling of various coal samples exposed to different gases such as He, N_2, CO_2. The coal samples that were 1 cm in length and 0.4 cm in diameter showed an increase in their length between 0.36% and 1.31% when exposed to carbon dioxide. Insignificant changes were observed when the coal was tested in both nitrogen and helium under the same conditions. Also, further experiments were conducted under a low pressure of 0.14 MPa, which is rather low compared with the existing in-situ coal gas pressures. Generally this approach, which is used for measuring surface area and porosity, is more useful for coking coal used in steel making and as therefore not considered in this research.

Gray (1987) examined the relationship between shrinkage, fluid pressure /effective stress and coal permeability. Gray stated, "shrinkage of the coal occurs on desorption, leading to an effective stress reduction. This opposes the effective stress increase that would normally be expected with a lowering of fluid pressure. Because permeability is a function of the effective stress, it may increase or decrease with stress changes associated with drainage". This implies that shrinkage of the coal matrix associated

with desorption opens up the cleat and results in an increase in the permeability of the coal.

Sethuraman (1987) studied the effect of gas pressure on the changing dimensions of coal. He found that there was a linear correlation between swelling and pressure. For methane pressures up to 1.5 MPa, there was a reported volume increase between 0.75% and 4.18%. He also found that the lower the carbon content, the higher the swelling of coal.

e) Studies in the 1990s

Stefanska (1990), a Polish researcher, tested some coal samples using both methane and carbon dioxide under pressures ranging from 0.5 MPa to 5 MPa. It was found that factors such as coal rank and moisture content affected coal sorption behaviour as well as coal matrix changes.

Harpalani (1989) conducted a series of sorption tests and found a relationship between gas sorption and changes in permeability. He confirmed that by desorption of coal gas, the coal matrix shrinks and the permeability increases.

Milewska-Duda, Cegarska-Stefanska and Duda (1994) studied the swelling of the coal matrix due to methane sorption at pressures from 0.5 MPa up to 4.5 MPa and at 298 K temperature. They claimed that coal matrix expansion caused by gas sorption plays an important role in determining mining method so far as outburst phenomena are concerned. Figure 3.9 indicates that at lower pressures the empirical measurements were in agreement with the theoretical data, but deviations were

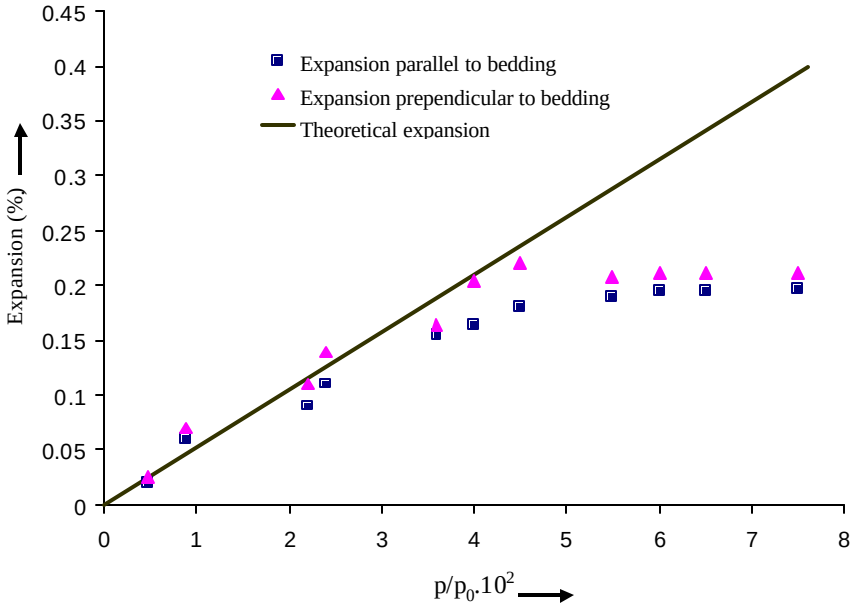

Figure 3.9 Linear expansion of coal (after Milewska-Duda, Cegarska-Stefanska and Duda, 1994).

observed at the higher pressures. The compression of cleats and pores was recognized as the reason for this difference. As can be seen from Figure 3.9, at the lower pressures the amount of expansion was dependent on the direction and expansion of the cleats. The expansion perpendicular to the bedding was more than in the parallel direction. At higher pressures the difference between those were decreased again because of closing the cleats and pores.

Seidle and Huitt (1995) measured the shrinkage of coal matrix with respect to desorption and the changing permeability of coal. They postulated that coal matrix shrinkage was more correlated to gas content than to gas pressure. They found that the amount of volumetric change depends on coal rank and sorbed gas type. It should be mentioned that their samples were placed in an oven at 48^{o}C, which is

significantly higher than the temperature of 20°C that is commonly used for tests. However they did not clarify the reasons for the more rapid desorption than adsorption. As will be shown in later chapters, this author believes that the discrepancy should be attributed to the porous structure of coal. In adsorption it takes a longer time for the gas molecules to get adsorbed in macropores and reach the end of their path in the pore space and micropores, However, in desorption the molecules that are in the vicinity of the free surface and in macropores are easily desorbed and leave their places immediately. Then the inner molecules will be able to quickly flow toward the surface until equilibrium is established.

Levine (1996) reported that with gas sorption during the gas drainage process, the coal matrix shrinks and causes permeability to significantly increase. Different factors affecting this phenomenon include coal rank, petrographic composition, mineral matter content and composition of gases.

Different coals exhibit different shrinking behaviour, and it is crucial to note that one of his significant results was that carbon dioxide causes a greater degree of coal matrix change compared to methane. This is one of the basic principles of carbon sequestration projects. Exposing coal to CO_2 causes different amounts of strain compared to methane or helium, and this difference is attributable to the different sorption capacities of the particular gases.

Levine (1996) also studied the mechanical strength of coal, which was described as the ability to resist stresses and change in dimensions. Figure 3.10 depicts the effective mechanical forces in relation to gas storage and movement in coal.

S is spacing and b the width of fractures, s_v and s_h are vertical and horizontal overburden stress, s_t is the tectonic stress, e_s and e_p are the matrix shrinkage and pore compressibility factors and finally P_f is the fluid pressure.

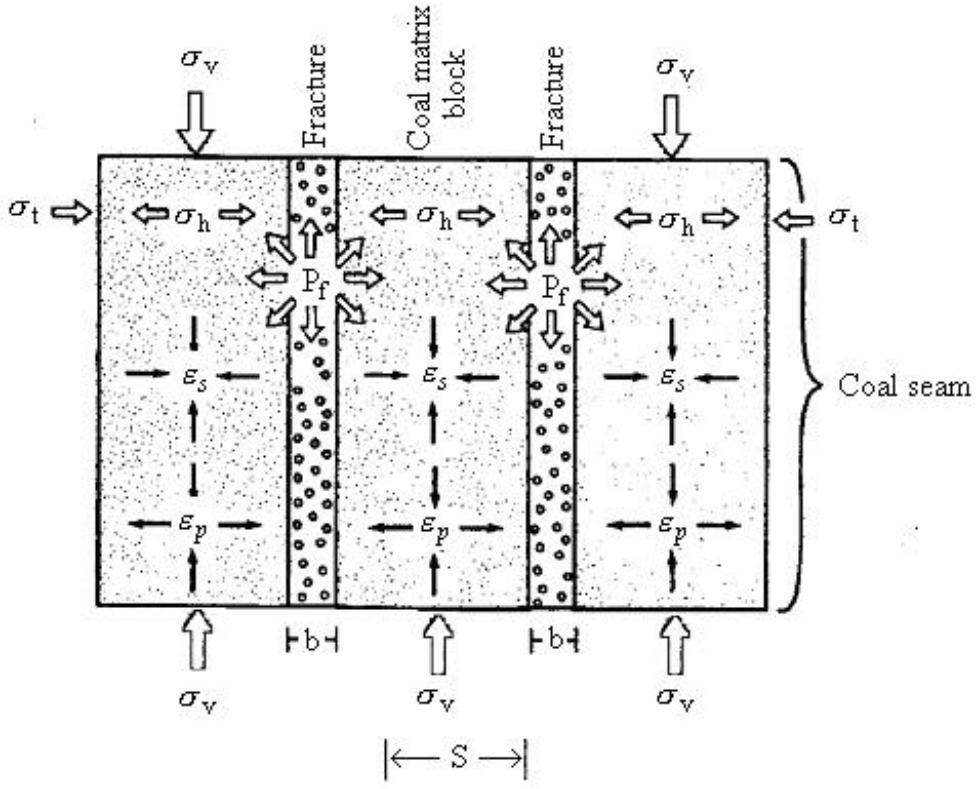

Figure 3.10 Schematic representation of the effective mechanical forces model of a coal bed reservoir. (after Levine, 1996).

Harpalani and Chen (1997) studied the drainage of coal gas (Figure 3.11), and its impact on the coal matrix and permeability. Based on their test results, they presented a relationship between changes in permeability and volumetric strains in the coal matrix, which was described as:

$$\Delta k = a\left(\frac{\Delta V_m}{V_m}\right) \qquad (3\text{-}2)$$

Where Δk is the change in permeability, a is a constant which depends on the coal

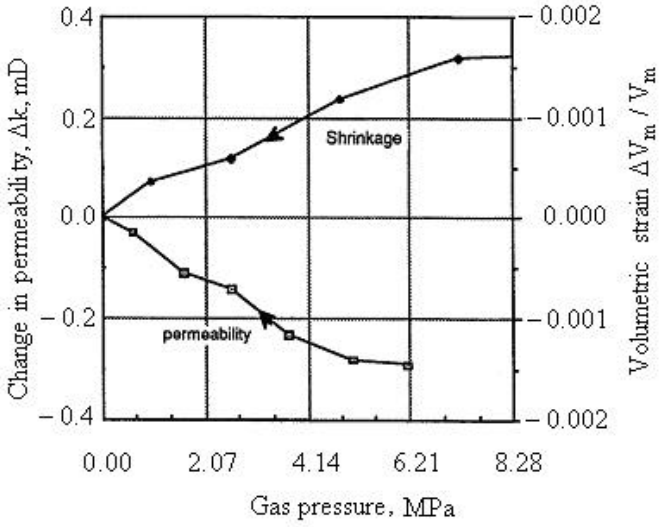

Figure 3.11 Relationship between volumetric strain and changes in permeability as a result of matrix shrinkage(after Harpalani and Chen, 1997).

type and its characteristics, and $(\Delta V_m / V_m)$ is the relative matrix volume change.

Volumetric strains also have a proportional relationship to the desorbed coal gas. Harpalani and Chen (1992) introduced the following equation:

$$\frac{\Delta V_m}{V_m} = bV_{des} \qquad (3\text{-}3)$$

where V_{des} and b are the volume of gas desorbed and a constant which depends on the coal type. In the conclusion to the results of their research they stated that: first, the permeability of coal was drastically increased by decreasing the gas pressure; second, by decreasing the fluid (gas) pressure the effective stress increases and tends to reduces the permeability, but coal matrix shrinkage influences the permeability and limits the decrease; third, permeability changes due to coal matrix shrinkage are dependent on the volumetric strain (Figure 3.12).

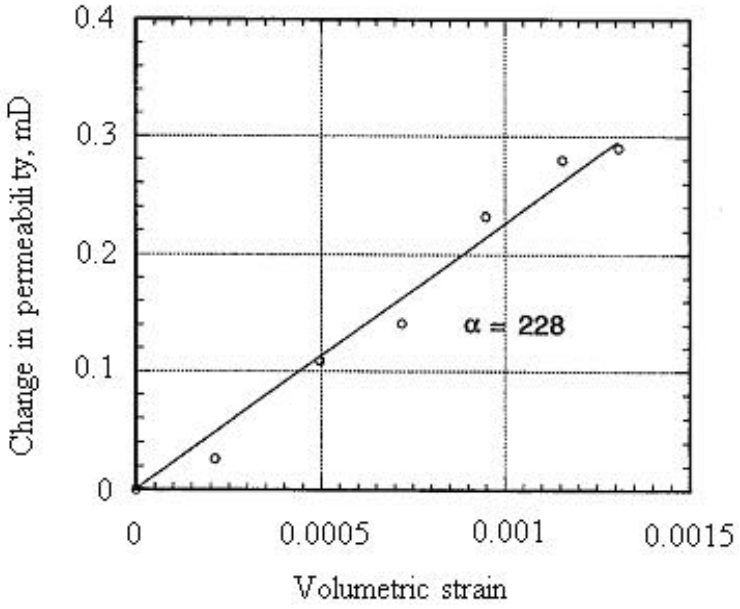

Figure 3.12 Linear relationship between volumetric strain and permeability.

Results of the research of Ceglarska-Stefanska and Holda (1994) on sorption of various gases by coal matrix are shown in Figure 3.13.

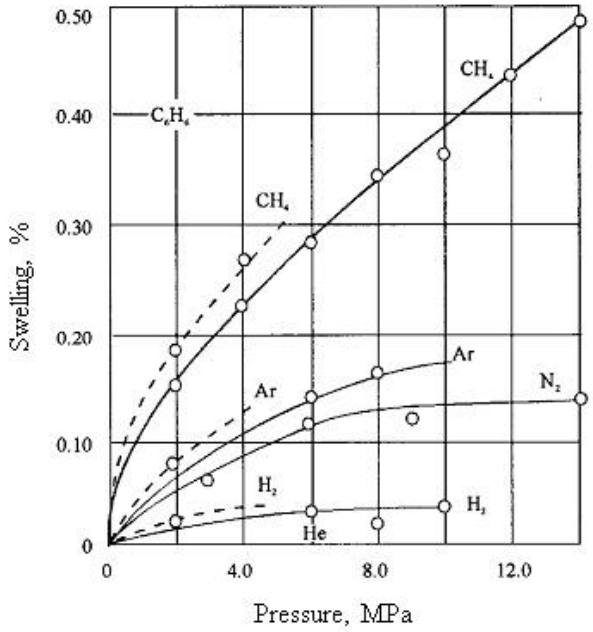

Figure 3.13 Swelling of coal as a function of pressure for different sorbates (after Ceglarska- Stefaneska and Holda, 1994).

It is obvious that the volumetric changes for coal matrix due to Helium gas were negligible, followed by Hydrogen gas which caused 0.05% swelling at 10 MPa, with nitrogen and Argon causing swelling amounts from 0.15% to 0.18%, respectively. The highest amount of swelling was related to Methane, which resulted in about 0.36% swelling. They concluded that by increasing the molecular weight of the gas the percentage of volumetric change would increase. However, one of the parameters, which was not mentioned, is the different affinity of those gases to the coal matrix, this is an important factor which should be taken into account. Figure 3.13 indicates that there isn't any interaction between Helium and the coal matrix, however, coal adsorbs methane immensely.

f) Studies in 2000 - present

St. George and Barakat (2001) demonstrated how desorption of coal gas affected the coal matrix and effective stress. They used sub-bituminous coal samples for their tests. The experimental set up was similar to the Harpalani and Chen (1995) apparatus. Tests were conducted on cylindrical, 54 mm diameter core samples and in four different gas environments. Gases used included CO_2, CH_4, N_2, and He. They found coal swelling due to sorption of carbon dioxide was about 12 times greater than for nitrogen and 8 times more than for methane. They also mentioned that the swelling due to applying helium was negligible. They postulated that the strength characteristics of coal could be affected by compressive strains due to gas pressure reduction and coal matrix shrinkage. Also, in the presence of carbon dioxide, the coal

underwent an initial contraction for a period of less than 45 seconds due to the hydrostatic pressure, which was then followed by expansion due to gas sorption. However, based on the experimental studies discussed later in this thesis, this initial shrinkage time period was found to be shorter than that reported by St. George and Barakat (2001).

The latest study as reported by Chikatamarla, Xiaojun and Bustin (2004) examined the shrinkage and swelling of various Canadian coal samples with different ranks from sub-bituminous to medium volatile coals. The tests were made with regard to determining the capacity of the various coals for sequestration by adsorption. By using various gases, CO_2, CH_4, H_2S, and N_2, they demonstrated that the volumetric strains are proportionally related to the amount of adsorbed gas. H_2S caused larger volumetric changes than the others, up to 15 times greater than carbon dioxide, 20 times more than methane and about 40 to 130 times more than nitrogen. In the second part of their experiments they compared the swelling and shrinkage of the coal matrix by introducing various gases to determine the effect on coal permeability. They reported that, by injecting carbon dioxide into the coal seam, the relative swelling of coal was markedly greater than the shrinkage of the coal matrix.

3.2.2 Modelling matrix shrinkage effects on coalbed methane recovery

Some attempts have been made to model the behaviour of coal matrix (swelling and shrinking) during methane desorption and its recovery from coal beds. Two different models are used to describe how the matrix shrinkage and swelling can cause

profound changes in the porosity and permeability of coal-bed methane reservoirs during depletion or when under injection processes, with associated implications for primary or enhanced methane recovery.

a) API model

Sawyer, Paul and Schraufnagel (1990) developed and presented the first model. Their model, which was called the API model, for the change of coal porosity due to pore compressibility, shrinkage and swelling, is defined as:

$$\Phi = \Phi_i[1 + c_p(P - P_i)] - c_m(1 - \Phi_i)\left(\frac{\Delta P_i}{\Delta C_i}\right)(C - C_i) \qquad (3\text{-}4)$$

Where:

Φ = Fracture system porosity, decimal fraction

Φ_i = Initial fracture system porosity, decimal fraction

c_P = Pore volume compressibility, psi^{-1}

P = Reservoir pore pressure, psi

P_i = Initial reservoir pore pressure, psi

c_m = Matrix shrinkage compressibility, psi^{-1}

ΔP_i = Maximum pressure change based on the initial desorb, psi^{-1}

ΔC_i = Maximum concentration change based on the initial desorb, dimensionless

C = Reservoir gas concentration, dimensionless

C_i = Initial reservoir gas concentration, dimensionless

b) Palmer and Mansoori model

Palmer and Mansoori (1996) established the second model by describing the dependence of permeability on stress and pore pressure in coal beds. Their published matrix shrinkage model was based on induced strains and the mechanical properties of coal. The Palmer and Mansoori model is presented as:

$$\Phi = \Phi_i + A_m (P - P_i) + C_o \left[\frac{K}{M} - 1\right](C - C_i) \qquad (3\text{-}5)$$

Where:

M = Constrained axial modulus, psi

K = Bulk modulus, psi

C_o = Langmuir dimensionless volumetric strain constant

The term A_m can be calculated from following equation:

$$A_m = \frac{1}{M} - \left[\frac{K}{M} + f - 1\right]g \qquad (3\text{-}6)$$

in which:

f = Grain thermal expansivity fraction, dimensionless

g = Grain compressibility, psi^{-1}

By equating the value of Φ from both models they can be combined (Pekot and Reeves, 2003):

$$\Phi_i[1 + c_p(P - P_i)] - c_m(1 - \Phi_i)\left(\frac{\Delta P_i}{\Delta C_i}\right)(C - C_i) = \Phi_i + A_m(P - P_i) + C_o\left[\frac{K}{M} - 1\right](C - C_i) \qquad (3\text{-}7)$$

If grain compressibility *g* is small and the second expression is negligible, then:

$$A_m = \frac{1}{M} \tag{3-8}$$

The pore volume compressibility c_p is found from the following equation:

$$c_p = \frac{1}{\Phi_i M} \tag{3-9}$$

By eliminating the common expressions from both side of Equation (3-7):

$$-c_m(1-\Phi_i)\left(\frac{\Delta P_i}{\Delta C_i}\right) = C_o\left[\frac{K}{M} - 1\right] \tag{3-10}$$

This model is based on changes in gas concentration and addresses how changes in permeability due to matrix shrinkage and internal stress affect the releasing and drainage of coal gas. If no gas desorption occurs, no shrinkage occurs.

It can be seen that the Sawyer, Paul and Schraufnagle model describes shrinkage in terms of matrix shrinkage compressibility and gas concentration change, whereas the Palmer and Mansoori model describes shrinkage in terms of rock mechanics moduli (Pekot and Reeves, 2003).

3.2.3 Numerical simulators of coal-bed methane based on coal matrix shrinkage

The software packages which are currently used for modelling coal bed methane and CO_2 sequestration are based on the above mentioned equations. Some of these are GEM, SIMEDII, ECLIPSE, COMET and GCOMP. These software packages

generally have some features for analysing the porosity system and the diffusional flow of gas between the coal matrix and cleats, as well as modelling the permeability and porosity of cleats as functions of effective stress (CMG, 2004). In Table 3.4 some features for ECBM (enhanced coal bed methane) modelling from different numerical models can be seen:

Table 3.4 Numerical models for enhanced coal bed methane recovery (after Law, 2002).

CBM Simulators	GEM	ECLIPSE	SIMED II	COMET 2	GCOMP
Multiple Gas Components (3 or more: CH_4, CO_2& N_2)	Y	N	Y	Y	Y
Dual Porosity Approach	Y	Y	Y	Y	N
Mixed Gas Diffusion	Y	Y	Y	Y	N
Mixed Gas Sorption (extended Langmuir Model)	Y	N	Y	Y	Y
Stress Dependent Permeability & Porosity	Y	Y	Y	Y	Y
Coal Shrinkage (Primary Process)	Y	N	Y	Y	Y
Coal Shrinkage/Swelling (ECBM Process)	Y	N	Y	Y	Y

3.3 COAL PERMEABILITY

Permeability is a physical property of porous materials, which determines the flow of fluid through the material by an applied pressure gradient. It may be described as the "fluid conductivity" of the porous material. Permeability is also used to describe the

resistance of strata to the passage of gas through it (Mordecai and Morris, 1974). Permeability is one of the most important parameters that affect gas production rates and reservoir recovery in coal-bed methane production (Wallace, 1990; Shi and Durucan, 2003).

One of the principal physical parameters governing gas emission from coal is cleat permeability (Jones et al., 1982). Permeability also is considered as a principal factor in controlling gas release into mine workings (Ramani and Owili-Eger, 1973; Guney, 1975). To properly plan the gas drainage system in a mine, information about gas pressure, gas composition, location of the gas reservoirs and permeability of the seam is required. Highly permeable coal offers a good opportunity to recover methane.

Permeability of coal can be calculated using the following Darcy's equation:

$$Q = -\frac{kA}{m}\frac{dP}{dx} \qquad (3\text{-}11)$$

where:

k = Permeability, Darcy

$\frac{dP}{dx}$ = Pressure gradient, atm/cm

A = Cross sectional area, cm^2

m = Viscosity of the fluid, centipoise

Q = Volumetric flow, cm^3/s

Permeability has units of area (m^2) in the SI system, but the usual unit for permeability is the Darcy. The Darcy unit represents the flow capacity required for 1

ml of fluid to flow through 1 cm^2 for a distance of 1 cm when 1 atmosphere of pressure is applied, that is;

$$1\ m^2 = 10000\ cm^2 = 1.01 \times 10^{12}\ \text{Darcy} \quad (3\text{-}12)$$

There are some conditions that are required for Equation (3-11) to be valid; they are:

- Porous medium is not reacting with the flowing fluid.
- Assumed single phase flow.
- Reynold's number is of the order of 1, based on superficial velocity.

According to Wallace (1990), the permeability of US coals is usually in the range of 1 to 60 mD. Hayes (1982) reported that the Bulli seam permeability is considerably less than 1 mD. Lingard, Phillips and Doig (1982) reported permeability of Australian coals from Appin, Westcliff and Leichhardt Collieries that varied from less than 0.1 mD to 100 mD.

The permeability values vary according to gas type and differential pressure across the coal seam. This effect was originally detected with the gas flowing through capillary tubes, and becomes more pronounced when the diameter of the capillary tubes approaches the mean free path of the gas molecule, which is a function of the molecular weight and kinetic energy of the gas. For equal pressures, a small molecule in the gas phase will exhibit significantly more slippage when travelling through the medium than a larger gas molecule. For a liquid that totally fills the medium, there will be no slippage. The effect of gas slippage on the permeability value was identified and quantified by Klinkenberg (1941).

3.4 FACTORS AFFECTING THE PERMEABILITY OF COAL

The following factors influence coal permeability (Enever and Hennig, 1997):

- Effective stress
- Coal petrography
- Mineralisation
- Degree of fracturing
- Gas type and pressure
- Water

3.4.1 Effective stress

Permeability is heavily influenced by the effective stress. In fractured reservoirs, such as coal-beds, the permeability of coal is sensitive to stress variation or pore pressure (Palmer and Mansoori, 1996). Lingard, Phillips and Doig (1982) stated that permeability cannot be studied without reference to in-situ stress conditions. Others examining the effect of stress on coal permeability include Patching, 1965; Gunther, 1968; Pomery and Robinson, 1967; Somerton, Soylemezoglu and Dudley, 1975; Hargraves, 1983; Rose and Foh, 1984; Puri and Seidle, 1992 and Duracan, 2003. A wide range of permeability values was measured under various stresses. The permeability of a particular coal was found to depend on the level of the confining stress. For example a permeability of 12 mD at 0.07 MPa confining pressure changed to 0.0035 mD at 20 MPa. Somerton, Soylemezoglu and Dudley (1975) found that increased applied stress in constrained coal samples caused a decrease in permeability

of several orders of magnitude, up to the point where microfracturing occurred, and permeability increased again beyond this point.

Limited tests on measuring the permeability of coal have been undertaken on different Australian coals. The measured permeability for the Bulli coal seam under triaxial conditions varies from 0.001 mD (Lingard, Phillips and Doig, 1984) to 0.15 mD (Somers, 1993). Their results also showed that in all tests the permeability could decrease with increasing stress. Xue and Thomas (1991) investigated the variation of Australian coal sample permeability with confining stress and changing gas mean pressure. They showed that the permeability of coal increased when the mean gas pressure was decreased. However, the coal samples were one to two orders of magnitude smaller in permeability as the confining stress increased from 1 MPa to 15 MPa.

Somers's (1993) work on Australian coal permeability found that under 5 MPa confining pressure Bulli coal samples had an average permeability of 30 mD, with Westcliff coal 21mD, Tower 45 mD, and Tahmoor 17 mD. Ulan coal permeability is around 16 mD. Gray (1987) also presented a relationship between effective stress and permeability for cores taken from Leichhardt Colliery in the Bowen Basin, The relationship, shown in Figure 4.1, is based on:

$$k = 1.013 \times 10^{-0.31\sigma} \qquad (3\text{-}13)$$

where k is the dry permeability in mD and "s" is the effective triaxial confining stress in MPa. As can be seen in Figure 3.14, there is an order of magnitude reduction in

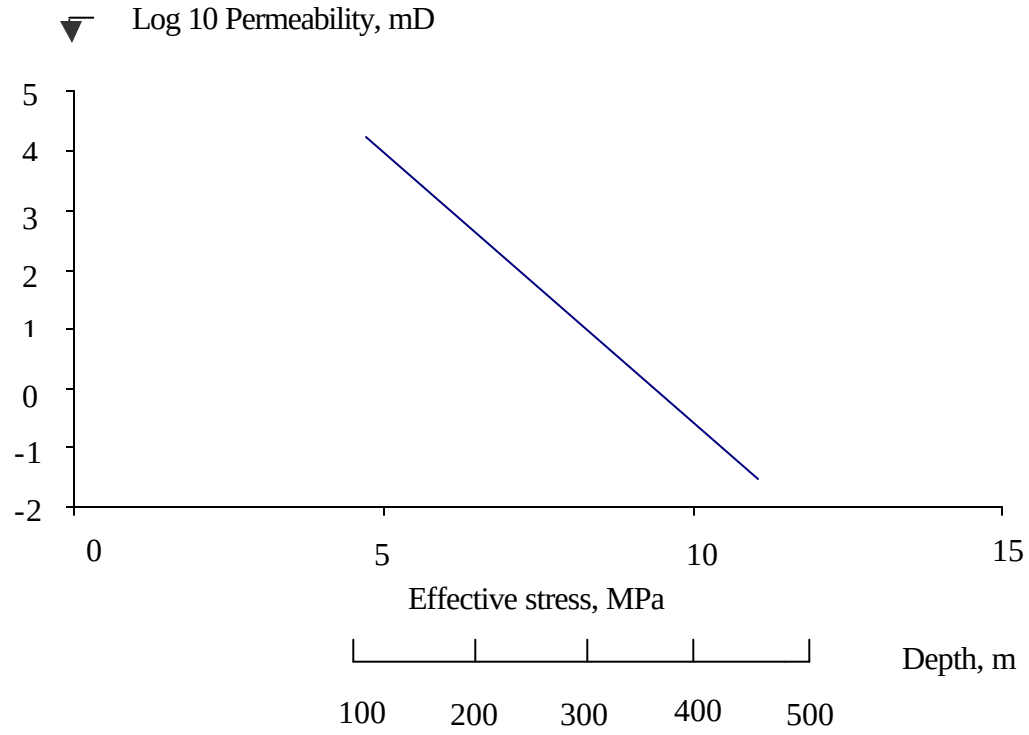

Figure 3.14 Relationship between permeability and effective stress based on field studies. (after Gray, 1995).

permeability with a 1.47 MPa increase in effective confining stress. Gray demonstrated that the graph in Figure 3.14 was also able to show the log of coal permeability declines linearly with increasing effective stress.

The permeability of coal samples is very sensitive to the overburden pressure, and it is significantly reduced as overburden pressure increases (Durucan and Edwards, 1986).

Enever and Hennig (1997) summarised the results of previous tests and stated, "for equal applied confining pressure, some Australian coal exhibited significantly lower

average permeability than either of the tested American coals", implying that in their tests, the Australian coals are more stress dependant than the American coals. Figure 3.15 shows this difference:

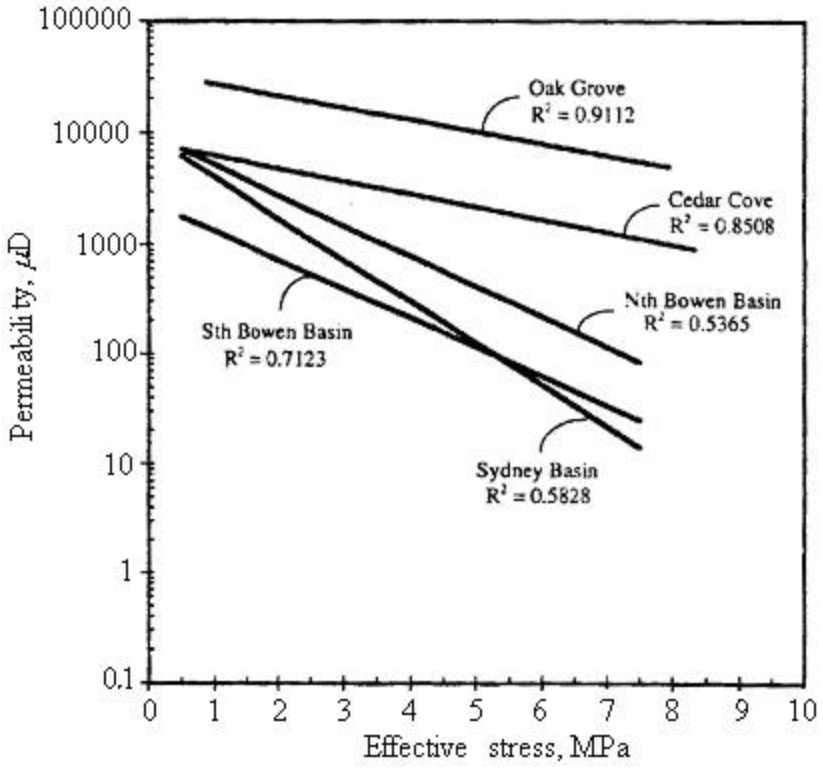

Figure 3.15 Average relationship between permeability and effective stress for several Australian regions compared to Black Warrior Basin (USA).

It should be mentioned there were only two samples from USA coal basins and three from Australia so, it could not be drawn a general conclusion unless there were more data and samples for tests. Also, the R^2 values were around 0.5, which shows that there was a significant variation for results.

Lingard, Phillips and Doig's (1984) study on Australian Coals found that the permeability reduction was between 2 to 3 orders of magnitude for an increase in the confining stress from 0 to 9 MPa.

Various researchers examined the recovery in permeability with respect to changing effective stresses. Harpalani and McPherson (1984) reported a partial recoverability property for some USA coals, and Paterson (1990) did work on Australian coal permeability hysteresis by cycling the confining stress. As can be seen from Figure 3.16, there was a considerable difference between the initial and last value of permeability for the same stress.

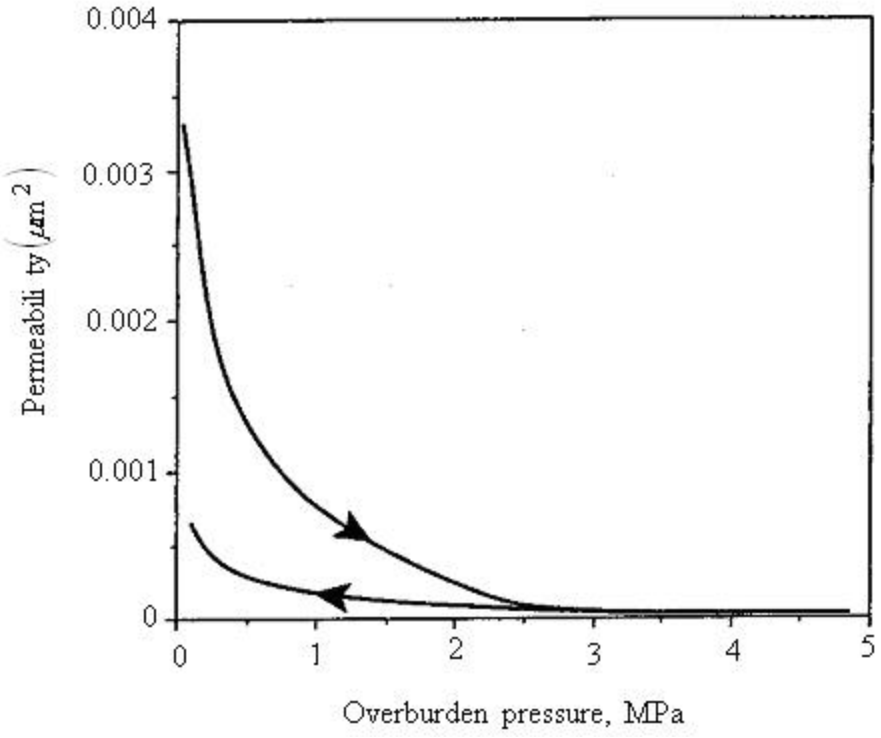

Figure 3.16 The hysteresis in coal permeability from cycling the confining stress (after Paterson, 1990).

3.4.2 Coal Petrography

The permeability of coal seams can be influenced by geological structure variations. Coal seam permeability is sometimes enhanced in the vicinity of a fault, dyke or fold.

Generally, favourable areas for coal bed methane drainage are likely to have a relatively simple geological structure to ensure the continuity of reservoirs. Wallace (1990) reported that gently folded areas in coal seams tend to have higher permeability than steeply folded and faulted areas. Since cleat orientation has proved to be an important parameter for the permeability of coal (Wolf et al., 2001 a & b), structurally complex areas tend to have damaged cleat systems resulting in low permeability, especially where severe structural compression has occurred.

The permeability among different coal litho-types varies even under the condition of similar coal rank. The coal petrological composition affects the overall permeability of the coal-bed through controlling the development of the pore and fissure system. The permeability of a vitrinite-rich coal reservoir is around 10 times higher than for an inertinite rich one (Symth, 1993). Also, the inertinite-rich coal absorbed more methane than a middle-rank coal sample, but absorbed the same amount as a high rank coal sample.

Bartosiewicz and Hargraves (1984) examined various coal samples from Australian coal basins, and the results showed significant variations in permeability in different directions. Bedding plane permeability is significantly greater than the permeability normal to the bedding. However, Lingard, Phillips and Doig (1982) reported no significant difference between coal samples cut parallel and perpendicular to the bedding plane. Gash et al. (1993) tested the permeability of American coal samples and found that the permeability in the face cleat direction was greater.

3.4.3 Mineralisation

There are some differences between low permeability and high permeability coal seams. These differences can be related to the presence of some specific pore and cleat fillings such as mylonite, the development of cleats and their mineralisation, and the mode of occurrence of minerals in coal macerals. Successful drainage and a suitable rate of gas flow through the coal can be influenced by coal microstructures, especially micro-cleat openings and mineral matters. In good drainage and high permeability coal seams, the micro-cleats are mostly empty, or only partly mineralised.

Stach et al. (1982) and Renton (1982) reported that most mineral matters are fine grained with an approximate size of $20\,m$, Faiz et al. (1992) stated, "the presence of mineral matter in coal mainly contributes to the volume of macropores". Speight (1983) has shown that increased mineral matter normally fills macropores and consequently the porosity of coal will be decreased, particularly in lower rank coals, causing a reduction in coal permeability.

There are various classifications of mineral matters in coal, based on their mode of origin (Gluskoter, Shimp and Ruch, 1981; Stach et al., 1982; Renton, 1982). Two of these classifications are as follows:

a) Renton classification:

Renton (1982) classified the mineral matters in coal based on their origin, as shown in the Figure 3.17. Detrital minerals such as clay and quartz are derived from an

external source and transported to the peat by water or occasionally by wind. Conner and Shacklette (1975) reported that inorganic materials exist in plants as contaminants. Vegetal group minerals such as silica and alumina originate from the inorganic constituents of swamp plants. Chemical mineral matters are subdivided into two divisions: in the first the minerals appear in coal as a result of direct chemical precipitation, and in second the minerals emerge from chemical reactions.

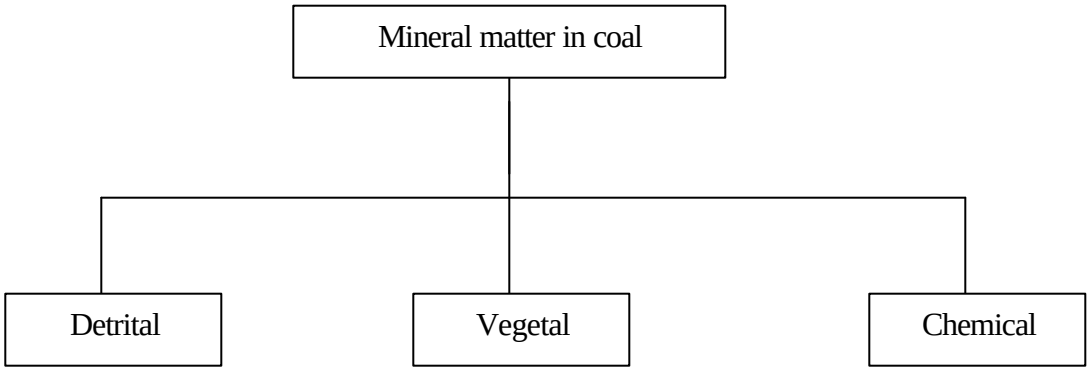

Figure 3.17 Classification of mineral matters based on their origin (after Renton, 1982).

b) Stach classification

In this method the mineral components are also classified according to their origin. However Stach et al. (1982) believed that in this classification there is no certainty in some conclusions, as is shown in Figure 3.18.

The first group comprises the minerals from plants, the second group formed in the first phase of the coalification process, consists of minerals transported into the

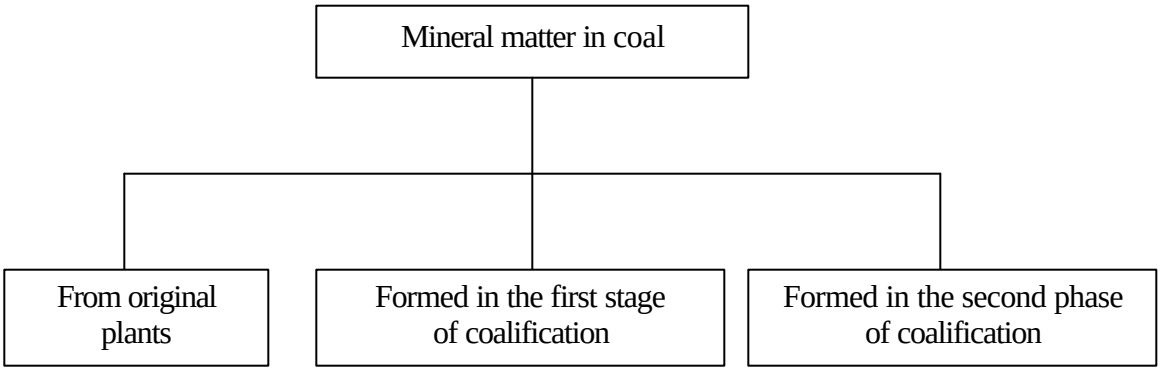

Figure 3.18 Classification of mineral matters based on their origin (after Stach et al., 1982).

swamp, and lastly the group of minerals that are introduced into the coal matrix by precipitation or alteration in fractures, cleats or fissures during the second phase of coalification. Some of the common minerals in coal are carbonates (Calcite), iron disulphides (Pyrite), clay minerals (Kaolinite) and salts, the most abundant being clays that have variable stochiometry. Dominant minerals include kaolinite, which is useful in marker beds to correlate seams across a coalfield. Clay has swelling properties and expands when it comes into contact with water. Wet clay reduces strength and can be hazardous during mining, because it acts as a weak point in the coal seam and a suitable place for the initiation of an outburst, when other factors such as high gas content, gas pressure, and stress are also present. Calcite and dolomite are the next most common minerals in coal. Pyrite is commonly present in older and more mature coal seams, which have more gas and less permeability because of the presence of pyrite mineral matter, and consequently an outburst prone zone can easily appear, for example the outburst zone in Central Colliery.

In coal seams with negligible quantities of mineral matter, the coal-bed gases flow and initially continue to flow when the pressure is lowered below the desorption pressure. The coal matrix shrinkage as a result of gas desorption may cause greater cleat openings than the effective stress. Titheridge (2004) stated, "In mineralised coal, the presence of calcite (or other minerals) in cleat or fractures adds an additional factor to the initial and subsequent drainage process. Mineralisation blocks cleat and fracture permeability routes that would otherwise transport gas". Thus, an increased presence of mineral matter in coal would cause a reduction in coal permeability, and the degree of permeability will be proportional to the extent of mineralisation. Furthermore, mineral matter impedes the gases from leaving their place by affecting the desorption and shrinkage properties of the coal matrix.

Gamson, Beamish and Johnson (1993) in an extensive study on Australian coals found that the amount of fracture infilling with minerals was one of the factors which influenced the effectiveness of methane flow through the coal matrix. They also noted that mineral matter such as clay, calcite and quartz block the methane flow path through cleats and interconnected pores by forming a compact amorphous or crystalline structure. The size of infillings influences gas diffusion as well as laminar flow in the coal matrix. Later Gurba (2002b) described her microscopic studies of some Australian coal samples and found that the Bulli seam had two different sets of cleats. One set of cleats is open and the other mineralised. Microscopic studies on coal samples from West Cliff Colliery showed micro-cleats totally mineralised by carbonates. Siderite nodules (Iron Carbonate) in the cleats were observed to cause difficulty in drilling and in drainage. Mylonite is also present in West Cliff coal

samples, and mylonitic type coal could be prone to outbursts (Gurba, 2002a). Additionally, microscopic examination of the coal samples from difficult drainage areas has shown that the presence of mylonite in micro-cleats is also likely to cause difficulties in gas drainage. As revealed by electron microprobe analysis the mylonite in micro-cleats is cemented by calcite, dolomite or kaolinite. In the coal samples from Central Colliery in the Bowen Basin that were collected from the low permeability area and outburst prone zone, the cleats were totally filled with calcite. In Appin Colliery coals, carbonates were present in the cleats as well as mylonite, which was cemented by carbonates so that there was not much space for gas flow.

Titheridge (2004), who did extensive work on Tahmoor Colliery Bulli coal and its calcite mineral matter, postulated that high fluid pressure was the major factor responsible for the fibrous veins in coal (sedimentary rock). He stated, "the origin of high fluid pressure was primarily due to the fluctuating NE-SW tensional – compressive stress field that was present during the burial phase of the Southern Sydney Basin". Calcite in Tahmoor coal (Figure 3.19) was formed from the combination of CO_2 and water, for which one of the CO_2 resources was magmatic

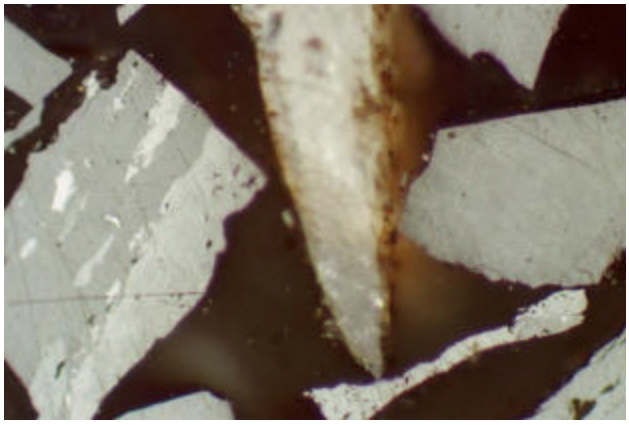

Figure 3.19 Calcite in Tahmoor coal.

intrusions (dyke), and that this mineralisation can extend a long way from the dyke.

At Tahmoor, a vein that was formed by the calcite accompanied by sideritic mudstone caused a large reduction in the permeability of coal between coal seam layers. It should be noted also that the carbonate ground water system is the main source of calcite penetration into the coal seam and its cleats (Drever, 1982; Williams and Elders, 1984; Barker, 1991).

3.4.4 Degree of fracturing

Coal seams have natural fractures, known as cleats. Cleats act as a major transport system for gas and water flow within a coal seam. There are two sets of cleats in coal, face and butt cleats. Face cleats are longer than butt cleats, hence directional anisotropy in coal permeability results from this phenomenon.

Permeability of coal increases with cleat density and cleat width. The flow capacity of fractured media depends almost entirely on the number and width of fractures and their continuity (Dabbous et al. 1974). Lingard, Phillips and Doig (1984) showed that the dimensions of fractures influence coal permeability. The greater the fracture, the higher is the permeability of the coal. Flow through cleats is generally laminar flow, and the following equation is used for measuring the laminar flow rate through a narrow channel (Muskat, 1949):

$$Q = \frac{10^8 W^3 \Delta P}{12 mL} \qquad (3\text{-}14)$$

where:

Q = Flow rate, cm/sec

W = Fracture width, cm

$\frac{\Delta P}{L}$ = Pressure differential over channel length, atm/cm

m = Viscosity of fluid, centipoise

As previously mentioned, Darcy's law expresses the fluid flow as:

$$Q = \frac{kA\Delta P}{mL} \tag{3-15}$$

By combining equations 3-14 and 3-15 (Somerton, Soylemezoglu and Dudley, 1975):

$$k_f = \frac{10^8 W^3}{12A} \tag{3-16}$$

k_f = Permeability of fracture, Darcy

W = Fracture width, cm

A = Cross-sectional flow area of fracture, cm^2

Information relative to the cleat size and spacing in coal are useful in predicting permeability, and generally the larger the cleat size and cleat density, the higher the permeability. Secondary cleats also occur in coal as a result of induced stress and changes to coal geological structure or mining. These fractures normally cause permeability to increase, but sometimes they do the opposite and reduce the permeability, and such situations tend to occur in shear zones or near magmatic intrusions. According to Hayes (1982) permeability in the fractured and crushed zone ahead of the face side during mining is greater than permeability in the intact and solid coal area.

3.4.5 Gas pressure and type

Figures 3.20 (a-b) shows test results from as discussed at the beginning of this

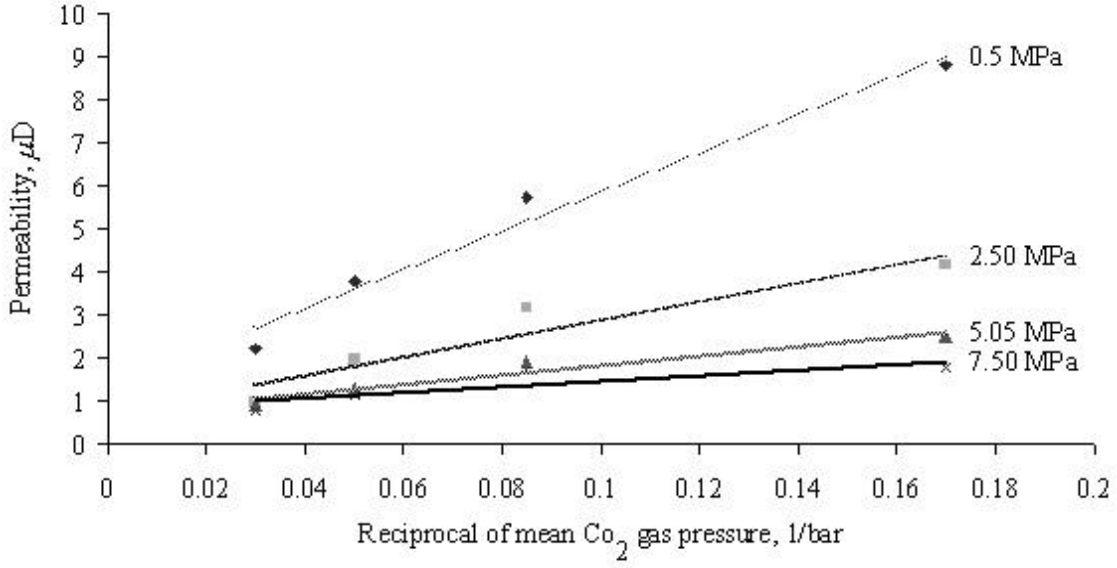

(a) Permeability from 0 to 10 *m*D

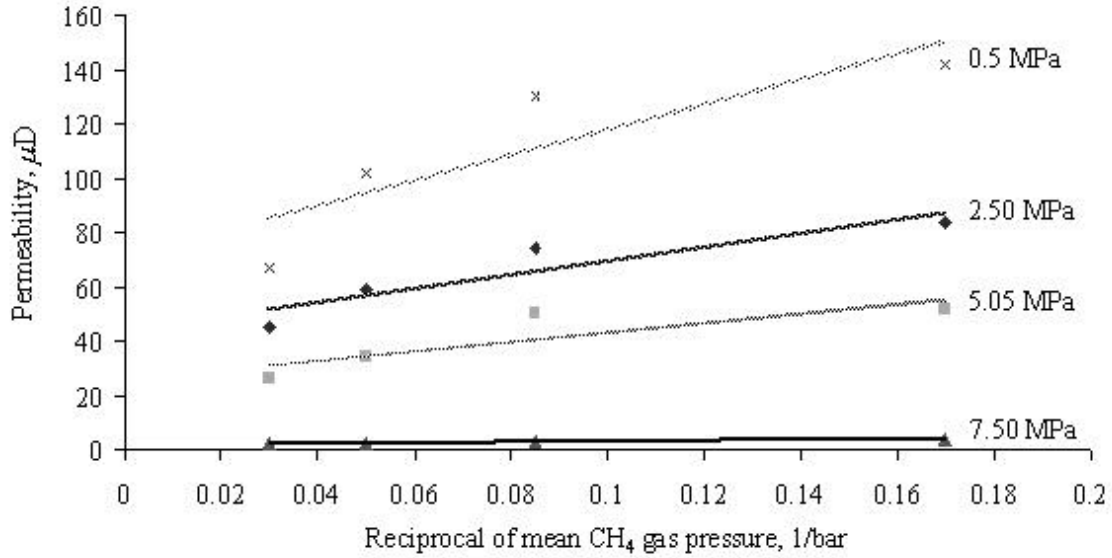

(b) Permeability from 0 to 160 *m*D

Figure 3.20 Effect of gas pressure on permeability of Bulli coal samples for (a) CO_2 and (b) CH_4 (after Lama, 1995a).

chapter, the Klinkenberg effect explains the effect of gas pressure on permeability of Bulli coal samples. For methane and carbon dioxide, increasing gas pressure decreases the permeability, but this reduction is greater for methane than carbon dioxide. This effect is remarkable at the lower pressures for both gases, but by increasing the pressure up to 7.5 MPa for carbon dioxide, the rate of decrease drops further. As for methane, the permeability decreases to half of its initial amount when the gas pressure increases from near 0.5 MPa to 2 MPa.

There appears to be limited research on the influences of gas type on coal permeability. Somerton, Soylemezoglu and Dudley (1975) used nitrogen and methane to study coal permeability and found that coal permeability to methane is lower than the permeability to nitrogen. The explanation provided was that the sorption of methane on coal was a possible cause of this phenomenon. Another possibility was previously presented by Patching (1965), who reported that permeability decreases linearly with increases in the square of the molecular diameters of different gases.

The ratio of CH_4/CO_2 in Australian coal seams varies; in some deposits CO_2 is the predominant gas, and in other areas methane is predominant. The permeability of coal is higher for methane than carbon dioxide (Lama, 1995a; Bartosiewicz and Hargraves, 1985). Australian researchers Xue and Thomas (1995) investigated the permeability of Australian coals to a mixture of CH_4/CO_2. They stated that by using the Darcy and Dalton pressure laws, the permeability of coal to a mixture of two gases can be derived theoretically from Equation 3-17:

$$k_m = \frac{N_1^2 \times m_m}{10^4 \times m_1} \times k_1 + \frac{N_2^2 \times m_m}{10^4 \times m_2} \times k_2 \qquad (3\text{-}17)$$

where:

N_1 = Volumetric percentage of gas No. 1

N_2 = Volumetric percentage of gas No. 2

K_1 = Permeability of coal to gas No. 1, Darcy

k_2 = Permeability of coal to gas No. 2, Darcy

k_m = Permeability of coal to mixture, Darcy

m_1 = Viscosity of gas No. 1, centipoise

m_2 = Viscosity of gas No. 2, centipoise

m_m = Viscosity of mixture gas, centipoise

Based on their results (Figure 3.21), Xue and Thomas (1995) found the difference between the theoretical calculated and the experimentally measured permeability was about $\pm$15%They also reported that by increasing the proportion of carbon dioxide in the mixture, the permeability of coal decreases till the point which the composition of mixture was approximately 60% CO_2 and 40% CH_4 and then begun to increase, the reason for such a difference will be discuss later in Chapter 6. Finally they explained the adsorption effect on the permeability of coal to methane and the carbon dioxide mixture by defining the mutual and individual adsorption effects, which are the effects of adsorption of a gas from a mixture and from an individual gas on coal permeability, respectively.

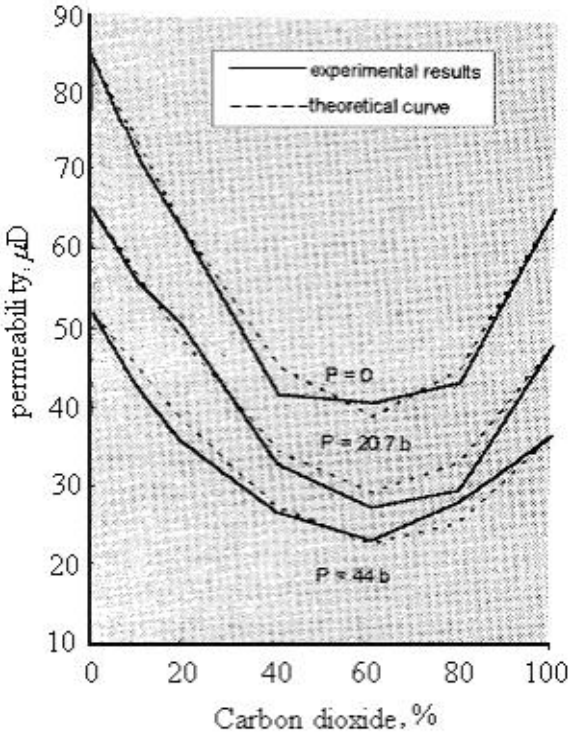

Figure 3.21 Permeability of coal sample to mixtures of CH_4 and CO_2. (after Xue and Thomas, 1995)

. As is shown in Figure 3.21, for a higher percentage of methane in a gas mixture, the experimental value of the coal permeability to the mixture is slightly smaller than the theoretical value because the effect of mutual adsorption is more significant than the combined effects of the individual adsorption of CH_4 and CO_2. However, at a lower percentage of methane, the experimental coal permeability is slightly larger than the theoretical value.

3.4.6 Water

In virgin coal seams, water normally fills pore spaces, cleats, and fractures and any gas present is dissolved within the seam water or absorbed on the internal surface of

the coal, while the reservoir and its fluid components are in equilibrium (Van der Meer, 2004). Permeability of a coal seam to gas is dependent on the concentrations of water (Thakur and Davis, 1977). Usually free gas only comes out of the coal into the cleat space when the water pressure drops below the sorption pressure (Gray, 2000). The permeability of coal to water is increased by decreasing the pressure (Dabbous et al., 1974). Kissell and Edwards (1975) reported that the relative permeability of a coal seam increases as the water in the seam decreases, thus making more space available for the gas phase to flow. It means that initially permeability will decrease with a drop in reservoir pressure around the production hole, followed by an increase, as significant desorption induced shrinkage occurs as water and gas are produced from the seam, with the effective stress increases leading generally to a reduction in permeability. However many coal seams exhibit an increase in permeability with production, because of seam de-stressing and coal shrinkage due to gas desorption. Coal shrinkage reduces the lateral stress in the seam and shifts the stress into the surrounding rocks. The opposing effects on effective stress mean that the permeability of the seam may either increase or decrease with the removal of gas and water from the seam.

Generally, permeability is reduced by an increase in moisture content (Bartosiewicz and Hargraves, 1985). However, it should be pointed out that the gas permeability of a coal mass is influenced by the degree to which the permeable volume of the pore is filled with natural moisture. Natural moisture decreases the permeable volume of pores by a factor of greater than two (Ayruni, 1981).

3.5 PERMEABILITY CLASSIFICATION OF COAL-BEDS

3.5.1 Drainage classification

Annually some 300,000 m of underground directional inseam drilling is carried out in Australia for degasification and drainage purposes (Thomson and MacDonald, 2003). Gas drainage is a technique that has proven to be successful in reducing the outburst hazard by reducing the insitu gas pressure. Influencing the effectiveness of gas drainage is the physical phenomenon of permeability. The permeability of coal has its importance in other stages of drainage such as continuing and developing the coal bed methane drainage system. Figure 3.22 shows the various factors that Wallace

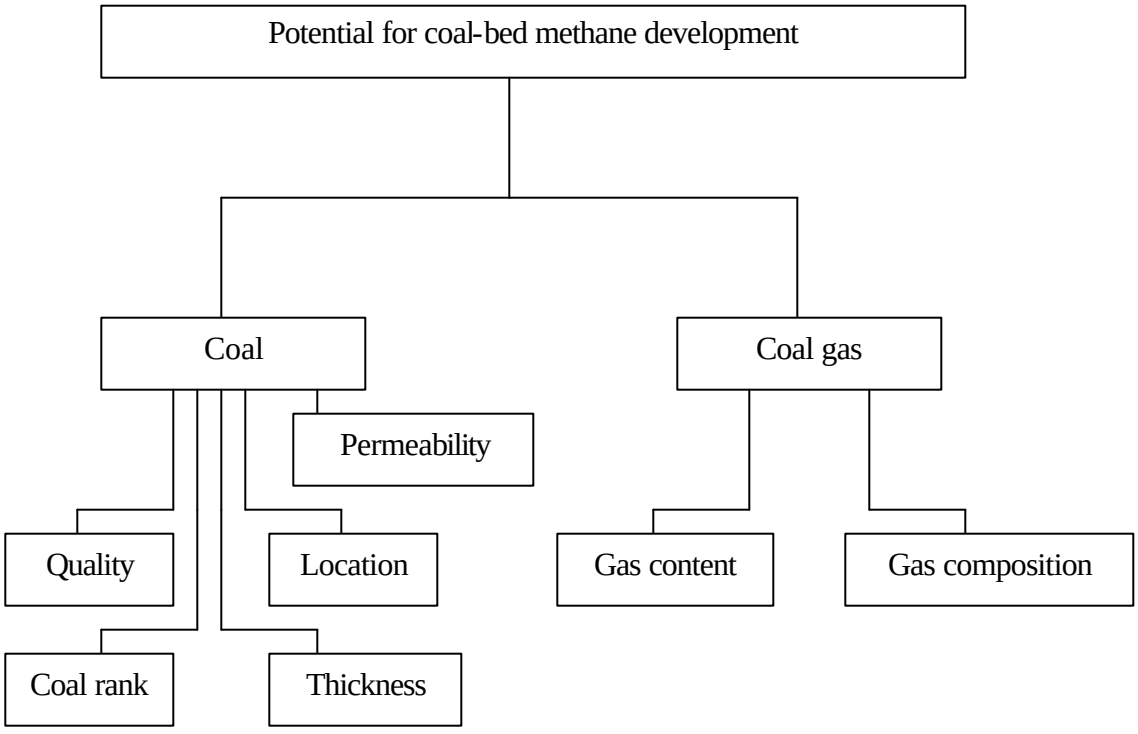

Figure 3.22 Important factors for coal bed methane development.
(modified from Wallace , 1990)

(1990) considered as important when dealing with the potential for coal bed methane development. Yong, Jianping and Dayang (1999) introduced a classification for coal bed methane resources in China. As shown in Figure 3.23, the coal beds are divided into three categories,

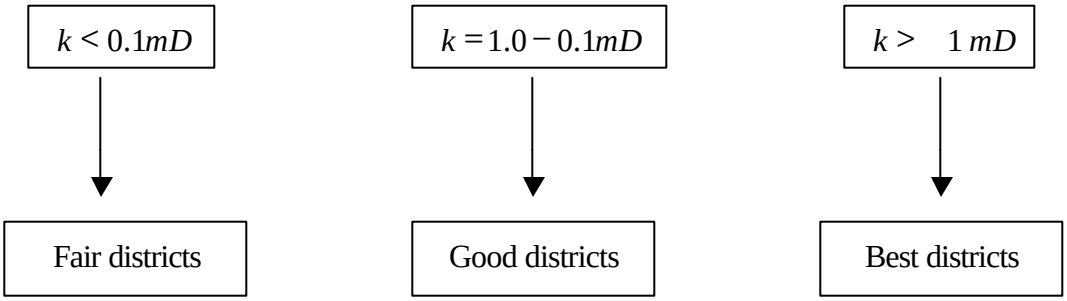

Figure 3.23 Chinese coal bed classification based on their permeability (after Yong, Jianping and Dayang, 1999).

Santillan (2004) classified coalbeds into four groups based on their insitu permeability (Figure 3.24).

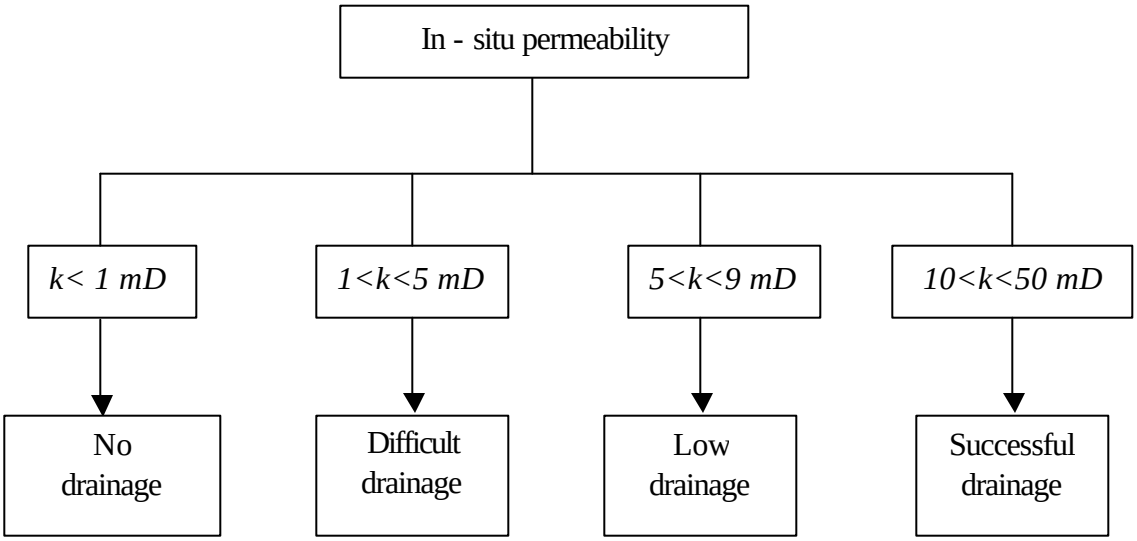

Figure 3.24 Classification of coal-beds based on their permeability (after Santillan, 2004).

Hughes and Logan (1990) stated that the minimum required permeability of coal for coal-bed gas drainage is generally greater than 1 mD. However for Australian coals, Thomson and MacDonald (2003), referring to the work by Williams (1999), indicated that the Australian coal seams suitable for drainage (medium radius drill method) should have a gas content of more than 6 m^3/t gas and permeability bigger than 2 mD at a depth of 150 to 500 m as illustrated in Figure 3.25.

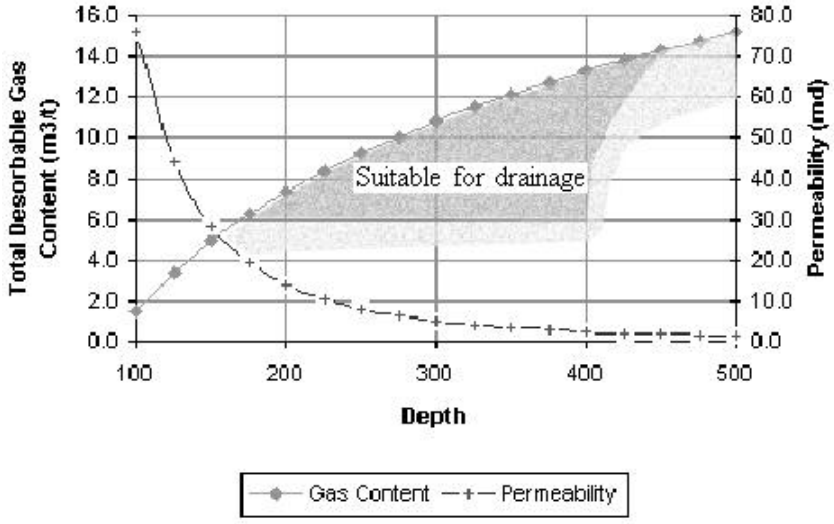

Figure 3.25 Permeability and gas content relationship with depth (after Thomson and MacDonald, 2003).

It should be mentioned that these classifications are based on using currently available technology and commercial conditions. In future, advanced development may occur to enhance drainage at lower coal permeability. None of these mentioned categories considered the coal gas content. Those coal-beds, which have low gas content (1.8 m^3/tonne) and high permeability can be subjected to drainage, however, some environmental limitations occur such as water disposal (Aluko, 2001).

3.5.2 Outburst classification

As defined in Chapter two, the tendency of a coal seam to outburst depends on a number of factors that includes the total gas content and gas type, coal seam permeability, rate of development, length of gas drainage time and the presence of geological structures (Thomson, 2004). By combining the data from Gil and Swidzinski (1988) and Lama and Bodziony (1998) a diagram (modified from the original by Gil and Swidzinski, 1988) can be produced, which shows the correlation of coal permeability to outburst proneness for some Russian, Ukrainian and Australian coal mines (Figure 3.26).

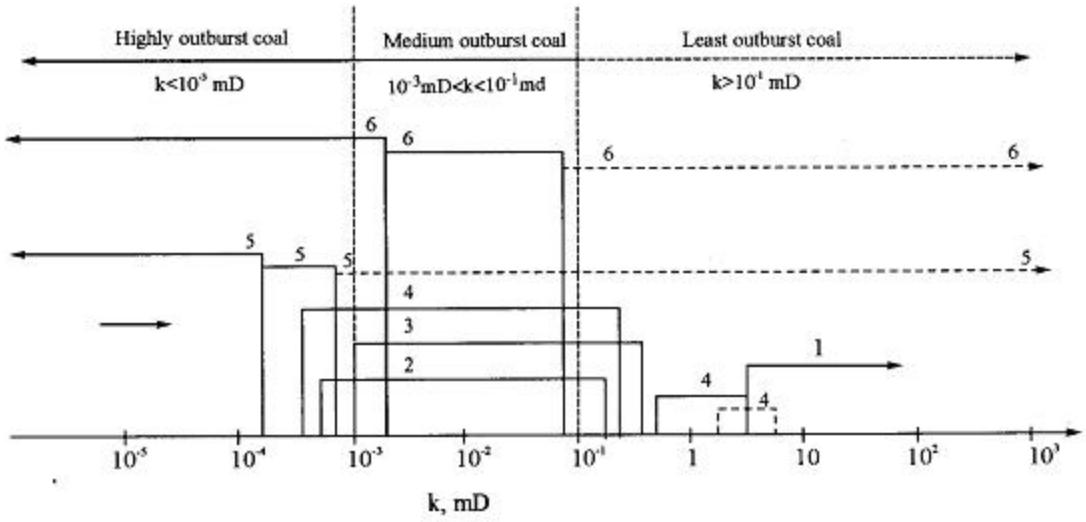

1. Lama and Bodziony
2. G. N. Feit
3. Institute IGC (Karaganda coal)
4. Institute IGC (Vorkuta coal)
5. O. J. Chemov (Kuznetsk coal)
6. Institute MakNII (Donetsk)

Figure 3.26 The relationship of permeability to outburst proneness (modified from Gil and Swidzinski, 1988).

The data presented in Figure 3.26 should be considered together with other factors such as coal gas content, the strength of the coal and geological aspects of the coal bed. For example, it must be noted that in low permeability coal-beds in the absence of outburst risk it may not be of great benefit to drain the gas from the coal-bed as a safety measure whereas it is possible that a coal-bed with high permeability can be subject to outburst. As is shown in Figure 3.27, an intrusion intersects a coalbed with high permeability, when mining towards the intrusion safe mining can be predicted

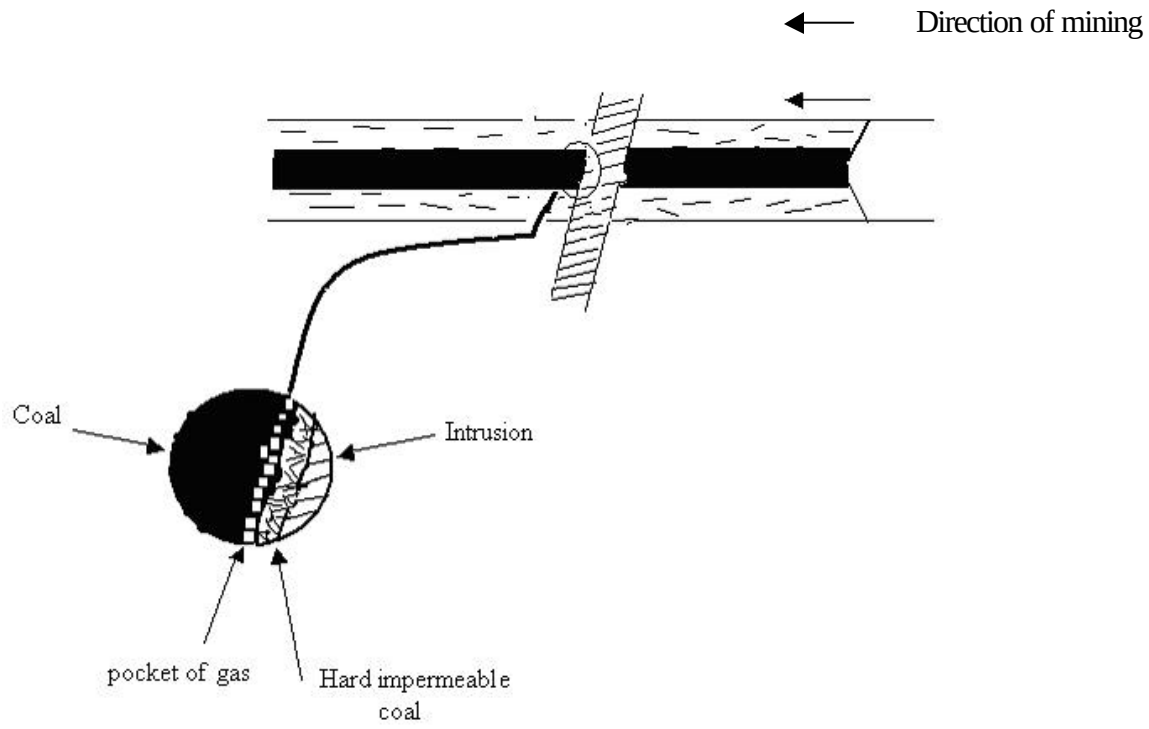

Figure 3.27 Intersection of an intrusion and a high permeability coal seam.

because of the easy release of gases due to the high permeability, however as mining approaches the intrusion an outburst prone zone will manifest. The reason is that at distance from the intrusion gas is released because of the high permeability of the

coal and the de-stressing and relaxation of the coal-bed near the face of the heading, but in the region of the intrusion it is held behind the intrusion, which acts as a barrier, resulting in an outburst prone zone. One of the ways of distinguishing these zones during pre-drainage drilling is explained by Hungerford (1995). He pointed out two characteristics, firstly, difficulty in penetration into the intrusion area and secondly, damaging the drill bits sooner than expected.

3.6 SUMMARY AND CONCLUDING REMARKS

This chapter provided evidence about the influence of coal matrix changes and permeability on coal drainage and outburst control phenomena. Gas drainage is a technique that has proved to be successful in reducing the outburst hazard by reducing the in-situ gas pressure. Coal seams with higher permeability show better gas drainage characteristics. However an outburst prone zone may be located beside an intrusion, even in a coal seam with high permeability.

Different factors such as petrography, mineral matters, stress and porosity play a significant role with respect to coal volume change and permeability. Accordingly, a series of experimental studies was undertaken to examine the interrelationships between various factors, which are the subject of study in the remaining chapters in this thesis.

The aims of matrix shrinkage tests are various. They are partly for measuring the internal pore surface of the coal matrix, also to provide the information to modify drainage system or mining method to reduce the risk of outburst. Some of the results, which have been reported by researchers, are as follows.

Expansion of the coal matrix parallel to the bedding is less than that perpendicular to the bedding. Gas type, coal type and rank play a significant role with respect to coal matrix swelling and shrinkage due to sorption / desorption.

There are different methods of measuring the in-situ permeability of coal, such as drilling boreholes from the surface for estimating the in-situ permeability before mining or using in-seam boreholes drilled from underground workings. It is preferable to conduct coal permeability tests in-situ, as it provides a true picture of the permeability properties of the coal. However, because of the cost of the field test process, the most widely used technique is by laboratory experimentation. Permeability is measured by the rate at which a fluid of standard viscosity can move along a given distance within a certain time.

CHAPTER FOUR

COAL PETROGRAPHY

4.1 INTRODUCTION

As discussed in the previous chapters, there are a number of factors that can contribute to the phenomenon of outburst in coal. The physical structure of coal has a significant influence on gas storage and its sorption. Also, the gas retention characteristics of coal for any type of gas are strongly influenced by the composition and mineralisation of the coal. A better knowledge of the coal mineralisation and composition constitute a realistic way to gain a better understanding of the role of coal composition in the outburst proneness of coal. This can be realised in practice by petrographic study of coals. Petrographic study involves the microscopic analysis of the mineral and maceral content of coal, such as vitrinite and inertinite. This chapter discusses the petrographic study of coal samples collected from a number of Australian underground mines and from one site in Iran. Details of the coal specimen preparation and the experimental apparatus used for the petrographic studies are described.

4.2 SAMPLE COLLECTION

Coal samples were obtained from different collieries in the Sydney Basin (Tahmoor,

Dartbrook, Metropolitan), the Bowen Basin (North Goonyella) and the Tabas coalfields in central Iran. Typical geological stratigraphy of the different sites is shown in Figure 4.1. (SS= Sandstone; LS= Limestone and Sha=Shale)

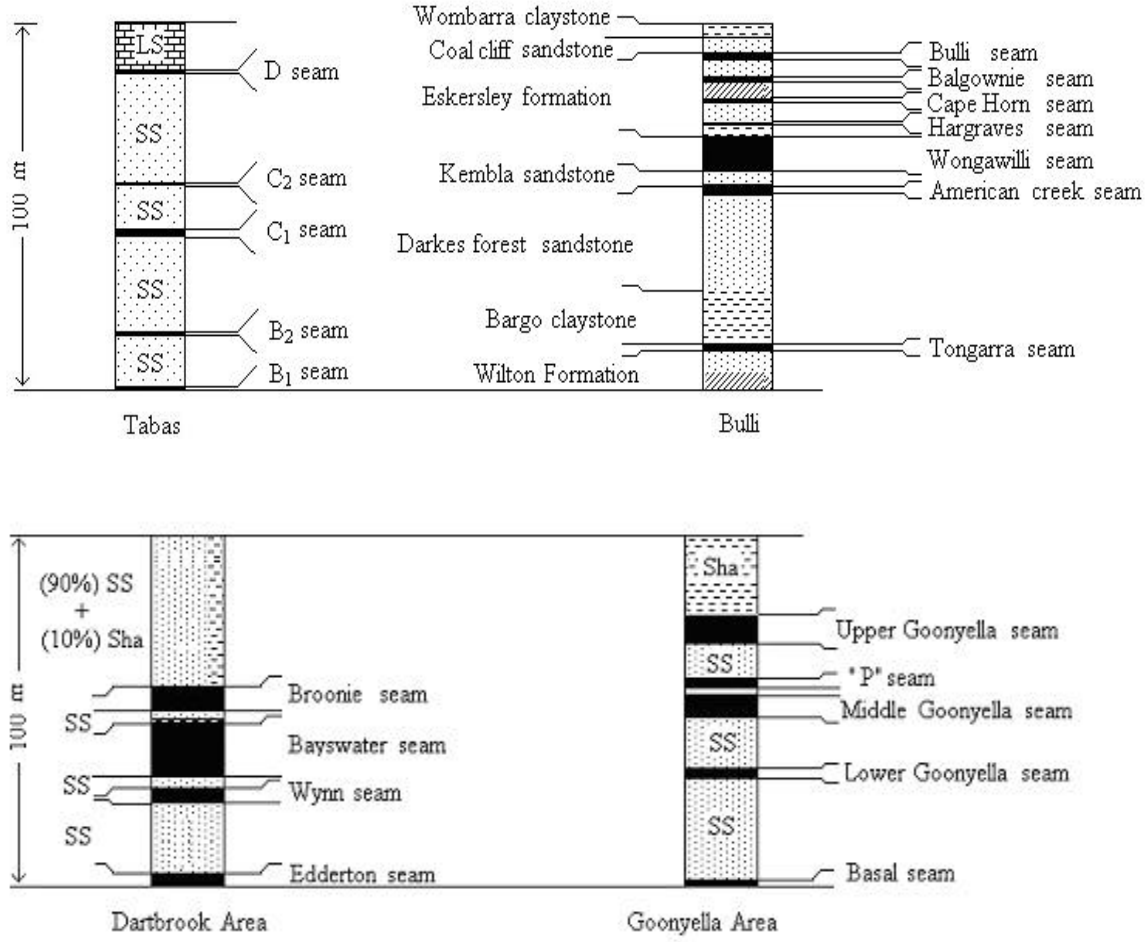

Figure 4.1 Representative lithological sections of the coal deposits.
(sources: Hulleatt, 1991, Jeffrey et al. 1997 and Fazl, 1990)

With the exception of Metropolitan Colliery Coal, coal samples were dug out from the freshly exposed coalface as lumps. Each lump of coal was immediately placed in a plastic bag and properly sealed to avoid prolonged exposure to air. Once in the

laboratory, the coal lumps were immersed in water to prevent oxidation and drying (Figure 4.2).

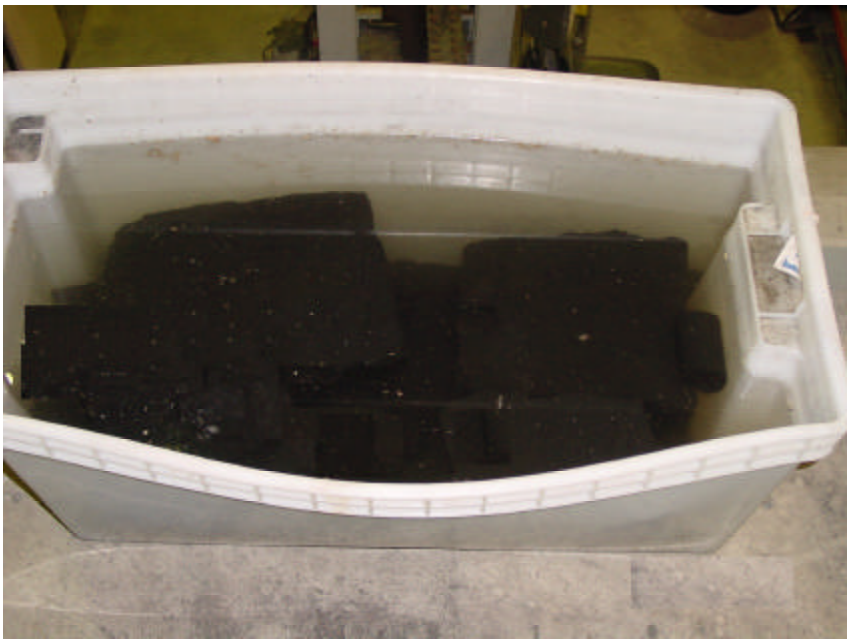

Figure 4.2 Coal lumps immersed in water.

Coal samples from Metropolitan Colliery were obtained as drilled cores and carted to the laboratory in sealed plastic pipe containers specially constructed for the purpose.

4.3 SAMPLE PREPARATION

The coal samples to be used for the petrographic study were made into polished cylinders approximately 20 mm in diameter using plastic moulds. Initially, the coal samples were initially crushed to particle sizes between approximately 100 *m*m and 0.7 mm. A 0.7 mm sieve was used to separate out large fractions. The oversize particles were re-crushed until all the coal particles were <0.7 mm. A riffle was used

to aid in the collection of sufficient representative samples to half fill the rubber mould. A cold setting polyester resin, consisting of 98% Astic resin and 2% hardener was mixed and added to fill the mould. The specimen and resin mixtures in the moulds were thoroughly stirred with a paper clip so that all coal grains were in direct contact with resin. The specimens were then placed in a special vacuum chamber at 70 kPa (absolute) for two minutes to remove air bubbles. Once the specimens were mixed and all air bubbles expelled, they were then left to set for 24 hours.

The final step in sample preparation was specimen polishing carried out on a rotating lapping machine (Figure 4.3). It was important to produce a highly polished face on the specimens to allow the collection of accurate reflectance data and to aid in maceral identification.

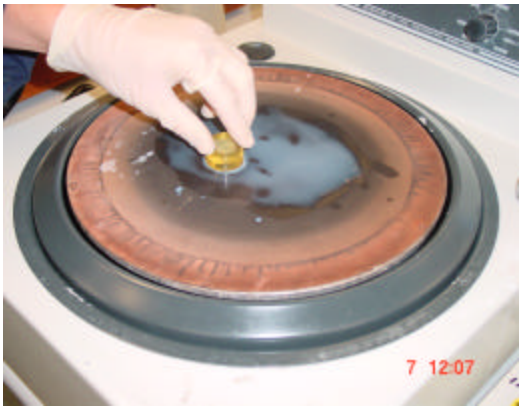

a) A sample polished on a lapping machine

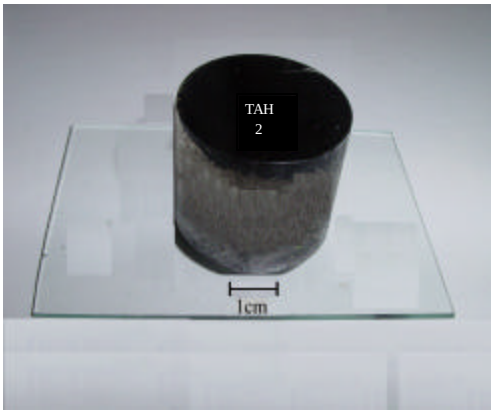

b) Finished sample

Figure 4.3 Polished sample on lapping machine.

A coarse carborundum paper was initially used to remove sharp edges from one face of the specimen to allow for easy handling. After this, 240 grit carborundum paper was used to polish the opposite face manually. After several strokes, the polished face was rotated 90 degrees and polishing continued.

The specimen face was periodically flushed and cleaned with soap and water, then alcohol was sprayed on the face and it was dried with an automatic heater. This process was repeated until a smooth and shiny face was created. The aim of this exercise was to successively polish the specimen to greater degrees of smoothness, so as to remove surface scratches and to create a surface of maximum quality free from surface roughness, using 400, 600 and 1200 grit papers successively and pouring "Diamond Polishing Solvent",

4.3.1 Microscopy

A Leitz MPV-2 microscope was used for maceral analysis. Reflected white light andfluorescence mode illumination were used with 32x and 50x oil immersion objectives giving a total magnification of approximately 400x to 500x. Figure 4.4 shows a general view of the Leitz orthoplan microscope and the Leitz MPV-2 photometer.

Point count analysis utilizes a swift automatic point counter and mechanical stage. The composition of the specimens was examined under oil immersion with the microscope at a total magnification of 320x. A mechanical stage was used to move the specimens under the objective lens in a regular manner.

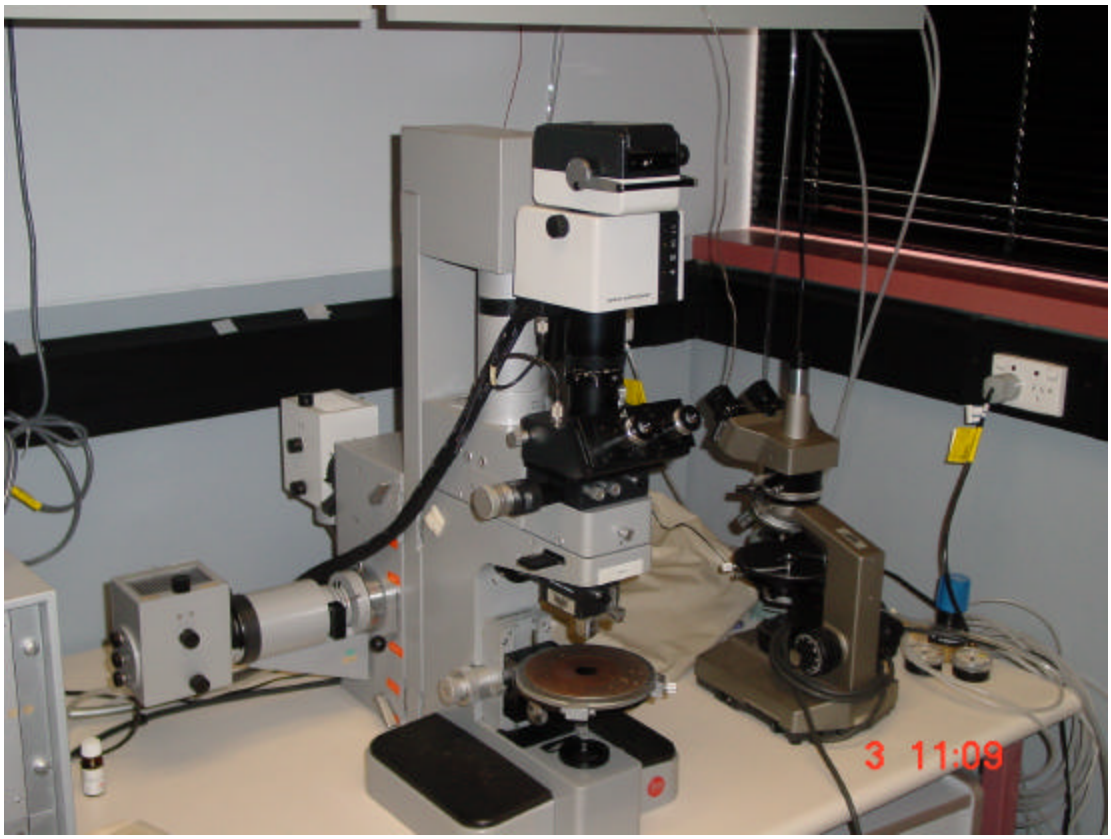

Figure 4.4 A general view of Orthoplan maceral microscope with MPV-2 photometer.

Point counts were thus carried out with a regular east west (or column) spacing of 0.6 mm and a north south (or row) spacing also of 0.6 mm. These spacing were selected so that the likelihood of counting any one particular grain (maximum size of 0.7 mm) twice was very low. The objective lens had a small cross-hair inscribed in its centre. Each time the lens was moved to a new position the coal component under the cross-hair was identified and recorded. Where the movement controller moved the objective lens and cross-hair over the specimen resin, the point was ignored and the lens moved to the next point.

A minimum of 500 points were counted for each specimen in this manner. Care was taken to ensure that point readings were taken at the end of the last row (the row in which the 500th point was recorded), so as not to create a composition bias due to grain sedimentation in the resin. Each coal component was classified into one of the following:

- Vitrinite (VIT)
- Inertinite (INT)
- Liptinite (LIP)
- Pyrite (PYR)
- Carbonate (CAR)
- Other Mineral Matter (OMM)
- Cavity (CAV)
- Fracture (FRA)
- Tabas coal sample (TAB)
- Tahmoor coal sample (TAH)
- Dartbrook coal sample (DAR)
- Metropolitan coal sample (MMP)
- North Goonyella coal sample (NGO)

4.4 PETROGRAPHICAL TEST RESULTS

4.4.1 Tabas coal samples

The Tabas coal deposit has three mineable seams (C_1, B_1, B_2) according to Fazl (1990), and the coal samples used in this study were all obtained from one location in deposit C_1. Table 4.1 shows the results of petrographic point counts. There appears to be no marked differences in the maceral and mineral content of all five samples being tested. Pyrite and carbonate elements are listed separately from the rest of the mineralisation column because of the role they play in coal sorption behaviour. Also listed independently is the cavity column, which describes the cracks and fissures which both play an important part in gas sorption in the coal mass.

Figure 4.5 shows how the pyritic matter occurs as individual crystals associated with vitrinite maceral. As can be observed, the Tabas coal samples were vitrinite rich (Table 4.1) and the average vitrinite point count numbers constituted around 72% of the total, which is within the range between 68% and 100% that was reported by Fazl (1990). Figure 4.6 shows a reflected white light image of a vitrinite rich sample from Tabas.

Table 4.1 Tabas coal composition and mineralisation.

Sample	VIT %	INT %	PYR %	MMO %	CAR %	CAV %	FRA %	TOTAL %
TAB 1			.0		.0	.0	.0	100
TAB 2	68.8	14.6	2.6	2.5	2.0	6.6	3	100
TAB 3	69.3	8.8	1.9	4.1	2.9	8.9	3.9	99.8
TAB 4	73.2	9.8	2.1	4.9	1.2	7.2	1.4	99.8
TAB 5	77.5	7.7	1.3	2.8	2.8	6.8	1.0	99.9
Average	**71.9**	**9.5**	**2.18**	**3.68**	**2.18**	**7.9**	**2.66**	

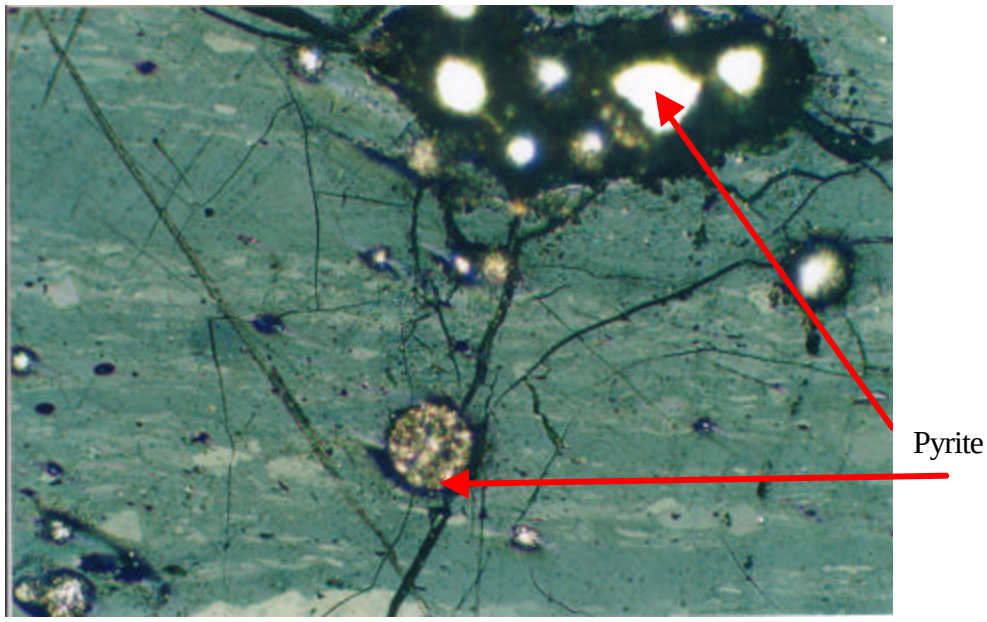

Figure 4.5 Framboidal pyrite (lower) and larger pyrite grains in vitrinite in Tabas coal sample. Reflected white light image; Field width = 0.54 mm

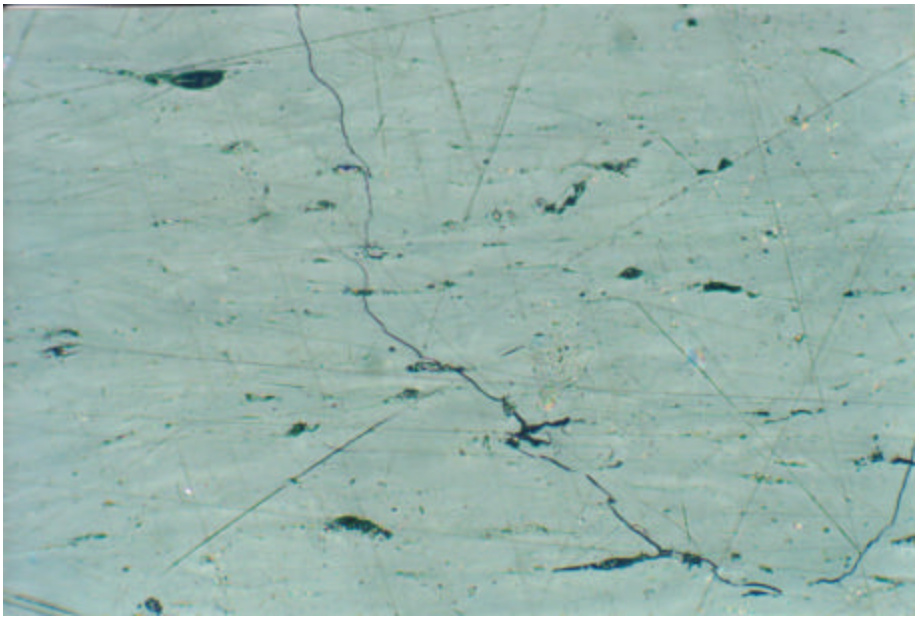

Figure 4.6 Vitrinite with cell lumen, originally filled with fine grained mineral matter, in Tabas coal sample.
Reflected white light image; Field width = 0.54 mm

4.4.2 Tahmoor coal samples

Coal samples from Tahmoor mine were collected from two panels in the Bulli seam. The 800 and 900 Panels, which were divided by a dyke. As a result the 800 Panel was in a benign zone while the 900 zone was described as geologically disturbed. Bulli seam coal, a high quality coking coal, is extensively mined within the Illawarra Coal Measure deposit of the Sydney Basin. The other seams in the Illawarra Coal Measure formation in descending order from the Bulli seam include, Balgownie, Cape Horn, Wongawilli, American Creek, Tongarra and Woonona seams. The thickness of the Bulli seam at Tahmoor Colliery generally varies from 1.6m to greater than 2.5m. The depth of workings can range from 380m to 450m below the surface. The Bulli seam section usually occurs as a single unit of coal, although shale and other dirt bands can occur from time to time in various portions near the floor and roof of this seam. Table 4.2 shows the mineral composition analysis obtained from both the 800 and 900 Panels, respectively.

Table 4.2 The results of petrographic point counts for Tahmoor Colliery samples.

Sample	VIT %	INT %	LIP %	MMO %	CAR %	CAV %	FRA %	TOTAL %
Panel 800								
TAH 1	75.8	22.7	0.8	0.8	0	0	0	100.1
TAH 4	75.0	19.7	1.8	0.9	0	2.5	0	99.9
TAH 5	71.4	21.8	1.8	1.0	0	3.8	0	99.8
TAH 7	77.8	20.2	0.0	0.8	0.2	0.8	0	99.8
TAH 8	77.4	19.1	0.7	0.6	0.2	1.8	0	99.8
Average	**75.5**	**20.7**	**1.0**	**0.8**	**0.2**	**1.8**	**0**	
Panel 900								
TAH 2	69.0	25.8	0.8	3.2	1.1	0	0	99.9
TAH 3	56.0	31.6	1.6	7.3	2.7	0.6	0	99.8
TAH 9	57.8	28.6	1.4	4.8	4.7	0.9	2	100.2
Average	**60.9**	**28.7**	**1.3**	**5.1**	**2.8**	**0.5**	**0.6**	

It can be noted from the Table 4.2 that the vitrinite content for the 800 zone is greater than for the 900 Panel, and this difference will be reflected in the permeability and coal volume change characteristics.

From Figure 4.7 it can be seen that typical grains have abundant vitrinite. Also present, but in lesser proportions, are a mixture of vitrinite and inertinite and a large piece of calcite that infilled a cleat prior to sample preparation. Calcite-filled cleats reduces coal permeability and impede gas desorption. Figure 4.8 shows the typical composition of the Tahmoor coal, which is characterized by inertinite layers and mixed vitrinite-inertinite layers. Figure 4.9 shows vitrinite with a clay-filled cell lumen. A clay filled lumen generally impedes permeability causing difficulties in effective coal degassing.

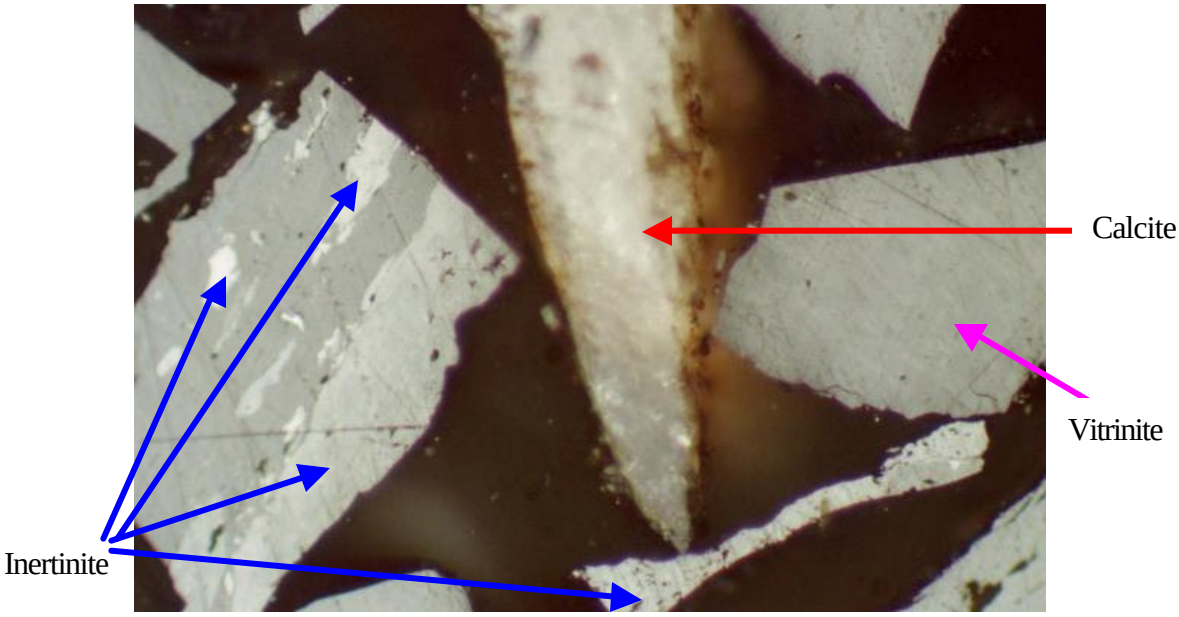

Figure 4.7 Tahmoor coal showing calcite, and coal grains with vitrinite/inertinite or vitrinite only. Reflected white light image; Field width = 0.54 mm

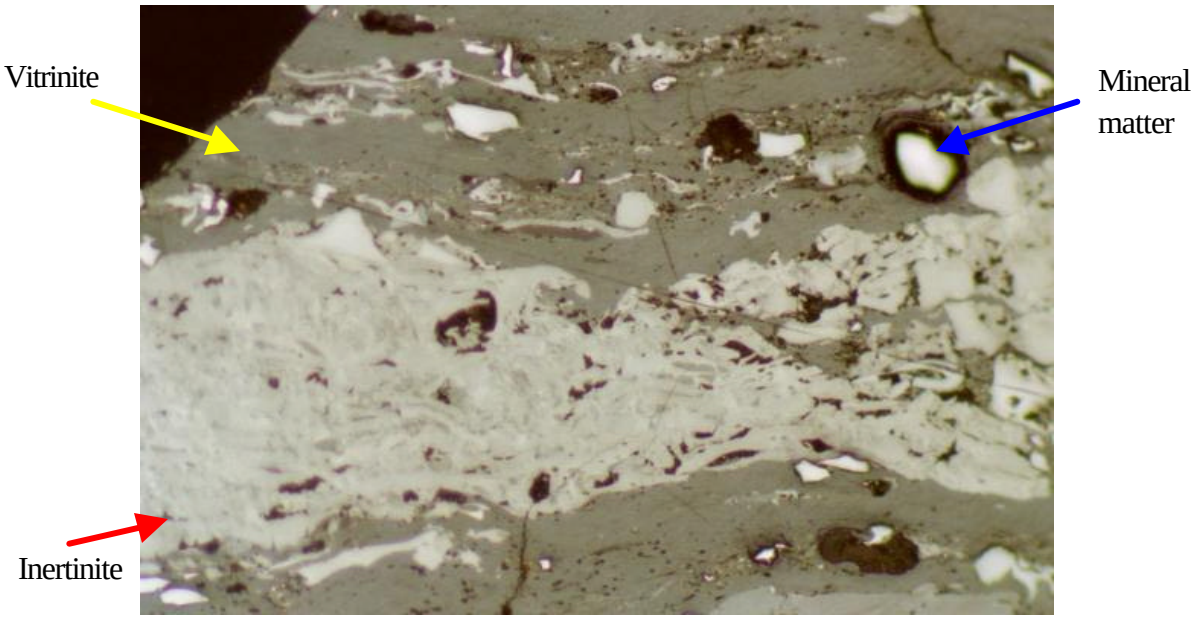

Figure 4.8 Tahmoor coal composed of inertinite (white) and vitrinite. Reflected white light image; Field width = 0.54 mm

Figure 4.9 Tahmoor coal with abundant clay filled cell lumen in vitrinite. Reflected white light image; Field width = 0.54 mm

As stated above, the coal composition is different between the 800 and 900 Panels with the 800 Panel coal having a greater percentage of vitrinite in comparison to the 900 Panel coals. The ramifications of these variations will be further examined when dealing with coal permeability and the shrinkage properties of coal later on.

4.4.3 Dartbrook coal samples

Coal samples from Dartbrook Colliery were collected from the Wynn seam. The mine commenced operation in 1996, mining coal by retreat longwall mining. The Wynn seam is a low sulphur, high volatile bituminous, thermal coal, situated about 350m below ground with a working section of between 4.0 and 4.5 m.

The coal cleats are filled by calcite, which greatly influences the permeability. Carbon dioxide is the dominant gas in Dartbrook Colliery with methane as a minor gas (Crosdale, 1998). The results of point counts are shown in Table 4.3.

Table 4.3 The results of petrographic point counts for Dartbrook Colliery samples.

Sample	Vit %	INT %	LIP %	MMO %	CAR %	CAV %	FRA %	TOTAL %
DAR 1	39.9	39.2	1.4	4.9	9.9	2.3	2.2	99.8
DAR 2	40.2	33.3	1.8	6.6	15.5	2.4	0	99.8
DAR 3	44.3	35.2	1.1	4.5	12.8	0.9	1.1	99.9
DAR 4						.7	0	99.8
DAR 5	39.8	31.5	0.6	4.8	16.1	5.6	1.4	99.8
Average	**40.68**	**35.56**	**1.1**	**5.28**	**13.88**	**2.38**	**0.94**	

It can be seen that the tested coal has a relatively low percentage of vitrinite, and its inertinite component is high in comparison with Tahmoor coal samples. Figure 4.10 shows inertinite as the major maceral, while in Figure 4.11 it is a combination of vitrinite and inertinite.

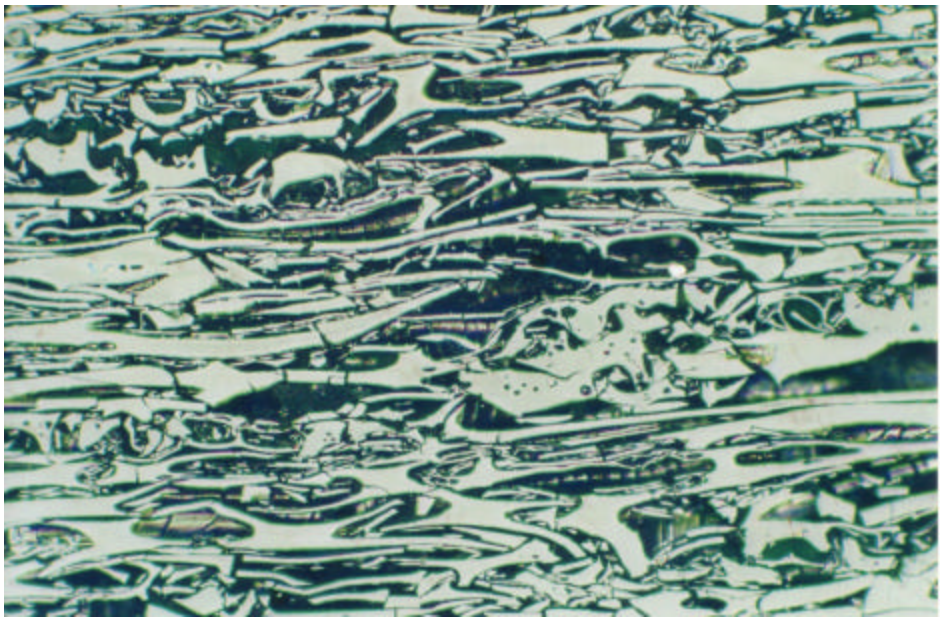

Figure 4.10 Inertinite in Dartbrook coal. Reflected white light image. Field width = 0.54 mm

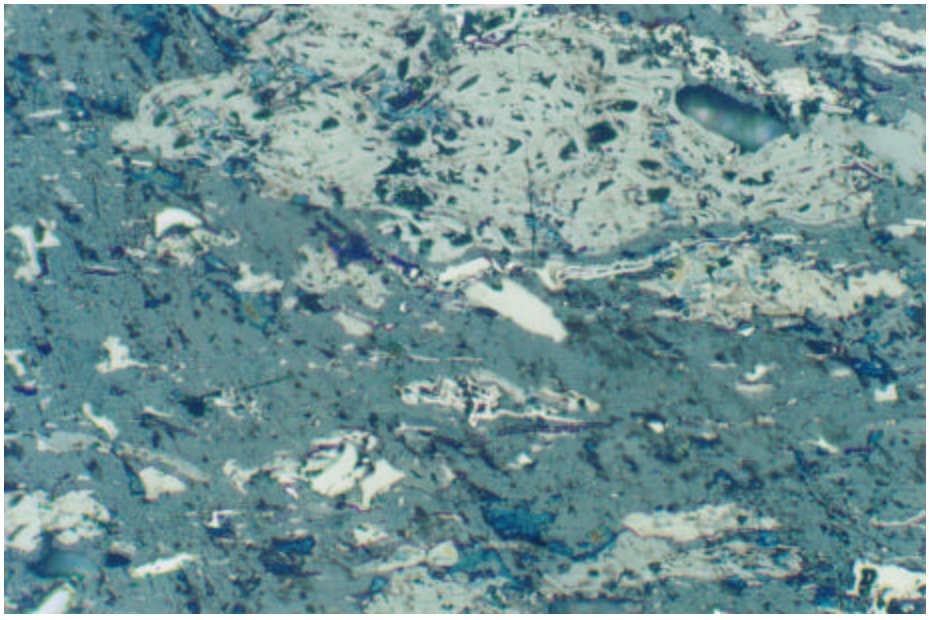

Figure 4.11 Dartbrook coal composed of vitrinite and inertinite (white). Reflected white light image; Field width = 0.54 mm

4.4.4 Metropolitan coal samples

Table 4.4 shows the petrographic point counts for coal samples collected from Metropolitan Colliery. Metropolitan Colliery has a long history of outbursts. 154 outbursts have occurred at Metropolitan Colliery from 1895 till now, and in the largest one nearly 250 tonnes of coal were ejected. The presence of dykes and faults has resulted in changes in the seam gas composition, and according to Lama (1995b) the dominant gas at Metropolitan Colliery is CO_2. Also the current gas composition of the active part of the mine is mainly CO_2. In fact, the overall composition of coal at Metropolitan Colliery was similar to Panel 900 coal at Tahmoor. Under white light incident microscopy, clay minerals were distinguished by their dark and grainy colours. Also present in the sample is a small amount of polishing powder (Figure 4.12). Figure 4.13 shows the inertinite present within vitrinite.

Table 4.4 Petrographic point counts for Metropolitan Colliery samples.

Sample	VIT %	INT %	MMO %	CAR %	CAV %	FRA %	TOTAL %
MMP 1	61.1	24.5	2.6	0	5.9	5.7	99.8
MMP 2	54.3	30.9	2.3	1.8	5.7	5.4	99.8
MMP 3	59.8	28.1	1.9	0	5.8	4.6	99.9
MMP 4	59.1	28.0	2.0	0	6.2	4.5	99.8
MMP 5	56.3	29.0	2.8	0.8	5.8	5.1	99.8
Average	**58.12**	**28.1**	**2.32**	**0.52**	**5.88**	**5.06**	

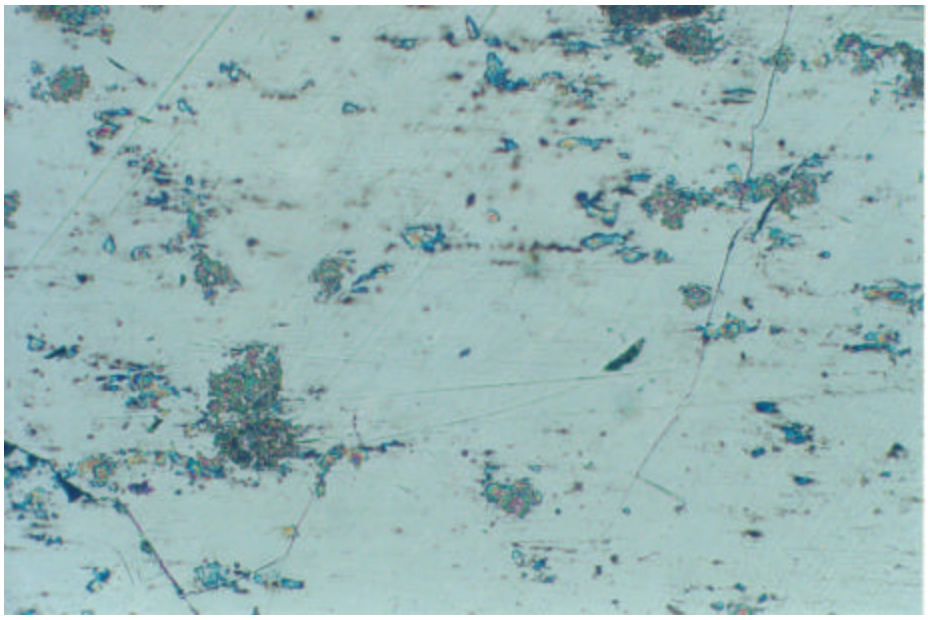

Figure 4.12 Metropolitan coal with vitrinite and polishing powder adhering to the surface. Reflected white light image; Field width = 0.54 mm

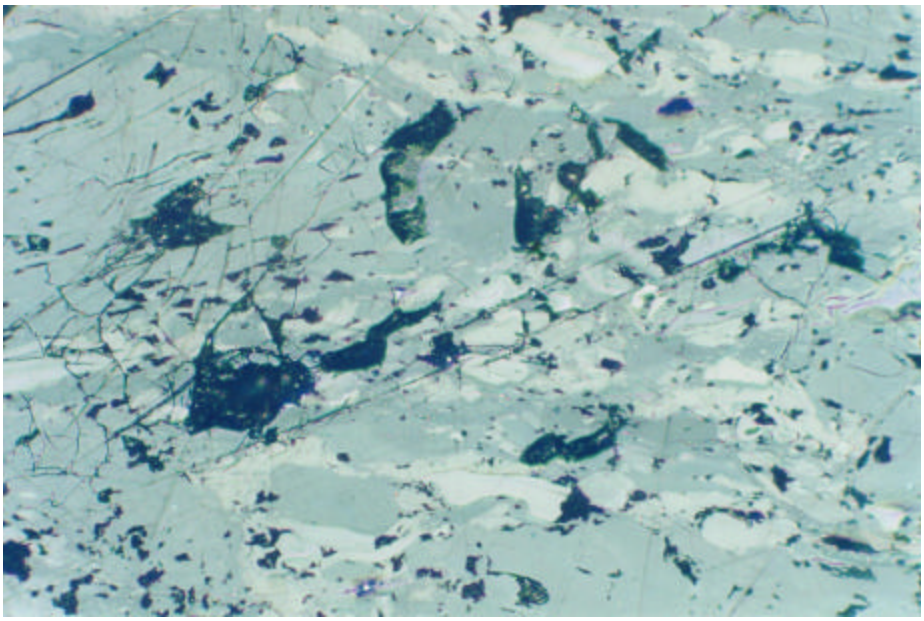

Figure 4.13 Metropolitan coal composed of inertinite (white) and vitrinite. Reflected white light image; Field width = 0.54 mm

4.4.5 North Goonyella coal samples

Table 4.5 shows the point counts for North Goonyella coal samples. North Goonyella coal has a very low percentage of vitrinite and a very high percentage of inertinite in its composition as shown in both Figures 4.14 and 4.15, respectively.

Table 4.5 Petrographic point counts for North Goonyella Colliery samples.

Sample	VIT %	INT %	PYR %	MMO %	CAV %	FRA %	TOTAL %
NGO 1	24.8	56.5	0.7	6.5	7.2	4.3	100.0
NGO 2	25.3	61.1	0.8	6.2	3.1	3.4	99.9
NGO 3	29.1	57.2	0.5	4.0	5.8	3.2	99.8
NGO 4	24.3	58.0	0.9	7.0	6.5	3.1	99.8
NGO 5	30.0	52.3	0.9	5.5	7.6	3.7	100.0
Average	**26.7**	**57.02**	**0.76**	**5.84**	**6.0**	**3.54**	

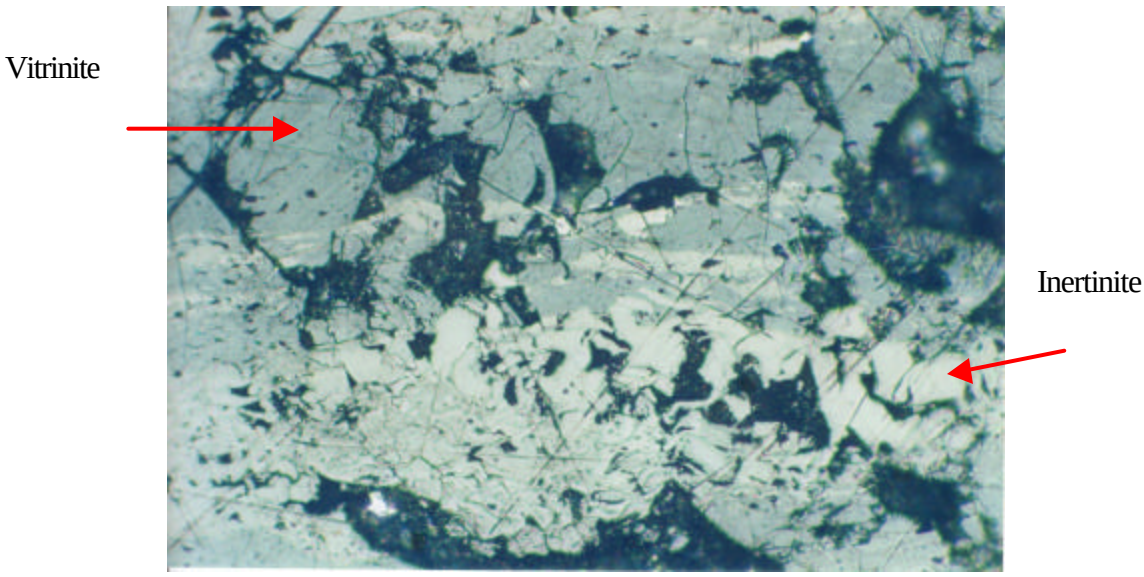

Figure 4.14 North Goonyella coal composed of inertinite with many cell lumen(white) and vitrinite with many fractures.
Reflected white light image; Field width = 0.54 mm

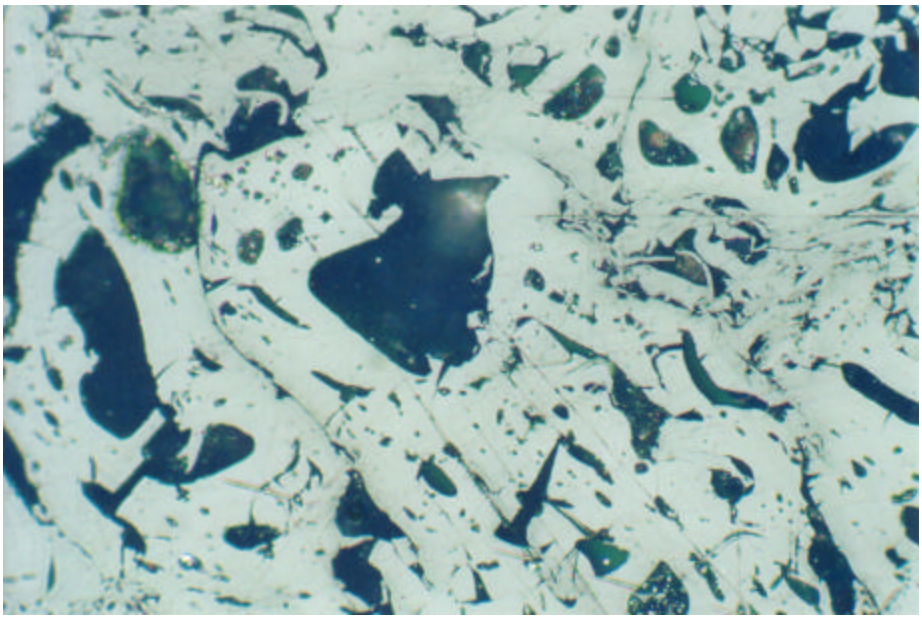

Figure 4.15 North Goonyella coal composed of inertinite with numerous cell lumen. Reflected white light image; Field width = 0.54 mm

It should be noted that at North Goonyella coal mine the dominant gas is CH_4. Hargraves (1986) related the CO_2 in the coal measures of eastern Australia to the progress of tertiary vulcanism. Where magmatic intrusions occur in coal seam, such as at Tahmoor, Dartbrook and Metropolitan coalmines, the likelihood of CO_2 presence is strong. This explains why there is the absence of CO_2 at North Goonyella and Tabas coalmines.

4.5 DISCUSSION AND SUMMARY

The point count analysis average results are shown in Figure 4.16. The bar chart shows correlations between different coal type compositions. Tabas Coal has the highest vitrinite concentration (70%) and lowest inertinite elements (9.46%) compared to the other coal samples. The lowest vitrinite content was obtained from

North Goonyella. The latter, however, had a significant proportion of inertinite, which makes it a poor quality coal in comparison with the other coals. The quality of Bulli coal is inferior to that of Tabas, but superior to other coals obtained from Dartbrook and North Goonyella respectively.

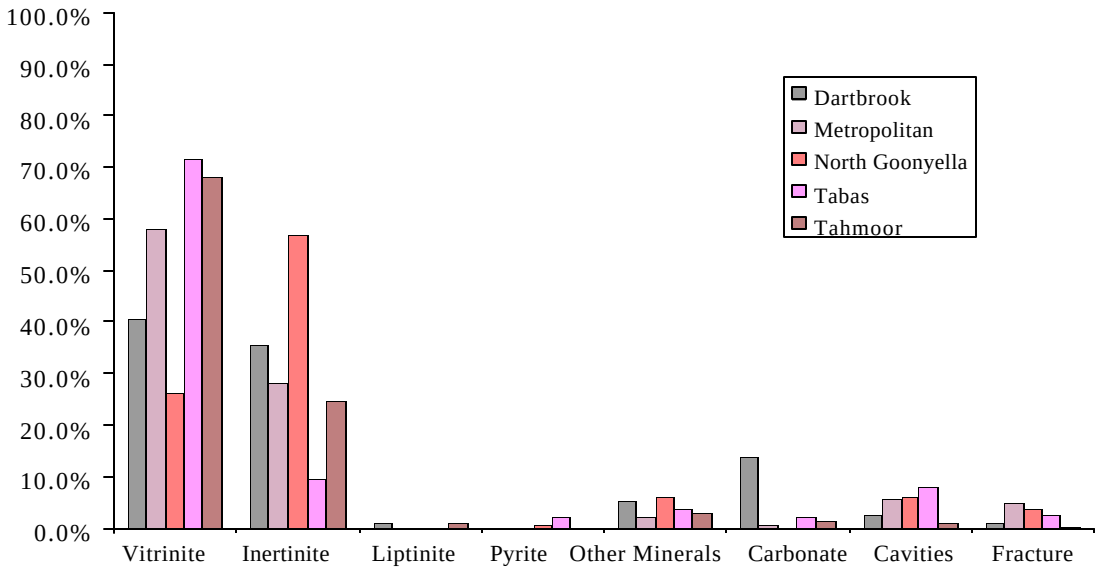

Figure 4.16 Bar chart of point count compositions of all the coals.

It is interesting to note that there is a marked similarity in coal composition between the Metropolitan coal sample and the Tahmoor 900 Panel coals. This is expected as both sample locations are geologically structured with some intrusions. It is a well-known fact that gas composition often changes in the Metropolitan Colliery Bulli seam between methane and carbon dioxide, and such variations may be the results of intrusions and geological disturbances.

Thus, the significance of this petrological study with respect to the proneness of coal to outburst will be brought to light when the coal composition elements are further assessed with respect to coal permeability and volumetric matrix change in different gas environments. This will be the subject of further research reported in the following chapters.

CHAPTER FIVE

INFLUENCES OF GAS ENVIRONMENT ON VOLUMETRIC COAL MATRIX CHANGE

5.1 INTRODUCTION

Significant studies are reported on coal matrix shrinkage tests conducted on coal samples from overseas and on a limited number from Australia. There is, however, limited reporting of the relationship between coal matrix shrinkage and parameters such as coal permeability, mineralogy and adverse geological conditions. This is of particular importance to the Australian coal industry, with regard to the establishment of a credible databank for Australian coals.

This chapter is primarily concerned with experimental studies related to coal volume change under various gas types and pressures. All these tests were performed at a constant normal temperature of 25^{o}C. The gases used in the study were CH_4, CO_2, CH_4/CO_2 (50%), and N_2. Two types of tests were conducted on each sample, the adsorption test for coal swelling and the desorption test for coal shrinkage. All tests were conducted at incremental pressure changes of 0.5 MPa. A total of 125 tests were conducted with respect to volumetric change behaviour in different gases.

5.2 COAL SAMPLE PREPARATION

Core samples 50 mm in diameter were drilled out of the coal lumps collected from five different locations as described in Chapter 4. Figure 5.1 shows the flow diagram for the coal sample preparation and testing procedure. Prior to drilling the cores, each irregularly shaped coal lump was first cast in a regular shaped concrete block base to permit easy drilling.

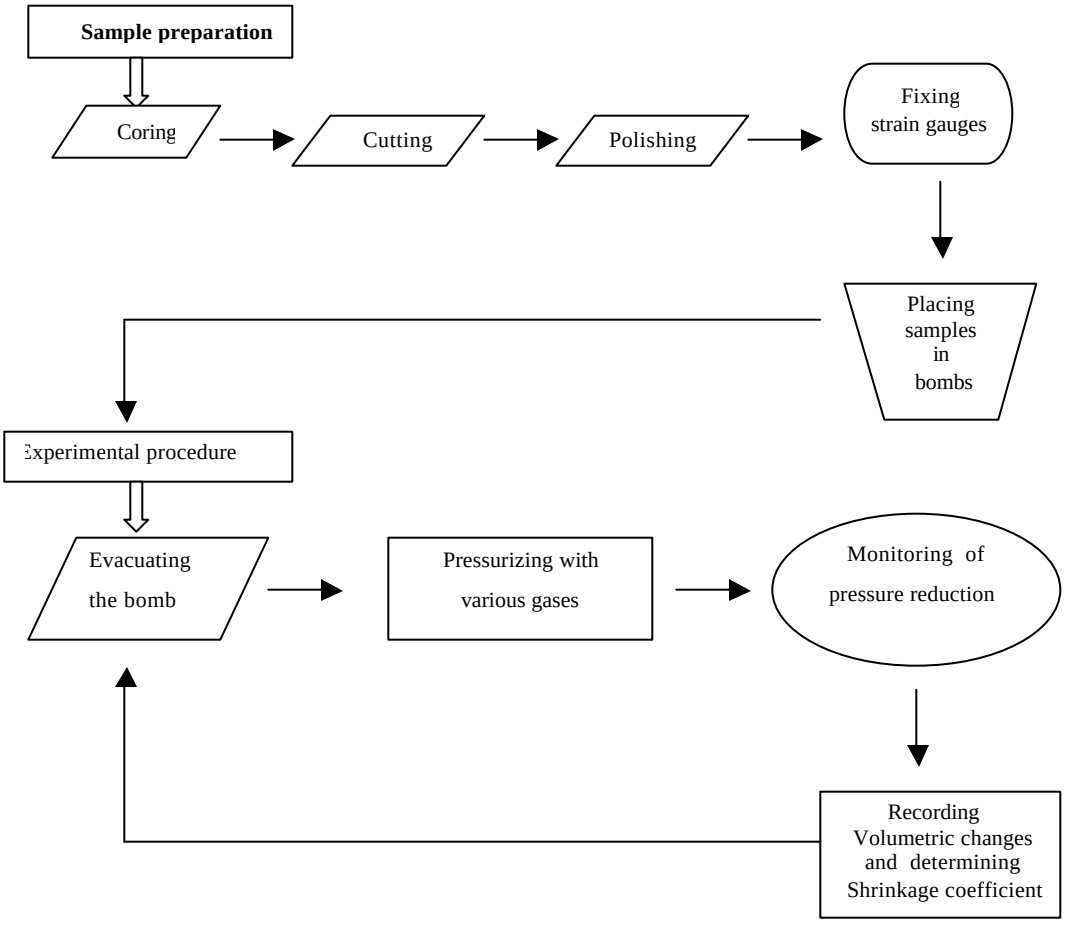

Figure 5.1 Flow diagram of coal sample preparation and shrinkage testing

A diamond tipped core drill was used to drill the cores as shown in Figure 5.2. The cored samples were then cut to 50 mm lengths using a circular saw. The ends of each core sample were cut, polished and ground flat with a lapping machine in accordance with the International Society of Rock Mechanics (ISRM) standards. Once the core samples were fully prepared they were re-immersed in water until the time of testing.

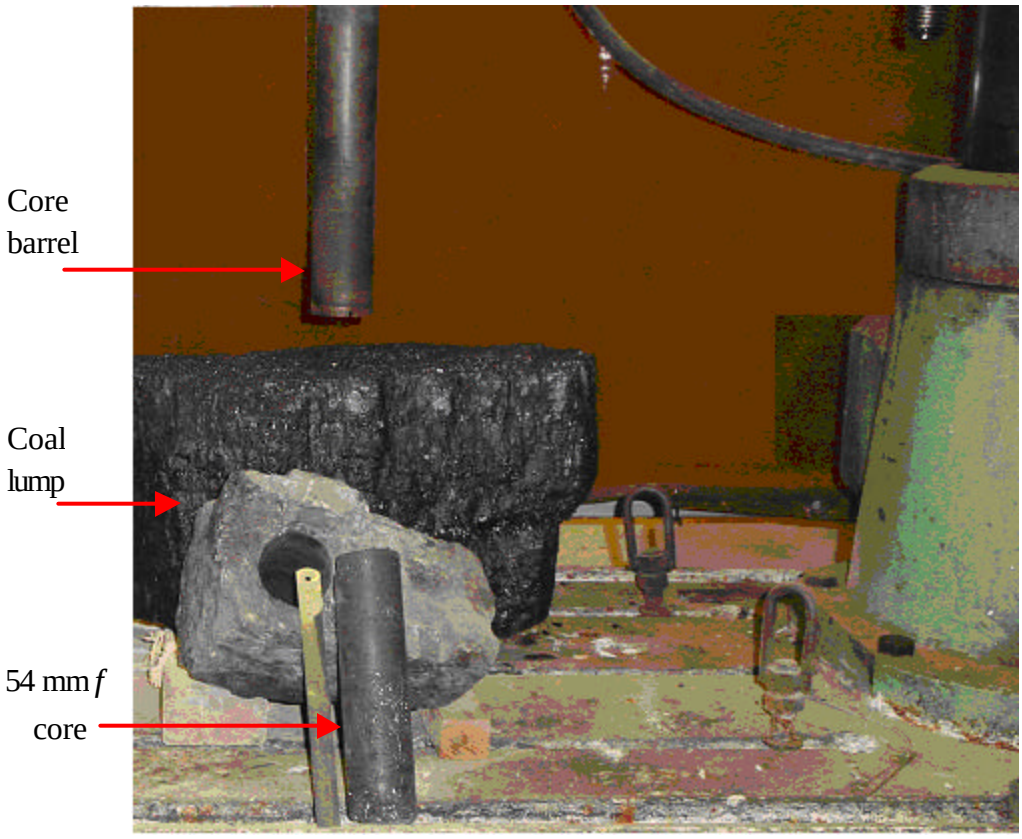

Figure 5.2 Coal core drilled out of coal lump.

5.2.1 Sample instrumentation

A set of four strain gauges was mounted at mid-height on each sample to monitor both the axial and radial strains in the coal sample. Two strain gauges were mounted

parallel to the sample axis, but diametrically opposite. The other two were circumferentially glued around the sample and 180^{o} apart. Figure 5.3 shows a typical specimen with instruments and wires attached, which were to be connected to the bomb lid terminals for data retrieval. A data-logger DT-500 (Data Taker brand) connected to a PC was used for data retrieval from the samples during the sorption process and subsequent analysis.

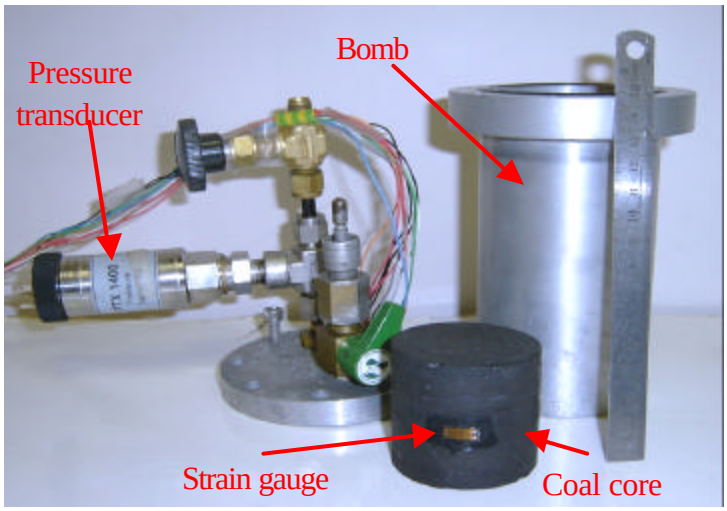

Figure 5.3 Coal sample with instruments.

5.2.2 Sample preconditioning and testing

Volumetric matrix change or coal swelling/shrinkage tests were conducted in pressure vessels in a adsorption / desorption apparatus as shown in Figure 5.4 and described elsewhere by Lama and Bartosiewicz (1982) and later by Aziz and Ming-Li (1999). The pressure vessels, known as 'Bombs' (Figure5.5) were modified to

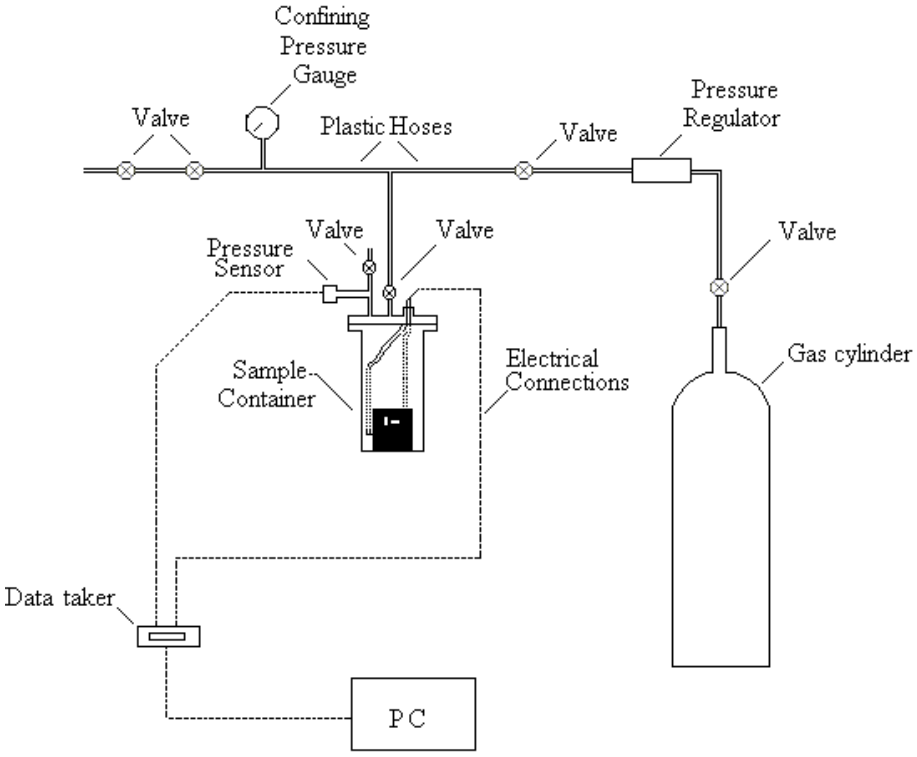

Figure 5.4 Schematic diagram of apparatus for testing volumetric change in coal

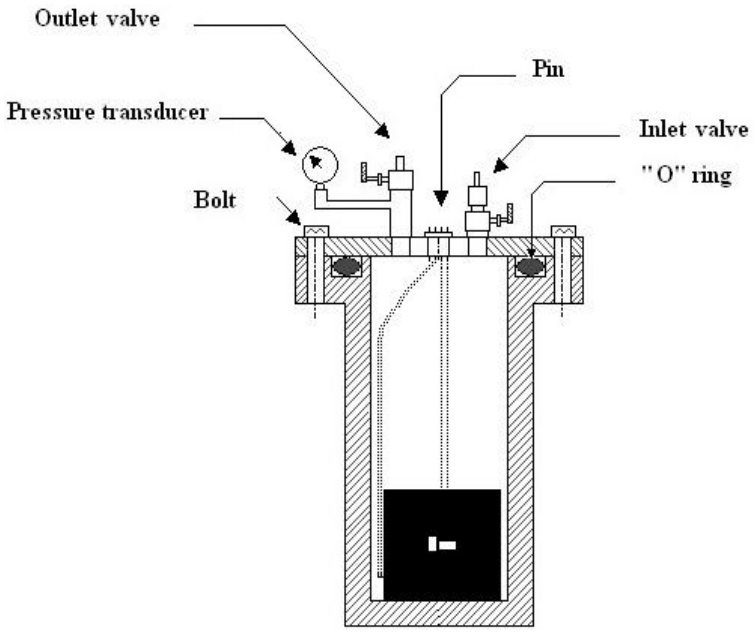

Figure 5.5 Sample container (Bomb)

include individual pressure transducers. A total of 18 bombs were constructed for two sets of sorption apparatus, and one set of six bombs was subsequently modified and used for coal shrinkage testing. Coal samples were sealed in the bombs and evacuated for 24 hrs in order to remove any other gases in the coal. They were then pressurised with a predetermined gas type up to 3 MPa pressure, which is typical of the gas pressures found in Australian coals, as measured by Lama and Bartosowicz (1983) in West Cliff Colliery. However, the Bulli seam gas pressure can reach up to 5 MPa, particularly in some parts of the seam near Tahmoor and in the now closed nearby Oakdale mine workings. The sample containers (bombs) were kept immersed in a constant temperature ($25^{o}C$) controlled water bath, but were isolated from the water bath by copper sleeves to keep them dry. Two types of test were made on each coal sample:

- Adsorption test to determine the volumetric swelling of coal in different gases and pressures
- Desorption test for coal volume shrinkage in different gases and pressures.

The sample was pressurised to 3MPa and then the gas was discharged in incremental steps of 0.5 MPa every 100 minutes. Changes in the volume of the coal were monitored and automatically recorded at regular intervals during the sorption and desorption process via the Data-Taker and PC.

Following completion of one set of tests for a given gas type, the bomb was evacuated and the procedure repeated for the other gases. Changes in the volume of

the coal matrix were calculated using the average of the two strains in the axial and radial directions. The calculation procedure was:

$$V = p \times r^2 \times h \tag{5-1}$$

$$\ln V = \ln (p \times r^2 \times h) \tag{5-2}$$

$$\ln V = \ln p + 2 \ln r + \ln h \tag{5-3}$$

As

$$\ln p = \text{Constant} \tag{5-4}$$

Then;

$$\frac{\Delta V}{V} = 2 (\frac{\Delta r}{r}) + (\frac{\Delta h}{h}) \tag{5-5}$$

Where:

h = The height of sample, cm

r = The radius of sample, cm

V = the volume of sample, cm^3

$\frac{\Delta V}{V}$ = Volumetric strain, dimensionless

$\frac{\Delta r}{r}$ = Average radial strain, dimensionless

$\frac{\Delta h}{h}$ = Average axial strain, dimensionless

5.3 VOLUMETRIC CHANGE DUE TO ADSORPTION – RESULTS AND DISCUSSION

Figures 5.6 to 5.9 show the volumetric strain variations versus time for Tabas coal samples in different gas environments. It can be observed that there are some variations in the volumetric change profiles for different samples tested under the same gas type and gas pressure. For example, at a 3 MPa gas pressure level (Figure 5.6), there is a difference in the volumetric strain of the order of 20% between Tabas coal samples 1 and 2, while the other samples (samples 3, 4 and 5), lie in between these two extremes. This is not unexpected, as the coal samples with very different volumetric strains may have come from different places in the long section (different horizons) cored out of the coal lumps.

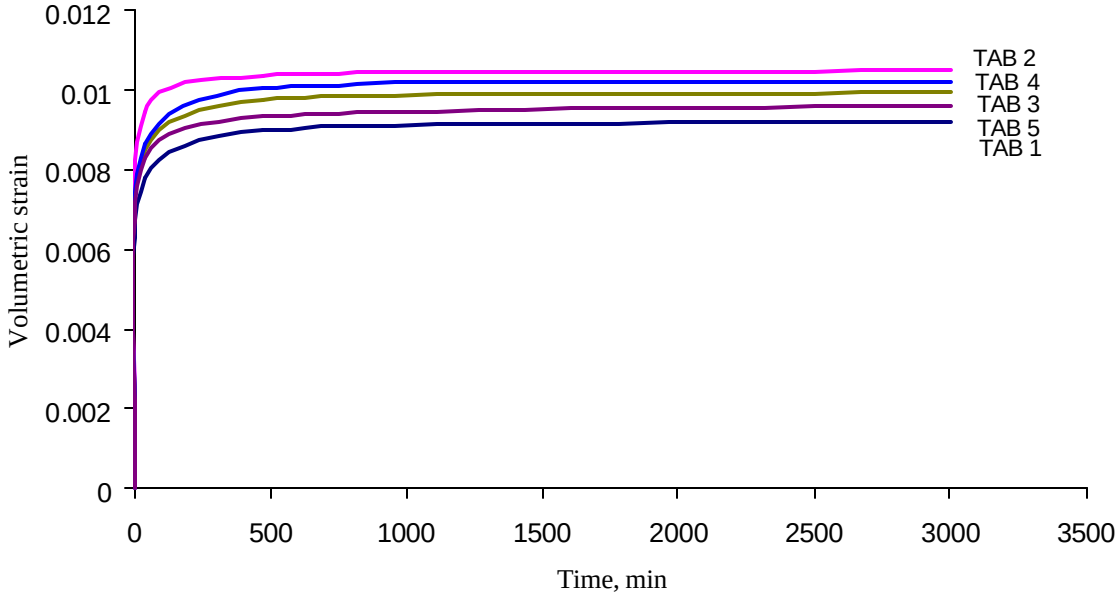

Figure 5.6 Volumetric strains for Tabas coal at 3 MPa in CO_2.

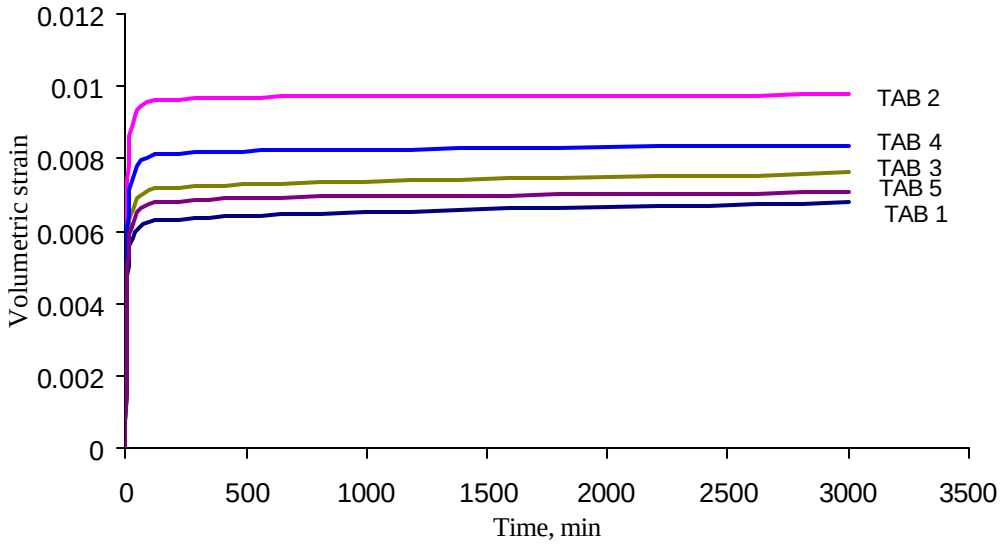

Figure 5.7 Volumetric strains for Tabas coal at 3 MPa in CH_4.

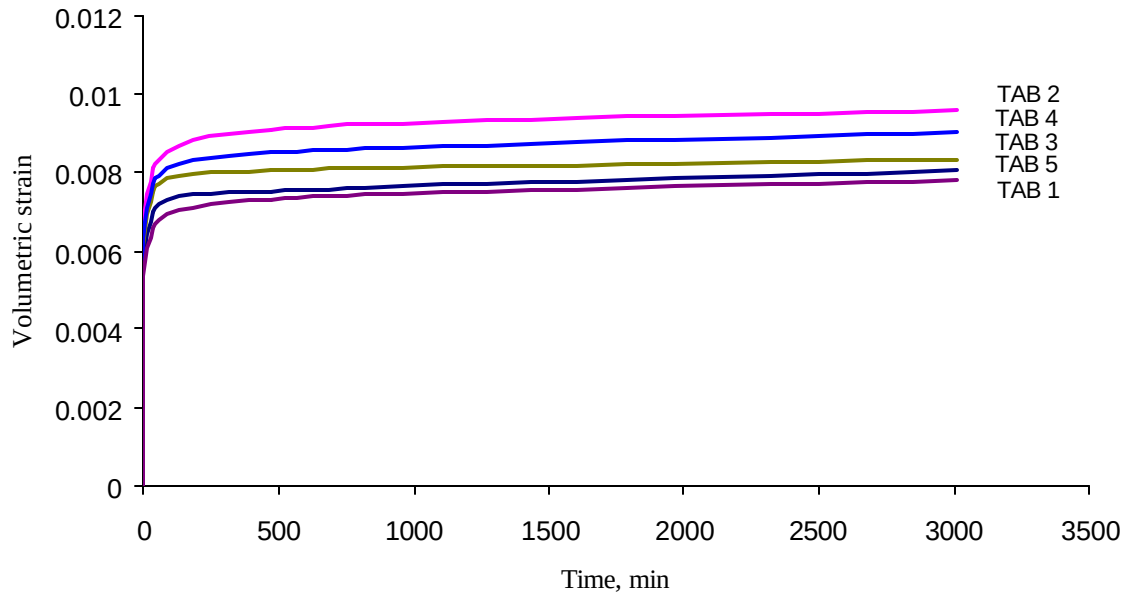

Figure 5.8 Volumetric strains for Tabas coal at 3 MPa in a 1:1 CH_4/CO_2 mixture.

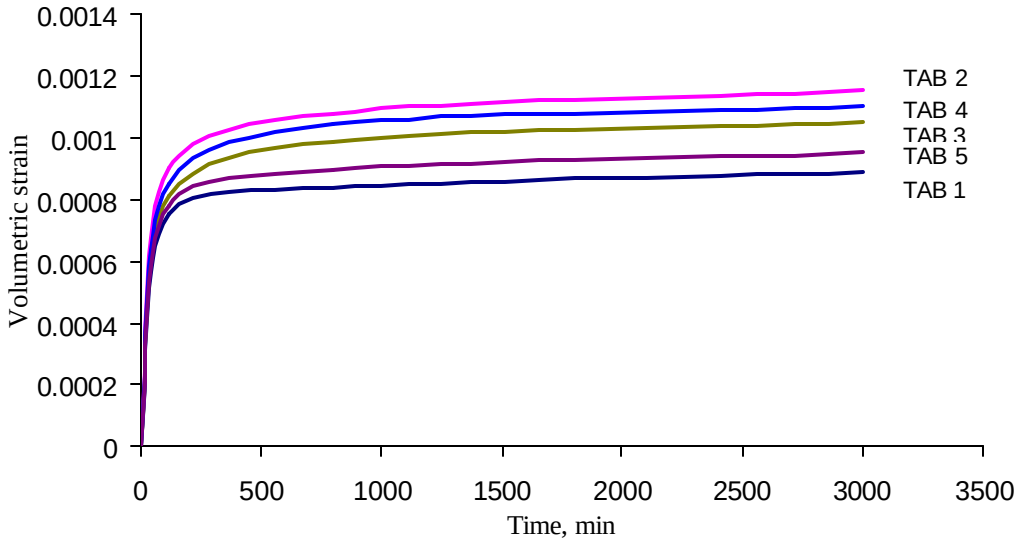

Figure 5.9 Volumetric strains for Tabas coal in N_2 gas at 3 MPa.

By comparing the volumetric strain curves it was found that CO_2 gas caused the highest coal volume expansion and N_2 the lowest (Figures 5.6 to 5.9). This trend was the same for all the coals tested. The low level of influence of N_2 gas can be explained by referring to its lack of attraction to coal. However the molecular size of nitrogen (36Å) is smaller than the methane (38Å) (Kaye and Laby, 1966) for example suggesting that it can reach to the smaller pores, but because there isn't any attraction between the pore walls and the N_2 molecule, the sorption rate of nitrogen will therefore be low. Also, Rodrigues and Sousa (2002) mentioned that carbon dioxide induces great swelling effect in the coal structure since its rate of sorbed and free gas is higher than the other gases such as nitrogen. In the case of the coal matrix higher affinity for carbon dioxide, Deitz, Carpenter and Arnold (1964) explained, "adsorption of carbon dioxide by the coal matrix is strengthening by the quadrupole

moment of the carbon dioxide molecule interacting with the oxygen present on the coal (carbon) surface". It can be concluded that, in the volume change measurements of coal with sorption of different gases, both size of the gas molecules and their relationship with the coal have to be considered.

More than 90% of the total increase in volume for any coal type occurred during the first 300 min after gas pressurisation, however this period varied with the gas type used. It occurred at a faster rate in CH_4, followed by the CO_2/CH_4 mixture, then CO_2 and finally N_2.

The volume increase for Tabas coal in CH_4 was around 0.08%, and in CO_2 it was around 0.1%. The significance of the coal swelling profiles with respect to time is that it clearly demonstrates that much of the coal matrix expansion occurs in the early stages of gas application, and is in line with the general sorption isotherms used for gas sorption as discussed by Lama and Bartosowicz, (1982). The volumetric strain due to sorption of the CH_4/CO_2 mixture was closer to that of carbon dioxide rather than that of methane, this is because of the greater affinity of CO_2 on coal.

A relatively greater variation of volume change "swelling" in coal samples with respect to changes in gas type and coal can be attributed to the coal matrix structure. The sorption capacity of coal appears to depend on its porous configuration, especially with respect to the micropores, as reported by various researchers. Lama (1988) stated, "Coals have a fairly complex and variable microstructure depending upon their metamorphic state (rank) and the percentage of each of the petrographic components". Ettinger et al. (1958) showed a clear connection between degree of metamorphism and gas sorption capacity of coals. Furthermore Gan, Nandi and

Walker (1972) demonstrated that pore volume distribution is dependent upon the rank of coal. Therefore it can be explained that rank and macerals dictate the development of the micropores in the coal matrix. When describing the differences between sorption rates, the discussion refers to the influence of maceral composition and mineral matter within the coal matrix (which will be discussed later in this thesis).

The volumetric strain curves of all the coal samples which were tested from the Tabas mine indicated that the higher the level of vitrinite maceral the greater the magnitude of strain. Many researchers have indicated that coal macerals influence gas sorption. These include Ettinger et al. (1966), Lamberson and Bustin (1993), Crosdale and Beamish (1993, 1995), Bustin, Clarkson and Levy (1995) and Crosdale, Beamish and Valix (1998) who observed that vitrinite-rich coals have a higher adsorption rate and a higher amount of swelling than inertinite-rich coals of equivalent rank. However, Faiz et al. (1992) mentioned that "poor or no correlation may be found between adsorption capacity and maceral composition".

The role of mineral matter in sorption is important. Mineral matter causes a reduction in gas sorption as it is not an adsorbent for the coal gases. This was clearly evident in the lower value of volumetric strain for the Dartbrook Wynne Seam coal (Figure 5.10), a coal that was relatively high in mineral matter in comparison to average values for the other coals. Thus higher amounts of mineral matter result in lower volumetric strain. The average values of volumetric strain profiles in different gases for Tabas coal and other coal samples from Dartbrook, Tahmoor, Metropolitan, Tabas and North Goonyella are shown in Figures 5.10 to 5.14 respectively.

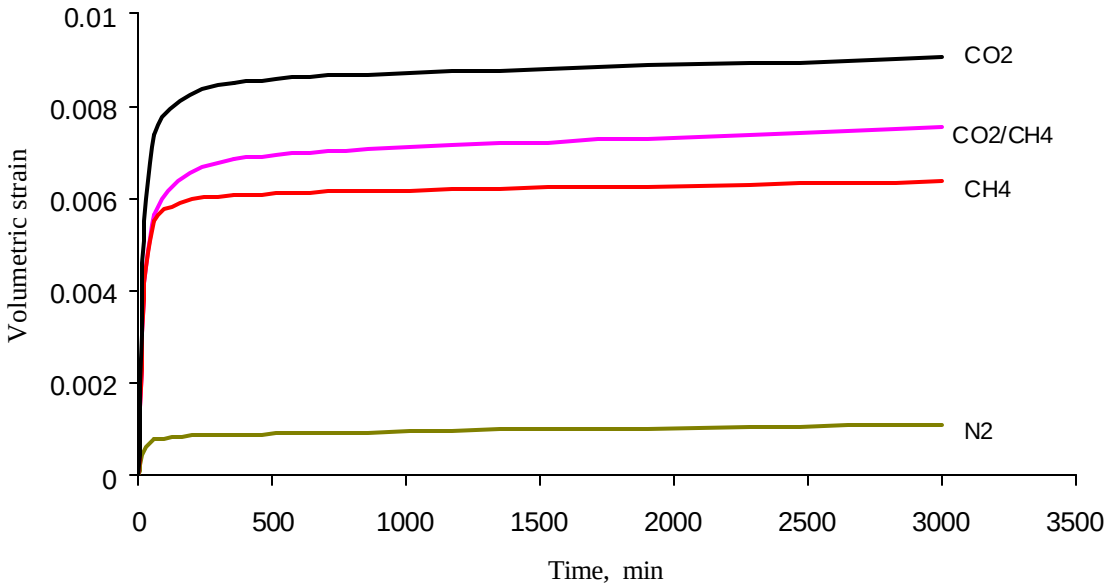

Figure 5.10 The average volumetric strain of Dartbrook coal associated with adsorption at 3 MPa for different gases.

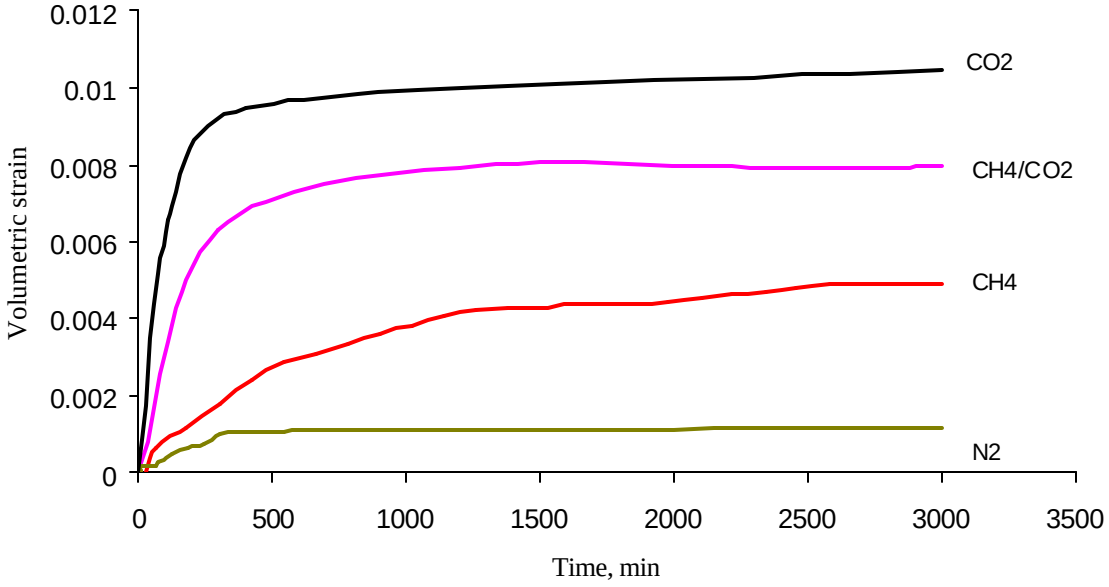

Figure 5.11 The average volumetric strain of Tahmoor coal associated with adsorption at 3 MPa for different gases.

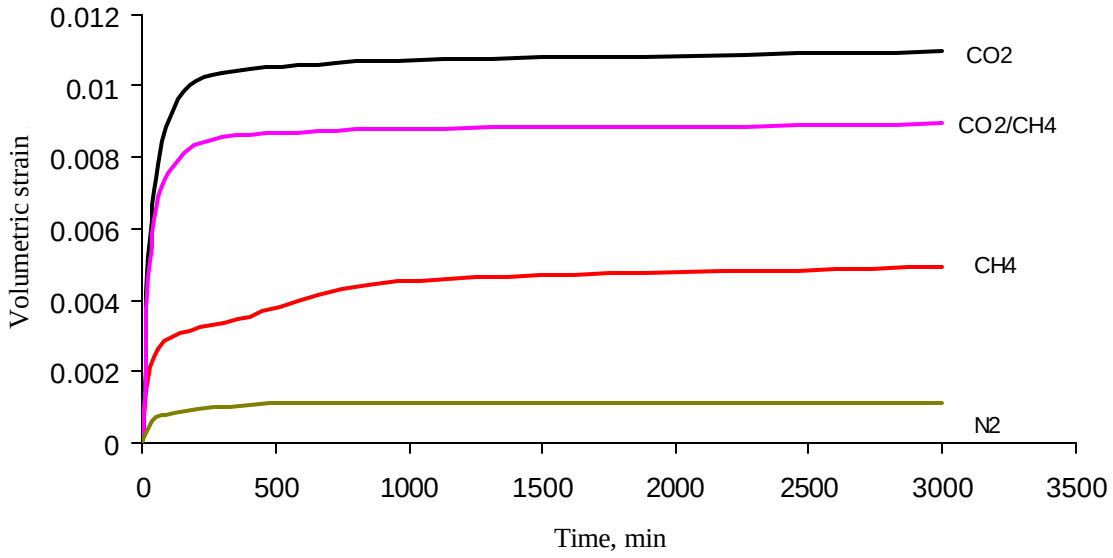

Figure 5.12 The average volumetric strain of Metropolitan coal associated with adsorption at 3 MPa for different gases.

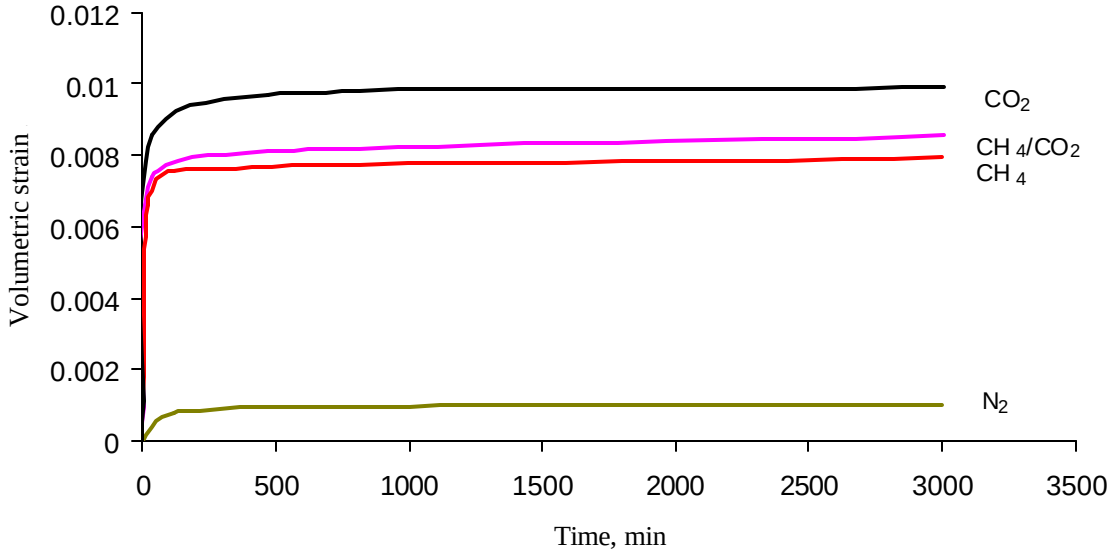

Figure 5.13 The average volumetric strain of Tabas coal associated with adsorption at 3 MPa for different gases.

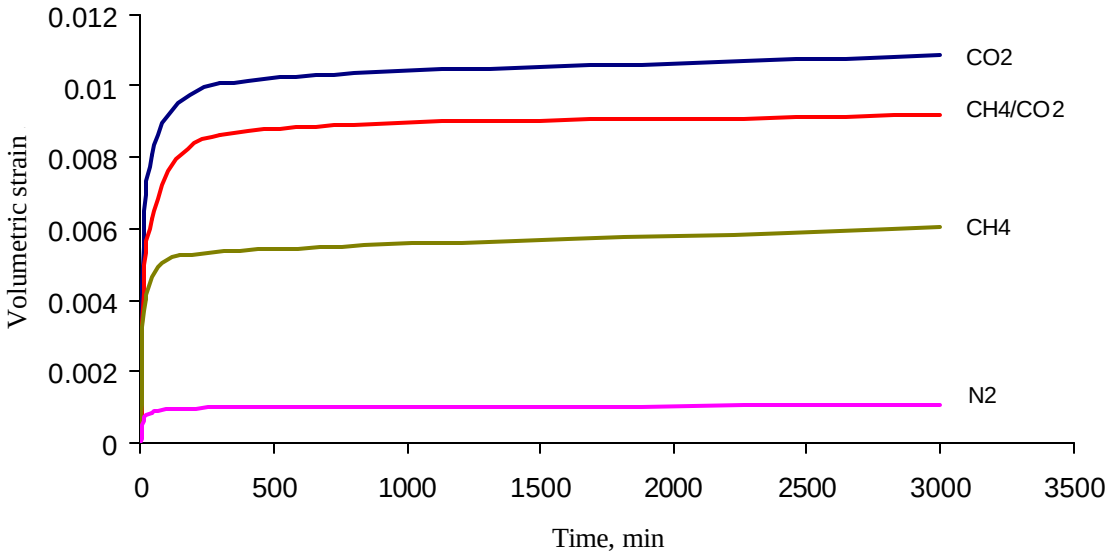

Figure 5.14 The average volumetric strain of North Goonyella coal (NGO) associated with adsorption at 3 MPa for different gases.

For coal samples from North Goonyella (NGO) the average volumetric change due to carbon dioxide sorption was about ten times higher than that due to nitrogen, and was approximately 2 and 1.2 times higher than for methane and the CH_4/CO_2 mixture, respectively. The ratio of the volumetric strain changes of CO_2 / N_2 measured for Tahmoor (TAH) coal samples was around 22, and for Dartbrook (DAR) coal it was eight (8). By comparing Figures 5.10 and 5.11 with the other sorption figures, it can be seen that the coal samples from the Bulli coal seam (Tahmoor and Metropolitan Collieries) had the least expansion in the methane gas environment. The ratio of their expansion for methane compared to carbon dioxide was 2.5 for Metropolitan coal samples (MMP) and 2 for Tahmoor coal samples (TAH).

5.4 COAL SHRINKAGE BY DESORPTION

In the second series of tests the strains due to desorption were measured. Incremental gas pressure reduction and its impact on various coal samples from North Goonyella (pressurised to 3 MPa) are shown in Figures 5.15 to 5.18, and Figure 5.19 shows the average values for all North Goonyella samples. The trend of the incremental decrease in coal volume as a result of gas pressure drop is similar for all five samples.

It is clear from Figure 5.19 that for any given pressure level the volume change is highest in a carbon dioxide environment, followed by the mixture CO_2/CH_4, then CH_4 and N_2. The incremental reductions in gas pressure were maintained constant at 0.5 MPa. All individual sample desorption graphs are listed in Appendix I.

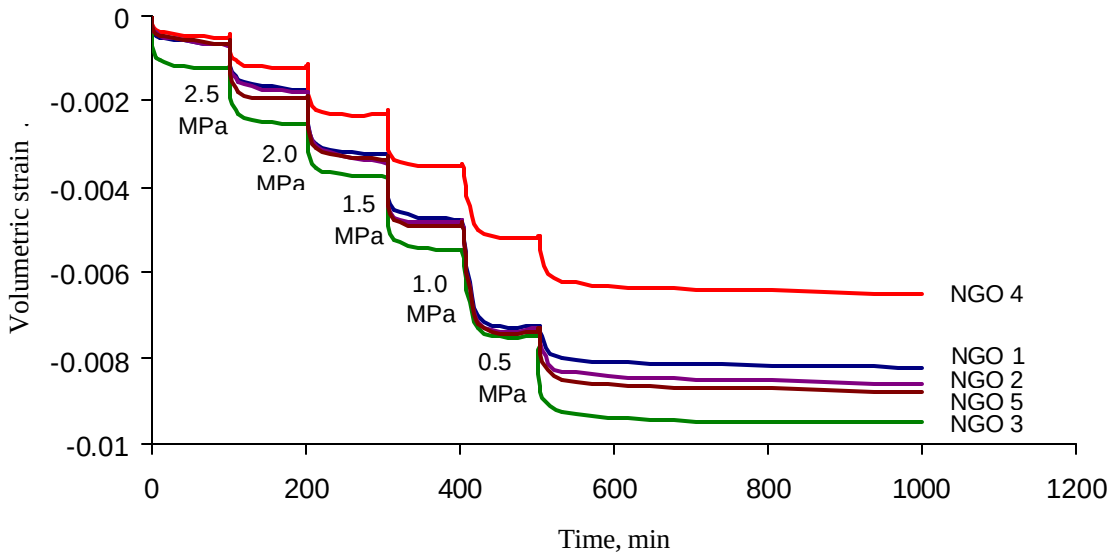

Figure 5.15 Volumetric strain in CO_2 for pressure reductions of 0.5 MPa from 3 MPa for North Goonyella samples.

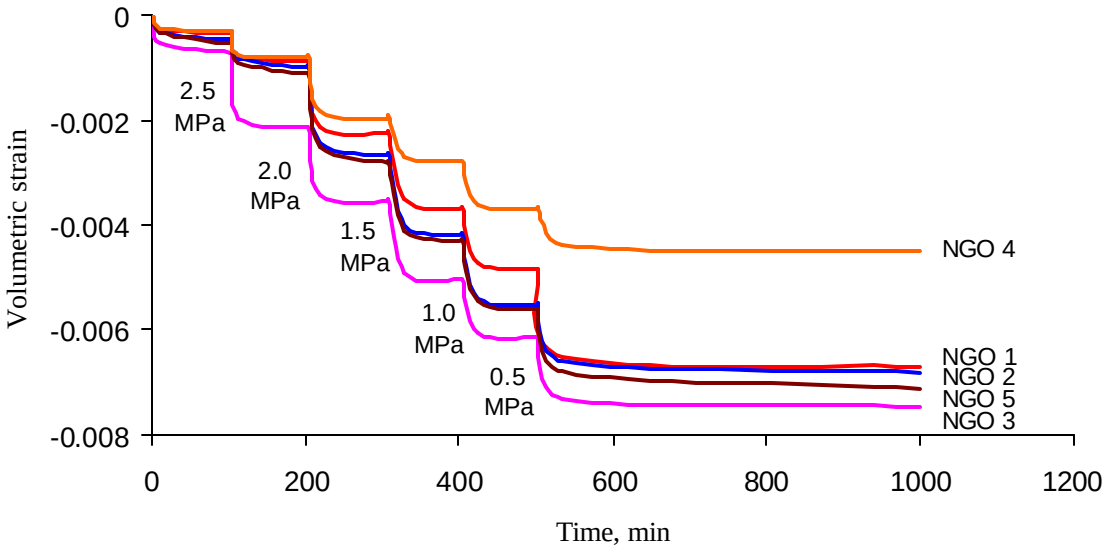

Figure 5.16 Volumetric strain in mixed CH_4/CO_2 for pressure reductions of 0.5 MPa from 3 MPa for North Goonyella samples.

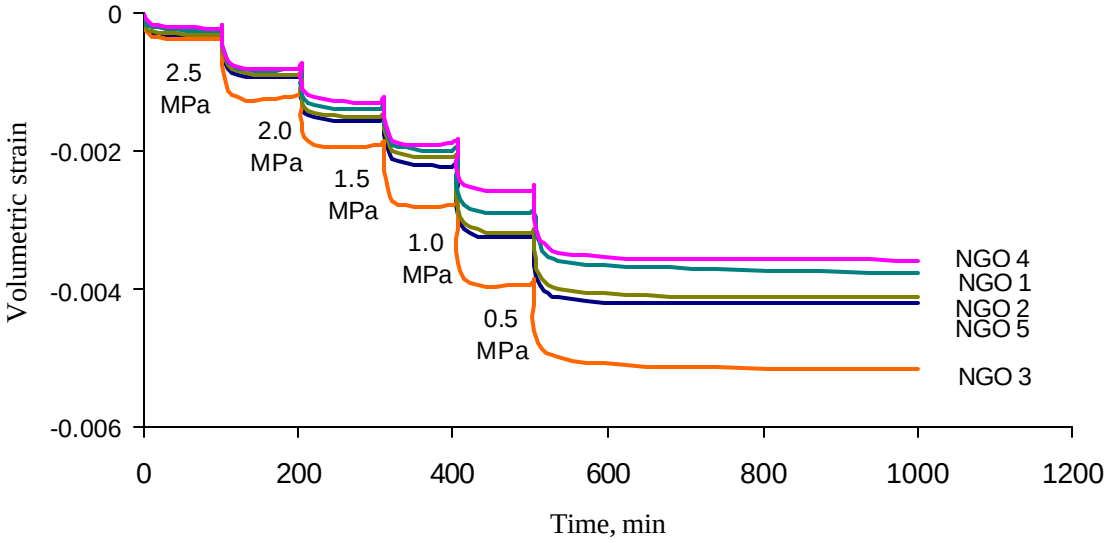

Figure 5.17 Volumetric strain in CH_4 gas for pressure reductions of 0.5 MPa from 3 MPa for North Goonyella samples.

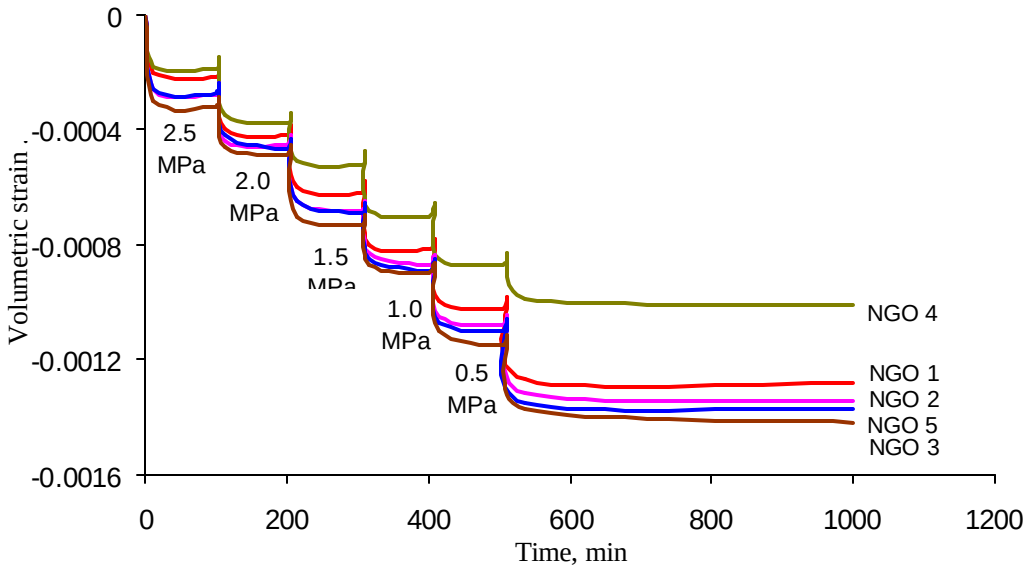

Figure 5.18 Volumetric strain in N_2 gas for pressure reductions of 0.5 MPa from 3 MPa for North Goonyella samples.

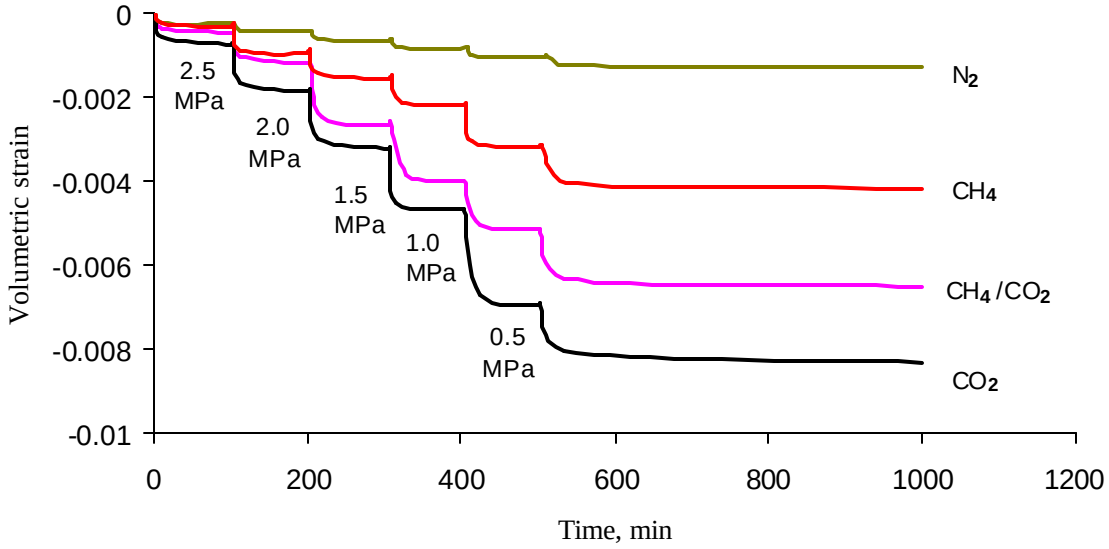

Figure 5.19 Average volumetric strain for various gases for pressure reductions of 0.5 MPa from 3 MPa for North Goonyella samples.

The rate and amount of volumetric change over the same time period were greater at lower pressures. A suitable explanation is that at lower pressure levels the sorbed gas

in coal can desorb more easily than at higher pressures; also, the inherent coal pores and microfractures open up at the lower pressures (Harpalani and Chen, 1995). The volumetric strains were higher for carbon dioxide than methane and nitrogen. Thus the shrinkage due to carbon dioxide was more than with the other gases. By comparing the desorption diagrams for the CH_4/CO_2 mixture with the desorption diagrams for CH_4 and CO_2, the desorption of the mixture can be divided into two stages. Initially the volumetric strains for the mixture were very similar to CH_4 strains. In the second stage, the mixed gas behaved in the same way as CO_2. This suggests that desorption of methane is more rapid than that of carbon dioxide, even in mixtures. This implication can be further justified by looking at the ratio of CO_2 / CH_4, which in the initial stages of desorption was low and in the later stages had increased; it confirms Lama's (1988) and Crosdale's (1999) findings, which showed that during CH_4/CO_2 mixture desorption from high pressure to low pressure, CH_4 is preferentially released and CO_2 preferentially retained by the coal. This suggests an explanation for the outburst phenomena, where in the early stage of outburst methane gas is the predominant gas and in the later stages the vast majority of the gas will be carbon dioxide.

The shrinkage coefficient (C_m) is defined as the rate of change of the coal matrix volume to the change in gas pressure and is given by:

$$C_m = \frac{1}{V_m}\left(\frac{dV_m}{dP}\right) \qquad (5–6)$$

V_m = Matrix volume, m^3

dV_m = Change in volume, m^3

dP = Change in applied pressure, MPa

C_m = Shrinkage coefficient, MPa^{-1}

However, the simple way to determine (C_m) is from the slope of the volumetric strain versus gas pressure plot. The volumetric strains were plotted with respect to decreasing gas pressures by allowing desorption to reach near equilibrium at each stage.

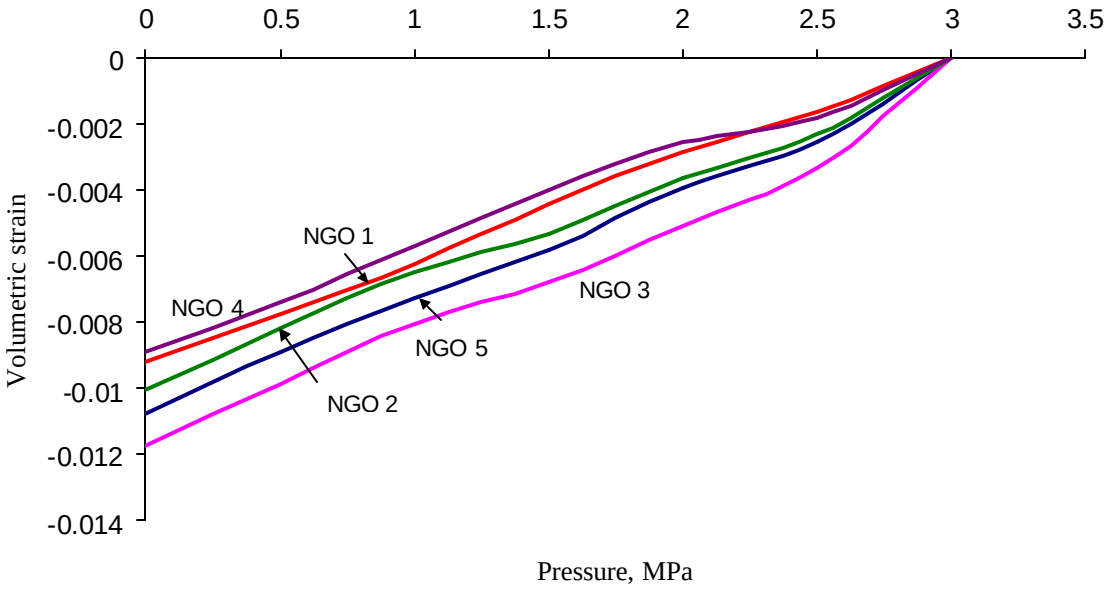

Figure 5.20 Volumetric strain of different North Goonyella coal matrix samples with decreasing CO_2 gas pressure from 3MPa to absolute pressure

According to Figures 5.20, as a general rule, the shrinkage coefficient increases with decreasing pressure. Table 5.1 shows the values of the shrinkage coefficient (C_m) for the various coal types in different gas sorption/desorption environments.

Table 5.1 Shrinkage coefficients (MPa^{-1}) for samples tested.

Coal samples	CO_2	CH_4	CH_4/CO_2	N_2
NGO 1	0.0092	0.0044	0.0067	0.0012
NGO 2	0.0099	0.0049	0.0070	0.0013
NGO 3	0.0118	0.0054	0.0081	0.0014
NGO 4	0.0087	0.0035	0.0051	0.0010
NGO 5	0.0108	0.0031	0.0061	0.0013
TAB 1	0.0047	0.0021	0.0037	0.0008
TAB 2	0.0073	0.0041	0.0059	0.0011
TAB 3	0.0058	0.0029	0.00 0	0.0009
TAB 4	0.0067	0.0033	0.0052	0.0010
TAB 5	0.0055	0.0026	0.0046	0.0008
MMP 1	0.0060	0.0016	0.0061	0.0009
MMP 2	0.0089	0.0022	0.0048	0.0012
MMP 3	0.0082	0.0020	0.0051	0.0011
MMP 4	0.0072	0.0017	0.0055	0.0010
MMP 5	0.0083	0.0021	0.0046	0.0011
DAR 1	0.0099	0.0039	0.0052	0.0012
DAR 2	0.0082	0.0031	0.0080	0.0010
DAR 3	0.0085	0.0034	0.0064	0.0010
DAR 4	0.0090	0.0035	0.0056	0.0011
DAR 5	0.0075	0.0029	0.0072	0.0010
	800 panel			
TAH 1	0.0098	0.0020	0.0065	0.0011
TAH 4	0.0091	0.0018	0.0053	0.0010
TAH 5	0.0080	0.0017	0.0053	0.0009
TAH 7	0.0114	0.0023	0.0078	0.0012
TAH 8	0.0105	0.0022	0.0075	0.0011
	900 panel			
TAH 2	0.0073	0.0013	0.0051	0.0007
TAH 3	0.0051	0.0010	0.0040	0.0007
TAH 9	0.0072	0.0011	0.0048	0.0007

These values clearly show the effects of variations of the matrix structure and composition of various coal types on C_m. C_m values determined from the current tests were in agreement with values obtained by previous researchers in this field, which were shown in Table 3.1. Also, the shrinkage coefficients of Metropolitan coal samples were approximately the same as for Tahmoor coal samples, which in both mines were extracted from the Bulli coal seam. Obviously, the variation in shrinkage coefficient is influenced by the coal composition, particularly, the variation in mineral matter.

It can be clearly seen that for all gas environments the coal matrix volume shrinks with reduction in pressure. As can be seen from Figure 5.21 for all tested samples the

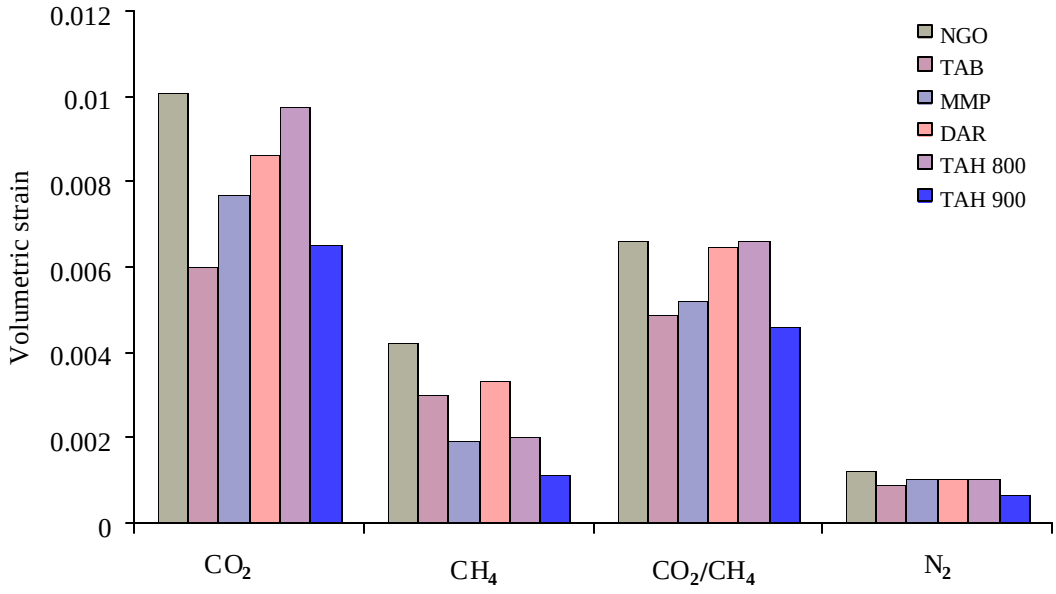

Figure 5.21 Average volumetric strain of tested coal samples

highest amount of volumetric strain was caused by carbon dioxide and the least by nitrogen. Also it can be deduced that the volumetric strain for CO_2/CH_4 is closer to that of CO_2 than to that of CH_4. Nitrogen as a neutral gas does not have much effect on the coal volume.

5.5 CONCLUSIONS

The experimental work reported in this chapter demonstrated the influence of increased coal sorption on coal volume change. The level of coal shrinkage is affected by the type of gas desorbed. Carbon dioxide appears to have the greatest influence on the matrix and nitrogen the least. This is understandable in view of the fact that carbon dioxide has a greater affinity to coal than the other gases. As well as the magnitude of shrinkage, the rate of shrinkage was also found to be influenced by the type of gas and the applied pressure. All mines' coal samples showed approximately the same behaviour, with Metropolitan coal samples having a greater average rate of shrinkage than the other coal samples. Such variation can be attributed to the coal composition. Further analysis of the results will be discussed in relation to coal permeability and coal composition in later chapters.

CHAPTER SIX

THE EFFECT OF GAS PRESSURE AND AXIAL STRESS ON COAL PERMEABILITY

6.1 INTRODUCTION

There are different methods of determining the permeability of coal. The in-situ field test method is generally superior as it represents a much more realistic way of determining permeability. In particular, the slug method reported by Koenig and Schraufnagel (1987) and Shu et al. (1995) is widely used for estimating insitu permeability, particularly in a water-saturated coal seam. In-situ permeability tests have their limitations, however, as the method can be laborious and access to the site is not always convenient. Accordingly, most of the permeability research conducted is laboratory based, often involving the use of some complicated apparatus, mostly built in-house for the specific task. Past laboratory-based studies on coal permeability include those by Lingard, Phillips and Doig (1982), Gray (1987), Wold and Jeffery (1999), and Lama and Bodziony (1996).

The experimental study reported in this chapter forms part of a comprehensive study aimed at establishing correlations between the gas environment, coal matrix change, coal composition and coal permeability for outburst control and management. Variation of ground stresses on coal is simulated by the application of variable

vertical loads on the coal samples, which are contained in a triaxial gas chamber that forms a significant part of the purpose built permeability apparatus.

6.2 EXPERIMENTAL PROCEDURE

Permeability tests were conducted in a Multi Function Outburst Research Rig (MFORR) (Figures 6.1 and 6.2). MFORR comprises a number of components which can be utilised in a variety of research studies, although it was initially built for the study of the influence of the gas environment on coal strength. The integrated components of the MFORR include:

1. Gas pressure chamber – also used for coal permeability studies
3. Drilling system
4. Drill support frame
5. Drill cutting collection system
6. Universal socket for vertical load application
7. Flow meters
8. Data acquisition system
9. Various components for coal strength properties tests.

The components of the MFORR were interchangeable with respect to the types of tests undertaken. All the above were held in a main frame that consisted of a sturdy steel structure, which housed the gas chamber and a universal thrust connector. The gas pressure chamber was a hollow rectangular prism of cast iron with removable front and back viewing plates. The dimensions of the box were 110 mm x 110 mm x

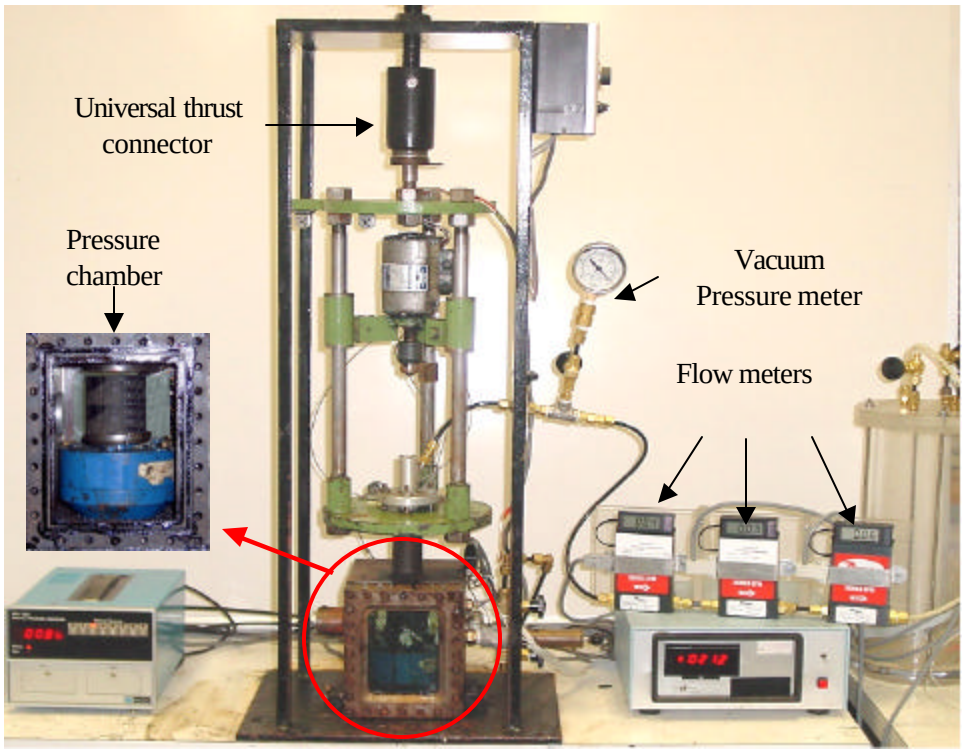

Figure 6.1 A general view of the MFORR.

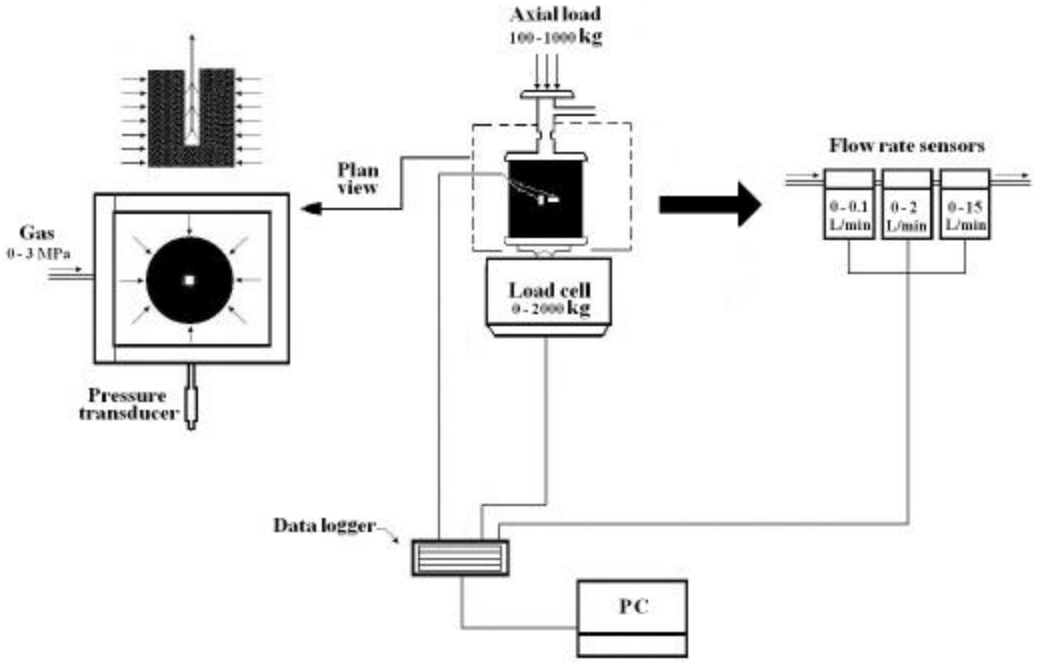

Figure 6.2 Schematic of the equipment for measuring the permeability of coal.

140 mm. The viewing windows were made of 20 mm thick glass in a cast iron frame. Access to the chamber was possible by unbolting the front cast iron frame with the glass window. Housed in the chamber was a 1210-BF interfaced load cell with a capacity of 40 kN for monitoring the load applied. A pair of specimen loading plates with locating lips was used for holding the samples and monitoring the load applied.

For the permeability tests the 50mm diameter, 50mm long core samples were placed between the loading plates of the permeameter chamber. Axial load was applied to the coal sample via a universal torque device. Changes in the sample's axial and lateral dimensions due to gas sorption were monitored by two sets of strain gauges, as shown in Figure 6.2 and described in detail in Chapter 5.

The procedure for conducting each test consisted of the sample being first mounted in the pressure chamber. The chamber was then sealed, the system evacuated to remove air and subsequently repressurised to a predetermined level and maintained at that level. The gas was allowed to permeate the coal sample and flow out through the central hole. The released gas from the coal flows through a measuring system consisting of a vacuum pressure sensor and gas flow meters with different measurement ranges:

- High range: 0-15 L/min (Type: Dwyer, Model: GFM 1111)
- Medium range: 0-2 L/min (Type: Dwyer, Model: GFM 1108)
- Low range: 0-100 mL/min (Type: Dwyer, Model: GFM 1104)
- Vacuum pressure sensor

The sequence of varying gas pressure and vertical load on the samples is illustrated in Figure 6.3. The load cell, flow meters, pressure transducer and strain gauges were connected to a PC through a data logger (Data taker D-500) for data collection. About 30 minutes were allowed to elapse before steady-state conditions could be reached and readings could be taken.

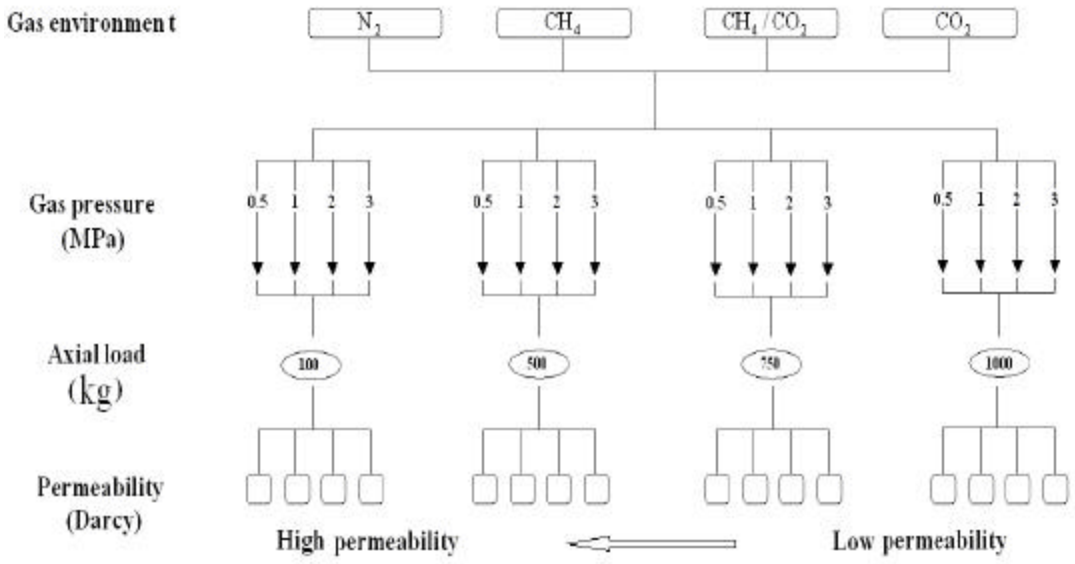

Figure 6.3 Sequence of varying pressures and loads in the permeability tests.

The permeability of the sample was calculated using the following Darcy's equation (Lama, 1995a):

$$K = \frac{mQ\ln\left(\frac{r_o}{r_i}\right)}{p\ell(P_o^{\,2} - P_u^{\,2})} \qquad (6\text{-}1)$$

where:

K = Permeability to gas, Darcy

ℓ = Height of the sample, cm

Q = Rate of flow of gas, cc/sec

P_o = Absolute pressure in the chamber, bars

r_o = External radius of sample, cm

P_u = Absolute pressure at the outlet, bars

r_i = Internal radius of sample, cm

m = Viscosity of tested gas, centipoise

6.3 TEST RESULTS

Permeability tests were conducted on coal samples from all five mines under consideration. The Tahmoor coal samples from two geologically different conditions were the subject of particular interest. Tables 6.1 - 6.2 contain the permeability test results of Tahmoor coals collected from 800 and 900 panels. The coal sample results from the other mines (Metropolitan, Dartbrook, North Goonyella, and Tabas) and additional Tahmoor samples are listed in Appendix II.

It can be seen from Tables 6.1 to 6.2 that there were variations in permeability between the two different coals from the Bulli seam at Tahmoor mine. Also, considerable variations in coal permeability were observed for different confining gas pressures under the same axial load. Similar findings were also reported by Enever and Henning (1997).

Table 6.1 Permeability test results for Tahmoor coal sample from panel 900(TAH 3).

Gas pressure (MPa)	Axial load (kg)	Permeability to CO_2 (Darcy)	Permeability to CH_4 (Darcy)	Permeability to CO_2/CH_4 (Darcy)	Permeability to N_2 (Darcy)
0.5	100	3.27E-06	2.43E-05	6.67E-06	4.91E-05
	500	2.27E-06	2.02E-05	4.63E-06	3.16E-05
	750	2.20E-06	1.73E-05	4.25E-06	2.78E-05
	1000	1.53E-06	1.53E-05	3.73E-06	2.57E-05
1.0	100	2.72E-06	1.95E-05	6.56E-06	4.56E-05
	500	2.07E-06	1.62E-05	4.09E-06	3.35E-05
	750	1.54E-06	1.55E-05	3.81E-06	2.53E-05
	1000	1.30E-06	9.00E-06	3.76E-06	2.19E-05
2.0	100	1.99E-06	1.71E-05	5.83E-06	4.24E-05
	500	1.91E-06	1.33E-05	4.23E-06	3.28E-05
	750	1.30E-06	7.48E-06	2.91E-06	2.28E-05
	1000	1.20E-06	6.07E-06	2.34E-06	1.91E-05
3.0	100	1.95E-06	9.26E-06	4.43E-06	1.76E-05
	500	1.32E-06	6.07E-06	3.82E-06	1.70E-05
	750	1.18E-06	4.96E-06	2.73E-06	1.30E-05
	1000	1.00E-06	3.78E-06	2.00E-06	1.03E-05

Table 6.2 Permeability test results for Tahmoor coal sample from panel 800(TAH7).

Gas pressure (MPa)	Axial load (kg)	Permeability to CO_2 (Darcy)	Permeability to CH_4 (Darcy)	Permeability to CO_2/CH_4 (Darcy)	Permeability to N_2 (Darcy)
0.5	100	5.95E-05	3.72E-04	8.28E-05	6.70E-04
	500	3.20E-05	3.50E-04	5.66E-05	5.77E-04
	750	2.97E-05	3.18E-04	5.13E-05	5.14E-04
	1000	1.81E-05	2.71E-04	4.43E-05	4.52E-04
1.0	100	3.88E-05	3.29E-04	7.93E-05	5.32E-04
	500	1.73E-05	2.73E-04	5.04E-05	4.42E-04
	750	1.63E-05	2.65E-04	4.78E-05	4.24E-04
	1000	3.70E-06	2.51E-04	4.24E-05	4.01E-04
2.0	100	2.00E-05	2.54E-04	6.11E-05	4.74E-04
	500	1.12E-05	2.31E-04	3.92E-05	4.51E-04
	750	6.50E-06	2.20E-04	3.71E-05	3.70E-04
	1000	2.53E-06	1.25E-04	3.00E-05	2.70E-04
3.0	100	9.10E-06	1.90E-04	4.73E-05	3.92E-04
	500	5.50E-06	1.60E-04	3.12E-05	3.10E-04
	750	5.00E-06	1.18E-04	1.87E-05	2.38E-04
	1000	2.15E-06	1.04E-04	1.29E-05	1.65E-04

6.3.1 The effect of applied load

In samples from all five coal mines, a strong correlation between permeability and stress was observed. By applying stress to the coal matrix the fractures and cleats are tightened or closed, the movement of gases is restricted and therefore permeability drops. In this study the permeability of Tahmoor coal samples decreased by an average factor of 1.5 to 2 when the axial load was increased from 100 kg to 1000kg under 0.5 MPa methane gas confining pressure.

It should be noted that if the applied load is greater than the mechanical strength of the coal, the coal matrix will be crushed, and this results in higher permeability. It is reasonable for the permeability of coal with a well developed cleat system to be much more stress dependent than for coal with less well developed cleats and pores.

The permeability of coal is also influenced by the confining gas pressure. As shown in Figures 6.4(a-b) to 6.7(a-b) the confining gas pressure has a remarkable influence on the permeability of all coal samples. With decreasing gas pressure the permeability increases. For example the permeability of the TAH 3 sample from 800 panel to methane decreased by a factor of around 2.6 (i.e., $k_3/k_{0.5}$=2.43/0.93) when the confining gas pressure was increased from 0.5 MPa to 3 MPa under a 100kg axial load. Thus it can be concluded that at higher confining gas pressures, the differences in the permeability of coal samples from the same seam decreases. Circumstances of low permeability can occur insitu as a result of geological anomalies such as intrusions, i.e. it is known that gas pressure increases and permeability decreases occur around the region of intrusions.

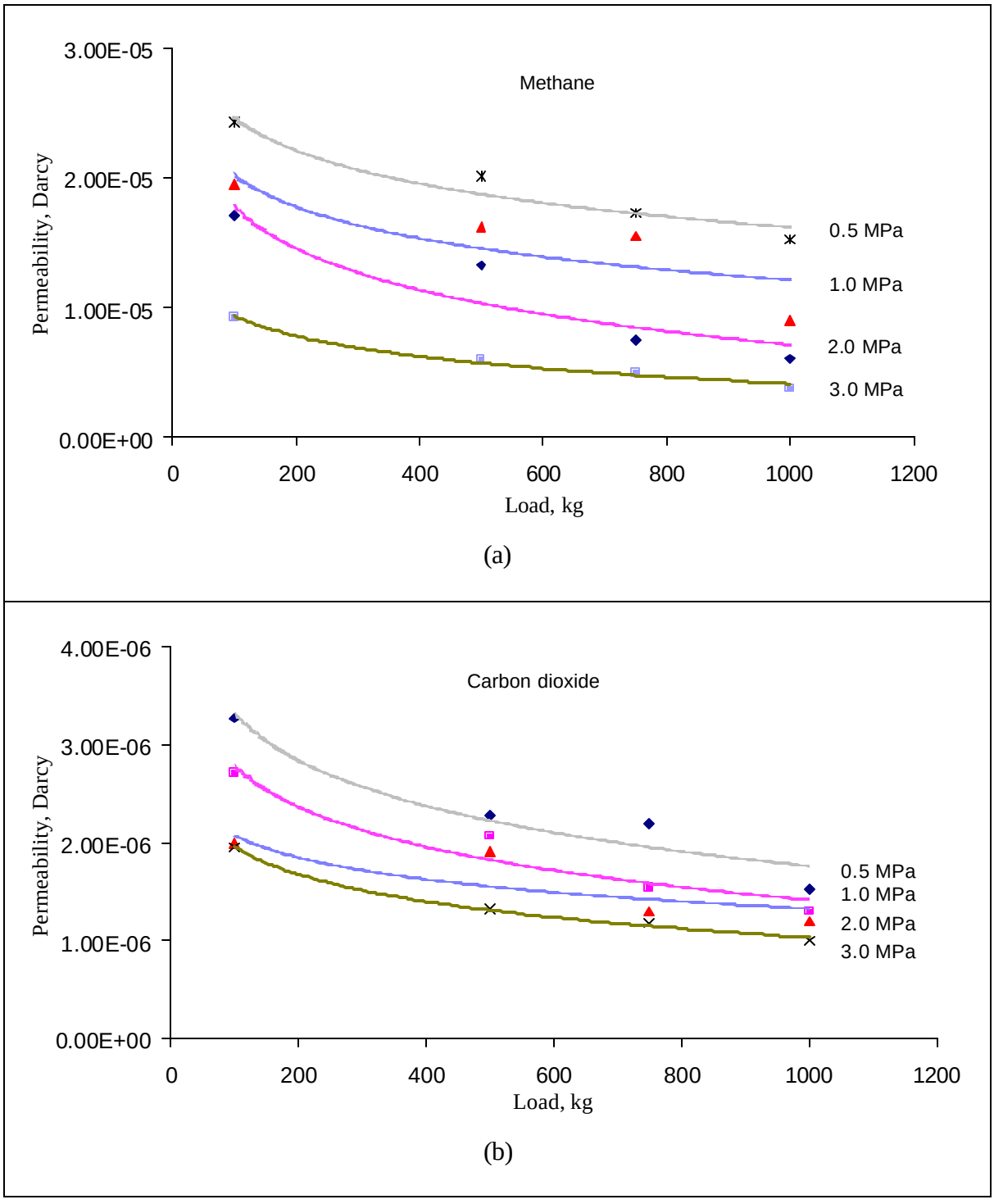

Figure 6.4 TAH 3 sample (900 panel) permeability for methane and carbon dioxide under various axial loads and confining pressures.

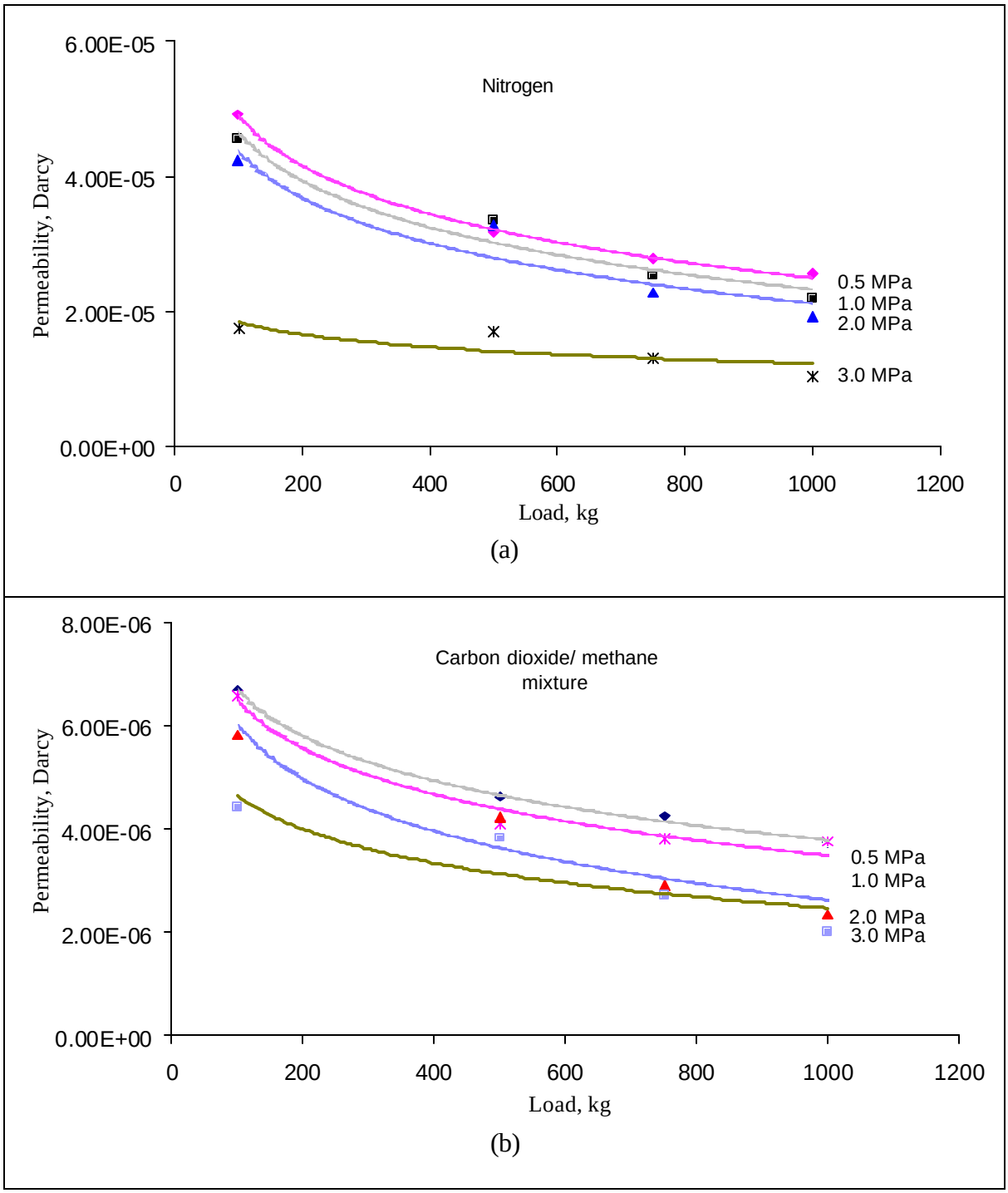

Figure 6.5 TAH 3 sample (900 panel) permeability for nitrogen and CH_4/CO_2 mixture under various axial loads and confining pressures.

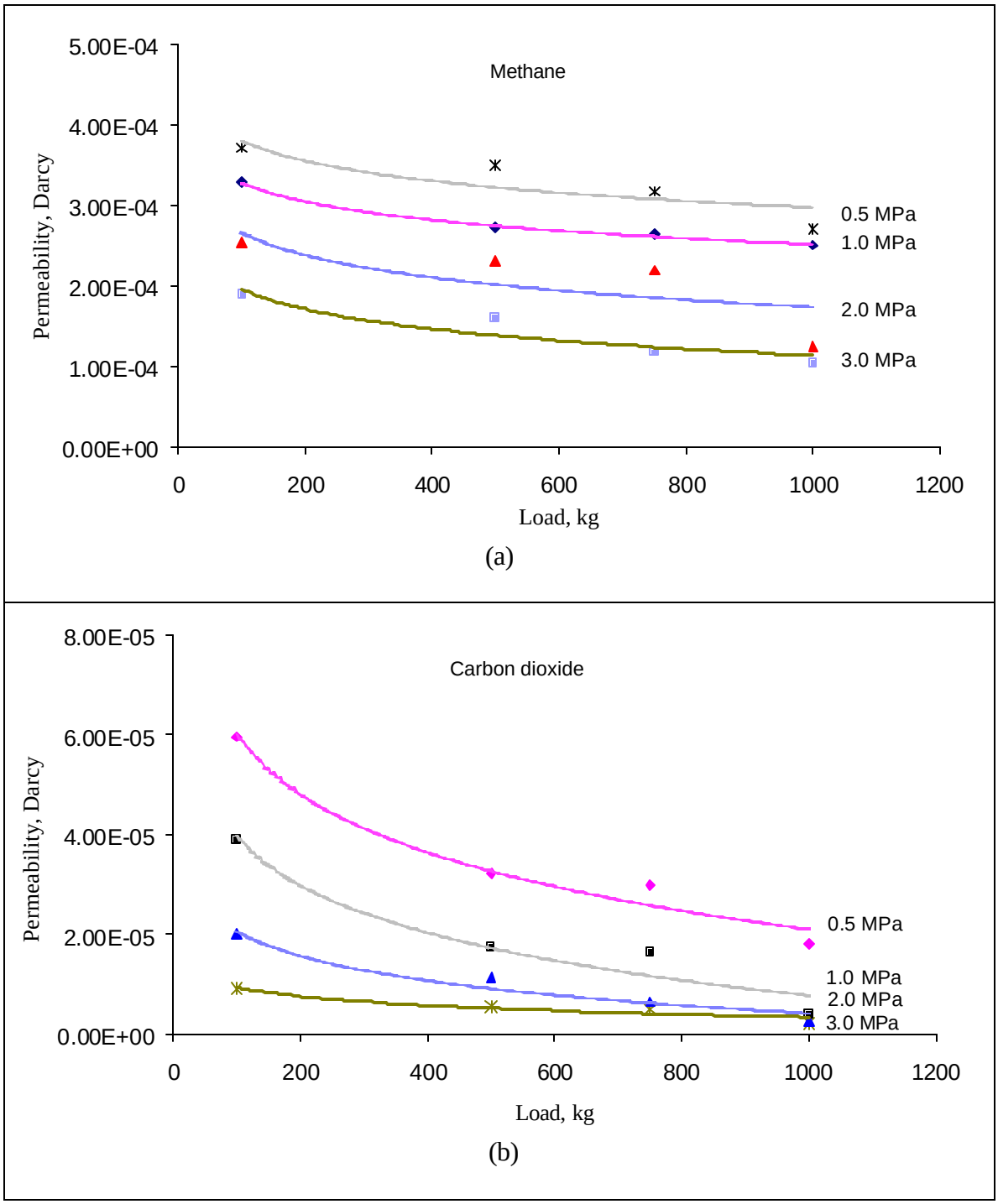

Figure 6.6 TAH 7 sample (800 panel) permeability for methane and carbon dioxide under various axial loads and confining pressures.

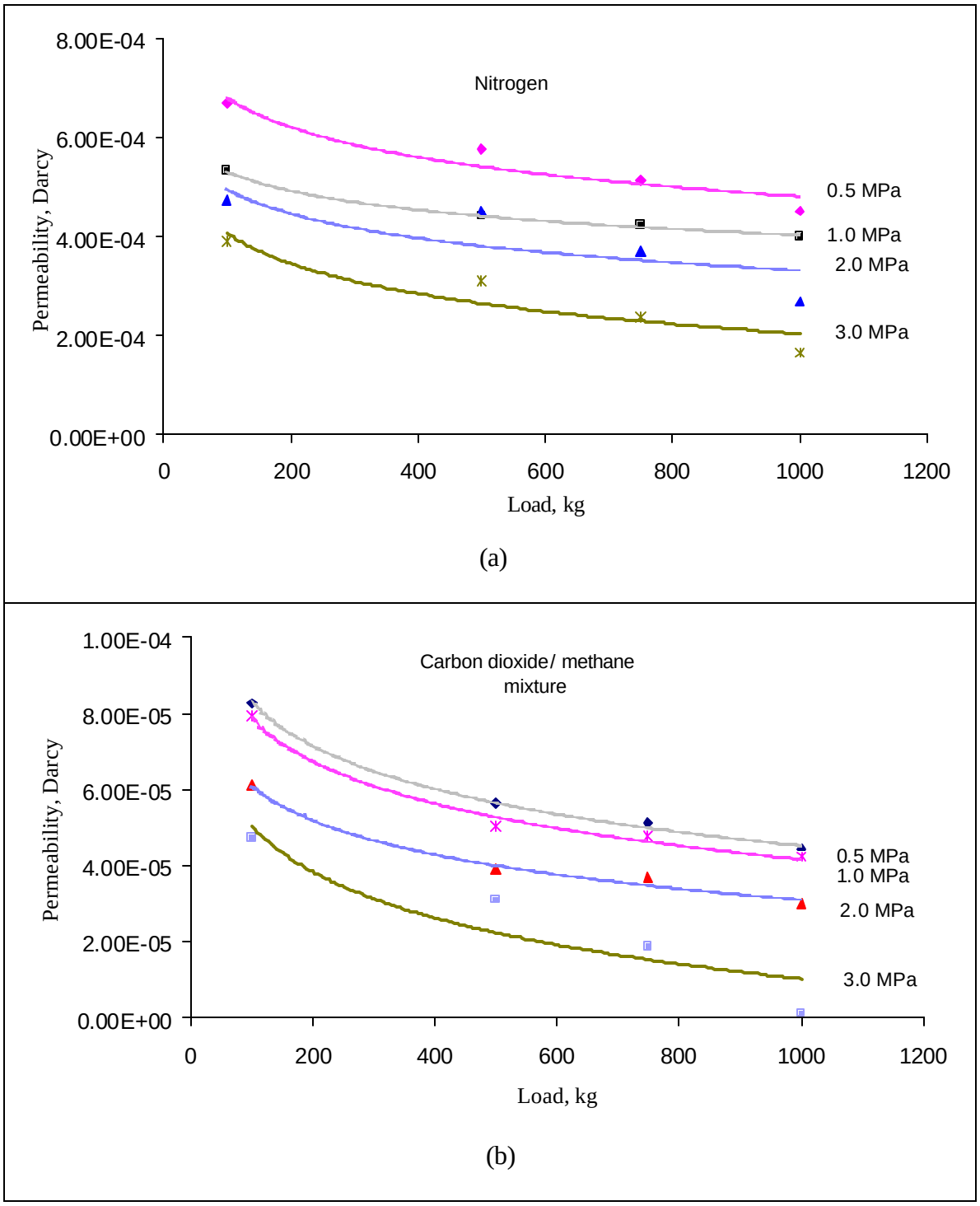

Figure 6.7 TAH 7 sample (800 panel) permeability for nitrogen and CH_4/CO_2 mixture under various axial loads and confining gas pressures.

6.3.2 The effect of coal composition

By comparing the Tahmoor coal sample permeability curves in Figures 6.4 to 6.7 with Tables 4.1 and 4.2 it can be shown that the permeability of coal is influenced by the mineral content and the carbonates, as well as the cavities. In particular:

- there was a reduction in coal permeability with increasing mineral and carbonate content of the coal;
- likewise, an increase in cavities and fractures causes an increase in the permeability of coal samples.

Further analysis of the role of coal composition on coal permeability will be introduced later in chapter seven.

6.3.3 The effect of gas Type

The results of the permeability measurements performed with different gases (N_2, CH_4, CO_2, CH_4/CO_2 mixture) at various pressures up to 3 MPa on the Tahmoor coal samples are documented in Figures 6.4 to 6.7. The coal samples had permeability to methane ranging from 0.00000378 (3.78E-06) up to 0.000372 (3.72E-04) for different axial loads. This variation was also found in other gas environments. The order of coal permeability from high to low was N_2, CH_4, CH_4/CO_2 mixture and finally CO_2 (Figures 6.4 to 6.7). The following is a possible explanation for this phenomenon.

Different gases have different molecular diameters, and the molecular diameters of methane and carbon dioxide are 38 Å and 41 Å, respectively. (Kaye and Laby, 1966). The flow of the gas through pores and cleats depends upon the size of the cleats and pores as well as the range and distribution. Small pores with diameters of a few Å can behave as a molecular sieve and permit some molecules to pass, while excluding others. Thus the flow rate of the gases that are passed will be reduced for gases with bigger molecules in the same dimension of pore sizes.

There are, however, two differing schools of thoughts on this issue. The first school of thought is attributed to Patching (1965). According to his experimental study, the permeability of coal depends on the size of the gas molecules and that permeability is not noticeably affected by gas sorption. The second school of thought is attributed to Somerton, Soylemezoglu and Dudley (1975), who challenged the notion that the permeability of coal can be explained solely on the basis of molecular diameter. Based on Patching's explanation, N_2 should show the highest permeability, followed by methane, carbon dioxide and then the CH_4/CO_2 mixture. The values obtained from the tests appear to be in good agreement with this theory. Somerton, Soylemezoglu and Dudley (1975), however, suggest that the difference in permeability as a result of molecular diameter alone should be around 7 per cent, but tests showed a value between 20 and 40 per cent. An initial hypothesis may be that sorption of methane is the reason for this discrepancy. Somerton reports this, and states that "Although these effects may explain the decreased permeability of the low permeability specimens, they can hardly explain the large changes observed for high permeability coals".

Somerton, however, provided no definitive reason for the discrepancy and suggested that further work was required. Others (Xue and Thomas, 1995) have suggested that the pathways for passing the gas molecules are narrow, thus acting as capillary tubes. The flow rate of the passing gas can be calculated from Equation 6-2 (Poiseuille's gas flow law):

$$V = (\frac{p\Delta P}{8hL})R^4 \qquad (6\text{-}2)$$

where:

V = Volume, cm^3 / second

h = The coefficient of viscosity, poise

ΔP = The difference in pressure between the two ends of the tube, dynes/cm^2

L = The length of the tube, cm

R = The radius of the tube, cm.

As can be seen from Equation 6-2 a small reduction in the effective radius of a capillary tube will cause a drastic reduction in the gas flow rate because the flow rate is proportional to the fourth power of the radius of the capillary tube. Thus gas flow through channels with dimensions near those of a capillary tube is governed by the pore or channel dimensions. From the tests results in Table 6.1 and illustrated in Figure 6.8a-d it is hypothesised that the sorption of molecules, especially carbon dioxide on the pores walls as a monolayer, reduces the effective radius of pathways

and hinders the passage of the gas through the pathways (interconnected pores or cleats), and does in fact reduce permeability.

Results show that permeability of coal to CH_4 is almost an order of magnitude greater than that of CO_2, while the molecular diameter is similar at 38 Å and 41 Å, respectively.

(a) methane (b) carbon dioxide (c) nitrogen (d) CH_4/CO_2 mixture

Figure 6.8 Schematic view of the passage of gas molecules through micropores with adsorbed gases.

It should also be noted, as was shown in the previous chapter, that when gases such as CO_2 and CH_4 are present in the coal matrix, the coal swells due to gas sorption (Harpalani and Zhao, 1991). This swelling effectively causes cleat closure and reduction in the transmissivity of the cleats.

The results of the four sets of experiments with different gases for coal samples from different mines that were conducted in this research are shown in Figures 6.9 to 6.13.

It is clear from Figures 6.9 to 6.13 that the permeability of coal from North Goonyella is greater than for the others. The order of permeability is North Goonyella, Dartbrook, Tahmoor, Metropolitan and the least permeability is Tabas.

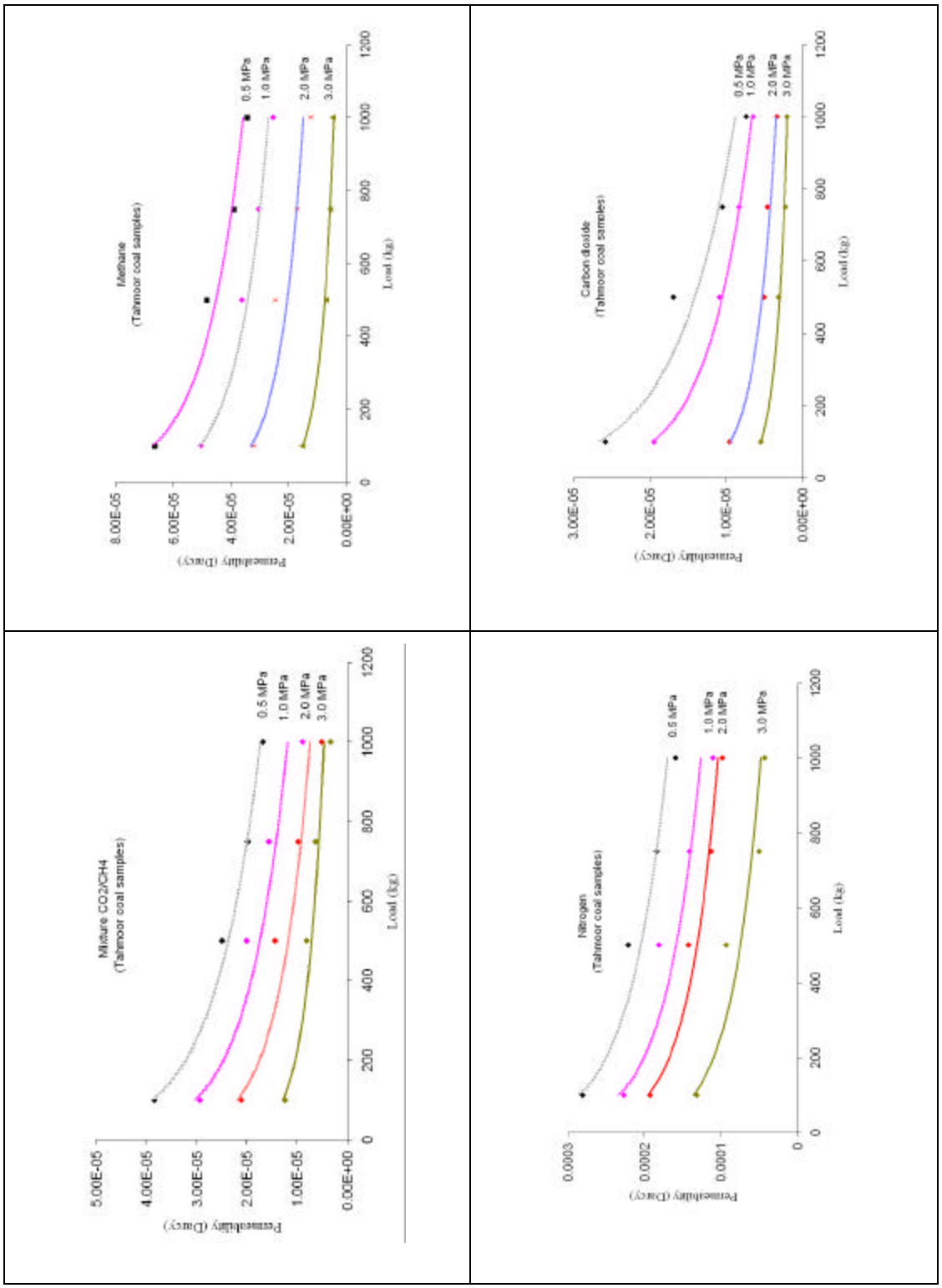

Figure 6.9 Average permeability of Tahmoor coal samples to gas under various axial loads.

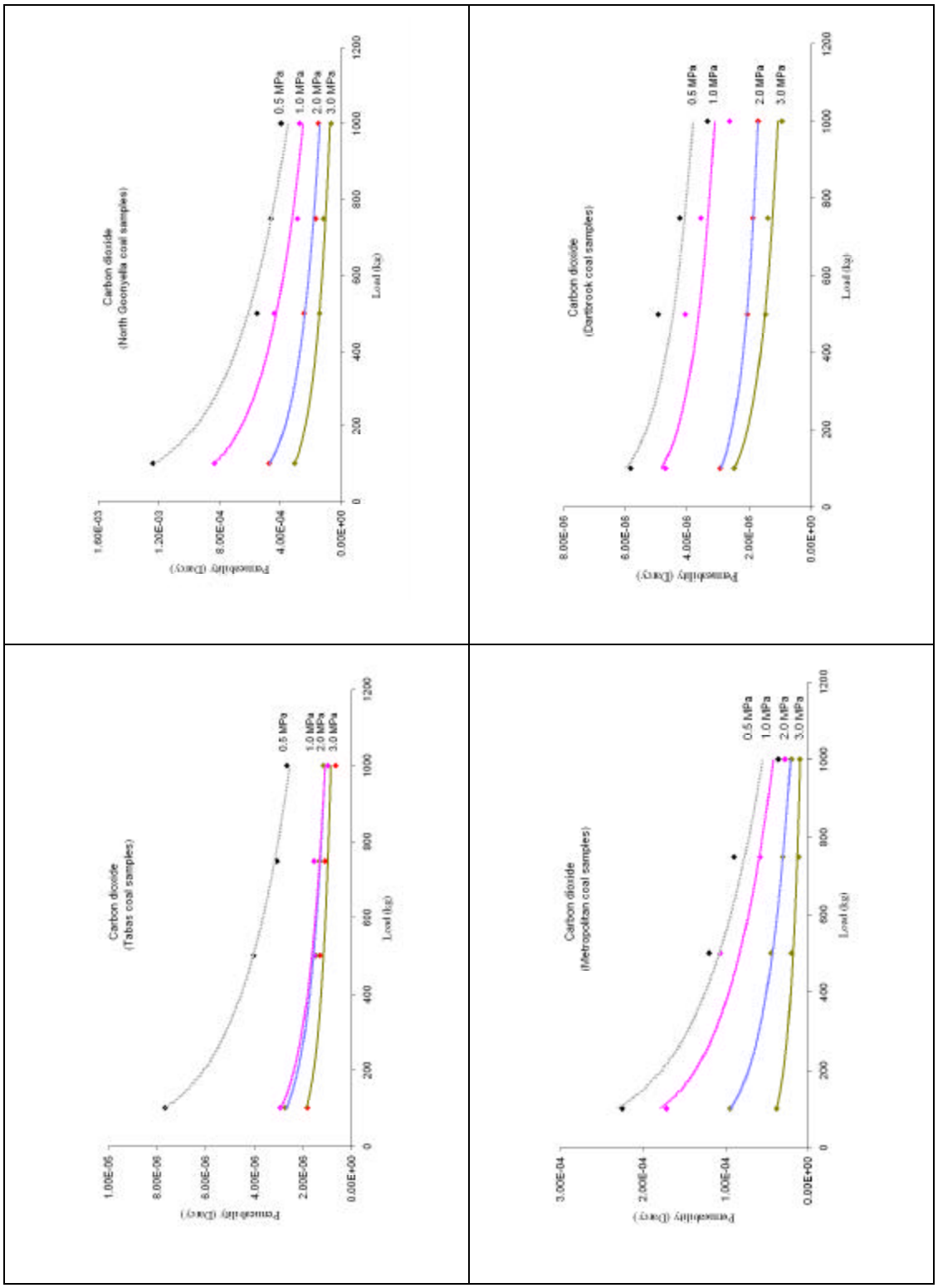

Figure 6.10 Average permeability of all samples to CO_2 under various axial loads.

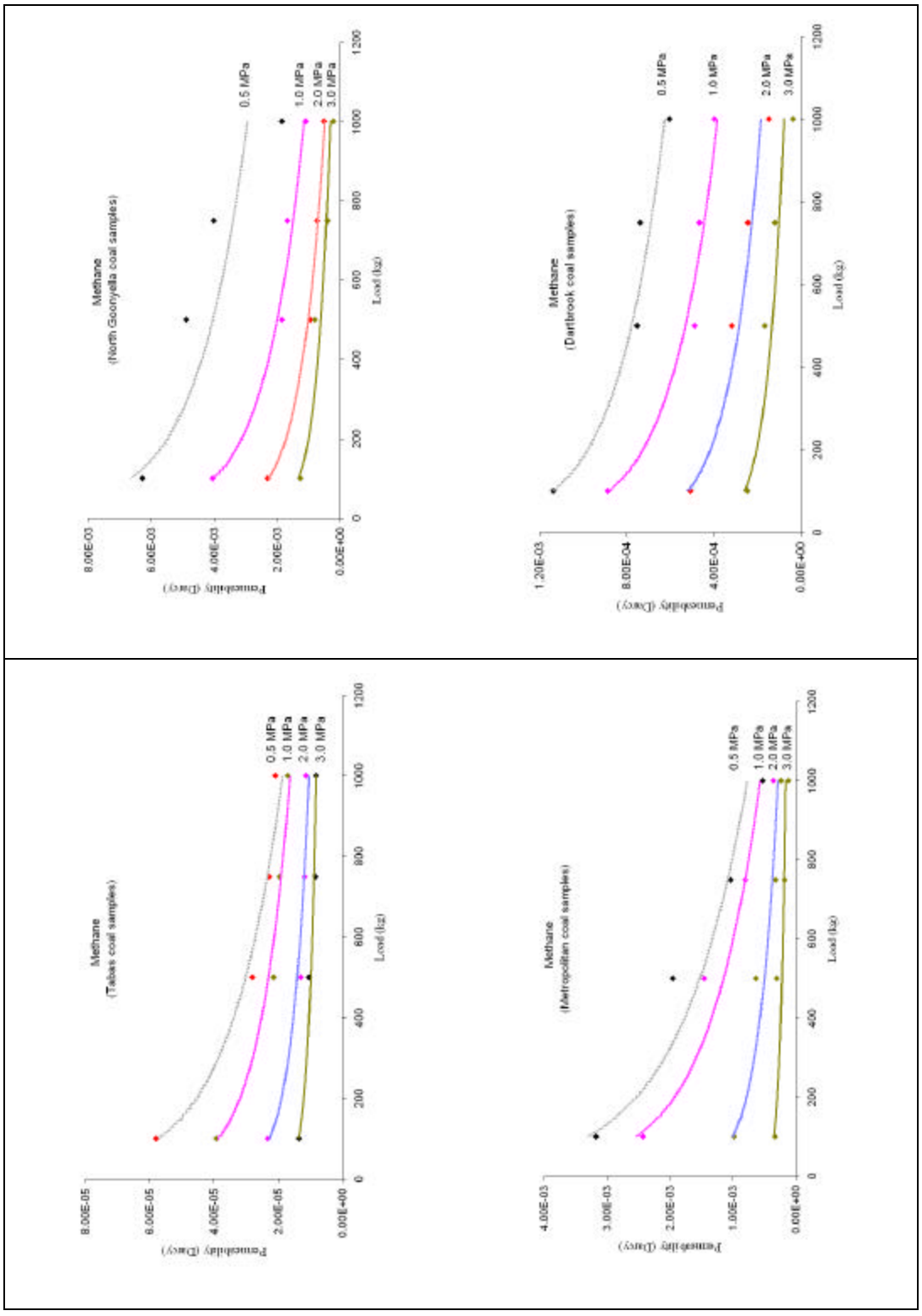

Figure 6.11 Average permeability of all samples to CH_4 under various axial loads.

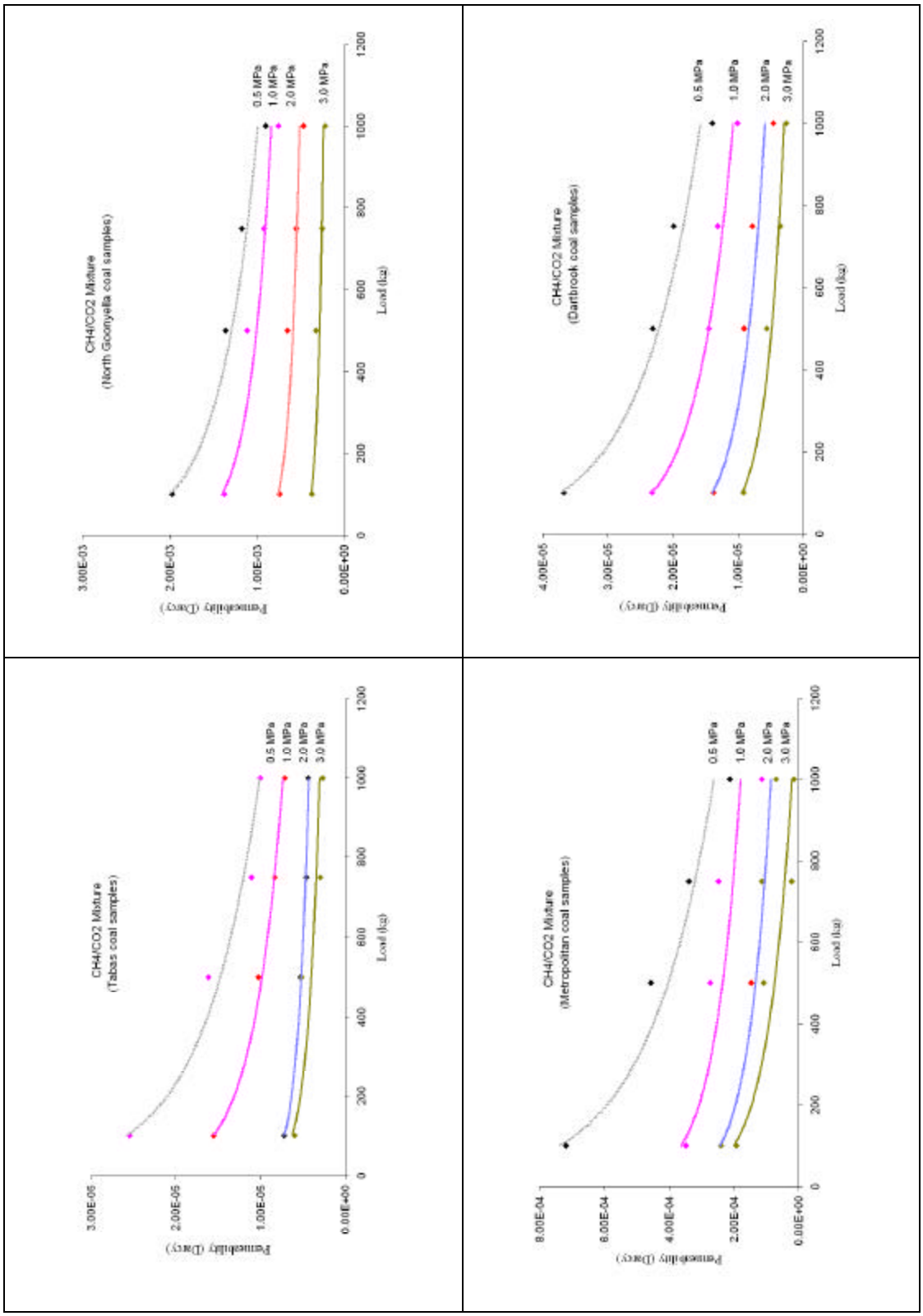

Figure 6.12 Average permeability of samples to CH_4/CO_2 under various axial loads.

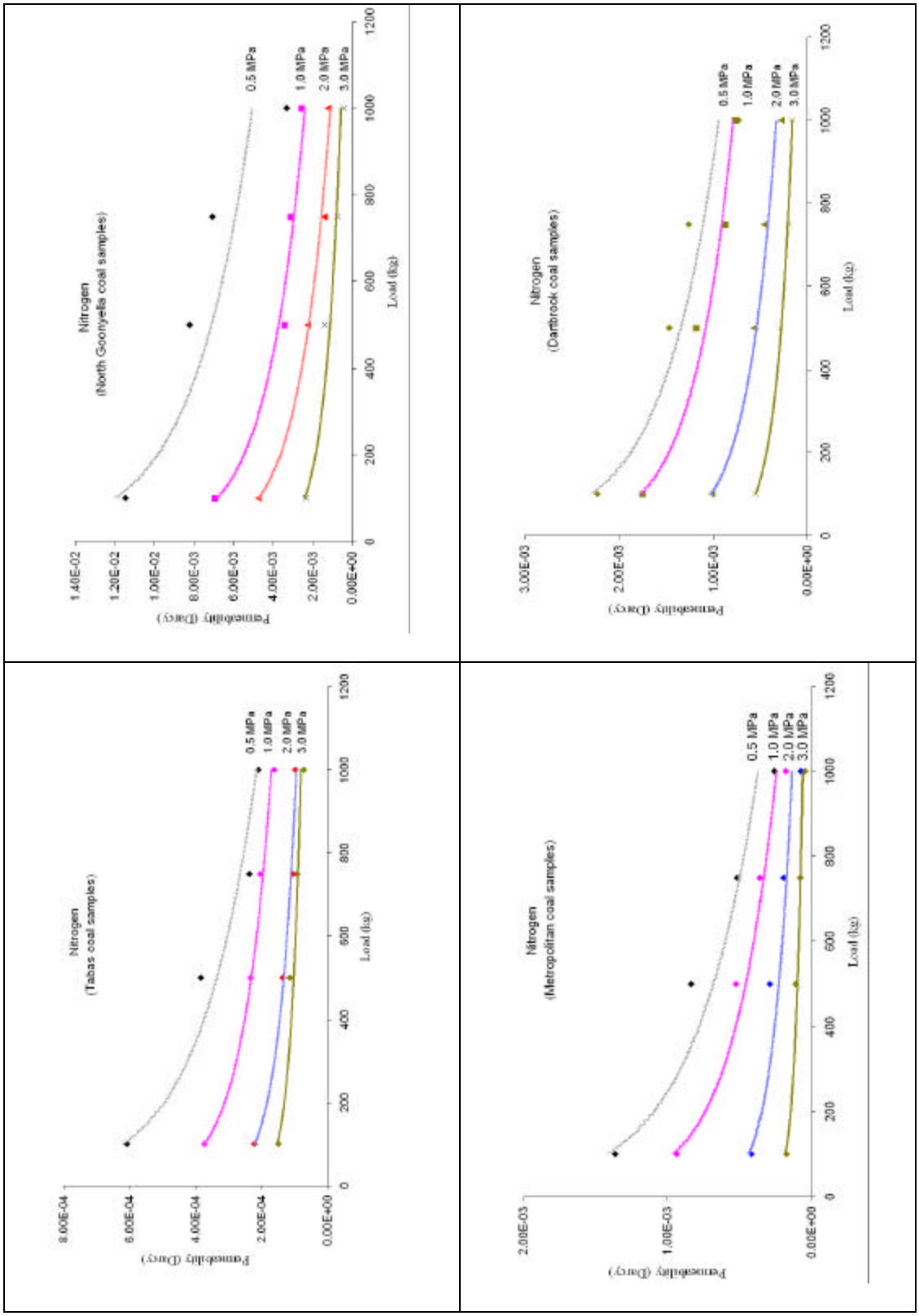

Figure 6.13 Average permeability of all samples to N_2 under various axial loads.

As stated above the Tabas coal samples had the lowest permeability. A closer analysis of the petrological composition, as explained in Chapter 4, indicated that Tabas coal had 70% vitrinite as well as having mineral matter such as pyrite, which is a typical characteristic of this type of coal. The vitrinite maceral pores were likely to be filled with mineral matter and pyrite, thus causing a reduction in permeability. Relatively low permeability was also observed in Tahmoor samples, especially from the 900 area, which after Tabas had the highest amount of vitrinite and were more than 7.8% rich in mineral matter. The North Goonyella coal samples, which had relatively higher permeability compared with the other samples, generally had a higher amount of inertinite and a smaller amount of vitrinite. This clearly demonstrates that coals with a higher percentage of vitrinite have lower permeability in comparison with the inertinite rich coals. It is the macropores or fractures that provide the main flow path for the methane (Curl, 1978). According to Mahajan (1982) the finest porosity that they observed in vitrinite ranged from 20 to 200 Å in diameter, with the majority of pores being at the smaller end of the size range, while inertinite was found to be the most porous maceral group and typically contained a broad range of pores from 50 to 500 Å. Also, Crosdale, Beamish and Valix (1998) have claimed, on the basis of his tests, that the inertinite-rich dull coals have greater total pore volume compared to bright coal (vitrinite-rich). Gamson and Beamish (1992) after tests on some Australian coals also claimed that dull coals have relatively large macropores, while in the bright coals the micropores are dominant, and thus the inertinite rich coals are better situated for laminar gas flow and better permeability.

The extent of gas flow through the microstructures will be influenced by the amount of mineral filling them, since many of the cleats and pores are commonly blocked by mineral matter such as pyrite and calcite, which restricts the area for the gas to pass through.

The tests in this research showed that in all cases except the Tahmoor 900 panel samples, the dull coal samples (with a higher percentage of inertinite) had a higher permeability than bright coal (vitrinite-rich). With the exception of Tahmoor 900 panel this is in general agreement with the results of the tests on various Australian coals that were conducted by Lama and Mitchell (1981). Similarly Creedy (1991) found that the greater the inertinite group content in coal the faster the coal degassed. In comparison, however, Clarkson and Bustin (1997) suggested that the permeability of Canadian coal increases with increasing vitrinite content.

6.3.4 Effect of loading stress

The test results were also used to investigate the relationship between coal permeability and confining gas pressure under various axial loads. Figures 6.14 to 6.17 show the experimental results for average change in permeability of all samples from Dartbrook with variation of axial load and gas pressures for different kinds of gases. From Figures 6.14 to 6.17 it can be seen that the permeability of coal to methane is reduced exponentially by increasing the load, irrespective of gas type. Furthermore not only is the permeability of coal very stress dependent, it is also dependent on the mean gas pressure so that by increasing the mean gas pressure up to 3 MPa the permeability was decreased.

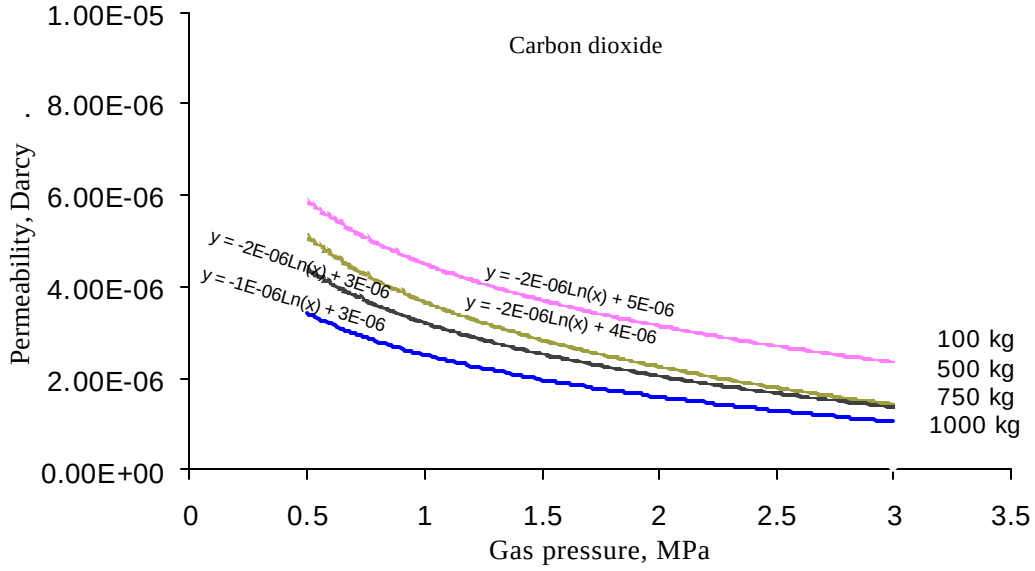

Figure 6.14 Dartbrook coal permeability under different CO_2 gas pressures and various axial stresses.

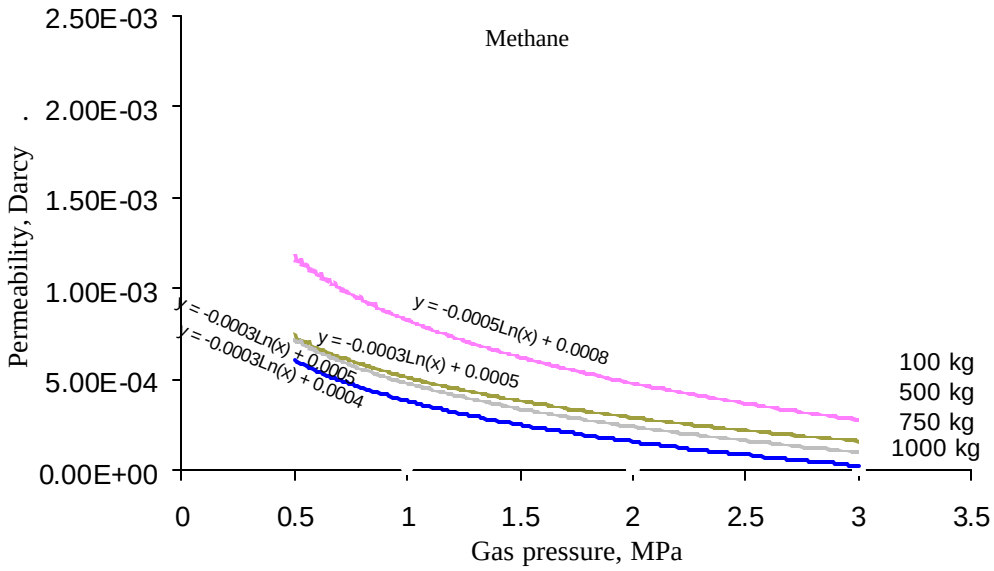

Figure 6.15 Dartbrook coal permeability under different CH_4 gas pressures and various axial stresses.

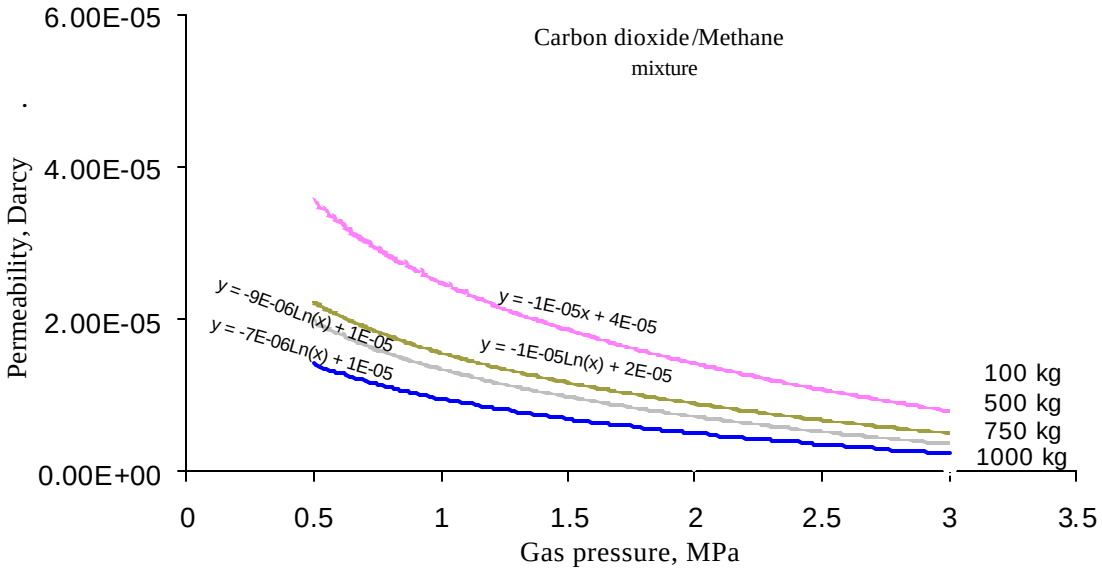

Figure 6.16 Dartbrook coal permeability under different CO_2/CH_4 (1:1 Mixture) gas pressures and various axial stresses.

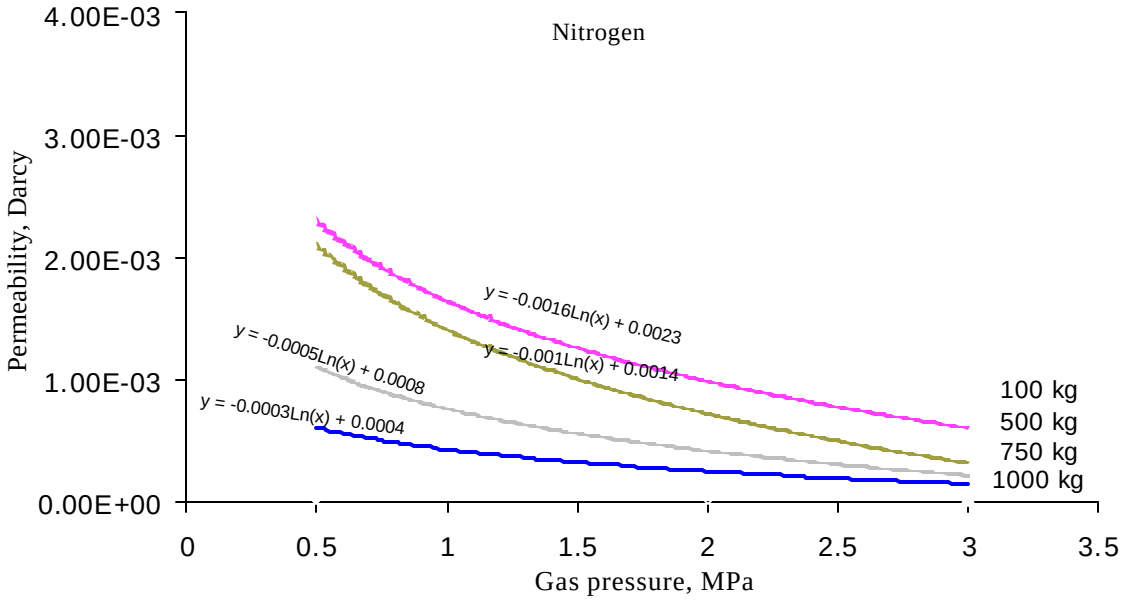

Figure 6.17 Dartbrook coal permeability under different N_2 gas pressures and axial stresses.

6.4 MODELLING THE FLOW OF GAS FROM COAL CORES

A numerical modelling study was undertaken to illustrate the influence of stress-dependent permeability on gas release and transportation. This work was undertaken by using the data obtained from the permeability tests conducted to determine the effect on permeability of applied vertical loads and different gas confining pressures.

The basic objectives of the numerical modelling study were:

- to compare the changes in gas pressure in the coal matrix due to changing permeability;
- to illustrate the influences of different gas environments on gas pressure gradient in the coal matrix.

6.4.1 Modelling procedure

The flow of gas in coal takes place under two simultaneous and parallel processes, Fick's diffusion and Darcy's laminar flow. Fick's diffusion takes place mainly in the micropore system whereas Darcy's flow occurs in the macropore channels and fractures.

For an isothermal system, the study of gas flow in porous media is based on a mass balance equation (Wu, Pruess and Persoff, 1998):

$$\tilde{N} \cdot (\rho \mathbf{u}) + f \frac{\partial \rho}{\partial t} = 0 \qquad (6\text{-}3)$$

where:

r = Gas density, kg/m^3

u = Darcy velocity of gas phase, m/s

f = Formation porosity, dimensionless

Also, Darcy's law can be used to investigate a single viscous fluid flowing through the porous medium. Darcy's law defines the relation between the flux of the fluid through the coal (medium) and the pressure gradient of the fluid:

$$\mathbf{u} = -\frac{k}{m}\tilde{\mathrm{N}}P \qquad (6\text{-}4)$$

Where:

k = Permeability, Darcy

m = Dynamic viscosity, centipoise

P = Pressure, Pa

By considering gas as an ideal fluid, the following equation can be used:

$$PV=nRT \qquad (6\text{-}5)$$

$$r = \frac{M}{V} \qquad (6\text{-}6)$$

$$r = \frac{M_m}{RT}P \qquad (6\text{-}7)$$

hence:

n = The quantity of gas, moles

R = Universal gas constant, m^3 Pa/mol K

T = Temperature, K

V = Volume, m^3

M = Mass, kg

M_m = Molecular mass, kg/mole

The result of combining of equations 6-1 and 6-2 will be:

$$\tilde{N}\chi(P\tilde{N}P) = \frac{mf}{k}(\frac{\partial P}{\partial t}) \qquad (6\text{-}8)$$

which can be written as:

$$\nabla^2 P^2 = \frac{mf}{kP}(\frac{\partial P^2}{\partial t}) \qquad (6\text{-}9)$$

Let P_{max} equal the lateral hydrostatic confining pressure applied in the gas pressure chamber containing the coal, and assuming that at the inner surface of the centrally drilled hole in the middle of samples the pressure was constant (atmospheric pressure), then it can be shown that gas pressure is only a function of time and the distance of the point from the inner hole axis (z axis). By using cylindrical coordinates, Equation (6-9) will be in the following form.

$$\frac{\partial^2}{\partial r^2}P(r,t)^2 + \frac{1}{r}\frac{\partial}{\partial r}P(r,t)^2 = \frac{mf}{kP(r,t)}\frac{\partial}{\partial t}P(r,t)^2 \qquad (6\text{-}10)$$

r = Radius of core, m

t = Time, s

Equation (6-10) may be written in the following compact form:

$$\frac{1}{r^2}\frac{\partial^2 P(r,t)^2}{(\partial(\ln r))^2} = \frac{mf}{kP(r,t)}\frac{\partial}{\partial t}P(r,t)^2 \qquad (6\text{-}11)$$

For optimising the computer efficiency, only dimensionless quantities, and not the existing real quantities for pressure and distance from the inner hole axis (A-A) were used in the above mentioned differential equations:

$$\frac{P}{P_{\max}} \rightarrow P'$$

$$\frac{r}{r_\circ} \rightarrow r'$$

P' = Dimensionless pressure $\qquad$ $P_{\max}$ = Inlet pressure, Pa

r' = Dimensionless radius $\qquad$ $r_\circ$ = Radius of hole, cm

$$\frac{P_{\max}^2 \partial^2\left(\frac{P^2}{P_{\max}^2}\right)}{r_\circ{}^2\left(\partial\frac{r}{r_\circ}\right)^2} + \frac{P_{\max}^2}{r_\circ^2}\frac{1}{\left(\frac{r}{r_\circ}\right)}\frac{\partial\left(\frac{P^2}{P_{\max}^2}\right)}{\partial\left(\frac{r}{r_\circ}\right)} = \frac{mf\ P_{\max}^2}{k\left(\frac{P}{P_{\max}}\right)P_{\max}}\frac{\partial\left(\frac{P^2}{P_{\max}^2}\right)}{\partial t} \qquad (6\text{-}12)$$

$$\left(\frac{P_{\max}^2}{r_\circ^2}\frac{\partial^2 P'^2}{\partial r'^2}\right) + \left(\frac{P_{\max}^2}{r_\circ^2}\frac{1}{r'}\frac{\partial P'^2}{\partial r'}\right) = \left(\frac{mfP_{\max}^2}{kP_{\max}}\right)\left(\frac{1}{P'}\frac{\partial P'^2}{\partial t}\right) \qquad (6\text{-}13)$$

$$\frac{\partial^2 P'^2}{\partial r'^2} + \frac{1}{r'}\frac{\partial P'^2}{\partial r'} = \left(\frac{mf\ r_\circ^2}{kP_{\max}}\right)\left(\frac{1}{P'}\frac{\partial P'^2}{\partial t}\right) \qquad (6\text{-}14)$$

Defining

$$t = \frac{mfr_\circ{}^2}{kP_{\max}} \qquad (6\text{-}15)$$

then:

$$\frac{\partial^2 P'^2}{\partial r'^2}+\frac{1}{r'}\frac{\partial P'^2}{\partial r'}=\frac{t}{P'}\frac{\partial P'^2}{\partial t} \qquad (6\text{-}16)$$

By dividing the radial distance between inner and outer surface of coal sample at an arbitrary z-component to "n" equal parts by n +1 points, Figure 6.18 can be developed.

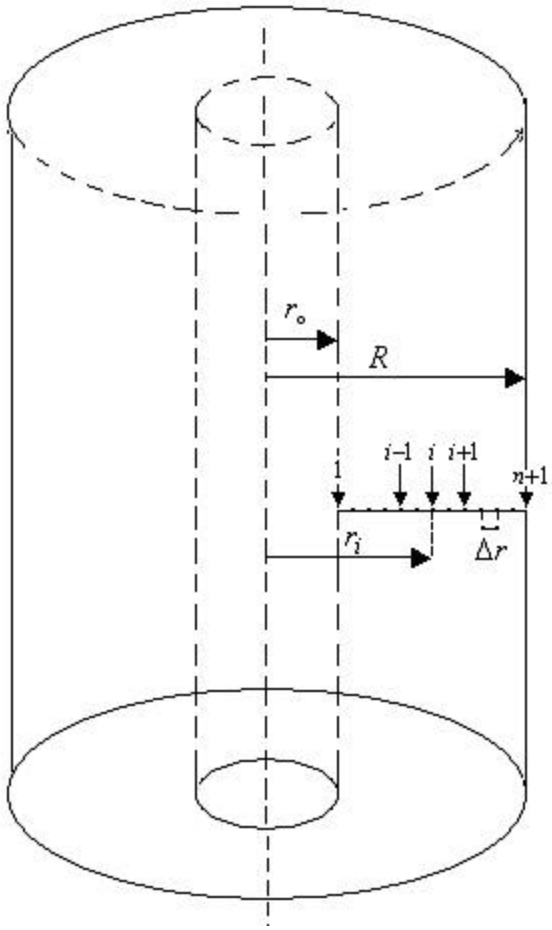

Figure 6.18 Time related division between inner and outer surface of coal sample

By dividing the distance of "ith" point from z-axis it could be found that:

$$r_i = r_\circ + (i-1)\Delta r$$

The situation in the system is being considered at incremental time steps, with each step equal to Δt. In "j" time steps ($t_j = j\Delta t$), for gas at a point with $r = r_i$, the pressure will be defined by P (r_i, t_j). For simplicity, P^2 (r_i,t_j) could be replaced by $Y(i, j)$, and for the above it classification can be written.

$$\frac{\partial Y}{\partial r} \rightarrow \frac{1}{2}\left[\frac{Y(i+1, j)-Y(i, j)}{\Delta r}+\frac{Y(i, j)-Y(i-1, j)}{\Delta r}\right] \tag{6-17}$$

$$\frac{\partial Y}{\partial r} \rightarrow \frac{1}{2\Delta r}\left[Y(i+1, j)-Y(i-1, j)\right] \tag{6-18}$$

then:

$$\frac{\partial^2 Y}{\partial r^2} \rightarrow \frac{1}{\Delta r}\left[\frac{Y(i+1, j)-Y(i, j)}{\Delta r}-\frac{Y(i, j)-Y(i-1, j)}{\Delta r}\right] \tag{6-19}$$

$$\frac{\partial^2 Y}{\partial r^2} \rightarrow \frac{1}{\Delta r^2}\left[Y(i+1, j)-2Y(i, j)+Y(i-1, j)\right] \tag{6-20}$$

also:

$$\frac{\partial Y}{\partial t} \rightarrow \frac{Y(i, j+1)-Y(i, j)}{\Delta t} \tag{6-21}$$

By substituting from Equations (6-18), (6-19) and (6-21), it will be found that:

$$a\left[\frac{\partial^2}{\partial r^2}+\frac{1}{r}\frac{\partial}{\partial r}Y\right]\cdot\sqrt{Y}=\frac{\partial Y}{\partial t} \tag{6-22}$$

Where:

$$a=\frac{1}{t} \tag{6-23}$$

Then:

$$a\left\{\frac{1}{\Delta r^{2}}\left[Y(i+1,j)-2Y(i,j)+Y(i-1,j)\right]+\frac{1}{(r_{\circ}+(i-1)\Delta r)}\left[\frac{1}{2\Delta r}\right]\left[Y(i+1,j)-Y(i-1,j)\right]\right\}\times$$

$$\times\sqrt{Y(i,j)}=\frac{Y(i,j+1)-Y(i,j)}{\Delta t} \qquad (6\text{-}24)$$

$$\Rightarrow Y(i,j+1)=a\ \Delta t\sqrt{Y(i,j)}\quad\left\{\frac{1}{\Delta r^{2}}\left[Y(i+1,j)-2Y(i,j)+Y(i-1,j)\right]\right.$$
$$\left.+\left(Y(i+1,j)-Y(i-1,j)\right)\frac{1}{2\Delta r(r_{\circ}+(i-1\Delta r))}\right\}+Y(i,j) \qquad (6\text{-}25)$$

The initial and boundary conditions are as follows:

for t = 0:

$$\{r_{\circ}\le r<R\Rightarrow P=0$$

$$\{r=R\Rightarrow P=P_{\max}$$

And for all t≥0:

$$r=r_{\circ}\Rightarrow P=0$$

$$r=R\Rightarrow P=P_{\max}$$

Because the initial values and the boundary conditions are completely specified, the differential equation can be solved by using a numerical method.

Figure 6.19 shows how different values of pressure in various places at each time step is being determined with regard to the quantities or pressures in different time steps.

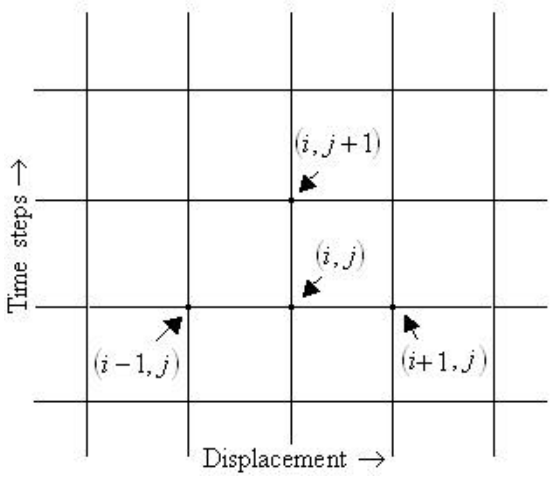

Figure 6.19 Determining gas pressure at any point and each time step taking into account the quantities in its neighbourhood at the previous time step.

Table 6.3 shows the model general input, these inputs were similar to the tested coal samples.

Table 6.3 Model input

Basic parameters of the model	
Coal sample height, mm	50
Coal sample diameter, mm	50
Diameter of inner hole, mm	6
Inlet gas pressure, MPa	0.5 - 1.0 - 1.5 - 2.0 - 2.5 - 3.0
Outlet gas pressure, MPa	Atmospheric pressure
Axial load, kg	100 - 500 – 750 - 1000
Porosity, %	2 (constant value)

The model responds to the changes to input values of any or all of the following parameters:

- Stress related permeability
- Applied inlet gas pressures

- Dynamic viscosity of tested gas
- Sample length and diameter
- Hole diameter
- Porosity of coal matrix

Using the data, obtained from permeability tests and the viscosity values for each of CH_4, CO_2, CH_4/CO_2 and N_2 as 0.0112, 0.0155, 0.0131 and 0.017 centipoise, respectively (Lide, 2000 and Jones, 2003). The gas flows through the coal matrix for four different axial loads were simulated Figures 6.20 to 6.23, shows that the increase in axial load has a detrimental effect on the passage of gas through the coal matrix.

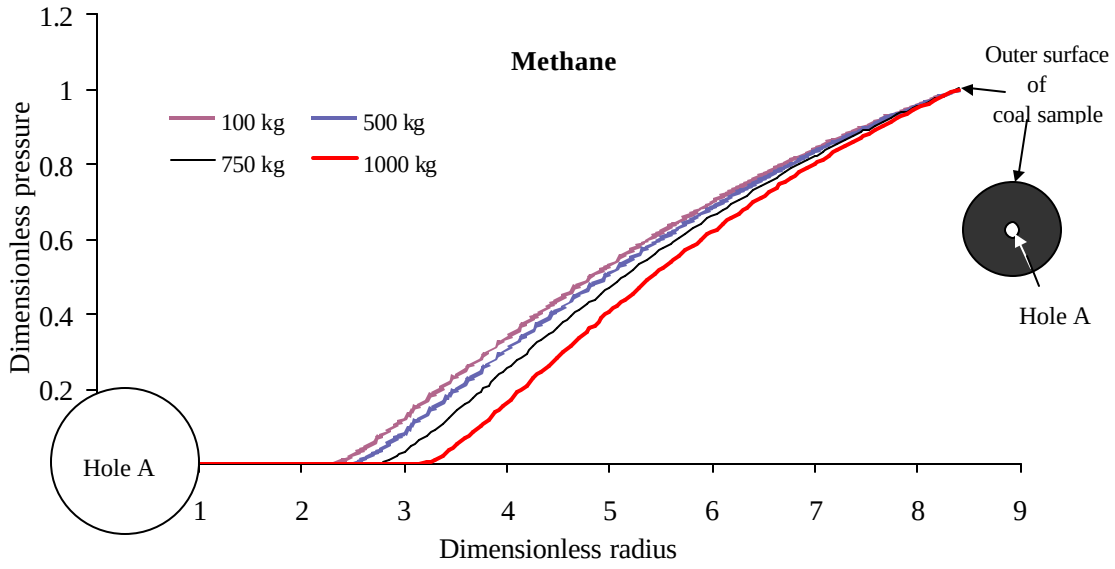

Figure 6.20 Methane gas radial flow through the coal sample at dimensionless pressure and dimensionless distance as a function of different axial loads in 0.1s duration.

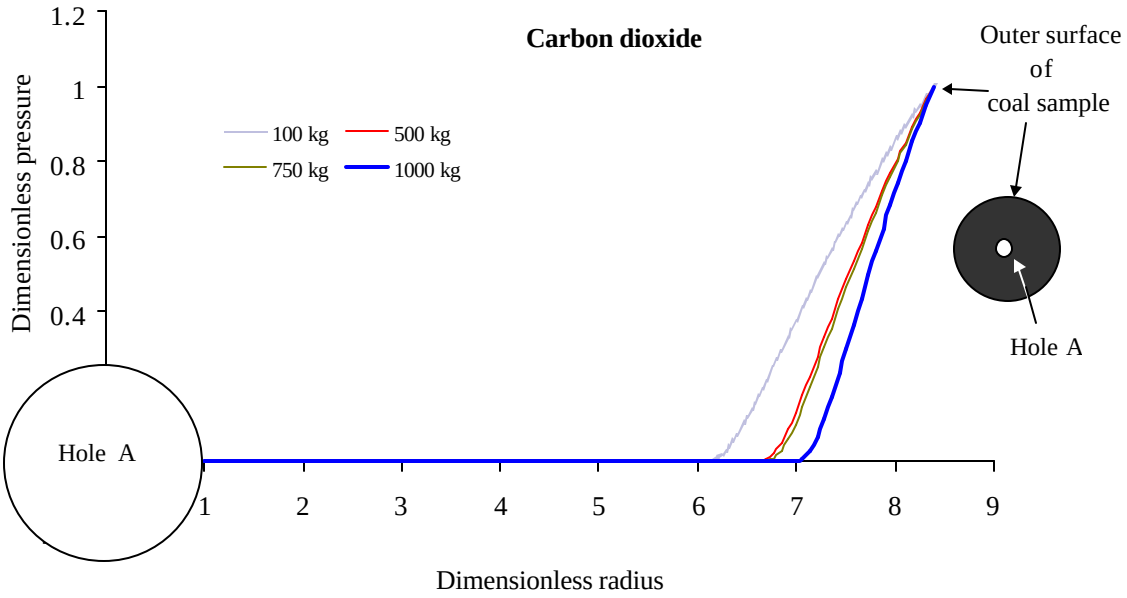

Figure 6.21 CO_2 radial flow within a coal sample and dimensionless pressure at dimensionless distance as a function of different axial loads, in 0.1s.

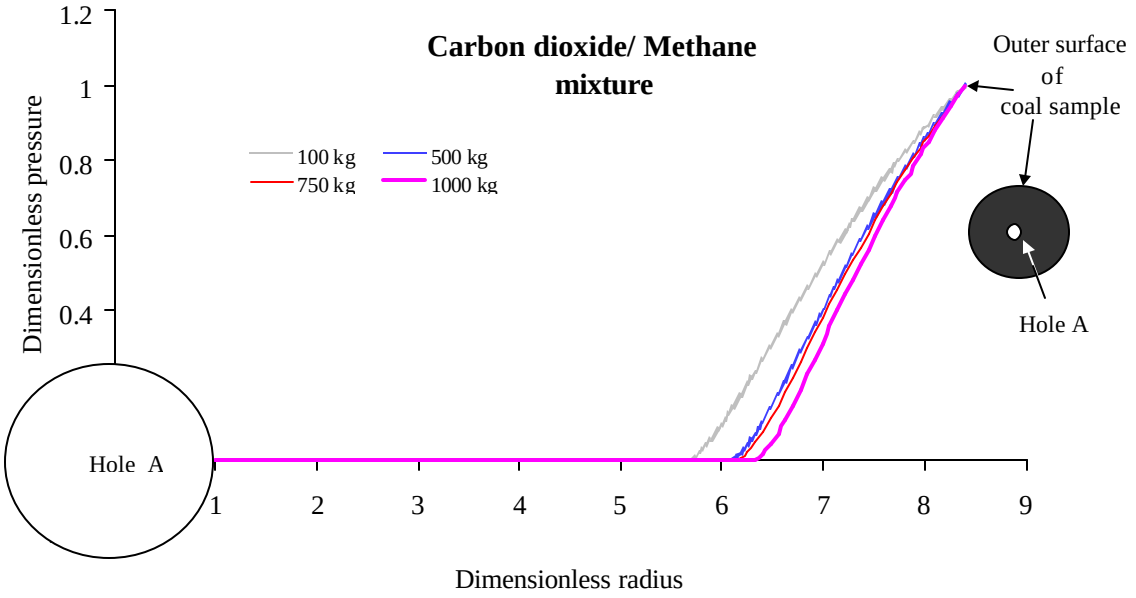

Figure 6.22 CO_2 / CH_4 radial flow within a coal sample and dimensionless pressure at dimensionless distance as a function of different axial loads in 0.1s duration.

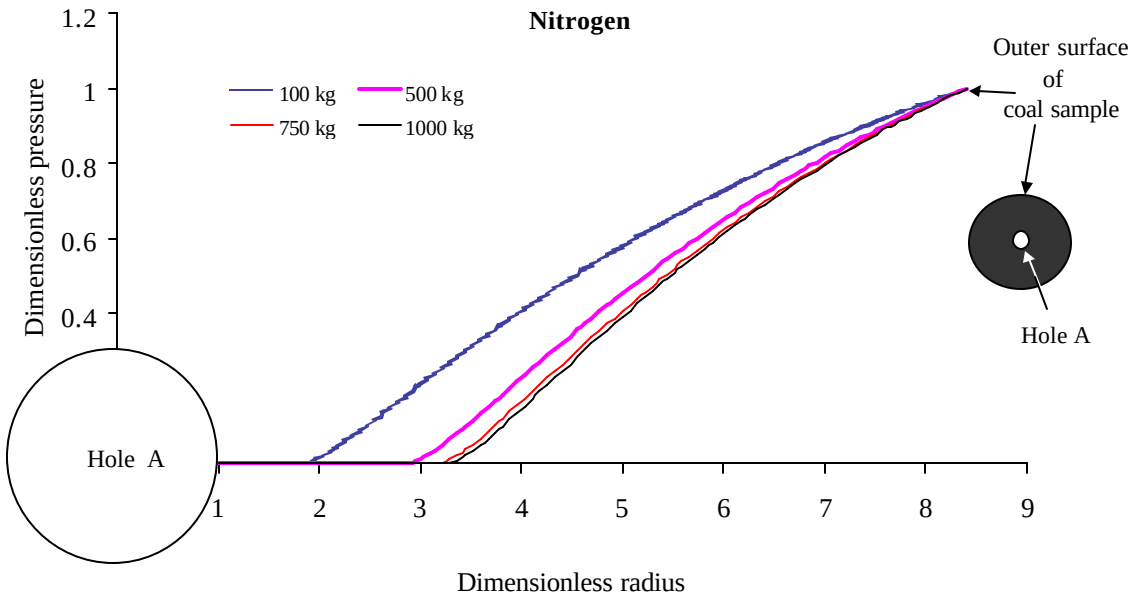

Figure 6.23 N_2 radial flow within a coal sample and dimensionless pressure at dimensionless distance as a function of different axial loads in 0.1s time.

As shown in Figures 6.20 to 6.23, the hydrostatic pressure around the outer surface of coal is obviously the highest and it is reduced gradually as the distance is reduced towards the inner hole wall. This is exactly what will occur in reality and demonstrates the validity and effectiveness of the model in simulating the real time pressure gradient across the coal sample radius. Increases in axial load will cause a reduction in the permeability for gas passing through the media. For each sample at lower axial loads the Darcy velocity of the gas phase will be higher, thus gas passing through the media will be faster and a quasi steady state flow and approximate saturation of gas in the pores will be achieved sooner. Considering the mass balance equation (6.3), at any applied axial load and for each sample, the pressure gradient and the radial velocity of the gas will be higher in the inner layers of the media (closer to hole) in a quasi steady state flow.

In the second series of RUNS, all conditions were maintained constant and results were plotted for different times. Results from RUN 2 are plotted in Figures 6.24 – 6.27. As can be seen, the order of gas release from hole "A" is in fair agreement with the behaviour of those gases in the laboratory tests. Nitrogen and methane reach the outlet during the first few moments, however, this time increases for the other two gases, CO_2 and CH_4/CO_2. After initial application of the inlet pressure and in the first steps of the flow process, gas will try to occupy the pores while it is passing through the coal media. Then, the pressure of gas in pores will increase until an approximately saturated situation occurs and achievement of a quasi steady state flow through the coal media is reached.

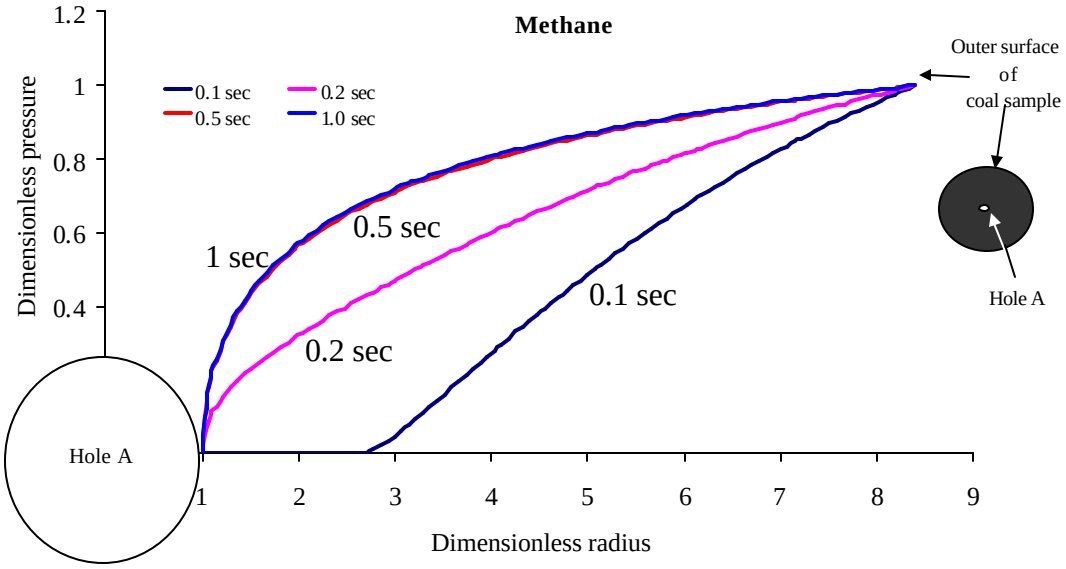

Figure 6.24 Radial flow within a coal sample and dimensionless pressure at dimensionless distance as a function of time and axial load 100 kg

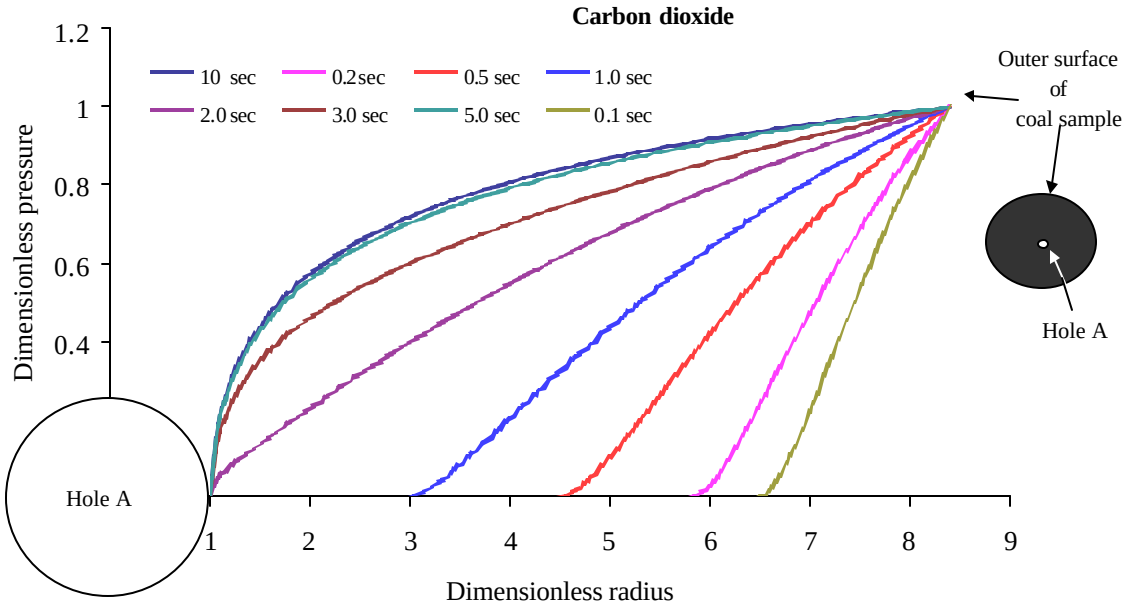

Figure 6.25 Radial flow within a coal sample and dimensionless pressure at dimensionless distance as a function of time, and axial load 100kg for CO_2.

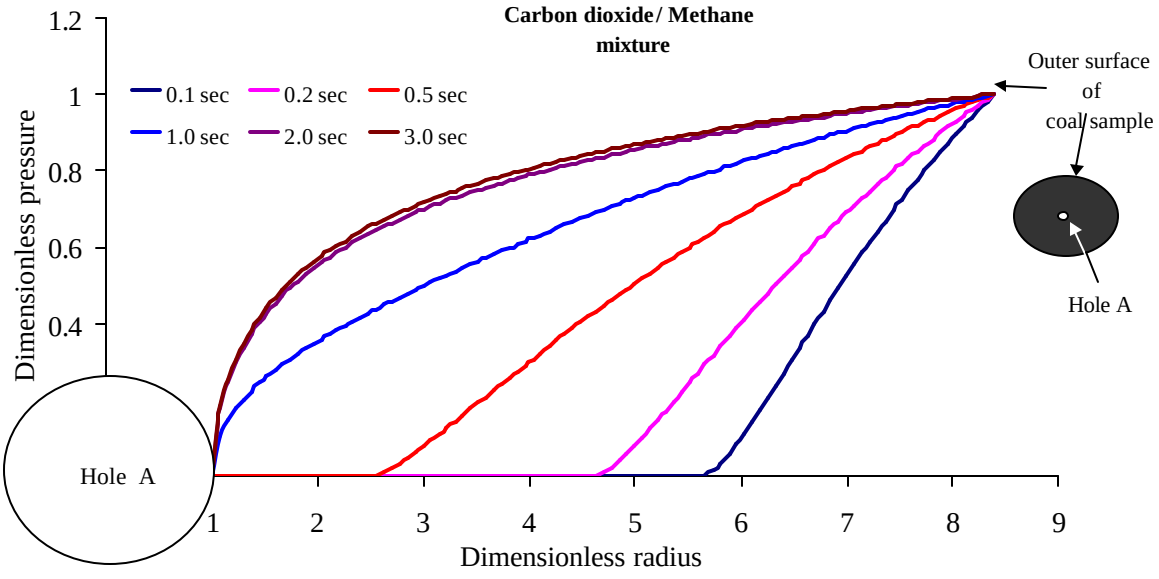

Figure 6.26 Radial flow within a coal sample and dimensionless pressure at dimensionless distance as a function of time and axial load 100 kg for CH_4/CO_2.

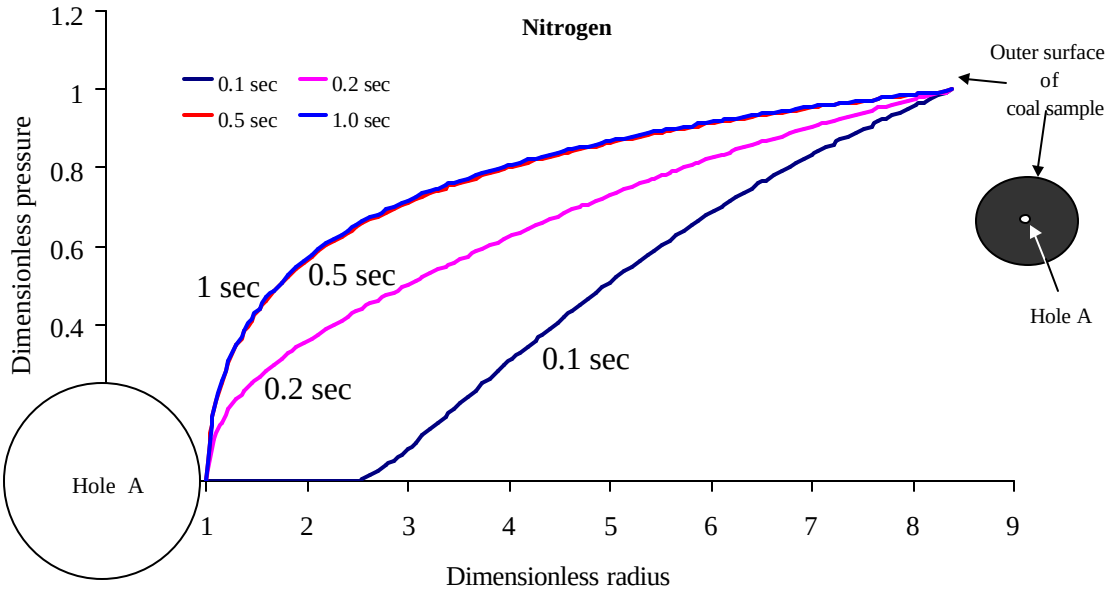

Figure 6.27 Radial flow within a coal sample and dimensionless pressure at dimensionless distance as a function of time and axial load 100 kg for N_2.

In the last series of RUNS the gas environments were changed while the uniaxial load and gas pressure were constant at any given time. As can be seen from Figures 6.28 and 6.29, methane and nitrogen reached the inner hole in a much shorter time than carbon dioxide and the CH_4/CO_2 mixture respectively. A faster drop in pressure or the high pressure gradient is a clear indication of the ease with which both N_2 and CH_4 would flow through the coal in comparison to CO_2 and the CO_2/CH_4 mix. The molecular weight, viscosity and most importantly, the affinity of coal to gases like CO_2 could be the major reasons for this phenomena. Each sample with a higher ratio of permeability to dynamic viscosity will pass gas faster so the achievement of quasi steady state flow will be naturally faster for that sample.

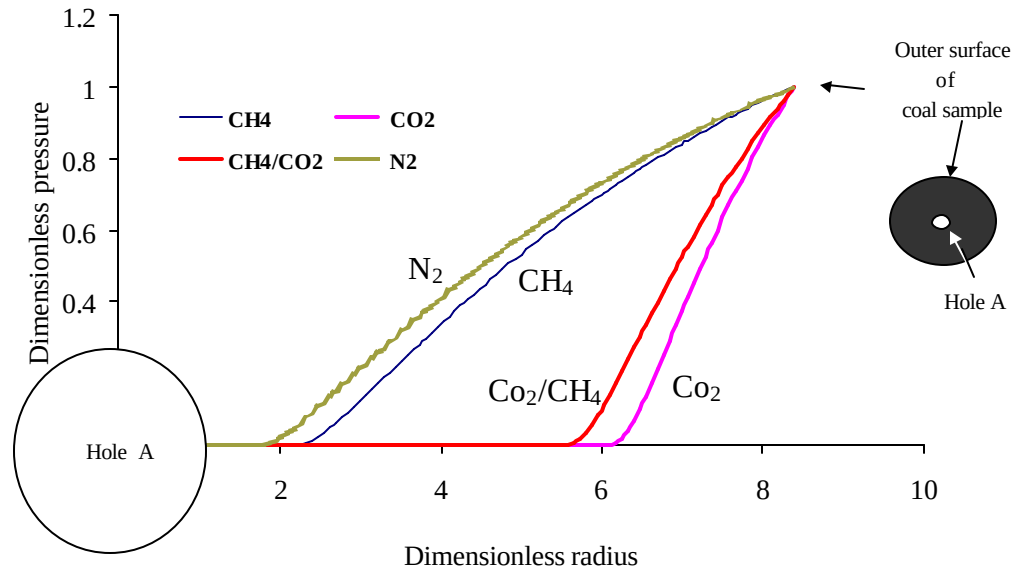

Figure 6.28 Radial flow within a coal sample and dimensionless pressure at dimensionless distance as a function of gas environment after 0.1 second.

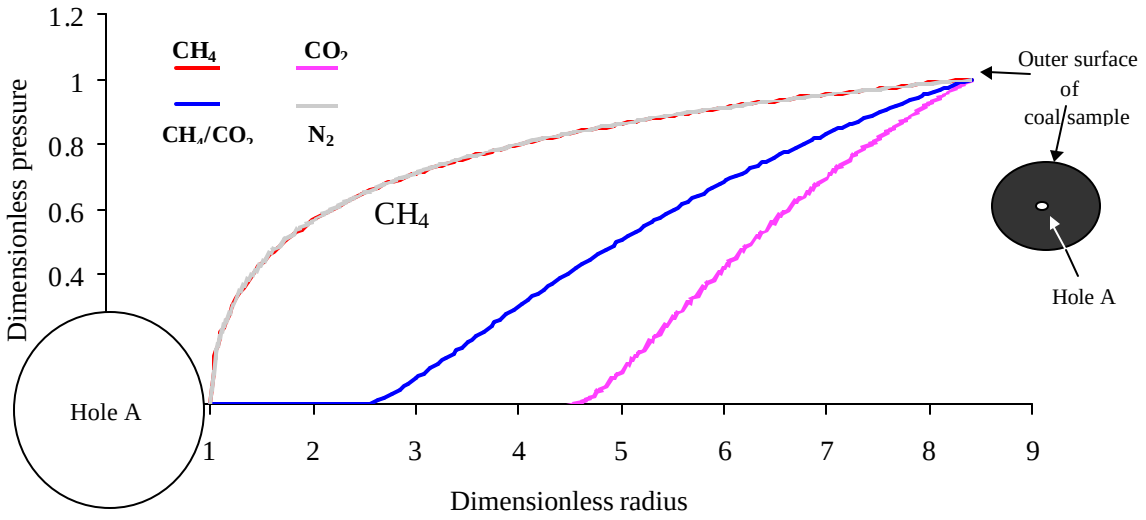

Figure 6.29 Radial flow within a coal sample and dimensionless pressure at dimensionless distance as a function of gas environment after 1 second.

N_2

Co_2/CH_4 Co_2

6.5 CONCLUSIONS

The MFORR apparatus has been demonstrated to be a reliable tool for conducting permeability testing of coal under different gas pressures. The unique feature of the rig is the ability to apply a vertical load on the sample while it is confined under a specified gas pressure. The permeability of coal:

- depends on the applied stress, particularly when the load is applied perpendicular to coal layering or lamination,
- is influenced by the gas type and pressure. Greater gas permeability was obtained in N_2 gas, and the lowest permeability was obtained in a CO_2 environment. The sorption characteristics of CO_2 gas is a major factor
- is reduced exponentially by increasing the applied load and also by increasing the confining gas pressure, irrespective of the gas type.
- in various gases is exponentially reduced at different rates. Lower permeability values were obtained for coal in CO_2 gas, and the highest permeability occurred in N_2 gas.
- The numerical model provided an opportunity to quantify the flow rate in coal. The simulation of different gases flow characteristics in coal supports the experimental results as demonstrated in this chapter. The numerical model developed in this thesis would have an immense potential for future application to insitu coal gas drainage rate estimation.

CHAPTER SEVEN

CASE STUDY AND OVERALL

DISCUSSION OF RESULTS

7.1 INTRODUCTION

This chapter will present a case study and an overall discussion of the findings presented earlier in this thesis, with the intention of comparing the general relations found through the different stages of this research. The case study will be based on Tahmoor Colliery, where coal shrinkage, permeability and coal petrography techniques have produced data that permits a better understanding of the gas regime in this mine. The results are important to the further understanding of the inter-relationship between gas flow, the coal matrix and permeability in what is considered to be 'normal' and 'tight' coal (locally referred to as disturbed coal), the latter being coal that degases slowly compared to normal coal.

7.2 SITE INVESTIGATION

A programme of site studies were undertaken to relate the changes in geological conditions to gas storage characteristics of the coal. Core samples were collected from two different locations in Tahmoor mine (Figure 7.1). Two areas, which were identified for the study, were designated as 800 and 900 locations. The geology of the Bulli coal seam in the area of 800 panel, from where the 'normal' coal in terms of

drainability comes, could be described as benign, with normal conjugate cleat sets and no adverse geological structures and thus the mining conditions were considered as favourable. The 900 panel on the other hand was in a difficult to drain area. The 900 panel could be described as being geologically disturbed, with significant alteration of coal cleat directions, calcite infill into the matrix structure, readily seen near the top of the seam, major geological structures such as thrust faulting of nominal size, as well as igneous dyke activity. Mining conditions were therefore not favourable, and at times the mine resorted to the grunching (drill and blast) method of heading development, particularly in areas where the gas content levels were greater than the allowable threshold limits as set by the Department of Mineral Resources (New South Wales, Australia).

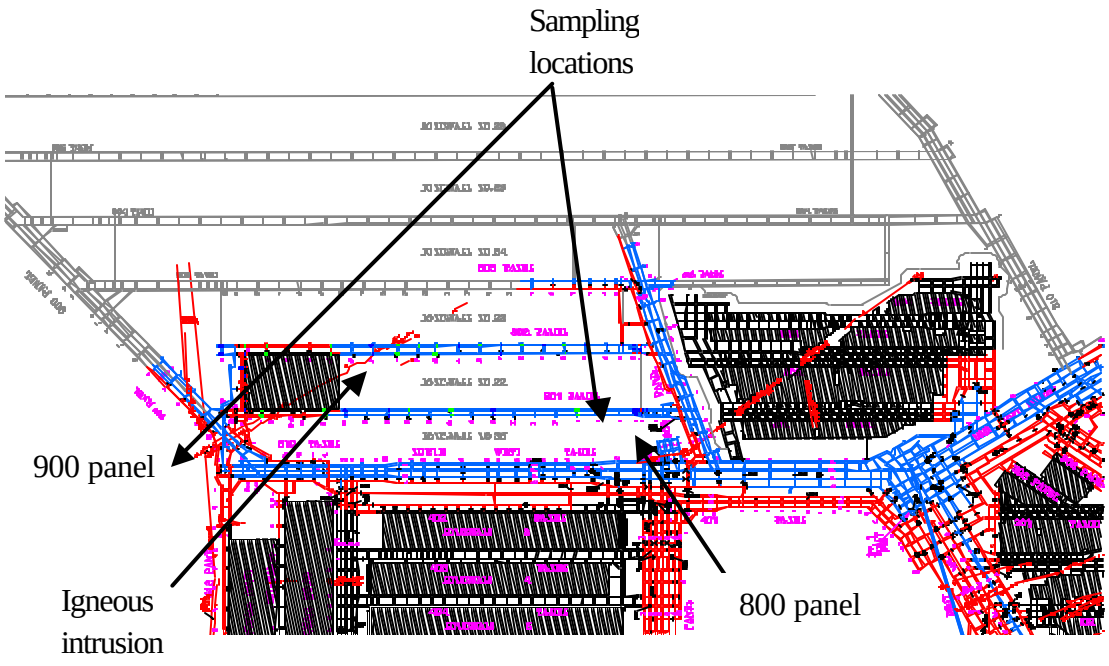

Figure 7.1 Tahmoor coal mine

From the above it is obvious that there exist significant differences in the permeability of the coal from one area to the other. In practical terms, this difference manifests as a relative difference in gas content after in seam drainage, if an overall inseam drainage time of 2–3 months is assumed. Table 7.1 shows the insitu gas content and composition around the 800 and 900 panel after drainage.

Table 7.1 Gas content and composition around 800 and 900 panels after inseam drainage (Bruggemann, 2005).

Panel Number	Total (m^3/tonne)	Methane (%)	Carbon Dioxide (%)
900	11.1	20.4	79.6
800	4.48	6.5	93.5

Of significance one the 900 panel samples which come from adjacent to the thrust fault and also from a non-structured area, both of which have significantly altered and mineralised coal. In its simplest terms, the 900 series coals had lower permeability compared to the 800 series coal, as shown in chapter 6 and again will be shown, later. The programme of study undertaken to examine the parameters affecting the gas drainage capability of the coal from both locations included an analysis of the gas content and gas composition, as well as determining the shrinkage and permeability characteristics of coal.

7.3 COAL PETROGRAPHY TESTS

After the experimental testing each sample was crushed to –2 mm and a representative sub sample mounted in polyester resin to form a block. Each block was cut in half perpendicular to any density separation, and the cut face from one of the halves polished. The maceral composition of each sample was determined by the method outlined in the Australian Standard AS2856.2-1998: Coal Petrography – Maceral Analysis. Maceral analyses for the samples are given in Figure 7.2.

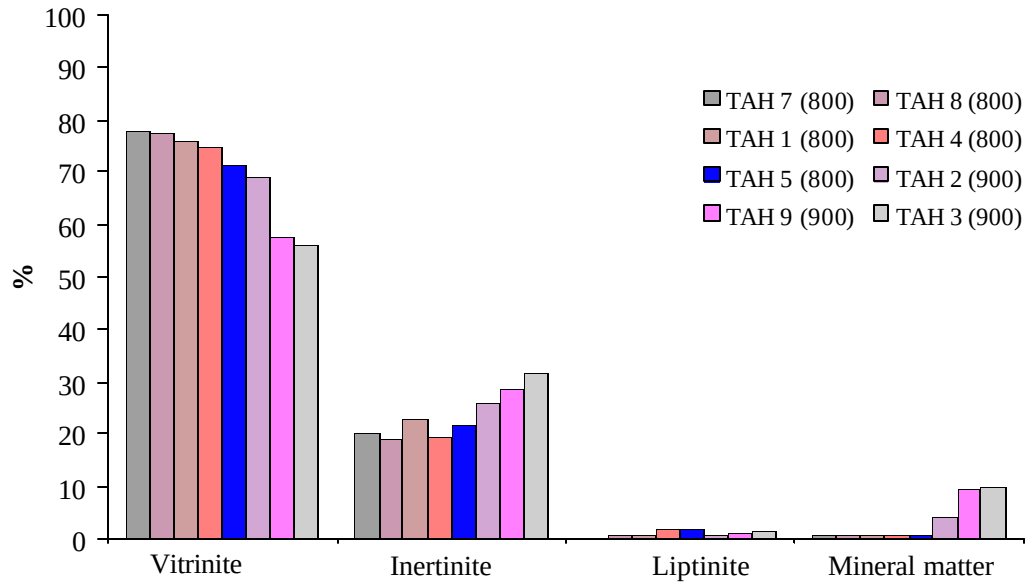

Figure 7.2 Maceral analyses of coal samples used in tests

Petrographically, the eight samples have similar organic components with vitrinite contents ranging from 56% to 78 %, inertinite from 18% to 32% and negligible liptinite. However, the mineral contents of the samples are quite different. All of the 900 panel coals have a higher mineral content than the 800 panel coals, while two in particular contain a significantly higher mineral content. In each of the three samples,

carbonate and clay filled the cleats and also some of the pores in the inertinite macerals. If the mineral content and species is common for the coal as a whole in 900 panel, the permeability and degassing problems associated with this panel can be explained in terms of petrography.

7.4 SHRINKAGE TESTS

Eight samples were tested for shrinkage, five samples were tested from 800 panel and three from 900 panel. Figures 7.3 and 7.4 show the incremental change in volumetric strain corresponding to the progressive reduction of gas pressure in the coal samples.

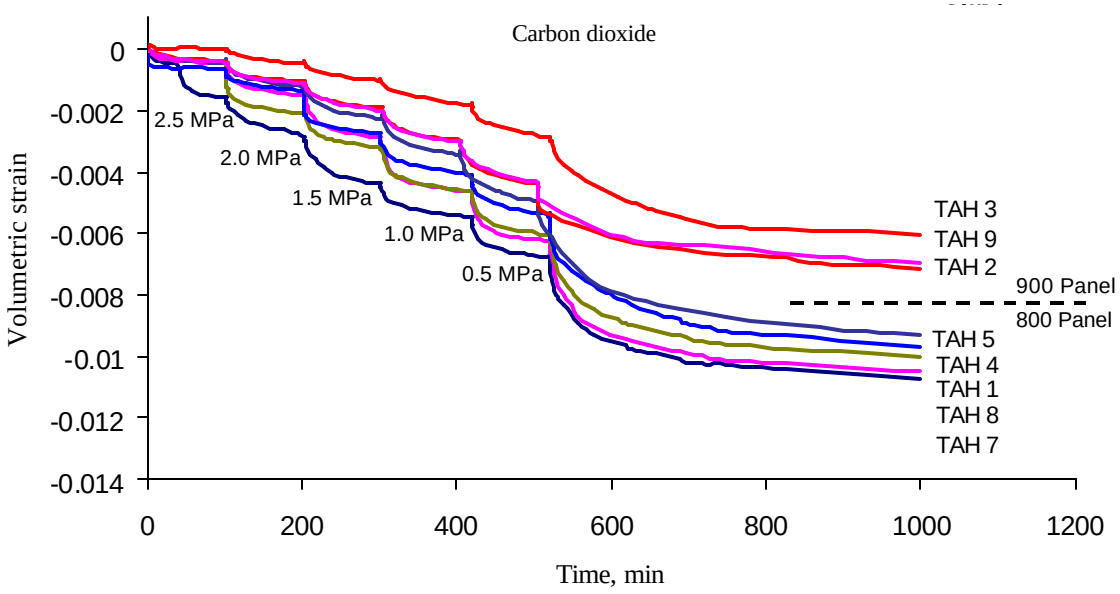

Figure 7.3 Volumetric strain for CO_2 and pressure reductions at increments of 0.5 MPa

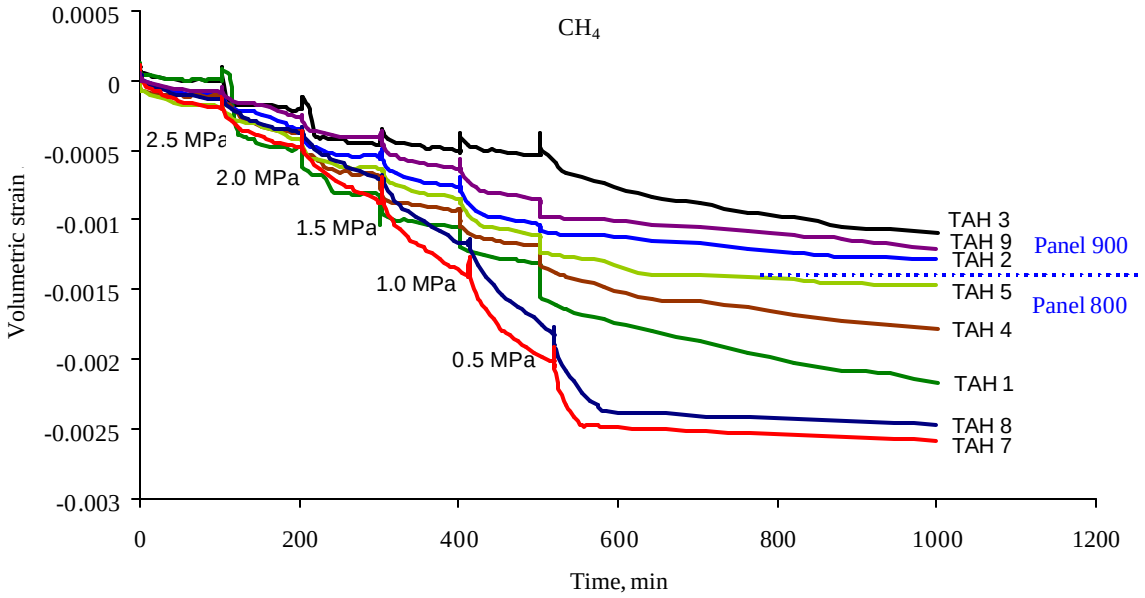

Figure 7.4 Volumetric strain for CH_4 and pressure reductions at increments of 0.5 MPa

It can be seen that the volumetric change for 800 panel samples was consistently higher than that for the geologically disturbed 900 panel.

7.5 PERMEABILITY TESTS

Full analysis of Tahmoor permeability tests was provided in Chapter 6, this section concentrates only on a direct comparison between 800 and 900 panels. The results show a marked difference in permeability between the 800 and 900 panel coals. The difference in permeability between 800 panel and the 900 panel coal for each of carbon dioxide and methane (Figures 7.5 and 7.6) is quite significant, with 800 panel having approximately three times greater permeability when compared to the 900 panel coals.

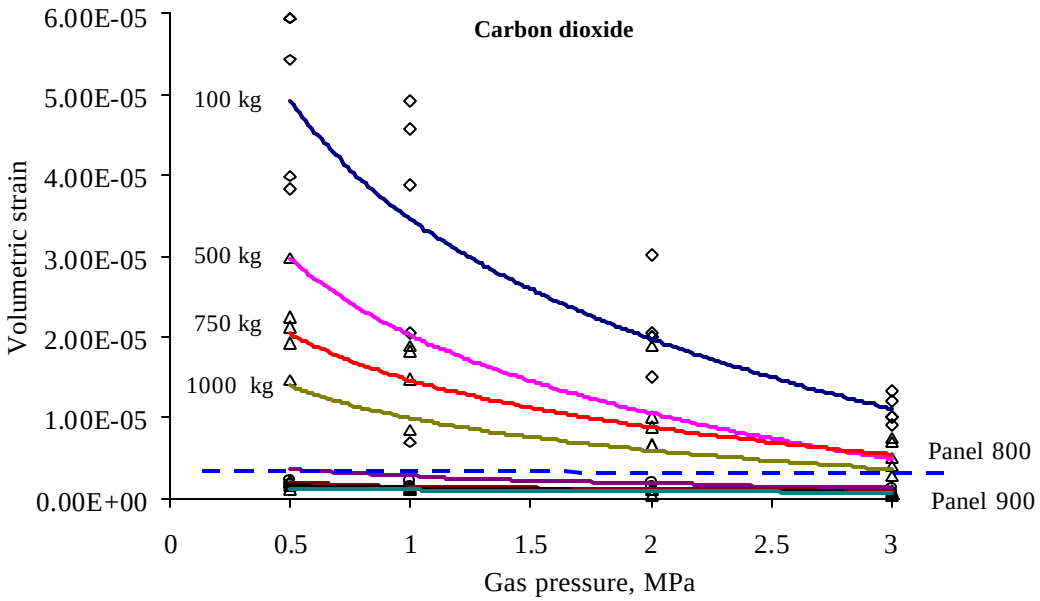

Figure 7.5 Permeability of samples from 800 and 900 panels to carbon dioxide at different axial loads.

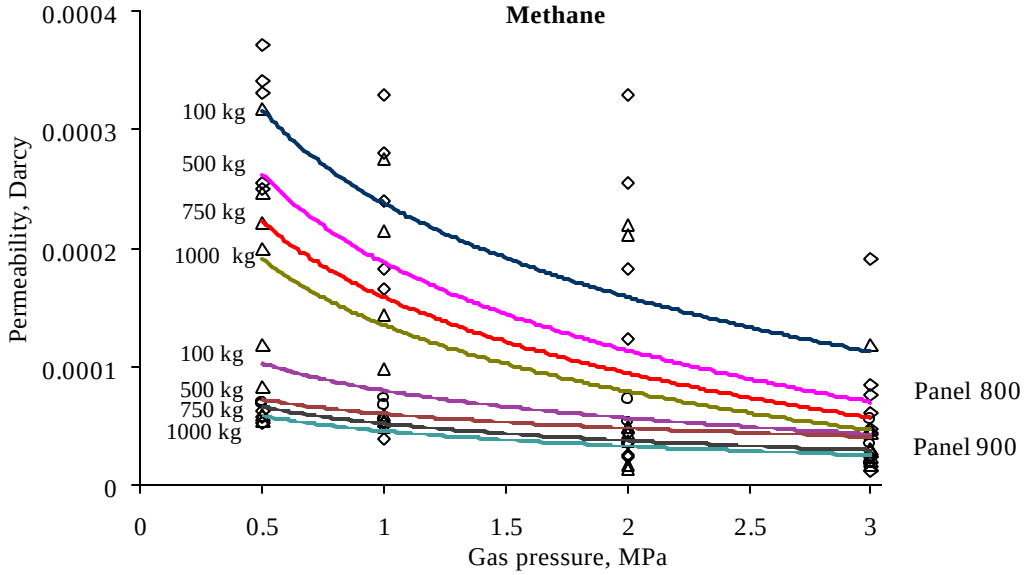

Figure 7.6 Permeability of samples from 800 and 900 panels to methane at different axial loads.

7.6 TEST RESULTS AND ANALYSIS

Results of the petrography tests on Tahmoor coal samples are summarised in the Figures 7.7 to 7.9. As it can be seen from Figure 7.7 the vitrinite content of coals from panel 800 were 20% times more than coals from 900 panel.

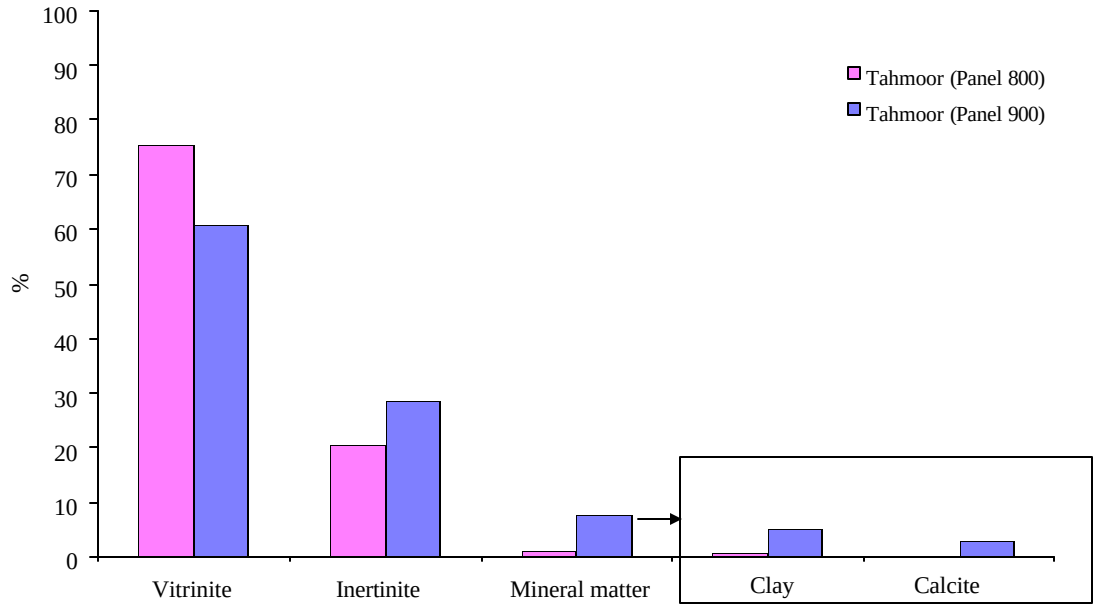

Figure 7.7 The petrographical test results for Tahmoor Colliery coal samples

On the other hand the 900 samples had more inertinite than 800 coals, around 30% more. Analysis of mineral matter indicated that the main minerals, carbonate and clay were found more in 900 samples than 800 coal samples (near 7 times as much). It may be noticed that there is not much difference between vitrinite values for the two panels, therefore the mineral matter and inertinite content (as a result of the contained mineral matter) is influencing the permeability and shrinkage characteristics of coals from the two panels.

Figure 7.8 illustrates that the shrinkage of Tahmoor coal samples increased 5 fold by changing the gas environment from CH_4 to CO_2. The effect of changing the tested gas on shrinkage of coal can be attributed to the affinity of gases to the coal.

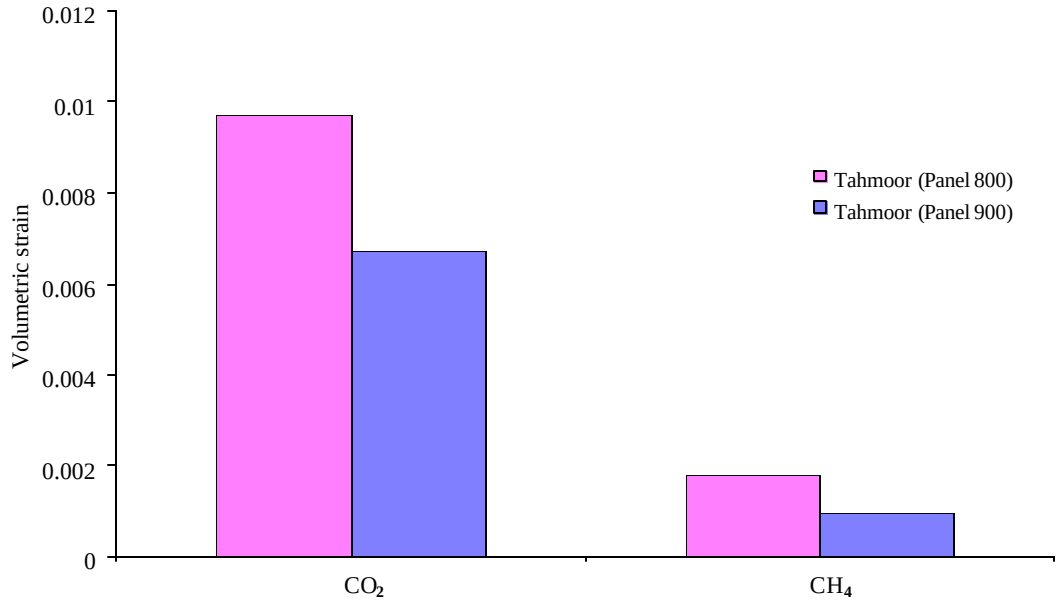

Figure 7.8 The shrinkage test results for coal samples from 800 and 900 panels (Tahmoor Colliery) under different gas environments.

The insitu gas drainage flow rates in the mine were (Bruggemann, 2005) between 0.1 l/m to 8.67 l/m (average around of 2 -3 l/m) for 800 panel, and in the range of 0.8 l/m and 2.6 l/m for 900 panel. From insitu observations and analysis of the flow rates from 900 panel it was apparent that CO_2 being dissolved in water results in lower coal matrix shrinkage and less drainage rates in comparison with 800 panel.

With the greater volume change occurring in 800 panel, the experiment clearly demonstrates that coal in this region has a greater capacity for inseam gas drainage than that of 900 panel, exactly what was experienced by the mine drainage system.

The 900 panel was considered to be a 'difficult to drain' area as it was highly stressed due to geological structures. After instigation of inseam drainage, the effective stress will change by a lesser magnitude as does the pore pressure, but not to the extent that free flowing drainage could be achieved. Unlike in the 800 panel area, which has shrinkage nearly twice that of the 900 panel area, this causes good drainage and greater change in effective stress from pore pressure is envisaged, particularly in the CO_2 environment.

The permeability tests results (Figure 7.9) for both carbon dioxide and methane show that the 900 panel coals have much lower permeability than the 800 panel coals.

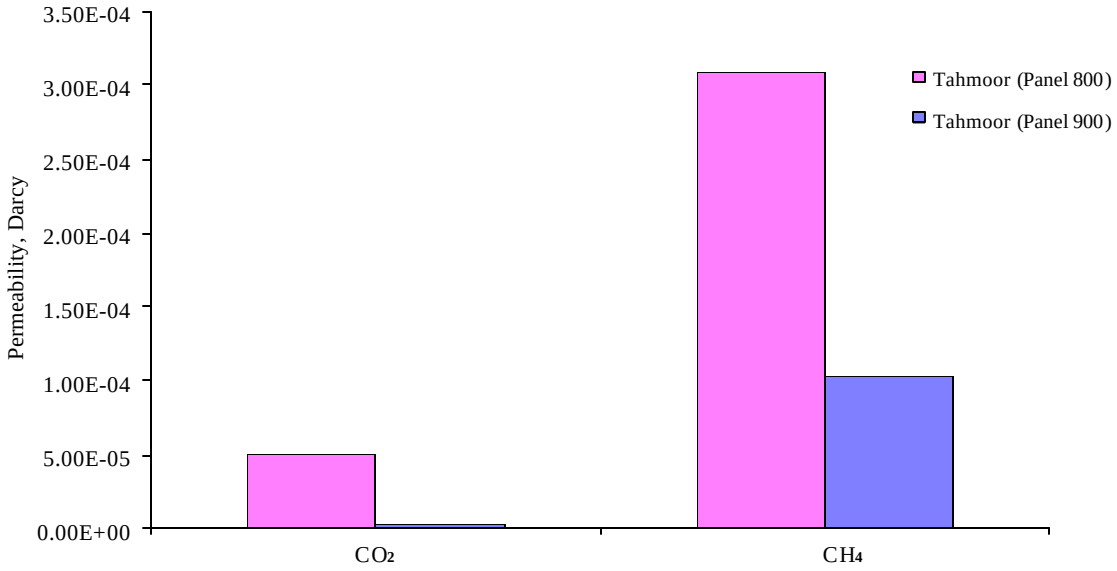

Figure 7.9 The permeability test results for 800 and 900 panels coal samples (Tahmoor Colliery) under 100 kg axial load and 0.5 MPa gas pressure.

Since permeability is a function of a number of parameters including size, distribution and frequency of cleats, any phenomenon that reduces cleat porosity will decrease permeability. Given that 900 panel coals contain a much higher mineral

matter content than the 800 panel coals, and also have the lowest permeability, it is suggested that the reduced porosity of the 900 panel coals is due to the infilling of the cleats with carbonate. The reduced permeability also explains why the 900 panel area is much harder to drain. The carbonate and clay infilled cleats restrict the movement of gases from the surrounding coal to the gas drainage holes. This is in agreement with the Titheridge (2004) explanation for the low permeability of Tahmoor coal samples, as stated in chapter three section 3.4.3. Also from Figure 7.9 it can be found that the permeability of 800 coal samples to CO_2 were near 16 times more than 900 samples however this ratio was decreased to 4 by switching the tested gas to CH_4. In chapter 6, analysis of the results suggested that inertinite rich coal would show better drainability characteristics than those that were vitrinite rich. This hypothesis, supported by the work of the Crosdale (1998), Gamson and Beamish (1992), (Curl, 1978) and Creedy (1991), but not by the work of Clarkson and Bustin (1997), is generally accepted for Australian coals. Analysis of Figure 7.7 to 7.9, however, does not support this view, as the inertinite rich coals of Tahmoor 900 panel are more difficult to drain than the vitrinite rich coals of 800 panel. Thus it can be concluded, that although under 'normal' circumstances, inertinite rich coals have higher permeability, when local alteration takes places (such an increase in mineral content) the opposite may occur. This is the situation for Tahmoor 900 panel, where a localised intrusion caused significant alteration to the coal in that immediate area.

7.7 SUMMARY AND OVERALL DISCUSSION

This results of the petrographic tests demonstrated that the Tabas and Tahmoor coal samples had the highest amount of vitrinite, while the North Goonyella and Dartbrook coal samples had higher inertinite contents when compared to the other coal samples (Figure7.10). Also from this, experimentation the highest amount of mineral matter was found to be approximately 20%, and belonged to the Dartbrook coal samples.

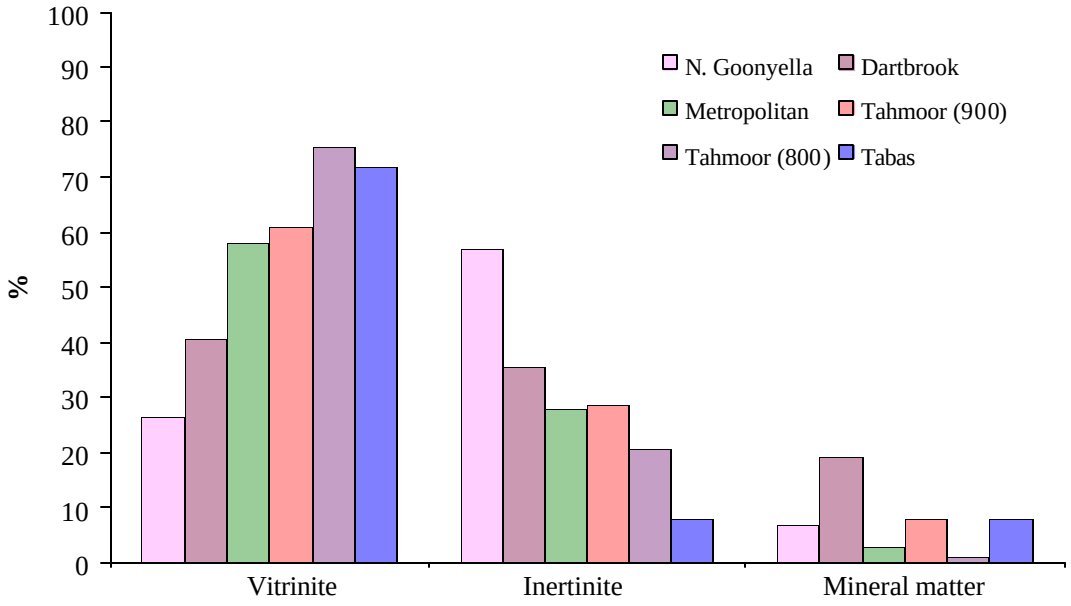

Figure 7.10 The composition of all tested coal samples

By observing the data from coal shrinkage tests, it was demonstrated that under the same testing conditions all samples showed higher shrinkage in a CO_2 environment than a CH_4 environment.

Based on analysis of the data shown in Figures 7.10 and 7.11, it can be concluded that, in general, with increasing inertinite content of coal the volumetric strain increases, however the relative increase for CH_4 was less than that CO_2.

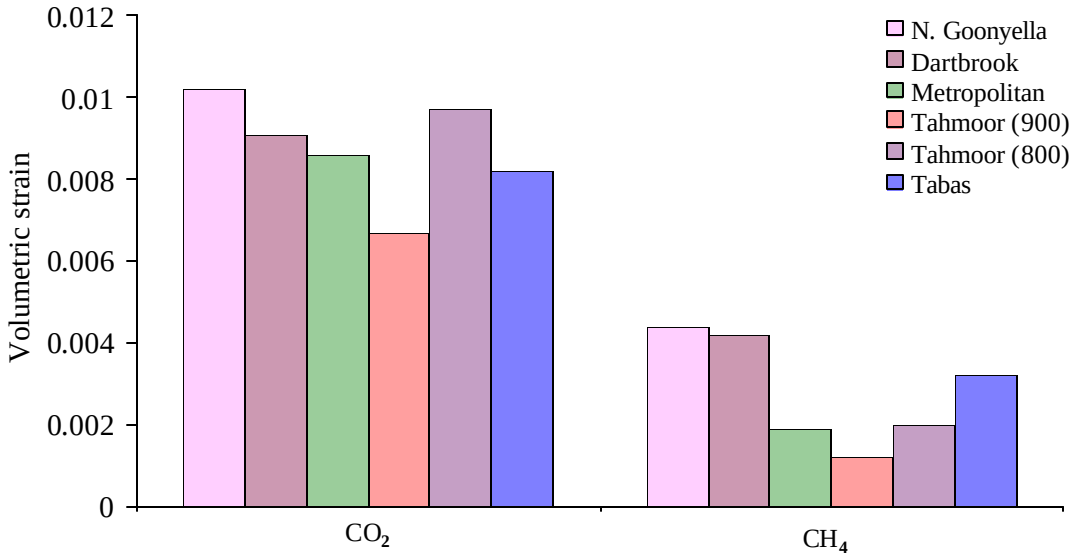

Figure 7.11 Average volumetric strains for tested coal samples.

On the other hand, an increase in the vitrinite content causes a decrease volumetric strain, but this relative decrease is significantly less for methane than that for CO_2. Figures 7.12 and 7.13 show that the above relationship is the same for permeability. It should be noted that this behaviour was not observed for all coal samples, Tabas coal was an exception. Tabas coal tests had one of the highest amounts of mineral matter, which was mostly pyrite (Fazl, 1990). The explanation for differing with other samples could be that the mineral matter infills the macropores of the coal matrix and causes the pores to become abandoned, resulting in less shrinkage, however as mentioned before, because of the small molecule size the methane could reach to

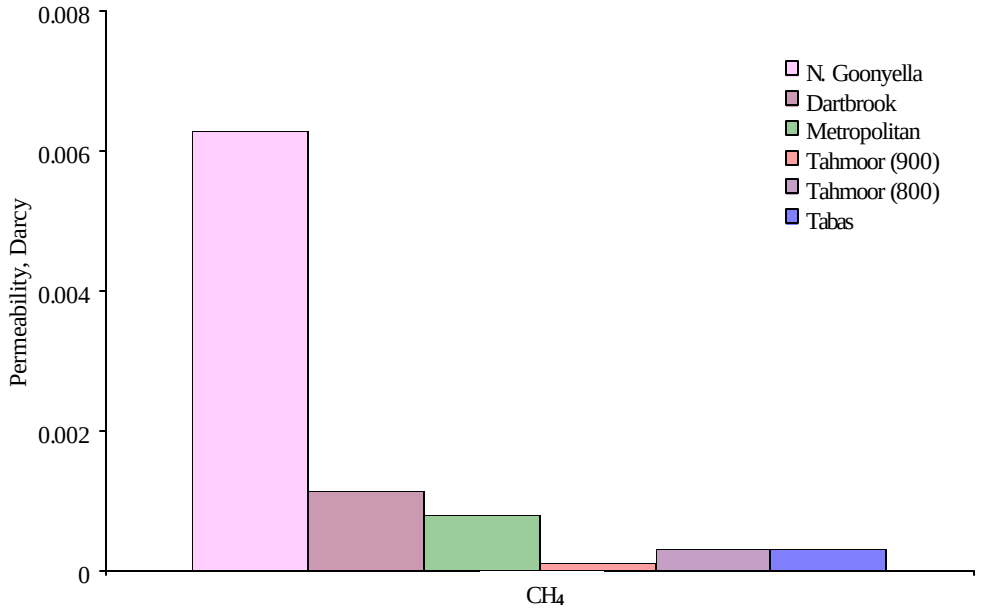

Figure 7.12 Permeability of tested coal samples to methane.

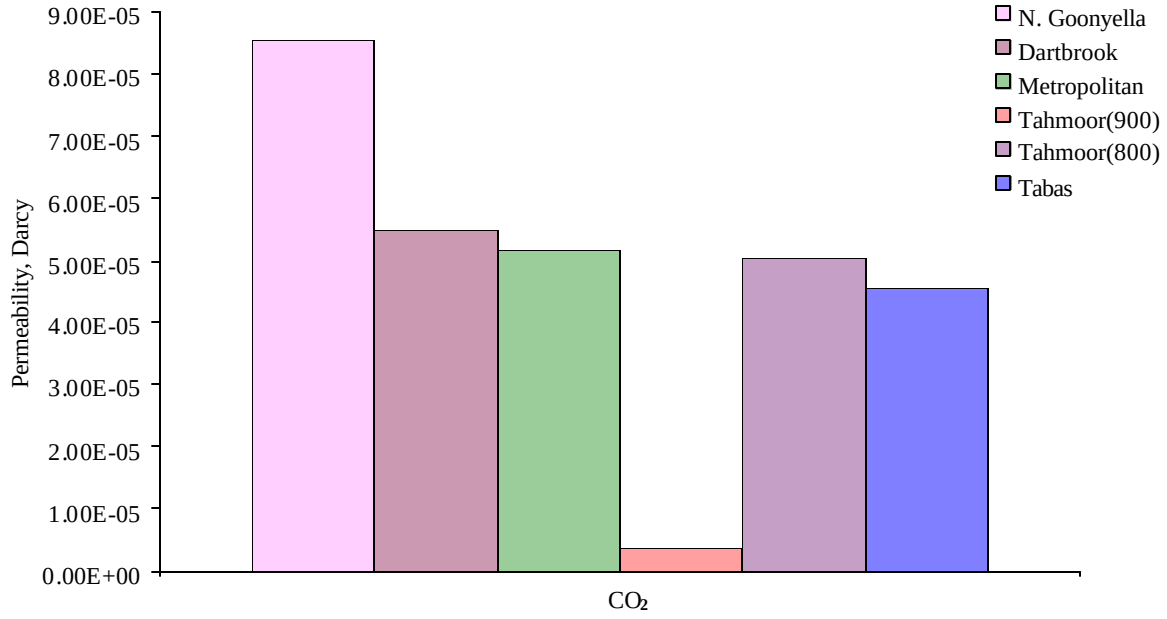

Figure 7.13 Permeability of tested coal samples to carbon dioxide.

micropore structure of coal and cause a high amount of shrinkage for methane desorption. It should be considered that it is possible for a coal sample to have relatively good permeability to methane (North Goonyella) but if the dominant gas is carbon dioxide, there isn't any guarantee that the coal still demonstrates a good drainability characteristics.

7.8 CONCLUSIONS

The material reported in this chapter has demonstrated the degree of influence factors such as gas type and pressure, and in particular coal composition have on permeability dependent on gas type and pressure. Carbon dioxide gas appears to cause the highest volume change. This is understandable in view of the fact that coal has higher affinity for carbon dioxide gas than the other gases tested.

Coals in the 800 locality have higher shrinkage coefficients than those obtained from the 900 area, suggesting that 800 area is more easily drained in comparison to 900 area. Permeability and petrographic data, as well as previously reported shrinkage results, confirm that the coals from the 900 and 800 panel area are markedly different. This has had consequential results for the efficiency of the mining cycle in these two areas of the mine.

CHAPTER EIGHT

CONCLUSIONS AND RECOMMENDATIONS

8.1 CONCLUSIONS

A number of important parameters have been identified which have a direct influence on the proneness of coal to outburst. Coal composition and abnormal geological conditions, as well as the stress regime are some of the factors which require careful attention for effective control of outburst. Accordingly, a series of experimental laboratory studies were undertaken and the findings were further enhanced with numerical modelling. The following paragraphs describe the main conclusions drawn from this research study.

Literature survey

- Outbursts of gas and coal have been a progressively increasing phenomenon in recent times, and therefore research on ways of combating this problem is warranted both in the laboratory and in the field.

- Effective planning of the mine gas drainage system can be facilitated by a clear understanding of the factors that influence the sorption and pressurisation of coal gases. Understanding the effect on the permeability of coal to different coal

gases and the changes in the coal matrix due to gas pressure plays an important role when planing an effective gas drainage programme.

- Carbon dioxide has a greater destructive effect in coal when compared to other coal gases. This is attributed to the greater amount of CO_2 generally adsorbed in coal and the high rate of desorption. CO_2 causes a reduction in coal strength, it has high viscosity, and has a lower diffusion rate and higher free pressure gradient than other gases.

- Increasing the area of cleats and joints affects the permeability of coal much more than factors causing volumetric strain changes in coal.

Experimental investigations

From the experimental work it can be concluded that:

- The MFORR apparatus was demonstrated to be a reliable tool for conducting permeability testing of coal under different gas pressures. The unique feature of the rig is its ability to apply a vertical load on a sample while it is confined under a specified gas pressure. The incorporation of selective capacity flow meters into the system provided the appropriate tools for effective monitoring of gas flow through the coal samples.

- The petrographical tests showed that most of the Australian coals tested were inertinite rich coals. The mineral matter in the Australian coal samples were

mostly carbonate (calcite) and clay, but the Iranian Tabas coal had pyrite as the dominant mineral matter.

- Volumetric strains during the adsorption stage in all gas environments were greater than the volumetric strains in the desorption stage.

- The level of coal shrinkage was affected by the type of gas desorbed. Carbon dioxide appears to have the greatest influence on the matrix and nitrogen the least. This is understandable in view of the fact that carbon dioxide has a greater affinity to coal than the other gases. As well as the magnitude of shrinkage, the rate of shrinkage was also found to be influenced by the type of gas and the applied pressure. The coal samples from all of the mines showed similar behaviour, with Metropolitan coal samples having a greater average rate of shrinkage than the other coal samples.

- The permeability of coal depends on the level of stress that is applied perpendicular to the coal layering or lamination. The permeability of coal was also influenced by the gas type and pressure. Greater gas permeability was obtained in N_2 gas, and the lowest permeability was obtained in a CO_2 environment. The sorption characteristics of CO_2 gas are a major factor

- The degree of coal permeability is reduced exponentially by increasing the applied stress and also by increasing the confining gas pressure, irrespective of the gas type. Similarly, the permeability of coal in various gases is exponentially reduced at different rates.

- For effective research and a better understanding of coal drainability, it is vitally important that due attention be paid to coal composition and in particular to the mineral content, as well as any other geological factors.

- Tahmoor coals from 800 and 900 Panels showed that the permeability of coal was influenced by the mineral content and the carbonates, as well as by the cavities. In particular, there was a reduction in coal permeability with increasing mineral content (other than inertinite) and carbonate content of the coal. Generally, with an increase in the percentage of inertinite, the permeability of coal increased. Likewise, any increase in cavities and fractures caused an increase in the permeability of coal. Naturally the permeability rates were dependent on the coal composition and geological conditions of the coals tested from different development panels under investigation.

- Tahmoor 900 Panel produced an exception to the increasing inertinite, increasing permeability rule. In this area increasing inertinite caused a reduction in permeability, the result of mineral matter filling up the inertinite macropores. This localised variation to the rule, was caused by alteration of the coal as a result of an igneous intrusion.

- A numerical model was developed to simulate single gas flow through coal. The numerical Simulation provided an opportunity to quantify flow mechanism in coal. It was possible to simulate the flow duration across the coal samples with different gases and coal type. Gases in general permeated at a much faster rate

through coal in the 800 Panel than in the 900 Panel. Naturally, the flow time was different for different gases and applied vertical stress.

- The numerical model developed in this thesis would have considerable potential for future application to in-situ coal gas drainage rate estimation and outburst risk assessment for improved mine safety and productivity.

8.2 SUGGESTIONS FOR FURTHER RESEARCH

This research has provided a comprehensive understanding of some of the important factors that influence outburst phenomena, such as permeability, shrinkage and the composition of coals, but there is still scope for further research in this area.

- The method of analysing the permeability, shrinkage and composition of coal represents a promising technique with great potential for use in the laboratory and in the field to provide a basis for the prediction of coal and gas outbursts as well as the drainability of a coal seam well in advance of mining the coal. It is recommended that use of these techniques be used for indication of potential outburst prone zones.

- Further studies on coal shrinkage and permeability are recommended to include testing of different coals using different gases under different axial loads at various gas pressures. A database should be established and maintained for the benefit of future research. Also it is suggested that the additional data can be used in the present numerical model for further analysis.

- The proposed programme continuing from the study reported in this thesis should be extended to field studies. By using the numerical model, better understanding of the flow of gas from drainage holes can be achieved.

- Modifications need to be made to the gas chamber and bombs so that testing can be conducted under higher pressures (more than 3 MPa), thus maximising the ability of the equipment for doing tests on different coal samples from different mines under actual conditions.

- Establishment of a time-related index for different coals and gases, based on both the experimental and numerical studies. These indices can then be used to categorise coals for outburst proneness even prior to mining.

REFERENCES

Ayruni, A. T. (1981). Theory and practice of mine gas control at deep mines, Nedra press, (Translated into English by Rockville, Maryland, USA), 355 p.

Aluko, N. (2001). Coalbed methane extraction and utilisation, Technology status report 016 August 2001, Department of Trade and Industry, UK.
http://www.dti.gov.uk/energy/coal/cfft/cct/pub/tsr016.pdf

Ates, Y. and Barron, K. (1987). The effect of gas sorption on the strength of coal, Mining science and Technology, Vol. 6, pp. 291-300.

Audibert, E. (1935). Ann. min., Paris series 13, Vol. 8, pp. 225(as cited in Moffat and Weale,1955).

Audibert, E. (1942). Ann. min., Paris series 14, Vol. 1, pp. 71(as cited in Moffat and Weale,1955).

Aziz, N. I. and Ming-Li, W. (1999). The effect of sorbed gas on the strength of coal-an experimental study, Geotechnical and Geological Engineering, Vol. 17, pp. 387-402.

Barker, C. E. (1991). Implications for organic maturation studies of evidence for a geologically rapid increase of vitrinite reflectance at peak temprature: Cerro Prieto geothermal system, Mexico, American association of petroleum geologists Bulletin, Vol. 75, pp. 1852-1863.

Bartosiewicz, H. and Hargraves, A. J. (1984). Catalog of gas properties of Australian gassy black coals., CSIRO Div. Geomech., AMIRA Project 82/P153, Final Report, 12 p.

Bartosiewicz, H. and Hargraves, A. J. (1985). Gas properties of Australian coal, Proc. Australas. Inst. Min. Metall., Vol. 290, pp. 71-77.

Beamish, B. B. and Gamson, P. D. (1993). Sorption behaviour and microsturcture of Bowen Basin coals, Coalseam Gas research institute, 195 p.

Bishop, R. and Battino, S. (1989). Extraction and utilization of coalseam methane-The Australian experience, *International coal bed methane symposium proceedings*, Tuscaloosa, AL, USA, pp. 107-115.

Boxho, J., Stassen, P., Mucke, G., Noack, K., Jeger, C., Lescher, L., Browning, E. J., Dunmore, R. and Morris, I. H. (1980). Firedamp drainage, handbook coal mining industry in European communities, Gluckauf, Essen, Germany, 450 p.

Briggs, H. and Sinha, R. P. (1933). Expansion and contraction of coal caused respectively by the sorption and discharge of gas, Proceedings of the royal society of Edinburgh, Vol. 53, pp. 48-53.

Bruggemann, D. (2005). Tahmoor Colliery, Austral Coal Pty Ltd, Personal communications.

Brunauer, S., Emmett, P. H. and Teller, E. (1938). Journal of Amer. Chem. Soc., Vol. 60, pp. 309-319.

Bustin, R. M. and Clarkson, C. R. (1998). Geological controls on coalbed methane reservoir capacity and gas content, International Journal of Coal Geology, Vol. 38, pp. 3-26.

Bustin, R. M. and Clarkson, C. R. (1999). Free gas storage in matrix porosity: a potentially significant coalbed resource in low rank coals, *International coal bed methane symposium*, University of Alabama, Tuscaloosa, AL, USA, pp. 197-214.

Ceglarska-Stefanska, G. and Holda, S. (1994). Effect of sorption of vapours of gases and fluids on properties of hard coal, Czaplinski, A. (ed.), Chap. 13, Academy of mining and metallurgy, Krakow, Poland, pp. 183-202 (as cited in Lama and Bodzinoy,1996).

Cervic, C. (1969). Behaviour of coal - Gas reservoirs, US Bureau of Mines, Methane Control Program Tech. Progress Report No: 10, (1967) 10p.

Chikatamarala, L., Xiaojun, C. and Bustin, R. M. (2004). Implications of volumetric swelling/ shrinkage of coal in sequestration of acid gases, *International coal bed methane symposium*, paper No.435, Tuscaloosa, Alabama USA, 22p.

Clark, D. A., Battino, S. and Lunarzewski, L. (1983). Prevention and control of outbursts by pre- drainage of seam gas at Metropolitan colliery- A review, *alleviation of coal and gas outbursts in coal mines*, Lama, R. D. (ed.), Wollongong, NSW, Australia, pp. 18(1- 42)

Clarkson and Bustin (1997). Variation in permeability with lithotype and maceral composition of Cretaceous coals of the Canadian Cordillera, International Journal of Coal Geology, Vol. 33, pp. 135- 151.

Close, J. C. (1993). Natural fractures in coal, in: Hydrocarbons from coal. AAPG studies in geology No.38, Law, B. E., Rice, D. D. (ed.), Tulsa, OK, USA, pp. 119-132.

CMG (2004). Software overview (Numerical simulators for reservoir management). *http://www.cmgl.ca/*.

Conner and Shacklette (1975). Geol. Surv. Prof. Pap., USA,.574p.

Coppens, L. (1937). Ann. min., Belg series 13,Vol. 38, pp. 137(as cited in Moffat and Weale,1955).

Cram, K. (2002). Coal services Pty. Limited data source 2002-2003, Corrimal, NSW, Australia. (personal communications)

Cram, K. (2003). New South Wales Coal Statistics 2002-03, Coal services Pty. Limited data source 2002-2003, Corrimal, NSW, Australia. 58p.

Creedy, D. P. (1991). An introduction to geological aspects of methane occurrence and control in British deep coal mines, Quarterly Journal of Engineering Geology, Vol. 24, pp. 209-220.

Creel, J. C. and Rollins, J. B. (1993). Mechanics of coalbed methane production, *Conference on Coalbed methane: understanding the technology and the new economics*, London, UK, 5p.

Crosdale, P. J. and Beamish, B. B. (1995). Methane diffusity at South Bulli (NSW) and Central (Qld) collieries in relation to coal maceral composition, *International symposium - cum- workshop on Management and control of high gas emissions and outbursts in underground coal mines*, Lama, R. D. (ed.), Wollongong, NSW, Australia, pp. 363-367

Crosdale, P. J., Beamish, B. B. and Valix, M. (1998). Coalbed methane sorption related to coal composition, International Journal of Coal Geology, Vol. 35, pp. 147-158.

Crosdale, P. J. (1999). Mixed methane/ carbon dioxide sorption by coal: New evidance in support of pore-filling models, *International coalbed methane symposium*, The University of Alabama, Tuscaloosa, Alabama, USA, pp. 359-366.

Cui, X., Bustin, R. M. and Dipple, G. (2004a). Differential transport of CO_2 and CH_4 in coalbed aquifers: Implications for coalbed gas distribution and composition, The American Association of Petroleum Geologists., Vol. 88, No.8, pp. 1149-1161.

Cui, X., Bustin, R. M. and Dipple, G. (2004b). Selective transport of CO_2, CH_4, and N_2 in coals: Insights from modeling of experimental gas adsorption data, Fuel, Vol. 83, pp. 293– 303.

Curl, S. J. (1978). Methane prediction in coal mines., IEA coal research, Report No. ICTIS/TR 04, London, UK, 77p.

Czaplinski, A. (1971). Simultaneous testing of kinetics of expansion and sorption in coal of carbon dioxide, Archivwum Gornickwa, Vol. 16, pp. 227-231.

Czaplinski, A. and Holda, S. (1982). Changes in mechanical properties of coal due to sorption of carbon dioxide vapour, Fuel, Vol. 61, pp. 1281-1282.

Czaplinski, A. and Holda, S. (1985). Changes in compressive strength of sandstones from the Nowwa Ruda Mine under the influence of the action of liquids and gases, Archiwum Gornictwa, Tom, Vol. 30, pp. 391-399.

Dabbous, M. K., Reznik, A. A., Taber, J. J. and Fulton, P. F. (1974). The permeability of coal to gas and water, SPE, Vol. 14, No. 6, pp. 563-572.

De Braaf, W., Itz, G. N. and Maas, W. (1952). 3rd Congr. stratigr. Geology. Carb, pp. 51 (as cited in Moffat and Weale, 1955).

Deitz, V. R., Carpenter, F. G.and Arnold, R. G. (1964). Interaction of carbon dioxide with carbon adsorbents below 400 °C, Carbon, Vol. 1, pp. 245-254.

Doscher, T. M., Kuuskraa, V. A. and Hammershaib, E. (1980). The controlling production mechanism of methane gas from coalbeds, Energy sources, Vol. 5, No. 1, pp. 71-85.

Drever, J. I. (1982). The geochemistry of natural waters: Englewood Cliffs, Prentice-Hall Inc., New Jersy, 388 p.

Dunn, P. G., and Alehossein, H. (2002). The development of an effective stress and permeability model for boreholes driven in coal for methane drainage, *NARMS-TAC 2002*, University of Toronto, pp. 73-81.

Durucan, S. and Edwards, J. C. (1986). The effects of stress and fracturing on permeability of coal, Mining science and technology, Vol. 3, pp. 205-216.

Durucan, S. (2003). Pore pressure dependent changes in coal permeability: The effect of matrix shrinkage and swelling on reservior response during primary and CO_2 enhanced recovery of methane, Environmental and mining engineering research group, The Society of Core Analysts.
http://www.scaweb.org/assets/symposium_2003/Workshop/Pore%20pressure%20dependent%20changes%20in%20coal%20permeability%20-%20S.%20Durucan.pdf

Eddy, G. E., Rightmire, C., T. and Byrer, C. W. (1982). Relationship of methane content of coal rank and depth theoretical vs. observed, *SPE/DOE Symposium on unconventional gas recovery*, Pittsburgh, Pa., USA.pp.117-122.

Ellis (1953). The adsorption of gas by coal, Colliery Engineering, pp. 17-21.

Enever, J. R. E. and Hennig, A. (1997). The relationship between permeability and effective stress for Australian coals and its implications with respect to coalbed methane exploration and reservoir modelling, *International coalbed methane symposium*, The university of Alabama, Tuscaloosa, AL, USA, pp. 13-22

Ettinger, I. L., Lidin, G. D.,Dimitiev, A. M. and Shaupachina, E. S. (1958). Systematic handbook for the determination of the methane content of coal seams from the seam gas pressure and the methane capacity of coal, USBM Translation No. 1501.

Ettinger, I. L., Eremin, I., Zimakov, B., and Yanovskaya, M. (1966). Natural factors influencing coal sorption properties, (I) Petrography and sorption properties of coals, Fuel, Vol. 45, pp. 267-275.

Ettinger, I. L. (1977). Swelling stress in the gas-coal system as an energy source in the development of gas outbursts, Soviet mining science, Vol. 15, No. 5, pp. 494-501.

Ettinger, I. L. (1979). Swelling stress in the gas-coal system as an energy source in the development of gas outbursts, Trans. From Russian, Soviet mining science, Vol. 15, No. 5, 1979, Fiziko-tekhnicheskie problemy razrabotki poleznykh iskopaemykh, Sept.-Oct. 1979, No. 5, pp. 78-87 (as cited in Lama and Bodziony, 1996).

Ettinger, I. L. and Serpinsky, V. V. (1991). On the state of methane in coal seam, Mining science and Technology, Vol. 13, pp. 403-407.

Faiz, M. M. and Cook, A. C. (1991). Influence of coal type, rank and depth on the gas retention capacity of coal in the Southern Coalfield, NSW, *Gas in Australian coals*, Bamberry, W. J. and Depers, A. M. (eds.), University of New South Wales, NSW, Australia, pp. 19-29.

Faiz, M. M., Aziz, N. I., Hutton, A., C. and Jones, B. G. (1992). Porosity and gas sorption capacity of some eastern Australian coals in relation to coal rank and composition, *Symposium on coalbed methane research and development in Australia*, Townsville, Australia, pp. 9-13.

Faiz, M. M. and Hutton, A., C. (1995). Geological controls on the distribution of CH_4 and CO_2 in coal seams of the Southern Coalfield, NSW, Australia, *Int. Symp. cum. Workshop on management & control of high gas emission outbursts*, Lama, R. D. (ed.), Wollongong, pp. 375-383.

Fazl, M. M. (1990). A summary of the reports on geology and exploration of Tabas coal basin. Report for National Iranian steel company, Ministry of mines and metals, Iran, 154p.

Gamson, P. D. and Beamish, B. B. (1992). Coal type, microstructure and gas flow behaviour of Bowen Basin coals, *Symposium on coalbed methane research and development in Australia*, Beamish, B. B. and Gamson, P. D. (eds.), James cook University of North Queensland, pp. 43-66.

Gamson, P. D., Beamish, B. B. and Johnson, D. P. (1993). Coal micropermeability and their effects on natural gas recovery, Fuel, Vol. 72, pp. 87-99.

Gamson, P., Beamish, B. and Johnson, D. P. (1996). Coal microstructure and secondary mineralization: their effect on methane recovery, Coalbed Methane and Coal Geology, Gayer, R. and Harris, I. (ed.), London. Geological Society Special Publication 109, pp. 165-179.

Gan, H., Nandi, S. P. and Walker, P. L. Jr. (1972). Nature of the porosity in American coals, Fuel, Vol. 51, pp. 272-277.

Garner, K. (1999). Mine gas exploitation at Appin and Tower collieries, New South Wales, Australia, The Australian Institution of Mining and Metallurgy, Vol. 108, pp. A212-A217.

Gash, B. W., Volz, R. f., Potter, G. and Corgan, M. (1993). The effects of cleat orientation and confining pressure on cleat porosity, permeability and relative permeability in coal, *International coalbed methane symposium*, The university of Alabama, Tuscaloosa, USA, pp. 247-255.

Gil, H., Swidzinski, A. (1988). Rock and Gas outbursts, Politechnika Slaska, Skrypty Uczelniane, no.1366, Wydanie II, Gliwice, Poland. 492p.

Giron, A., Pavone, A. M. and Schwere, F. C. (1984). Matemathical models for productiion of methane and water from coal seams, Quarterly review of methane from coal seams technology, Vol. 2, Gas Research Institute, Chicago, Illinois, USA, pp. 19-34.

Gluskoter, H. J., Shimp, N. F. and Ruch, R. R. (1981). Coal analysis, trace elements and mineral matter, Chemistry of coal utilization, Elliot, M. A. (ed.), New York, pp. 369- 424.

Gould, K. W., Hargraves, A. J. and Smith, J. W. (1987). Variation in the composition of seam gases issuing from coal, Bulletin proceedings of Australiasian institute of mining and metallurgy, Vol. 292, No5, pp. 69-73.

Gray, I. (1987). Reservoir engineering in coal seams: Part1- The physical process of gas storage and movement in coal seams.
http://www.sigra.com.au/ppr_reseng1.htm.

Gray, I. (1995). Stress, gas, water and permeability - their interdependence and relation to outbursting, *International symposium - cum- workshop on Management*

and control of high gas emissions and outbursts in underground coal mines, Lama, R. D. (ed.), Wollongong, NSW, Australia, pp. 331-334.

Gray, I. (2000). Determining gas production characteristics of coal seams. *http://www.sigra.com.au/ppr_csgdet.html.*

Gregg, S. J. and Sing, K. S. W. (1967). Adsorption, surface area and porosity, 1st Edition, Academic Press, London, 371 p.

Gregg, S. J. and Sing, K. S. W. (1982). Adsorption, surface area and porosity, 2nd Edition Academic press, London, 303 p.

Guney, M. (1975). Investigation of methane in carboniferous rocks, Journal of the Mine Ventilation Society of South Africa, Vol. 28, No. 7, pp. 101- 111.

Gunter, J. (1968). Investigation of the relationship between coal and the gas contained in it, Revue de l'Industrie Minerale, Vol. 47, No. 10, pp. 693-708 (French). SMRE translation No. 5134.

Gurba, L. W. (2002a). Microscopic studies of low permeability coal, In: "Outburst and gas drainage workshop", Hanes, J., Australian coal association research program, pp. 53-67

Gurba, L. W. (2002b). Gas migration in coal on the microscopic scale, In: Gas and coal outburst committee half day seminar, NSW Department of mineral resources, Wollongong, NSW, Australia,

Gustkiewcz, J. (1985). Deformation and failure of the Nowa Ruda sandstone in a three-axial state of stress with gas under pressure in pore, Archiwum Gornictwa, Tom, Vol. 30, pp. 401-424.

Hanes, J., Lama, R. D. and Shepherd, J. (1983). Research into the phenomenon of outbursts of coal and gas, *5th Int. Cong. Rock mechanics*, Melbourne, ISRM, pp. E79-E85

Hargraves, A. J. (1963a). Some variations in the Bulli seam, AusIMM, Vol 208, pp. 251-283.

Hargraves, A. J. (1963b).Instantaneous outbursts of coal and gas, Mining department for the degree PhD, University of Sydney.

Hargraves, A. J. (1966). Occurence, investigation and control of instantaneous outburst of coal and gas in Australian mines, *International congress on problems of sudden outburst of gas and rock*, Leipzig, Germany.

Hargraves, A. J. (1983). Instantaneous outbursts of coal and gas, a review in the proceeding, The Australian Institute of Mining and Metallurgy, Vol. 285, pp. 1-37.

Hargraves, A. J. (1986). Seam gases in major Australian coalfields, *proceeding of 13th congress of council of mining and metallurgical institutions*, Vol. 3, pp. 103-112. (The Australian Institute of Mining and Metallurgy: Melbourne).

Hargraves, A. J. (1990). Coal seam gas and atmosphere, Greenhouse and energy, Swaine, D. J. (ed.), Northryde, NSW, Australia, pp. 147-156

Harpalani, S. and McPherson, M. J. (1984). The effect of gas evacuation on coal permeability test specimen, Int. J. Rock Mech. Sci. & Geomech., Abstr., Vol. 21, No. 3, pp. 161-164.

Harpalani, S. (1989). Permeability changes resulting from gas desorption, Quarterly review of Methane from coal seams technology, pp. 58-61.

Harpalani, S. and Schraufnagel, R. A. (1990). Shrinkage of coal matrix with release of gas and its impact on permeability of coal, Fuel, Vol. 69, pp. 551–556.

Harpalani, S. and Zhao, X. (1991). Microstructure of coal and its influence on flow of gas, Energy Sources, Vol. 13, No.2, pp. 229-242.

Harpalani, S., and Chen, G. (1992). Effects of gas production on porosity and permeability of coal, *Symposium on coalbed methane research and development in Australia*, (Beamish, B. B. and Gamson P. D. (eds.), James cook University of North Queensland, Townsville, Australia, pp. 67-79

Harpalani, S., and Chen, G. (1992). Estimation of changes in fracture porosity of coal with gas emission, Fuel, Vol. 74, No. 10, pp. 1491-1498.

Harpalani, S. and Chen, G. (1997). Influence of gas production induced volumetric strain on permeability of coal, Geotechnical and Geological Engineering, Vol. 15, pp. 303–325.

Harpalani, S. and Ouyang, S. (1999). A new laboratory technique to estimate gas diffusion characteristics of coal, *International coalbed methane symposium*, Tuscaloosa, Alabama, USA, pp. 141-149

Harvey, C. R. (2001). Analysis and management of outbursts with particular reference to the Bulli coal seam, PhD Thesis in School of Civil, Mining and Environment Engineering, Faculty of Engineering, University of Wollongong, 210p.

Hayes, P. J. (1982). Factors affecting gas release from the working seam, *Seam gas drainage with particular reference to the working seam*, Hargraves, A. J. (ed.), University of Wollongong, Wollongong, Australia, pp. 62-69

Hiramatsu, Y., Saito, T. and Oda, N. (1983). Studies on mechanism of gas and coal burst in Japanese coalmine, *International congress on Rock Mechanics*, Melbourne, pp.7-10

Holda, S. (1986). Investigation of adsorption, dilatometry and strength of low rank coal., Archiwum Gornictwa, Tom, Vol. 31, pp. 599-608.

Hughes, B. D. and Logan, T. L. (1990). How to design a Coalbed methane well, Petroleum Engineer International, Vol. 5, No.62, pp. 16-20.

Hungerford, F. (1995). Status of Underground Drilling Technology, *International Symposium cum Workshop on Management & Control of High Gas Emission & Outbursts*, Lama, R. D. (ed.), Wollongong, pp. 397-404.

Jackson, L. J. (1984). Outbursts in coal mines, IEA coal research, London, Report No. ICTIS/TR25.

Jolley, D. C., Morris, L. H. and Hinsley, F. B. (1968). An investigation into the relationship between the methane sorption capacity of coal and gas pressure, The Mining Engineer, Vol. 127, No. 94, pp. 539-548.

Jones, A., Ahmed, U., Abou-Sayed, A. S., Mahyera, A. and Sakashita, B. (1982). Fractured vertical wells versus horizontal boreholes for methane drainage in advance of mining U.S. coals, *Seam gas drainage with particular reference to the working seam*, (Hargraves, A. J. (ed.), University of Wollongong, Wollongong, Australia, pp. 172-201

Jones, F. E. (2003). Viscosity of gases, Flow control network (F. C. N.). *http://www.flowcontrolnetwork.com/PastIssues/jul2003/3.asp*.

Juntgen, H. (1987). Research for future in situ conversion of coal, Fuel, Vol. 66, No.4, pp. 443-453.

Kaye, G. W. C. and Laby, T. H. (1966). Table of Physical and Chemical Constants and some Mathematical Functions, Longmans, Green and Co Ltd, London, 249p.

Kim, A. G. (1977). Estimating methane content of bituminous coalbeds from adsorption data., US Bureau of Mines, Report of investigations, RI 8245, 22pp.

Kim, A. G. and Kissell, F. N. (1986). Methane formation and migration in coalbeds In: Methane control research: summary of results, Bureau of Mines Bulletin/ Deul M. and Kim A. G. (eds.), pp. 18-25.

Kissell, F. N. and Edwards, J. C. (1975). Two-phase flow in coalbeds, U.S. Bureau of Mines, Report of Investigations 8066, USA, 16 p.

Klinkenberg, L. J. (1941). The Permeability of Porous Media to Liquidsand Gases, API Drilling And Production Practice, USA, pp. 200-213.

Koenig, R. A. and Schraufnagel, R. A. (1987). Application of the slug test in coalbed methane testing in Coalbed methane, *International coalbed methane symposium*, University of Alabama, Alabama, USA, pp. 16-19.

Kvalnes, H. M. and Gaddy, V. L. (1931). The compressibility isotherms of methane at pressures to 1000 atmospheres and at temperatures from -70° to 200°, Journal of the American Chemical Society, Vol. 53, pp. 394-399.

Lama, R. D. and Mitchell, G. W. (1981). Investigations of geochemical parameters in relation to outbursts of gas and coal at Leichardt Colliery, CSIRO Division of Applied Geomechanics, GCM Report No.9, 49 p.

Lama, R. D. and Bartosiewicz, H. (1982). Determination of gas content of coal seams, *Seam gas drainage with particular reference to the working seam*, Hargraves, A. J. (ed.), The Australian Institute of mining and metallurgy, Illawara Branch, University of Wollongong, pp. 36-52

Lama, R. D. (1988). Adsorption and desorption of mixed gases on coal and their implications in mine ventilation, *Fourth international mine ventilation congress*, Brisbane, Qld, Australia, pp. 161-174.

Lama, R. D. (1991). Methane gas emmisions from coal mining in Australia: estimates and control strategies, *Proceedings of the IEA/OECD Conference on coal, the environment and development: technologies to reduce greenhouse gas emissions*. Sydney, NSW, Australia,18-21Nov1991. Paris, France, IEA/OECD, pp. 255-266

Lama, R. D. (1995a). Effect of stress, gas pressure and vaccum on permeability of Bulli coal samples, *Int. Symp. cum Workshop on Management and Control of High Gas Emissions and Outbursts in Underground Coal Mines*, Lama, R. D. (ed.), Wollongong, NSW, Australia, pp. 293-301

Lama, R. D. (1995b). Safe gas content threshold value for safety against outbursts in the mining of the Bulli seam, *Int. Symp. cum Workshop on Management and Control of High Gas Emissions and Outbursts in Underground Coal Mines,* Lama, R. D. (ed.), Wollongong, Australia, pp. 175–189

Lama, R. D. and Bodziony, J. (1996). Outburst of gas, coal and rock in underground coal mines, R. D. Lama & Associates. 499 p.p.

Lama, R. D. and Bodziony, J. (1998). Management of outburst in underground coal mines, International Journal of Coal Geology, Vol. 35, pp. 83–115

Langmuir, I. (1918). The adsorption of gases on plane surfaces of glass, Mica and Platinum, Amer. Chem. Soc., Vol 40, pp. 1361-1403.

Laubach, S. E., Marrett, R. A., Olson, J. E. and Scott, A. R. (1998). Characteristics and origins of coal cleat: a review, Int. J. Coal Geol., Vol. 35, pp. 175–207.

Law, D., H. –S. (2002). Numerical Model Comparison Study for Greenhouse Gas Sequestration in Coalbeds, *Symposium of COAL-SEQ I, Houston*, Texas, U.S.A., *http://www.coal-seq.com/Proceedings/DavidLaw-CO2-Presentation.pdf.*

Levine, J. R. and Deul, M. (1989). Introduction to coal petrology with application to coalbed methane research and development, Paper to short course No 1. At: *The 1989 International coal bed methane symposium*, Tuscaloosa, Al.

Levine, J. R. (1996). Model study of the influence of matrix shrinkage on absolute permeability of coal bed reservoirs, Coal bed methane and coal geology, Geologic society special publication, Vol. 109, pp. 197-212.

Li, H., Ogawa, Y. and Shimada, S. (2003). Mechanism of methane flow through sheared coals and its role on methane recovery, Fuel, Vol. 82, pp. 1271-1279.

Lide, D. R. (ed.) (2000). CRC handbook of Chemistry and Physics, CRC Press, Cleveland, Ohio, USA, ISSN 0147-6262.

Lingard, P. S., Phillips, H. R. and Doig, I. D. (1982). The permeability of some Australian coals, *Seam gas drainage with particular reference to the working seam*, (Hargraves, A. J. (ed.), University of Wollongong, Wollongong, Australia, pp. 70-80

Lingard, P. S., Phillips, H. R. and Doig, I. D. (1984). Laboratory studies of the sorption characteristics and permeability of triaxially stressed coal samples, *Proceeding 3rd Int. congress on mine ventilation*, Harrogate, pp. 143-150

Littke, R. and Leythaeuser, D. (1993). Migration of oil and gas in coals, In: Hydrocarbons from coal, AAPG studies in Geology 338, Law, B., E. and Rice, D. D. (eds.), pp. 219-236.

Lohe, E. M. (1990). Geological parameters in coalbed methane generation and exploration, Methane drainage from coal, *presented in the CSIRO workshop meeting*, Paterson, L. (eds.), held at the division of Div. Geomech., Syndal, Victoria, pp.4-11.

Mackay, J. (1983). Mt. St. Helen, Creation, Key to rapid coal formation?, Vol. 6, No. 1, pp. 6-8.

Mahajan, O. P. and Walker, P. L., Jr. (1978). Analytical Methods for coal and coal products, New York, pp.125-162

Mahajan, O. P. (1982). Coal porosity, in: Coal structure, Meyers, R. A. (ed.) Academic press, New York, NY, USA, pp.51-86.

Maidebor, V., N. (1973). Production from fractured oil reservoirs, Institut Francais du Petrole (IFP), text No. 21820 (1 and 2).

Massarotto, P., Rudolph, V. and Golding, S. (2000). New 3-D Permeability Equipment, *Second Int'l Methane Mitigation Conference*. Russian Academy of Sciences, Novosibirske.

McCulloch, C. M., Duel, M. and Jeran, P. W. (1974). Cleat in Bituminous coalbeds, US Bureau of Mines, Report of investigations 7910, 25p.

McElhiney, J. E., Paul, G. W. and Young, G. B. C. (1993). Reservoir engineering aspects of coalbed methane, In: Hydrocarbons from coal, Law, B., E. and Rice, D. D.

(eds.) The American association of petroleum geologists, Tulsa, Oklahoma, USA, pp. 361-372.

McPherson, M. J. (1993). Ventilation and environmental engineering, University press, Cambridge, London, 903 p.

Meehan, F. T. (1927). Proceedings of the royal society of Edinburgh, Vol. CXV, pp. 119(as cited in Briggs and Sinha(1933)).

Milewska-Duda, J., Cegarska-Stefanska, G. and Duda, J. (1994). A comparison of theoretical and empirical expansion of coals in the high-pressure sorption of methane, Fuel, Vol. 73, pp. 971-974.

Moffat, D. H. and Weale, K. E. (1955). Sorption by coal of methane at high pressures, Fuel, Vol. 34, pp. 449-462.

Mordecai, M. and Morris, L. H. (1974). The effect of stress on the flow of gas through coal measure strata, Mining engineer, Vol. 133, pp. 435- 443.

More, R. D. and Hanes, J. (1980). Bursts in coal at Leichhardt Colliery, Central Queensland and the apparent benefits of Mining by shotfiring, *Symposium on occurence, prediction & control outbursts in coal mines*, Brisbane, Qld., Australia, pp.71-84.

Mostade, M. (1999). Coalbed methane potential of the southern coal basin of Belgium, *International coalbed methane symposium*, Tuscaloosa, Alabama, USA, pp. 35-41

Murry, D. K. (1991). Coal bed methane; natural gas resources from coal seams,USA, pp. 97-103.

Muskat, M. (1949). Physical principies of oil production, McGraw-Hill, New York.246p.

Ogle, M. (1984).Determining the gas content of coal seams using adsorption/desorption techniques. B.E. thesis, Department of Civil and Mining Engineering. University of Wollongong, 158 p.

Palmer, I. and Mansoori, J. (1996). How permeability depends on stress and pore pressure in coal beds: A new model, paper SPE36737, *Proceeding of the 71st annual technical conference*, Denver, CO.

Patching, T. H. (1965). Variations in permeability of coal, In proceedings of rock mechanics symposium, University of Toronto, pp. 185-194

Patching, T. H. (1970). The retention and release of gas in coal-a review, Canadian mining and metallorgical Bull., Vol. 63, pp. 1302-1308.

Paterson, L. (1990). Laboratory measurment of coal permeability, In: Methane drainage from coal, Paterson, L. (ed.) CSIRO division of geomechanics, Synadal, Victoria, pp. 33-38.

Pekot, L. J. and Reeves, S. R. (2003). Modelling the effects of matrix shrinkage and differential swelling on coalbed methane recovery and carbon sequestration. *http://www.coal-seq.com/Proceedings2003/40924R02.pdf*

Peng, S. S. and Chiang, H. S. (1984). Longwall mining, Wiley, Interscience Publication, New York, 708p.

Pomeroy, D. C. and Robinson, D. J. (1967). Effect of applied stress on permeability of middle rank coal to water, Int. J. Rock Mechn. Min. Sci., Vol. 4, pp. 329- 343.

Protodyakonov, M. M. (1963). Mechanical properties and drillability of rocks, *Proc. of 5th Symp. Rock Mech*., Fairhurst, C. (ed.), Minneapolis, Minnesota, pp. 103– 118

Puri, R. and Seidle, J. P. (1992). Measurment of stress- dependant permeability in coal and its influence on coalbed methane production, In situ, Vol. 16(3), pp. 183-202.

Rabia, H. (1988). Mine environmental engineering, Entrac Software, Newcastle, UK. 425 p.

Ramani, R. V. and Owili-Eger, A. (1973). Engineering aspects of coal mine ventilation systems, American Chemical Society, Division of Fuel Chemistry, Vol. 18, No.3, pp. 158- 164.

Reiss, L. H. (1980). The reservoir engineering aspects of fractured formations, Editions Technip, Paris, France, 108 p.

Renton, J. J. (1982). Mineral matter in coal, In: Coal structure, Meyers, R. A. (ed.), Academic Press, New York, 340 p.

Reucroft, P. J. and Patel, K. B. (1983). Surface area and swellability of coal, Fuel, Vol. 62, pp. 279-284.

Reucroft, P. J. and Patel, K. B. (1986). Gas-induced swelling in coal, Fuel, Vol. 65, pp. 816-820.

Rice, D. D. (1993). Controls of coalbed gas composition, *International coalbed methane symposium*, Uni. of Alabama, Tuscaloosa, pp.577-582.

Rightmire, C. T. (1984). Coalbed Methane Resource, *Coalbed Methane Resources of the United States*, Rightmire, C. T., Eddy, G. E., Kirr, J. N. (eds.), Tulsa, Oklahoma, pp. 1-13.

Rodrigues, C. F. and Lemos de Sousa, M. L. (2002). The measurement of coal porosity with different gases, International Journal of Coal Geology, Vol 48, pp. 245-251.

Rose, R. E. and Foh, S. E. (1984). Liquid permeability of coal as a function of net stress, *Unconventional Gas Recovery Symposium*, Pittsburgh, PA, USA, pp. 253-259.

Ruff, O. and Gessele, P. Z. (1930, 1940) BergHutton salinenwesen, No. 10, 84(1936), No. 7, 88(1940)(in German), (as cited in Lama and Bodziony, 1996).

Ruppel, T. C., Grein, C. T. and Bienstock, D. (1974). Adsorption of methane on dry coal at elevated pressure, Fuel, Vol. 53, pp. 152-162.

Ryan, B. D. (1995). Calcite in coal from the Quinsam mine, British Colombia, Canada; its origin, distribution and effects on coal utilization.
http://www.em.gov.bc.ca/DL/GSBPubs/GeoFldWk/1994/243-260-ryan.pdf

Saghafi, A. (2001). Coal seam gas reservoir characterisation, 14p.
http://www.australiancoal.csiro.au/pdfs/saghafi.pdf.

Santillan, M. (2004). Underground Desgasification and Coal Mine Methane Projects at Minerales Monclova, Minerales Monclova, S.A. de C.V.
http://www.epa.gov/coalbed/pdf/desgasification_mexico.pdf

Sawyer, W. K., Paul, G. W. and Schraufnagel, R. A. (1990). Development and application of a 3D coal bed simulator, Paper CIM/SPE 90-119, *Proceedings of the petroleum society CIM*, Calgary, Canada, pp. 119 (1-9)

Scott, A. R. (1994). Composition of coalbed gases, In situ, Vol. 18, No. 2, pp. 185-208.

Seidle, J. P. and Huitt, L. G. (1995). Experimental measurement of coal matrix shrinkage due to gas desorption and implications for cleat permeability increases, paper SPE 30010, *Proceedings of the international meeting on petroleum engineering*, Beijing, China, pp.575-582

Sethuraman, A. R. (1987). Gas and vapour induced coal swelling, American Chemical Society, Vol. 32, pp. 259–264.

Shi, J. Q. and Durucan, S. (2003). Modelling of enhanced methane recovery and CO_2 sequestration in deep coal seams: the impact of coal matrix shrinkage / swelling on cleat permeability, *International coal bed methane Symposium*, Tuscaloosa, Alabama, pp. 0343 (1-12)

Shu, D. M., Chamberlain, J. A., Lakshmanan, C. C. and White, N.(1995). Estimation of in-situ coal permeability and modeling of methane pre-drainage from in-seam holes, *Int. Symp. cum Workshop on Management and Control of High Gas Emissions and Outbursts in Underground Coal Mines*, Lama, R. D. (ed.), Wollongong, Australia, pp. 303-310

Smith, J. W. and Gould, K. W. (1980). An isotopic study of the role of carbon dioxide in outbursts in coal mines, Geochemistry, Vol. 14, pp. 27-32.

Somers, M. L. (1993). Industrial drainage of mine gas from coal seams, PhD Thesis, Chem. engineering and ind. chem., University of New South Wales, Sydney, 552p.

Somerton, W. H., Soylemezoglu, I. M. and Dudley, R. C. (1975). Effect of stress on permeability of coal, Int.J. Rock M. M. Sci., Vol. 12, pp. 129-145.

Speight, J. G. (1983). The chemistry and technology of coal, Marcel Dekker, Inc., New York and basel, 528 p.

St.George, J. D. and Barakat, M. A. (2001). The change in effective stress associated with shrinkage from gas desorption in coal, International Journal of Coal Geology, Vol. 45, pp. 105-113.

Stach, E., Mackowsky, M. T., Teichmuller, M., Taylor, G. H., Chandra, D. and Teichmuller, R. (1975). Stach's textbook of coal petrology, 2nd Ed., Gebruder Borntraeger,Berlin, Stuttgart.428 p.

Stach, E., Mackowsky, M. T., Teichmuller, M., Taylor, G. H., Chandra, D. and Teichmuller, R. (1982). Stach's textbook of coal petrology, 3rd Ed., Gebruder Borntraeger,Berlin, Stuttgart.535 p.

Stefanska, C. G. (1990). Influence of carbon dioxide and methane on changes of sorption, and dilatometric properties of bituminous coals, Archiwum Gornictwa, Poland, Vol. 35, pp. 105–113.

Su, X., Feng, Y., Chen, J. and Pan, J. (2001). The characteristics and origins of cleat in coal from Western North China., Int. J. Coal Geol, Vol. 47, pp. 51-62.

Symth, M. (1993). Statistics of coal micro lithotypes and their correlation to permeability of coal seams., Int. J. of Coal Geol, Vol. 22, No. 2, pp. 167-187.

Tankard, J. H. G. (1958). The effect of sorbed carbon dioxide upon the strength of coals, The M.S. thesis, Department of Mining Engineering, The university of Sydney, 149 p.

Temmel (1990). Coalbed methane : Criteria for the production of methane from coal: applied to Styrian brown coals. MSc thesis.

Thakur, P. C. and Davis, J., G. (1977). How to plan for methane control in underground coal mines., Mining Engineering, Vol. 29, No.10, pp. 41- 45.

Thakur, P. C. and Dahl, H. D. (1982). Methane drainage, In: Mine ventilation and air conditioning, Hartman, H., Mutmansky, J. M. and Wang, Y. J. (eds.), John Wiley& Sons, New York, pp.69-83.

Thomson, C. and MacDonald, D. (2003). Ryde, NSW, Australia. *http://www.lucas.com.au/index.cfm?section=1&homeContentID=28*.

Thomson, S. (2004). The role of directional drilling for safety in coal mining, CoalBed concepts Pty Limited for Advanced Mining Technologies Pty Ltd (AMT). *http://www.advminingtech.com.au/Paper3.htm#5.%20ACKNOWLEDGEMENTS*

Titheridge, D. (2004). Low permeability coal: toward an exploration model based on macroscopic features of calcite mineralisation and a knowledge of tectonic history, *Gas and coal outburst committee half day seminar*, NSW Department of mineral resources, Wollongong, NSW, Australia, pp. 1-28

Van der Meer, L. G. H. (2004). An excellent simulation tool SIMED II™, TNO-NITG, Information. *http://www.nitg.tno.nl/eng/pubrels/infor_mation/nr13art4.pdf*.

Van Krevelen, D. W. (1981). Coal, Elsevier, Amsterdam, 514 p.

Vutukuri, V. S. and Lama, R. D. (1986). Environmental engineering in mines, Syndicate of the University of the Cambridge, Cambrige, 504p.

Wallace, J. A. (1990). Coalbed methane production- an operator's perspective, Coalbed methane in Alberta what's it all about?, Nikols, D., Treasure, S., Stuhec, S., Goulet, D. (eds.),Edmonton, Alberta Canada, 17 p.

Wang, Y. and Yang, Q. (1987). Prediction of outburst hazard of coal and gas, *Proc. 22nd int. Conf. Safety in mines Res. Inst.,* Beijing, China, pp. 347-355

Williams, A., E. and Elders, W. A. (1984). Stable isotope systematics of oxygen carbon in rocks and minerals from the Cerro Prieto anomaly, Baja California, Mexico, Geothermics, Vol. 14, pp. 49-63.

Williams, R. J. (1991). Carbon dioxide and methane emission at Tahmoor Colliery, In: Gas in Australian coals, *A symposium on seam gas*, Bamberry, W. J. and Depers, A. M. (eds.), University of New South Wales, pp. 141-156

Williams, R. J. (1999). Assessment and control of gas hazards in Queensland collieries, Longwall Mining Summit, Capricorn Resort, Yeppoon.

Wold, M. B. and Jeffrey, R. G. (1999). A comparison of coal seam directional permeability as measured in laboratory core tests and in well interference tests, SPE paper 55598, *Proceedings SPE Rocky Mountain Regional Meeting,* Gillette, Wyoming, pp. 185-193

Wolf, K. H. A. A., Ephraim, R., Bertheux, W. and Bruining, J. (2001a). Coal Cleat Classification and Permeability Estimation by Image Analysis on Cores and Drilling Cuttings, *Int. Coalbed Methane Symp.,* Tuscaloosa, Alabama, USA. Paper No 0102., pp. 1-10

Wolf, K. H. A. A., Bertheux, W., Bruining, J. and Ephraim, R. (2001b). CO2 Injection in and CH4 production from coal seams: laboratory experiments and image

analysis for simulations, *First National Conference on Carbon Sequestration*, Washington, DC, USA.
http://www.netl.doe.gov/publications/proceedings/01/carbon_seq/p22.pdf

Wu, Y. S., Pruess, K. and Persoff, P. (1998). Gas flow in porous media with Klinkenberg effects, Transport in Porous Media, Vol. 32, pp. 117–137.

Wubben, P., Seewald, H. and Jurgen, K. (1986). Permeation and sorption behaviour of gas and water in coal, *Proceedings of the twelfth annual underground coal gasification symposium*, August 24-28.

Xue, S. and Thomas, L. J. (1991). The permeability of coal under various confining stresses, *Gas in Australian Coals*, Bamberry, W. J. and Depers, A. M. (eds.), School of mines, University of New South Wales, pp. 157-162

Xue, S. and Thomas, L. J. (1995). Laboratory investigation on the permeability of coal to mixture of methane and carbon dioxide, *Int. Symp. cum Workshop on Management and Control of High Gas Emissions and Outbursts in Underground Coal Mines*, Lama, R. D. (ed.) Wollongong, Australia, pp. 311-315

Yee, D., Seidle, J. P. and Hanson, W. B. (1993). Gas sorption on coal and measurement of gas content, Hydrocarbons from Coal, American Association of Petroleum Geologists, Tulsa, Oklahoma, pp.203-218

Yong, Q., Jianping, Y. and Dayang, L. (1999). Methodology of optimum seeking to the potential exploring and mining areas of coalbed methane resources in China, *International coalbed methane symposium*, University of Alabama, Alabama, USA, pp. 187-195

Zwietring, P. and Van Krevelen, D. W. (1954). Chemical structure and properties of coal. IV. Pore structure, Fuel, Vol. 33, pp. 331-337.

APPENDIX I

RESULTS OF PERMEABILITY OF COAL SAMPELS TESTS

UNDER DIFFERENT AXIAL LOAS AND

GAS PRESSURES FOR VARIOUS GASES

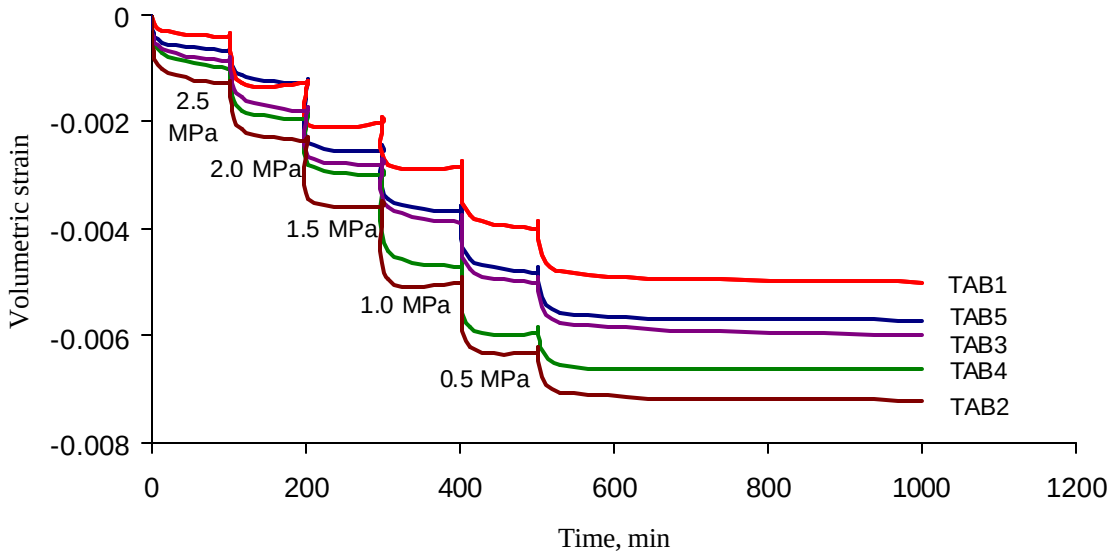

Figure A.I.1 Volumetric strain in CO_2 for pressure reductions of 0.5 MPa from 3 MPa for Tabas samples.

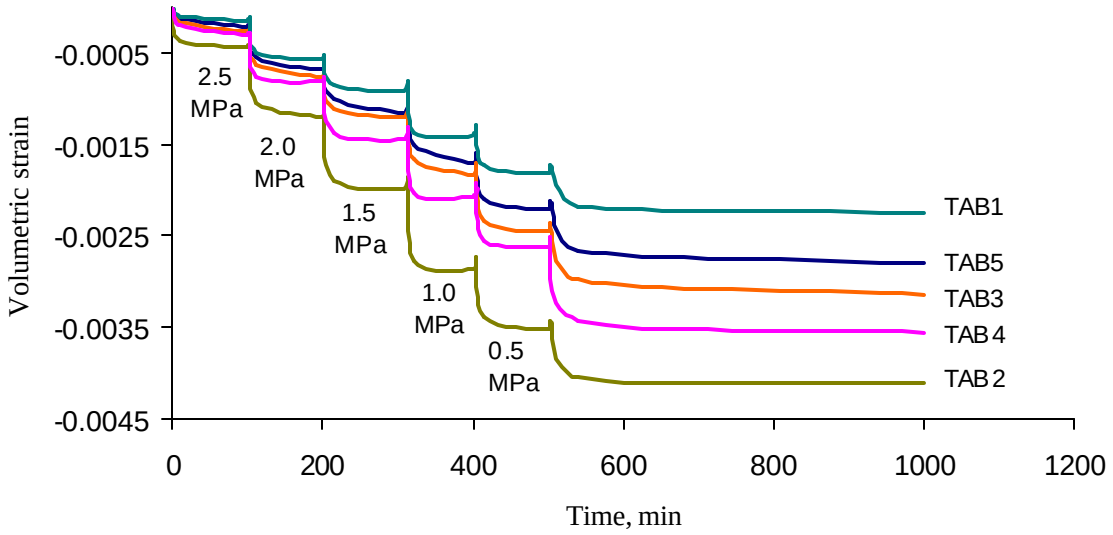

Figure A.I.2 Volumetric strain in CH_4 for pressure reductions of 0.5 MPa from 3 MPa for Tabas samples.

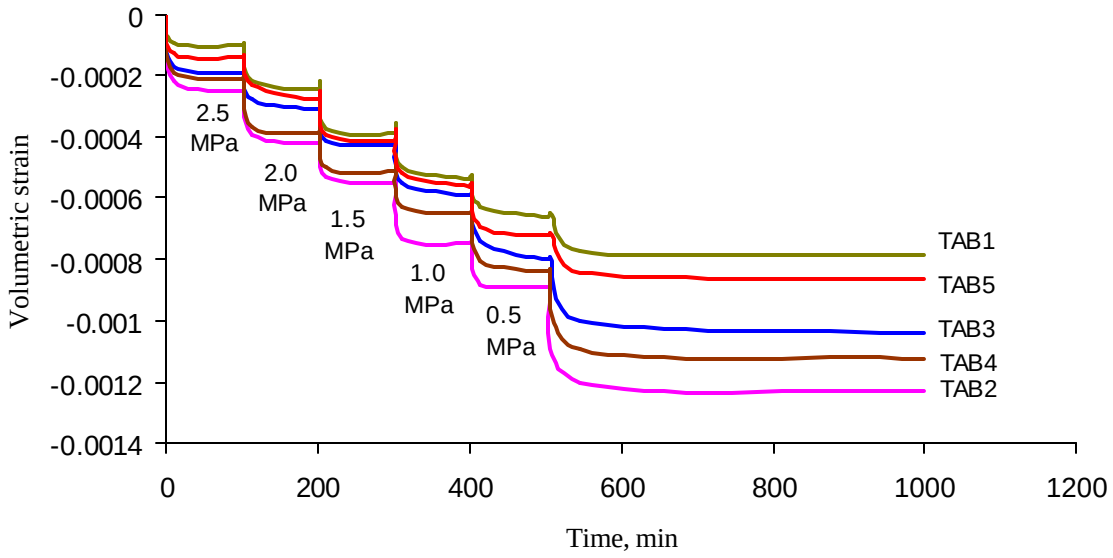

Figure A.I.3 Volumetric strain in N_2 for pressure reductions of 0.5 MPa from 3 MPa for Tabas samples.

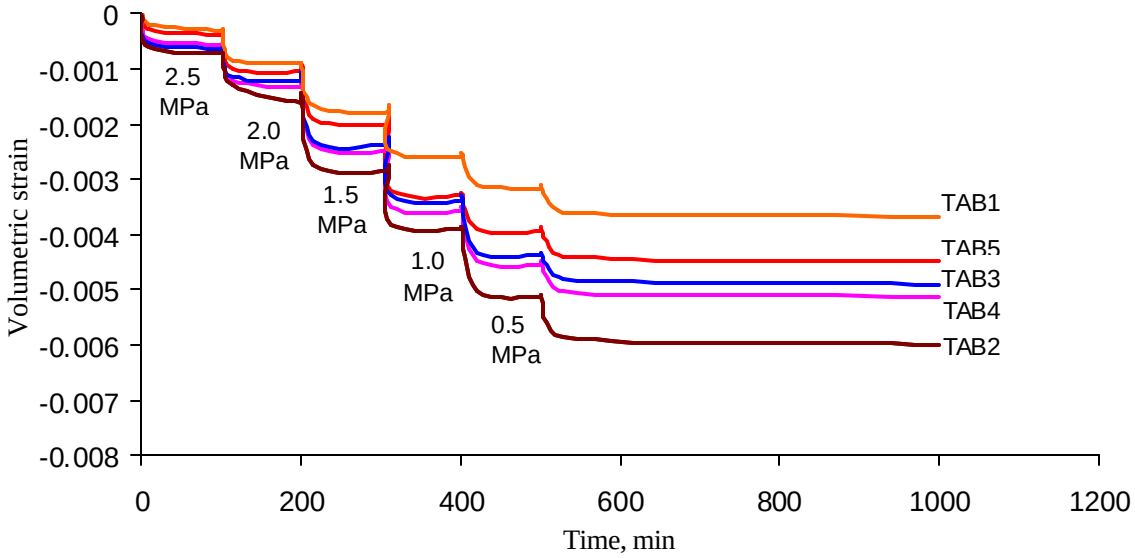

Figure A.I.4 Volumetric strain in CO_2/CH_4 mixture or pressure reductions of 0.5 MPa from 3 MPa for Tabas samples.

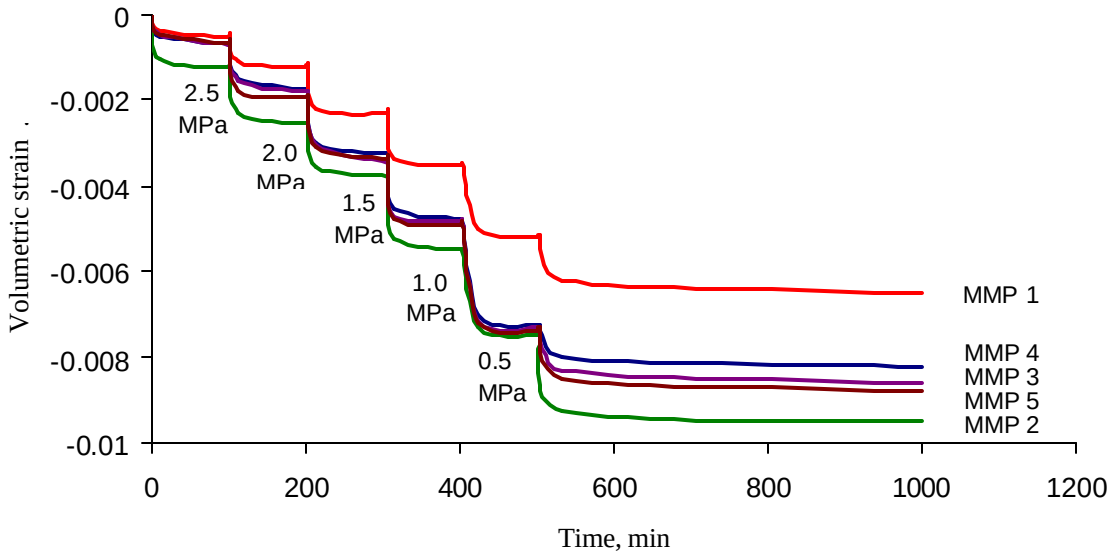

Figure A.I.5 Volumetric strain in CO_2 for pressure reductions of 0.5 MPa from 3 MPa for Metropolitan samples.

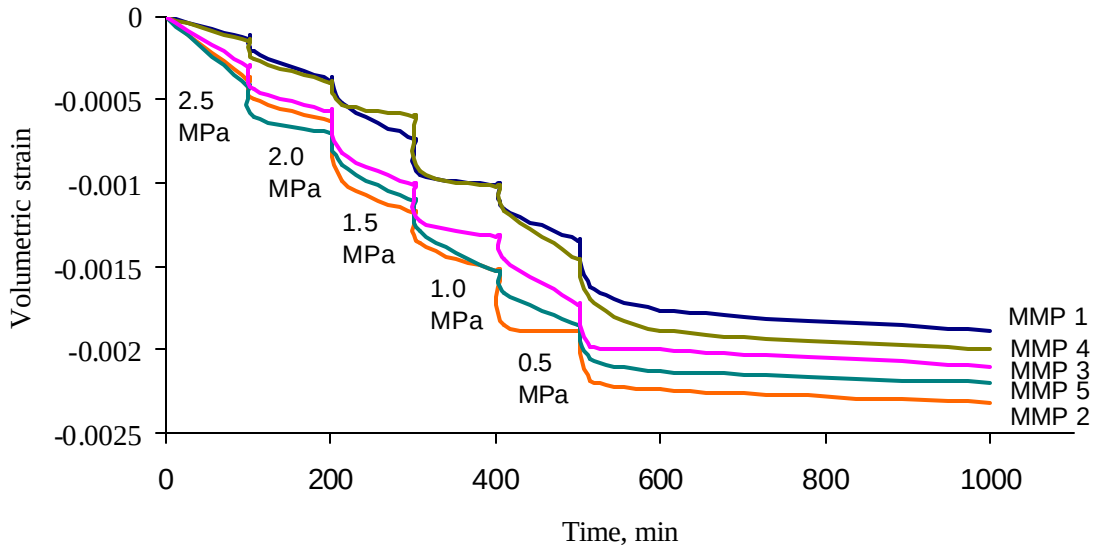

Figure A.I.6 Volumetric strain in CH_4 for pressure reductions of 0.5 MPa from 3 MPa for Metropolitan samples.

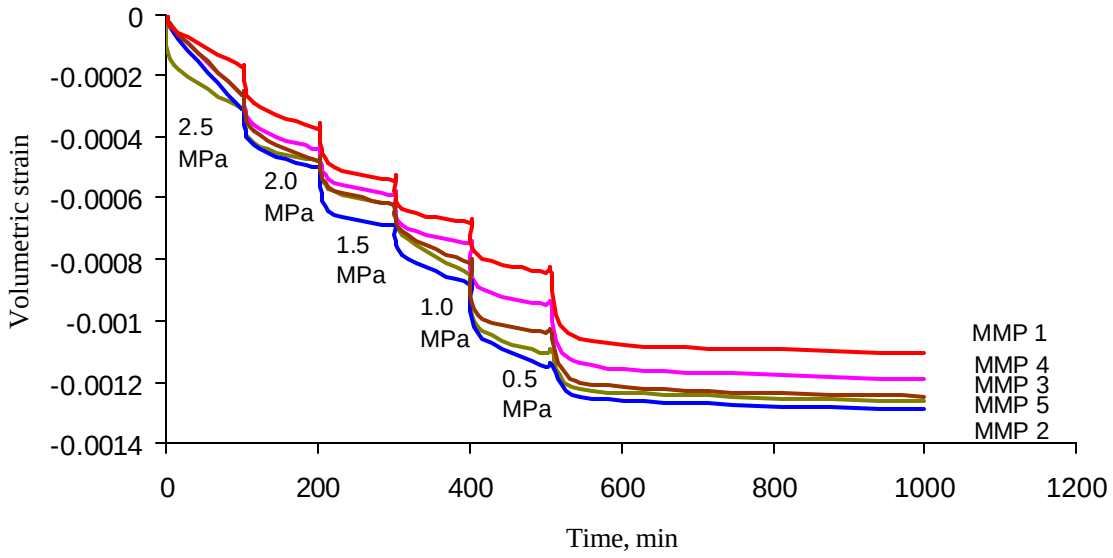

Figure A.I.7 Volumetric strain in N_2 for pressure reductions of 0.5 MPa from 3 MPa for Metropolitan samples.

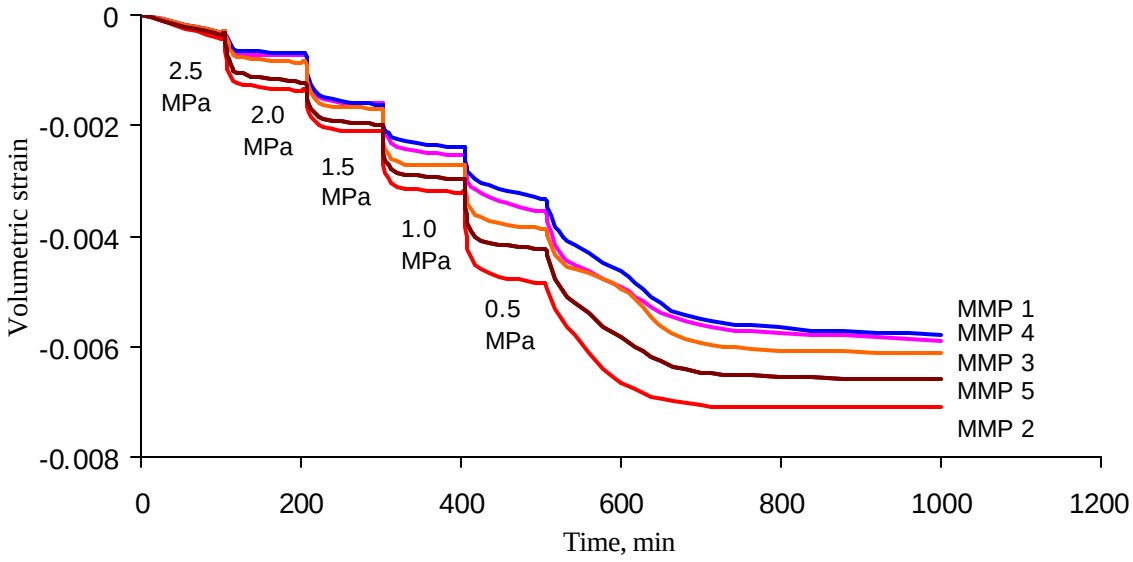

Figure A.I.8 Volumetric strain in CO_2/CH_4 for pressure reductions of 0.5 MPa from 3 MPa for Metropolitan samples.

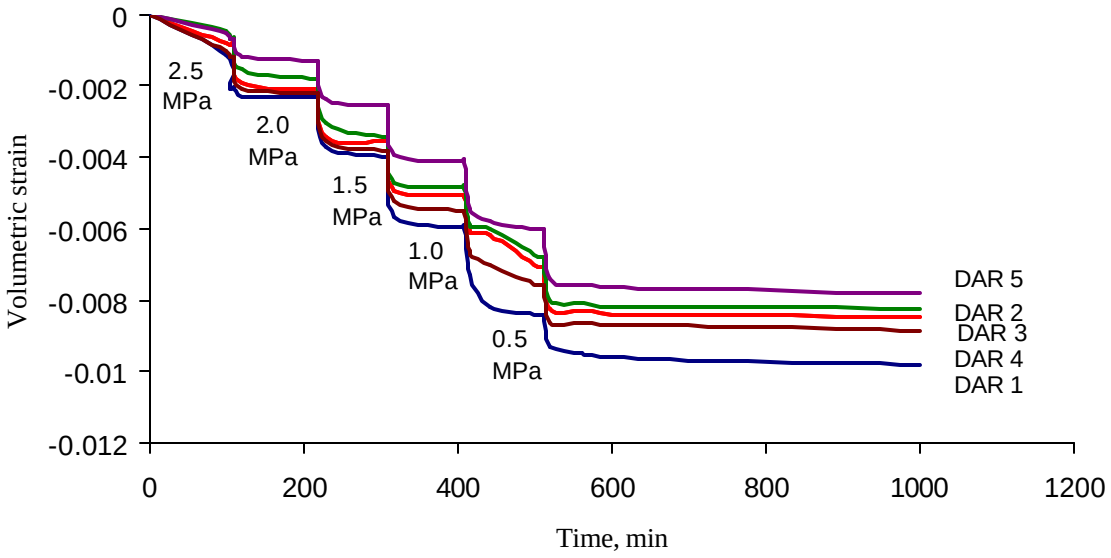

Figure A.I.9 Volumetric strain in CO_2 for pressure reductions of 0.5 MPa from 3 MPa for Dartbrook samples.

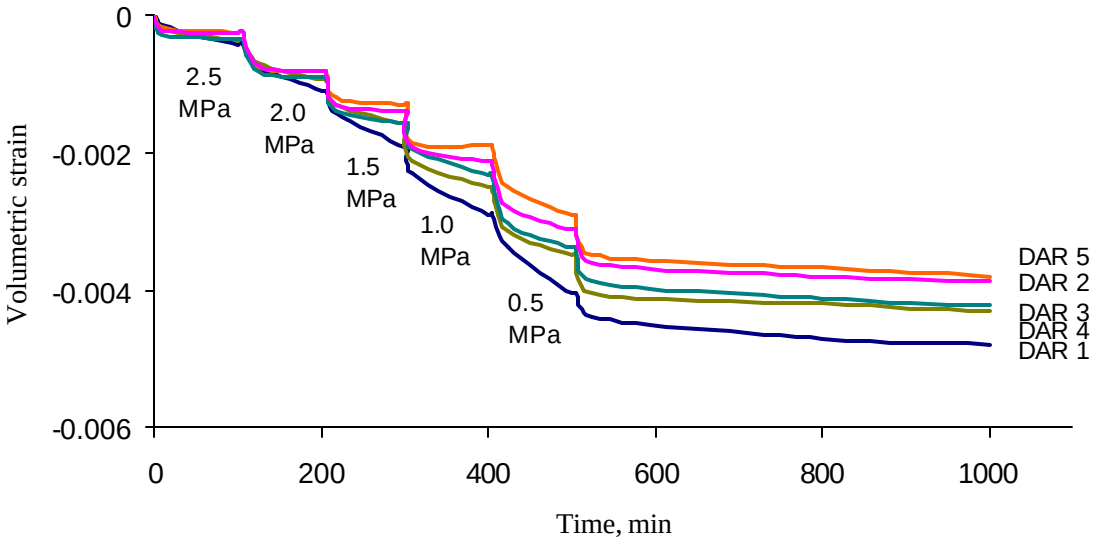

Figure A.I.10 Volumetric strain in CH_4 for pressure reductions of 0.5 MPa from 3 MPa for Dartbrook samples.

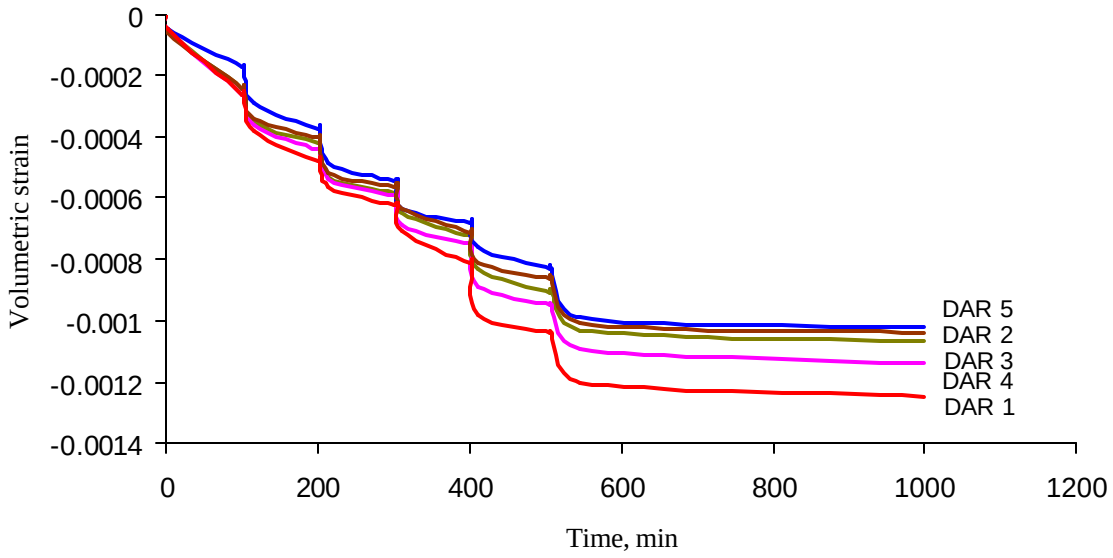

Figure A.I 11 Volumetric strain in N_2 for pressure reductions of 0.5 MPa from 3 MPa for Dartbrook samples.

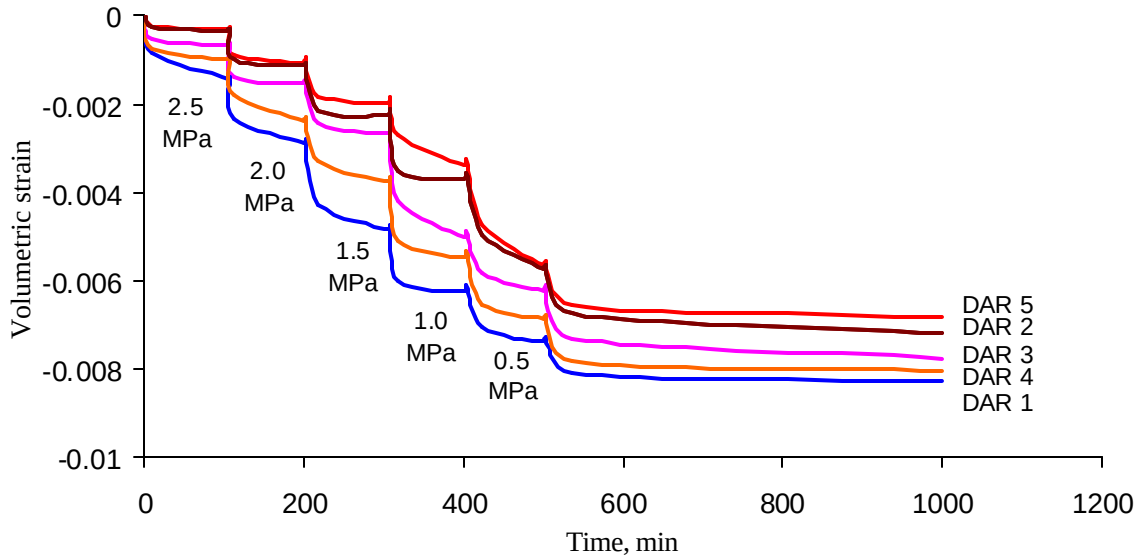

Figure A.I 11 Volumetric strain in CO_2/CH_4 for pressure reductions of 0.5 MPa from 3 MPa for Dartbrook samples.

APPENDIX II

PERMEABILITY OF COAL SAMPELS TEST RESULTS

UNDER DIFFERENT AXIAL LOAS AND

GAS PRESSURES FOR VARIOUS GASES

Table AII.1 Permeability test results for North Goonyella coal sample (NGO 1).

Gas pressure (MPa)	Axial load (kg)	Permeability to CO_2 (Darcy)	Permeability to CH_4 (Darcy)	Permeability to CO_2/CH4 (Darcy)	Permeability to N_2 (Darcy)
0.5	100	9.76E-04	5.40E-03	1.65E-03	8.85E-03
	500	4.45E-04	4.45E-03	1.08E-03	7.56E-03
	750	3.66E-04	4.01E-03	9.36E-04	6.71E-03
	1000	3.10E-04	1.66E-03	7.12E-04	2.81E-03
1.0	100	5.88E-04	2.66E-03	9.13E-04	4.71E-03
	500	2.93E-04	1.01E-03	7.28E-04	2.01E-03
	750	2.28E-04	7.60E-04	6.40E-04	2.41E-03
	1000	1.90E-04	6.82E-04	4.94E-04	2.06E-03
2.0	100	3.55E-04	1.33E-03	4.50E-04	3.03E-03
	500	1.94E-04	8.46E-04	3.95E-04	2.25E-03
	750	1.28E-04	6.56E-04	3.36E-04	1.46E-03
	1000	1.14E-04	3.96E-04	2.82E-04	1.21E-03
3.0	100	2.32E-04	9.50E-04	2.74E-04	1.77E-03
	500	1.07E-04	7.13E-04	2.28E-04	1.40E-03
	750	8.79E-05	3.48E-04	1.90E-04	6.05E-04
	1000	4.88E-05	1.94E-04	1.66E-04	3.45E-04

Table AII.2 Permeability test results for North Goonyella coal sample (NGO 2).

Gas pressure (MPa)	Axial load (kg)	Permeability to CO_2 (Darcy)	Permeability to CH_4 (Darcy)	Permeability to CO_2/CH_4 (Darcy)	Permeability to N_2 (Darcy)
0.5	100	1.22E-03	5.45E-03	1.78E-03	9.20E-03
	500	5.32E-04	4.24E-03	1.19E-03	6.90E-03
	750	4.45E-04	3.33E-03	1.03E-03	5.76E-03
	1000	3.87E-04	1.45E-03	7.90E-04	2.55E-03
1.0	100	6.99E-04	3.35E-03	1.14E-03	5.50E-03
	500	3.64E-04	1.32E-03	9.42E-04	2.35E-03
	750	2.49E-04	1.07E-03	7.91E-04	2.32E-03
	1000	2.24E-04	9.90E-04	6.39E-04	1.41E-03
2.0	100	4.16E-04	2.00E-03	6.49E-04	4.41E-03
	500	1.90E-04	9.04E-04	5.63E-04	2.21E-03
	750	1.51E-04	6.97E-04	4.72E-04	1.32E-03
	1000	1.32E-04	4.76E-04	4.02E-04	9.62E-04
3.0	100	2.84E-04	1.01E-03	3.01E-04	1.90E-03
	500	1.32E-04	6.85E-04	2.52E-04	9.85E-04
	750	1.08E-04	4.55E-04	2.08E-04	6.11E-04
	1000	5.89E-05	2.14E-04	1.82E-04	4.34E-04

Table AII.3 Permeability test results for North Goonyella coal sample (NGO 3).

Gas pressure (MPa)	Axial load (kg)	Permeability to CO_2 (Darcy)	Permeability to CH_4 (Darcy)	Permeability to CO_2/CH_4 (Darcy)	Permeability to N_2 (Darcy)
0.5	100	1.49E-03	8.50E-03	2.57E-03	1.91E-02
	500	7.31E-04	6.22E-03	1.84E-03	1.06E-02
	750	5.89E-04	4.46E-03	1.58E-03	8.40E-03
	1000	5.00E-04	1.98E-03	1.22E-03	3.73E-03
1.0	100	1.22E-03	5.65E-03	1.93E-03	9.95E-03
	500	6.41E-04	2.53E-03	1.70E-03	4.53E-03
	750	5.89E-04	2.44E-03	1.30E-03	4.24E-03
	1000	4.08E-04	1.50E-03	1.09E-03	4.03E-03
2.0	100	5.81E-04	3.38E-03	1.07E-03	6.76E-03
	500	2.97E-04	1.02E-03	9.53E-04	2.41E-03
	750	2.06E-04	9.85E-04	8.12E-04	1.72E-03
	1000	1.83E-04	7.68E-04	6.81E-04	1.62E-03
3.0	100	3.80E-04	1.85E-03	5.16E-04	3.33E-03
	500	1.76E-04	9.51E-04	4.52E-04	1.59E-03
	750	1.44E-04	5.33E-04	3.77E-04	8.80E-04
	1000	7.99E-05	3.57E-04	3.28E-04	6.00E-04

Table AII.4 Permeability test results for North Goonyella coal sample (NGO 4).

Gas pressure (MPa)	Axial load (kg)	Permeability to CO_2 (Darcy)	Permeability to CH_4 (Darcy)	Permeability to CO_2/CH_4 (Darcy)	Permeability to N_2 (Darcy)
0.5	100	1.13E-03	5.01E-03	1.65E-03	8.56E-03
	500	5.22E-04	3.95E-03	1.17E-03	6.57E-03
	750	4.41E-04	3.15E-03	1.01E-03	5.25E-03
	1000	3.79E-04	1.93E-03	7.76E-04	3.31E-03
1.0	100	6.90E-04	2.85E-03	9.92E-04	4.98E-03
	500	3.70E-04	9.51E-04	8.00E-04	2.51E-03
	750	2.39E-04	8.76E-04	6.52E-04	1.73E-03
	1000	2.21E-04	8.43E-04	5.53E-04	1.71E-03
2.0	100	3.96E-04	1.40E-03	4.79E-04	3.62E-03
	500	2.04E-04	7.76E-04	3.84E-04	1.87E-03
	750	1.33E-04	4.44E-04	3.27E-04	9.24E-04
	1000	1.18E-04	3.26E-04	2.74E-04	8.10E-04
3.0	100	1.18E-04	9.45E-04	2.96E-04	1.85E-03
	500	1.30E-04	8.25E-04	2.84E-04	1.45E-03
	750	1.06E-04	3.10E-04	1.77E-04	9.60E-04
	1000	5.89E-05	2.06E-04	1.55E-04	4.99E-04

Table AII.5 Permeability test results for North Goonyella coal sample (NGO 5).

Gas pressure (MPa)	Axial load (kg)	Permeability to CO_2 (Darcy)	Permeability to CH_4 (Darcy)	Permeability to CO_2/CH_4 (Darcy)	Permeability to N_2 (Darcy)
0.5	100	1.39E-03	7.10E-03	2.22E-03	1.16E-02
	500	5.34E-04	5.62E-03	1.53E-03	9.49E-03
	750	4.76E-04	5.10E-03	1.31E-03	9.14E-03
	1000	4.00E-04	2.28E-03	1.01E-03	4.16E-03
1.0	100	9.88E-04	5.72E-03	1.90E-03	9.49E-03
	500	5.41E-04	3.43E-03	1.40E-03	5.63E-03
	750	3.71E-04	3.34E-03	1.21E-03	5.55E-03
	1000	3.37E-04	1.45E-03	9.95E-04	2.46E-03
2.0	100	6.18E-04	3.41E-03	1.08E-03	6.00E-03
	500	3.47E-04	1.23E-03	9.60E-04	2.53E-03
	750	2.30E-04	9.12E-04	8.18E-04	1.62E-03
	1000	2.05E-04	6.09E-04	4.86E-04	1.46E-03
3.0	100	3.80E-04	1.62E-03	4.65E-04	2.83E-03
	500	1.76E-04	8.54E-04	3.84E-04	1.54E-03
	750	1.44E-04	3.75E-04	3.20E-04	6.31E-04
	1000	7.99E-05	1.20E-04	8.80E-05	2.31E-04

Table AII.6 Permeability test results for Tabas coal sample (TAB 1).

Gas pressure (MPa)	Axial load (kg)	Permeability to CO_2 (Darcy)	Permeability to CH_4 (Darcy)	Permeability to CO_2/CH_4 (Darcy)	Permeability to N_2 (Darcy)
0.5	100	4.81E-05	3.60E-04	1.30E-04	6.06E-04
	500	3.00E-05	1.69E-04	8.46E-05	3.79E-04
	750	2.17E-05	1.57E-04	8.46E-05	2.59E-04
	1000	1.61E-05	1.24E-04	6.36E-05	2.05E-04
1.0	100	2.30E-05	2.36E-04	8.34E-05	3.74E-04
	500	1.65E-05	1.28E-04	5.84E-05	2.41E-04
	750	1.19E-05	1.26E-04	5.40E-05	2.41E-04
	1000	1.24E-05	1.03E-04	4.22E-05	1.63E-04
2.0	100	1.56E-05	1.58E-04	4.02E-05	2.96E-04
	500	9.18E-06	9.90E-05	3.60E-05	1.76E-04
	750	7.32E-06	5.94E-05	3.04E-05	1.03E-04
	1000	7.74E-06	5.93E-05	2.77E-05	9.90E-05
3.0	100	1.03E-05	8.16E-05	3.80E-05	1.54E-04
	500	6.78E-06	6.36E-05	3.15E-05	1.14E-04
	750	7.56E-06	6.06E-05	2.42E-05	1.03E-04
	1000	3.48E-06	4.97E-05	2.29E-05	7.92E-05

Table AII.7 Permeability test results for Tabas coal sample (TAB 2).

Gas pressure (MPa)	Axial load (kg)	Permeability to CO_2 (Darcy)	Permeability to CH_4 (Darcy)	Permeability to CO_2/CH_4 (Darcy)	Permeability to N_2 (Darcy)
0.5	100	4.51E-05	3.35E-04	1.77E-04	5.80E-04
	500	2.14E-05	1.70E-04	9.72E-05	3.73E-04
	750	1.83E-05	1.32E-04	6.18E-05	2.24E-04
	1000	1.64E-05	1.26E-04	6.00E-05	2.18E-04
1.0	100	2.66E-05	2.36E-04	9.90E-05	3.78E-04
	500	1.94E-05	1.28E-04	5.62E-05	2.11E-04
	750	1.72E-05	1.07E-04	4.76E-05	1.79E-04
	1000	1.19E-05	1.03E-04	3.86E-05	1.75E-04
2.0	100	2.12E-05	1.17E-04	4.78E-05	1.93E-04
	500	9.36E-06	8.22E-05	3.73E-05	1.42E-04
	750	9.60E-06	6.72E-05	3.36E-05	1.15E-04
	1000	7.92E-06	6.24E-05	3.28E-05	1.04E-04
3.0	100	1.67E-05	8.10E-05	3.86E-05	1.45E-04
	500	1.67E-05	6.30E-05	3.32E-05	1.15E-04
	750	7.14E-06	5.52E-05	6.84E-06	9.24E-05
	1000	2.76E-06	4.88E-05	6.66E-06	8.22E-05

Table AII.8 Permeability test results for Tabas coal sample (TAB 3).

Gas pressure (MPa)	Axial load (kg)	Permeability to CO_2 (Darcy)	Permeability to CH_4 (Darcy)	Permeability to CO_2/CH_4 (Darcy)	Permeability to N_2 (Darcy)
0.5	100	4.58E-05	3.48E-04	1.61E-04	6.24E-04
	500	2.59E-05	1.69E-04	1.00E-04	3.78E-04
	750	1.55E-05	1.31E-04	5.99E-05	2.36E-04
	1000	1.40E-05	1.27E-04	5.96E-05	2.02E-04
1.0	100	2.55E-05	2.06E-04	8.94E-05	3.57E-04
	500	1.46E-05	1.30E-04	6.06E-05	2.68E-04
	750	1.49E-05	1.19E-04	4.78E-05	2.08E-04
	1000	1.30E-05	7.68E-05	4.46E-05	1.23E-04
2.0	100	1.76E-05	1.56E-04	4.87E-05	2.56E-04
	500	9.18E-06	8.34E-05	3.01E-05	1.36E-04
	750	9.36E-06	5.82E-05	2.68E-05	9.42E-05
	1000	5.98E-06	5.54E-04	2.60E-05	9.18E-05
3.0	100	9.42E-06	7.98E-05	3.67E-05	1.28E-04
	500	8.04E-06	6.24E-05	3.32E-05	1.07E-04
	750	6.66E-06	5.09E-05	2.14E-05	8.58E-05
	1000	5.32E-06	3.62E-05	1.93E-05	5.94E-05

Table AII.9 Permeability test results for Tabas coal sample (TAB 4).

Gas pressure (MPa)	Axial load (kg)	Permeability to CO_2 (Darcy)	Permeability to CH_4 (Darcy)	Permeability to CO_2/CH_4 (Darcy)	Permeability to N_2 (Darcy)
0.5	100	4.39E-05	3.47E-04	1.46E-04	6.30E-04
	500	2.47E-05	1.66E-04	1.11E-04	4.33E-04
	750	1.81E-05	1.32E-04	6.72E-05	2.51E-04
	1000	1.52E-05	1.23E-04	6.06E-05	2.11E-04
1.0	100	2.47E-05	2.37E-04	1.02E-04	3.77E-04
	500	1.51E-05	1.28E-04	7.26E-05	2.18E-04
	750	1.49E-05	1.14E-04	5.30E-05	1.99E-04
	1000	1.13E-05	1.03E-04	4.15E-05	1.78E-04
2.0	100	1.01E-05	1.47E-04	4.21E-05	1.73E-04
	500	7.62E-06	6.18E-05	2.83E-05	1.06E-04
	750	5.96E-06	6.18E-05	1.95E-05	1.00E-04
	1000	6.24E-06	5.38E-05	1.97E-05	8.88E-05
3.0	100	8.88E-06	1.01E-04	3.59E-05	1.91E-04
	500	7.14E-06	6.42E-05	2.63E-05	1.25E-04
	750	4.64E-06	3.25E-05	1.39E-05	8.40E-05
	1000	5.05E-06	3.17E-05	1.40E-05	5.60E-05

Table AII.10 Permeability test results for Tabas coal sample (TAB 5).

Gas pressure (MPa)	Axial load (kg)	Permeability to CO_2 (Darcy)	Permeability to CH_4 (Darcy)	Permeability to CO_2/CH_4 (Darcy)	Permeability to N_2 (Darcy)
0.5	100	4.69E-05	3.48E-04	1.49E-04	5.95E-04
	500	1.90E-05	1.70E-04	9.12E-05	3.56E-04
	750	1.88E-05	1.32E-04	5.93E-05	2.11E-04
	1000	1.79E-05	1.26E-04	5.75E-05	2.06E-04
1.0	100	2.76E-05	2.35E-04	9.30E-05	3.79E-04
	500	1.93E-05	1.29E-04	5.91E-05	2.29E-04
	750	1.37E-05	1.16E-04	4.82E-05	1.88E-04
	1000	1.38E-05	1.03E-04	4.80E-05	1.72E-04
2.0	100	1.75E-05	1.18E-04	3.85E-05	1.94E-04
	500	8.46E-06	6.54E-05	2.73E-05	1.19E-04
	750	7.50E-06	6.48E-05	2.71E-05	1.12E-04
	1000	7.26E-06	6.42E-05	2.52E-05	1.03E-04
3.0	100	9.48E-06	6.60E-05	3.14E-05	1.26E-04
	500	8.46E-06	6.24E-05	2.98E-05	1.12E-04
	750	6.96E-06	5.40E-05	2.23E-05	8.94E-05
	1000	3.46E-06	4.82E-05	1.84E-05	7.74E-05

Table AII.11 Permeability test results for Metropolitan coal sample (MMP 1).

Gas pressure (MPa)	Axial load (kg)	Permeability to CO_2 (Darcy)	Permeability to CH_4 (Darcy)	Permeability to CO_2/CH_4 (Darcy)	Permeability to N_2 (Darcy)
0.5	100	6.31E-06	1.03E-04	2.62E-05	1.37E-04
	500	3.21E-06	5.98E-05	1.35E-05	1.15E-04
	750	1.12E-06	1.92E-05	1.42E-05	4.29E-05
	1000	1.11E-06	1.56E-05	8.16E-06	2.56E-05
1.0	100	9.75E-06	7.77E-05	1.85E-05	1.28E-04
	500	4.82E-06	3.15E-05	1.19E-05	7.20E-05
	750	2.44E-06	1.74E-05	1.08E-05	2.33E-05
	1000	1.63E-06	1.22E-05	5.61E-06	2.16E-05
2.0	100	2.04E-06	2.70E-05	1.10E-05	5.17E-05
	500	1.20E-06	2.08E-05	4.62E-06	3.74E-05
	750	5.96E-07	1.10E-05	3.94E-06	1.96E-05
	1000	4.42E-07	8.61E-06	4.22E-06	1.46E-05
3.0	100	6.05E-07	1.07E-05	4.88E-06	1.75E-05
	500	5.10E-07	9.67E-06	3.32E-06	1.55E-05
	750	3.78E-07	6.81E-06	3.15E-06	1.27E-05
	1000	2.49E-07	5.43E-06	2.42E-06	1.12E-05

TableAII.12 Permeability test results for Metropolitan coal sample (MMP 2).

Gas pressure (MPa)	Axial load (kg)	Permeability to CO_2 (Darcy)	Permeability to CH_4 (Darcy)	Permeability to CO_2/CH_4 (Darcy)	Permeability to N_2 (Darcy)
0.5	100	1.22E-04	1.93E-03	3.34E-04	3.69E-03
	500	7.30E-05	1.40E-03	2.35E-04	2.26E-03
	750	4.16E-05	6.53E-04	1.90E-04	1.33E-03
	1000	2.03E-05	3.43E-04	1.23E-04	6.34E-04
1.0	100	9.66E-05	1.53E-03	1.78E-04	2.53E-03
	500	5.94E-05	9.26E-04	1.34E-04	1.09E-03
	750	2.90E-05	5.15E-04	1.37E-04	8.61E-04
	1000	1.71E-05	2.68E-04	6.23E-05	5.51E-04
2.0	100	5.37E-05	8.63E-04	1.67E-04	1.40E-03
	500	3.12E-05	5.77E-04	1.19E-04	9.91E-04
	750	1.95E-05	3.95E-04	8.82E-05	7.49E-04
	1000	1.52E-05	1.09E-04	8.82E-05	2.63E-04
3.0	100	2.71E-05	2.89E-04	1.37E-04	6.24E-04
	500	1.59E-05	2.55E-04	8.78E-05	3.93E-04
	750	8.01E-06	1.59E-04	1.46E-05	2.59E-04
	1000	4.86E-06	8.09E-05	8.95E-06	1.33E-04

Table AII.13 Permeability test results for Metropolitan coal sample (MMP 3).

Gas pressure (MPa)	Axial load (kg)	Permeability to CO_2 (Darcy)	Permeability to CH_4 (Darcy)	Permeability to CO_2/CH_4 (Darcy)	Permeability to N_2 (Darcy)
0.5	100	8.78E-06	1.38E-04	2.51E-05	2.29E-04
	500	5.37E-06	8.63E-05	1.93E-05	1.44E-04
	750	4.64E-06	8.09E-05	1.94E-05	1.43E-04
	1000	2.00E-06	3.48E-05	1.08E-05	6.37E-05
1.0	100	6.01E-06	1.07E-04	1.56E-05	1.99E-04
	500	4.86E-06	8.53E-05	1.30E-05	1.50E-04
	750	2.66E-06	4.24E-05	9.04E-06	7.54E-05
	1000	1.59E-06	2.73E-05	5.10E-06	4.47E-05
2.0	100	3.81E-06	8.11E-05	1.47E-05	1.49E-04
	500	3.10E-06	5.77E-05	1.32E-05	9.57E-05
	750	2.20E-06	3.95E-05	7.57E-06	7.05E-05
	1000	7.04E-07	1.09E-05	4.42E-06	2.50E-05
3.0	100	3.04E-06	4.58E-05	1.39E-05	7.88E-05
	500	1.64E-06	2.86E-05	1.03E-05	6.42E-05
	750	1.15E-06	2.53E-05	2.42E-06	4.55E-05
	1000	1.34E-06	1.56E-05	2.22E-06	2.58E-05

TableAII.14 Permeability test results for Metropolitan coal sample (MMP 4).

Gas pressure (MPa)	Axial load (kg)	Permeability to CO_2 (Darcy)	Permeability to CH_4 (Darcy)	Permeability to CO_2/CH_4 (Darcy)	Permeability to N_2 (Darcy)
0.5	100	7.22E-06	1.18E-04	2.22E-05	1.93E-04
	500	4.86E-06	8.35E-05	1.82E-05	1.53E-04
	750	2.40E-06	4.00E-05	1.29E-05	7.77E-05
	1000	1.74E-06	2.83E-05	4.82E-06	5.69E-05
1.0	100	5.37E-06	9.26E-05	1.25E-05	1.51E-04
	500	3.65E-06	6.34E-05	9.77E-06	1.27E-04
	750	2.01E-06	3.22E-05	8.56E-06	6.19E-05
	1000	1.22E-06	2.08E-05	3.76E-06	3.51E-05
2.0	100	4.22E-06	7.18E-05	1.12E-05	1.15E-04
	500	3.12E-06	4.19E-05	9.75E-06	7.67E-05
	750	1.46E-06	2.16E-05	7.13E-06	4.37E-06
	1000	1.03E-06	1.76E-05	2.57E-06	3.09E-06
3.0	100	1.46E-06	2.40E-05	7.94E-06	5.49E-05
	500	7.24E-07	1.63E-05	6.36E-06	2.65E-05
	750	6.40E-07	1.35E-05	1.48E-06	2.48E-05
	1000	4.88E-07	1.03E-05	9.92E-07	1.73E-05

Table AII.15 Permeability test results for Metropolitan coal sample (MMP 5).

Gas pressure (MPa)	Axial load (kg)	Permeability to CO_2 (Darcy)	Permeability to CH_4 (Darcy)	Permeability to CO_2/CH_4 (Darcy)	Permeability to N_2 (Darcy)
0.5	100	1.03E-04	1.58E-03	3.83E-04	2.57E-03
	500	4.55E-05	9.07E-04	2.15E-04	1.50E-03
	750	4.84E-05	5.56E-04	1.37E-04	9.65E-04
	1000	1.41E-05	2.60E-04	8.60E-05	5.04E-04
1.0	100	7.06E-05	9.91E-04	1.59E-04	1.67E-03
	500	4.38E-05	7.38E-04	1.32E-04	1.17E-03
	750	2.73E-05	4.13E-04	1.08E-04	7.59E-04
	1000	8.58E-06	1.32E-04	4.88E-05	2.43E-04
2.0	100	3.98E-05	1.66E-04	5.98E-05	3.74E-04
	500	1.02E-05	8.19E-05	1.36E-05	2.54E-04
	750	9.46E-06	5.77E-05	1.78E-05	1.28E-04
	1000	4.84E-06	3.04E-05	1.09E-05	5.80E-05
3.0	100	9.50E-06	5.51E-05	4.88E-05	1.06E-04
	500	2.90E-06	3.67E-05	1.19E-05	6.01E-05
	750	2.27E-06	3.46E-05	2.71E-06	5.49E-05
	1000	3.52E-06	2.50E-05	2.42E-06	4.68E-05

Table AII.16 Permeability test results for Dartbrook coal sample (DAR 1).

Gas pressure (MPa)	Axial load (kg)	Permeability to CO_2 (Darcy)	Permeability to CH_4 (Darcy)	Permeability to CO_2/CH_4 (Darcy)	Permeability to N_2 (Darcy)
0.5	100	2.91E-06	2.12E-03	1.12E-05	4.44E-03
	500	2.19E-06	1.50E-03	5.89E-06	2.84E-03
	750	2.19E-06	1.49E-03	5.40E-06	2.47E-03
	1000	1.56E-06	1.04E-03	4.83E-06	2.01E-05
1.0	100	2.39E-06	2.01E-03	1.08E-05	4.22E-03
	500	1.59E-06	1.16E-03	5.55E-06	2.11E-03
	750	1.49E-06	1.06E-03	4.67E-06	1.88E-03
	1000	1.04E-06	7.27E-04	4.92E-06	1.67E-03
2.0	100	1.30E-06	7.73E-04	5.42E-06	1.81E-03
	500	8.21E-07	6.97E-04	5.32E-06	1.09E-03
	750	5.07E-07	4.18E-04	1.58E-06	8.75E-04
	1000	4.66E-07	3.99E-04	1.67E-06	7.55E-04
3.0	100	8.46E-07	6.54E-04	1.69E-06	1.66E-03
	500	6.38E-07	6.13E-04	1.35E-06	9.93E-04
	750	5.26E-07	4.01E-04	1.26E-06	6.46E-04
	1000	2.07E-07	2.96E-04	9.04E-07	5.92E-04

Table AII.17 Permeability test results for Dartbrook coal sample (DAR 2).

Gas pressure (MPa)	Axial load (kg)	Permeability to CO_2 (Darcy)	Permeability to CH_4 (Darcy)	Permeability to CO_2/CH_4 (Darcy)	Permeability to N_2 (Darcy)
0.5	100	2.60E-05	7.17E-04	1.56E-04	1.61E-03
	500	2.20E-05	6.26E-04	9.79E-05	1.02E-03
	750	1.79E-05	5.31E-04	7.11E-05	9.21E-04
	1000	1.19E-05	4.51E-04	4.48E-05	8.31E-04
1.0	100	1.82E-05	2.12E-04	8.34E-05	6.41E-04
	500	1.92E-05	1.41E-04	6.31E-05	3.01E-04
	750	1.28E-05	1.18E-04	4.96E-05	2.21E-04
	1000	1.14E-05	8.21E-05	3.38E-05	1.52E-04
2.0	100	5.72E-06	1.27E-04	3.71E-05	2.80E-04
	500	3.57E-06	4.55E-05	1.29E-05	9.50E-05
	750	2.68E-06	3.67E-05	7.79E-06	7.60E-05
	1000	1.96E-06	2.18E-05	5.21E-06	4.00E-05
3.0	100	2.51E-06	6.00E-05	3.02E-05	1.17E-04
	500	2.13E-06	2.08E-05	7.94E-06	4.84E-05
	750	1.52E-06	1.99E-05	7.68E-06	3.57E-05
	1000	3.78E-07	9.00E-06	3.29E-06	1.95E-05

Table AII.18 Permeability test results for Dartbrook coal sample (DAR 3).

Gas pressure (MPa)	Axial load (kg)	Permeability to CO_2 (Darcy)	Permeability to CH_4 (Darcy)	Permeability to CO_2/CH_4 (Darcy)	Permeability to N_2 (Darcy)
0.5	100	2.05E-05	8.59E-04	1.58E-04	1.81E-03
	500	1.83E-05	4.23E-04	9.90E-05	1.00E-03
	750	1.68E-05	4.21E-04	9.71E-05	8.91E-04
	1000	1.50E-05	4.15E-04	7.14E-05	8.56E-04
1.0	100	1.94E-05	3.97E-04	1.12E-04	6.11E-04
	500	1.65E-05	1.52E-04	6.05E-05	3.53E-04
	750	1.58E-05	1.47E-04	5.94E-05	2.64E-04
	1000	1.50E-05	1.21E-04	4.96E-05	1.99E-04
2.0	100	1.66E-05	1.42E-04	7.51E-05	3.72E-04
	500	1.18E-05	9.92E-05	5.80E-05	2.23E-04
	750	1.18E-05	9.61E-05	5.72E-05	1.71E-04
	1000	1.14E-05	9.30E-05	3.00E-05	1.58E-04
3.0	100	1.60E-05	1.16E-04	4.71E-05	1.92E-04
	500	9.42E-06	7.58E-05	3.65E-05	1.37E-04
	750	9.20E-06	7.29E-05	1.90E-05	1.22E-04
	1000	6.48E-06	6.75E-05	1.54E-05	1.02E-04

Table AII.19 Permeability test results for Dartbrook coal sample (DAR 4).

Gas pressure (MPa)	Axial load (kg)	Permeability to CO_2 (Darcy)	Permeability to CH_4 (Darcy)	Permeability to CO_2/CH_4 (Darcy)	Permeability to N_2 (Darcy)
0.5	100	2.64E-06	1.87E-03	1.14E-05	3.01E-03
	500	1.98E-06	1.13E-03	8.57E-06	2.33E-03
	750	1.48E-06	1.17E-03	6.25E-06	1.92E-03
	1000	1.27E-06	1.03E-03	5.23E-06	1.84E-03
1.0	100	2.22E-06	1.78E-03	6.69E-06	3.09E-03
	500	1.30E-06	1.65E-04	4.29E-06	2.98E-03
	750	1.00E-06	1.01E-03	6.14E-06	1.82E-03
	1000	1.18E-06	1.00E-03	3.63E-06	1.70E-03
2.0	100	1.94E-06	1.47E-03	5.85E-06	2.47E-03
	500	1.15E-06	7.21E-04	6.29E-06	1.30E-03
	750	1.16E-06	6.43E-04	4.29E-06	1.09E-03
	1000	9.99E-07	2.01E-04	2.87E-06	3.51E-04
3.0	100	1.80E-06	3.81E-04	3.08E-06	6.88E-04
	500	1.17E-06	9.71E-05	2.55E-06	2.32E-04
	750	9.25E-07	8.11E-05	2.11E-06	1.56E-04
	1000	7.62E-07	7.05E-05	1.58E-06	1.21E-04

Table AII.20 Permeability test results for Dartbrook coal sample (DAR 5).

Gas pressure (MPa)	Axial load (kg)	Permeability to CO_2 (Darcy)	Permeability to CH_4 (Darcy)	Permeability to CO_2/CH_4 (Darcy)	Permeability to N_2 (Darcy)
0.5	100	3.29E-06	1.14E-04	1.29E-05	2.92E-04
	500	2.43E-06	7.74E-05	8.19E-06	1.51E-04
	750	2.00E-06	6.55E-05	9.52E-06	1.02E-04
	1000	2.01E-06	6.05E-05	6.12E-06	1.00E-04
1.0	100	2.47E-06	9.57E-05	7.18E-06	1.81E-04
	500	1.88E-06	7.97E-05	5.51E-06	1.53E-04
	750	1.76E-06	7.47E-05	3.91E-06	1.44E-04
	1000	1.58E-06	5.93E-05	4.09E-06	8.99E-05
2.0	100	2.36E-06	7.52E-05	7.03E-06	1.55E-04
	500	2.11E-06	6.61E-05	4.86E-06	1.12E-04
	750	1.72E-06	5.62E-05	3.48E-06	1.00E-04
	1000	1.35E-06	5.21E-05	3.88E-06	9.97E-05
3.0	100	2.36E-06	4.75E-05	5.02E-06	1.02E-04
	500	1.58E-06	1.39E-05	4.45E-06	2.57E-05
	750	1.16E-06	1.12E-05	3.27E-06	2.49E-05
	1000	1.05E-06	1.00E-06	3.50E-06	2.01E-06

Table AII.25 Permeability test results for Tahmoor (800 panel) coal sample (TAH 1).

Gas pressure (MPa)	Axial load (kg)	Permeability to CO_2 (Darcy)	Permeability to CH_4 (Darcy)	Permeability to CO2/CH4 (Darcy)	Permeability to N_2 (Darcy)
0.5	100	5.95E-05	3.29E-04	8.35E-05	5.11E-04
	500	3.73E-05	2.45E-04	5.25E-05	4.11E-04
	750	2.12E-05	2.12E-04	3.63E-05	3.71E-04
	1000	1.81E-05	1.99E-04	2.93E-05	3.11E-04
1.0	100	4.91E-05	2.49E-04	7.32E-05	4.73E-04
	500	2.11E-05	1.85E-04	5.25E-05	3.07E-04
	750	1.88E-05	1.61E-04	3.70E-05	2.99E-04
	1000	1.83E-05	1.42E-04	1.43E-05	2.39E-04
2.0	100	2.05E-05	1.66E-04	3.53E-05	4.54E-04
	500	1.79E-05	1.50E-04	3.20E-05	2.87E-04
	750	1.01E-05	9.79E-05	1.42E-05	2.85E-04
	1000	1.23E-05	7.06E-05	3.45E-06	2.38E-04
3.0	100	1.00E-05	7.62E-05	1.03E-05	2.99E-04
	500	9.20E-06	2.90E-05	7.43E-06	2.55E-04
	750	6.94E-06	2.45E-05	5.11E-06	1.32E-04
	1000	6.91E-06	2.16E-05	2.56E-06	9.55E-05

Table AII.22 Permeability test results for Tahmoor (900 panel) coal sample (TAH 2).

Gas pressure (MPa)	Axial load (kg)	Permeability to CO_2 (Darcy)	Permeability to CH_4 (Darcy)	Permeability to CO2/CH4 (Darcy)	Permeability to N_2 (Darcy)
0.5	100	4.22E-06	3.60E-05	5.99E-06	6.99E-05
	500	1.80E-06	2.70E-05	4.52E-06	5.04E-05
	750	1.47E-06	2.20E-05	4.00E-06	3.74E-05
	1000	1.33E-06	2.10E-05	3.40E-06	3.74E-05
1.0	100	3.51E-06	2.73E-05	5.71E-06	5.79E-05
	500	1.59E-06	2.22E-05	3.99E-06	3.94E-05
	750	1.40E-06	2.00E-05	3.61E-06	3.66E-05
	1000	1.05E-06	1.60E-05	2.88E-06	2.90E-05
2.0	100	2.55E-06	2.87E-05	4.24E-06	5.30E-05
	500	1.41E-06	2.12E-05	3.21E-06	3.86E-05
	750	1.20E-06	1.80E-05	2.63E-06	3.30E-05
	1000	1.00E-06	9.56E-06	2.15E-06	2.59E-05
3.0	100	1.12E-06	1.38E-05	2.94E-06	2.99E-05
	500	8.12E-07	1.36E-05	2.31E-06	2.86E-05
	750	6.88E-07	1.17E-05	1.85E-06	2.18E-05
	1000	6.20E-07	9.52E-06	1.35E-06	1.78E-05

Table AII.24 Permeability test results for Tahmoor (800 panel) coal sample (TAH 4).

Gas pressure (MPa)	Axial load (kg)	Permeability to CO_2 (Darcy)	Permeability to CH_4 (Darcy)	Permeability to CO_2/CH_4 (Darcy)	Permeability to N_2 (Darcy)
0.5	100	3.83E-05	2.54E-04	5.99E-05	4.68E-04
	500	2.34E-05	2.15E-04	4.52E-05	3.78E-04
	750	2.25E-05	1.79E-04	4.00E-05	2.91E-04
	1000	1.15E-05	1.25E-04	3.40E-05	2.12E-04
1.0	100	2.05E-05	2.39E-04	5.25E-05	3.96E-04
	500	1.79E-05	1.47E-04	3.47E-05	3.68E-04
	750	8.50E-06	1.44E-04	3.01E-05	2.71E-04
	1000	8.20E-06	1.09E-04	2.50E-05	1.81E-04
2.0	100	1.51E-05	1.22E-04	4.80E-05	3.29E-04
	500	8.20E-06	5.46E-05	3.01E-05	2.95E-04
	750	6.50E-06	3.76E-05	2.92E-05	1.07E-04
	1000	6.40E-06	3.25E-05	1.83E-05	8.41E-05
3.0	100	1.21E-05	6.07E-05	3.80E-05	2.19E-04
	500	5.00E-06	2.92E-05	2.40E-05	1.04E-04
	750	4.10E-06	2.00E-05	2.35E-05	6.12E-05
	1000	4.00E-06	1.88E-05	1.19E-05	4.63E-05

Table AII.23 Permeability test results for Tahmoor (800 panel) coal sample (TAH 5).

Gas pressure (MPa)	Axial load (kg)	Permeability to CO_2 (Darcy)	Permeability to CH_4 (Darcy)	Permeability to CO2/CH4 (Darcy)	Permeability to N_2 (Darcy)
0.5	100	3.99E-05	2.50E-04	5.73E-05	4.98E-04
	500	2.62E-05	1.90E-04	2.93E-05	3.68E-04
	750	1.92E-05	1.18E-04	2.85E-05	2.60E-04
	1000	1.21E-05	1.44E-04	2.56E-05	2.05E-04
1.0	100	3.01E-05	1.82E-04	3.85E-05	3.45E-04
	500	2.11E-05	5.64E-05	2.50E-05	3.01E-04
	750	1.88E-05	5.51E-05	2.33E-05	1.79E-04
	1000	1.01E-05	5.08E-05	1.46E-05	1.03E-04
2.0	100	1.33E-05	3.53E-05	2.37E-05	7.72E-05
	500	7.10E-06	7.80E-06	1.20E-05	3.35E-05
	750	7.60E-06	1.27E-05	9.40E-06	2.79E-05
	1000	1.20E-06	6.40E-06	1.13E-05	2.76E-05
3.0	100	7.00E-06	8.47E-05	1.80E-05	1.32E-04
	500	5.30E-06	2.47E-05	9.60E-06	5.98E-05
	750	1.17E-06	3.04E-05	6.30E-06	3.62E-05
	1000	5.81E-07	2.26E-05	6.70E-06	3.50E-05

Table AII.21 Permeability test results for Tahmoor (800 panel) coal sample (TAH 8).

Gas pressure (MPa)	Axial load (kg)	Permeability to CO_2 (Darcy)	Permeability to CH_4 (Darcy)	Permeability to CO2/CH4 (Darcy)	Permeability to N_2 (Darcy)
0.5	100	5.43E-05	3.41E-04	8.28E-05	5.37E-04
	500	4.14E-05	3.18E-04	5.66E-05	4.43E-04
	750	1.47E-05	2.21E-04	3.94E-05	4.10E-04
	1000	1.21E-05	1.90E-04	3.29E-05	4.10E-04
1.0	100	4.57E-05	2.79E-04	5.20E-05	3.90E-04
	500	2.07E-05	2.43E-04	3.50E-05	3.15E-04
	750	1.48E-05	2.15E-04	2.29E-05	2.46E-04
	1000	1.15E-05	1.71E-04	7.40E-06	2.45E-04
2.0	100	2.01E-05	1.82E-04	4.68E-05	4.83E-04
	500	2.47E-06	5.64E-05	3.15E-05	3.68E-04
	750	8.93E-06	4.85E-05	1.79E-05	3.59E-04
	1000	3.61E-06	5.80E-05	1.30E-06	3.32E-04
3.0	100	9.98E-06	4.73E-05	2.31E-05	2.93E-04
	500	2.82E-06	4.50E-05	1.55E-05	2.22E-04
	750	2.65E-06	3.80E-05	9.50E-06	9.95E-05
	1000	2.38E-06	1.20E-05	5.00E-07	9.86E-05

Table AII.26 Permeability test results for Tahmoor (900 panel) coal sample (TAH 9).

Gas pressure (MPa)	Axial load (kg)	Permeability to CO_2 (Darcy)	Permeability to CH_4 (Darcy)	Permeability to CO2/CH4 (Darcy)	Permeability to N_2 (Darcy)
0.5	100	3.40E-06	3.60E-05	5.73E-06	5.61E-05
	500	1.30E-06	2.77E-05	3.16E-06	4.32E-05
	750	1.27E-06	2.35E-05	2.95E-06	3.85E-05
	1000	1.15E-06	2.32E-05	2.65E-06	3.64E-05
1.0	100	2.01E-06	3.42E-05	3.24E-06	5.29E-05
	500	1.21E-06	2.67E-05	2.65E-06	4.16E-05
	750	1.17E-06	2.34E-05	2.21E-06	3.46E-05
	1000	5.81E-07	2.12E-05	1.72E-06	3.26E-05
2.0	100	1.40E-06	2.25E-05	2.60E-06	4.99E-05
	500	6.67E-07	1.40E-05	1.47E-06	4.27E-05
	750	5.71E-07	1.01E-05	1.25E-06	3.19E-05
	1000	5.13E-07	6.76E-06	9.98E-07	3.01E-05
3.0	100	6.10E-07	7.57E-06	1.43E-06	3.11E-05
	500	4.31E-07	7.33E-06	1.32E-06	2.91E-05
	750	3.83E-07	6.51E-06	1.02E-06	1.92E-05
	1000	3.31E-07	4.84E-06	8.30E-07	1.89E-05